1871
ИнБЮМ – IBSS

ISSN 2499-9768 print

МОРСКОЙ БИОЛОГИЧЕСКИЙ ЖУРНАЛ

MARINE BIOLOGICAL JOURNAL

Vol. 10 No. 2
2025

МОРСКОЙ БИОЛОГИЧЕСКИЙ ЖУРНАЛ
MARINE BIOLOGICAL JOURNAL

Журнал включён в перечень рецензируемых научных изданий, рекомендованных ВАК Российской Федерации, а также в базу данных Russian Science Citation Index (RSCI).
Журнал реферируется международной библиографической и реферативной базой данных Scopus (Elsevier), международной информационной системой по водным наукам и рыболовству ASFA (ProQuest), Всероссийским институтом научно-технической информации (ВИНИТИ), а также Российским индексом научного цитирования (РИНЦ) на базе Научной электронной библиотеки elibrary.ru.
Все материалы проходят независимое двойное слепое рецензирование.

Адрес учредителя, издателя и редакции:
ФИЦ «Институт биологии южных морей имени А. О. Ковалевского РАН».
Пр-т Нахимова, 2, Севастополь, 299011, РФ.
Тел.: +7 8692 54-41-10. E-mail: *mbj@imbr-ras.ru*.
Сайт журнала: https://marine-biology.ru.

Адрес соиздателя:
Зоологический институт РАН.
Университетская наб., 1, Санкт-Петербург, 199034, РФ.

Founder, Publisher, and Editorial Office address:
A. O. Kovalevsky Institute of Biology of the Southern Seas of Russian Academy of Sciences.
2 Nakhimov ave., Sevastopol, 299011, Russia.
Tel.: +7 8692 54-41-10. E-mail: *mbj@imbr-ras.ru*.
Journal website: https://marine-biology.ru.

Co-publisher address:
Zoological Institute Russian Academy of Sciences.
1 Universitetskaya emb., Saint Petersburg, 199034, Russia.

ZOOLOGICAL INSTITUTE OF RAS
A. O. KOVALEVSKY INSTITUTE OF BIOLOGY OF THE SOUTHERN SEAS OF RAS

МОРСКОЙ БИОЛОГИЧЕСКИЙ ЖУРНАЛ

MARINE BIOLOGICAL JOURNAL

2025 Vol. 10 No. 2

Established in February 2016 SCIENTIFIC JOURNAL *4 issues per year*

CONTENTS

Scientific communications

Chronicle and information

1871
ИнБЮМ – IBSS

Морской биологический журнал
Marine Biological Journal
2025, vol. 10, no. 2, pp. 3–17
https://marine-biology.ru

SCIENTIFIC COMMUNICATIONS

UDC [574.5:[582.272:661.635]](262.5)

MACROPHYTOCENOSES AS BIOGEOCHEMICAL BARRIERS TO WATER HYPEREUTROPHICATION BY MINERAL PHOSPHORUS OFF THE SOUTHWESTERN CRIMEA

© 2025 **V. Egorov, N. Milchakova, N. Bobko, and Yu. Marchenko**

A. O. Kovalevsky Institute of Biology of the Southern Seas of RAS, Sevastopol, Russian Federation
E-mail: *egorov@ibss-ras.ru*

Received by the Editor 30.07.2024; after reviewing 16.01.2025;
accepted for publication 20.03.2025.

The aim of the work was to study mineral phosphorus concentration by brown algae *Cystoseira crinita* and *Cystoseira barbata* listed in the Red Book of the Republic of Crimea and to assess the role of macrophytobenthos in the coastal ecosystem of the Southwestern Crimea in formation of biogeochemical barriers that regulate competitive relations of producers for biogenic elements. As established, *Cystoseira crinita* and *Cystoseira barbata* accumulate mineral phosphorus to levels of 170.0–377.1 mg·kg^{-1}, a mean of (224.7 ± 55.7) mg·kg^{-1} wet weight, with accumulation factors of 15,454–92,244 units, a mean of (35,300 ± 27,800) units. According to the updated nomenclature of the family Sargassaceae Kützing, these algae species belong to the *Ericaria*-dominated phytocenosis: *Ericaria crinita* + *Gongolaria barbata* – *Cladostephus spongiosus* – *Ellisolandia elongata* (*Ericaria* sp.). In general, brown algae of coastal biotopes uptake and retain over 80% of mineral phosphorus occurring in the aquatic environment and release back only up to 16% of maximum absorbed flux daily. This highlights their critical role in conditioning the biogenic composition of waters.

Keywords: biogenic elements, macrophytobenthos, pool of mineral phosphorus in water and algae, Southwestern Crimea, Black Sea

According to experts in environmental science, excessive influx of biogenic elements has caused hypereutrophication and a decline in water quality in the Black Sea, particularly in its coastal areas. Adverse effects of hypereutrophication on the marine ecosystem induced phytoplankton blooms, hypoxia and fish kills, outbreaks of Cyanobacteria and gelatinous plankton, reduced water transparency, increased organic matter fluxes from the photosynthetic zone, and shifts in key trophic chain balance [Fiori et al., 2016; Gubanov et al., 2004; Ivanov et al., 2006; Kuftarkova et al., 2006; Mee, 1992; Oguz, Gilbert, 2007; Yunev et al., 2019; Zaitsev et al., 1989]. Despite reduced regional economic activity in the 1990s, the Black Sea ecosystem did not return to its pre-eutrophication state [Slepchuk et al., 2017; Yunev et al., 2019]. To date, research on de-eutrophication is focused on enhancing standards to mitigate marine pollution caused by excess anthropogenic organic compounds and biogenic elements. Promising strategies in this field involve using macrophytes to reduce phytoplankton primary production. In this respect, key directions are as follows:

1) developing technologies for safe intervention in natural ecosystem functioning processes to remove the excess of biogenic elements [Kompleksnaya adaptatsiya, 1985];
2) creating geochemical barriers on biopositive surfaces to limit biogenic element availability for primary production [Aleksandrov, 2008];
3) developing methods to regulate permissible pollution limits for the marine environment based on biogeochemical criteria [Egorov, 2019, 2021; Polikarpov, Egorov, 1986].

The issue of preserving the ecological state of marine natural complexes is especially critical in the Southwestern Crimea: this area is recognized by the International Union for Conservation of Nature as both a European biodiversity hotspot and a major recreational and a tourist destination [Marine Protected Areas of the Crimea, 2015]. Consequently, 31 specially protected natural areas (hereinafter SPNAs) have been established along the Crimean coast; there, economic activities are legally restricted.

Interest in natural water self-purification driven by biogeochemical mechanisms has led to the development of a semi-empirical theory of mineral metabolism in hydrobionts [Polikarpov, Egorov, 1986] and the advanced theory on radiation and chemical homeostasis of marine ecosystems [Egorov, 2019, 2021]. The application of balance-based methods of mathematical modeling, which account for biogeochemical interactions within the ecosystems, supports the hypothesis of Academician V. Vernadsky that the reproduction of living and non-living matter simultaneously sustains their habitat conditions [Vernadsky, 1965]. This has enabled the development of methods to regulate thresholds for permissible anthropogenic load based on biogeochemical criteria: ecological capacity of marine ecosystems [Polikarpov, Egorov, 1981] and their assimilative capacity [Egorov, 2019, 2021; Izrael, Tsyban, 1983].

As established, the concentration of nearly all chemical substances in both living and abiotic components of ecosystems depends on their specific content in water [Polikarpov, 1964]. Concentration functions of hydrobionts are mediated by physicochemical forms of absorbed substances, with sorption, metabolic, and trophic interactions, and also reactions of their mineral and energy metabolism. These interactions are generally governed by the principles of water mineralization, Stokes' law, Freundlich and Langmuir models, Monod equation, and Michaelis–Menten kinetics, as well as the energetic aspects of trophodynamics [Polikarpov, Egorov, 1986; Popovichev, Egorov, 2009]. As known from the literature, the primary production–limiting biogenic elements are nitrogen and phosphorus [Redfield, 1958]. According to modern concepts [Zilov, 2009], the production of 1,000 g of primary organic matter requires 80 g of carbon, 14 g of nitrogen, and 2 g of phosphorus. The limiting factor in production is the biogenic element, proportion of which is lower in the aquatic environment compared to the stoichiometric ratio N : P = 16 : 1 (molar concentration) or N : P = 7 : 1 (by mass). If the ratio exceeds this value, the system is phosphorus-limited; if it is lower, the system is nitrogen-limited. Evidently, the availability of biogenic elements for sustaining primary production depends on their dissolved forms in the aquatic environment. Their pools in other biotopes act as barriers to water eutrophication. Therefore, assessing the contribution of individual biocenoses to the formation of biogenic element pools allows for an evaluation of their barrier role in mitigating eutrophication and competitive relations of producers in coastal photic zones.

Within the framework of this study, the authors aimed to assess pools of biogenic elements in macrophytocenoses by examining the accumulation patterns of mineral phosphorus in brown algae from coastal waters of the Southwestern Crimea. The research was focused on the Streletskaya Bay (Sevastopol) inhabited by brown algae *Cystoseira crinita* and *Cystoseira barbata* listed in the Red Book of the Republic of Crimea [2015], as well as macrophytobenthos and *Ericaria*-dominated phytocenosis,

Ericaria crinita + *Gongolaria barbata* – *Cladostephus spongiosus* – *Ellisolandia elongata*, in coastal zones of SPNAs, the Sevastopol Bay, and the Crimean Peninsula. To achieve the aim, the following issues were solved:

1) to analyze the annual variation in mineral phosphorus concentrations in both the water column and brown algae *Cystoseira crinita* and *Cystoseira barbata* in the inner part of the Streletskaya Bay based on monthly monitoring of 09.04.2023–31.03.2024;
2) to identify the mechanisms regulating mineral phosphorus accumulation in the studied *Cystoseira* species in relation to its varying concentrations in algae and water;
3) to assess the vertical biomass distribution of *Ericaria* sp. *crinita* (Duby) Molinari & Guiry and *Gongolaria barbata* (Stackhouse) Kuntze in waters of SPNAs, the Sevastopol Bay, and the Crimean Peninsula;
4) to quantify mineral phosphorus pools in macrophytobenthos and evaluate its functions in extracting biogenic elements from the dissolved phase of the aquatic environment and acting as a biochemical barrier to water hypereutrophication.

MATERIAL AND METHODS

Material was sampled during hydrobiological surveys in the Streletskaya Bay (44.59597108177086°, 33.46977409556002°) in 2023–2024 and off the Southwestern Crimea (Sevastopol region) in 2015–2024 (Fig. 1).

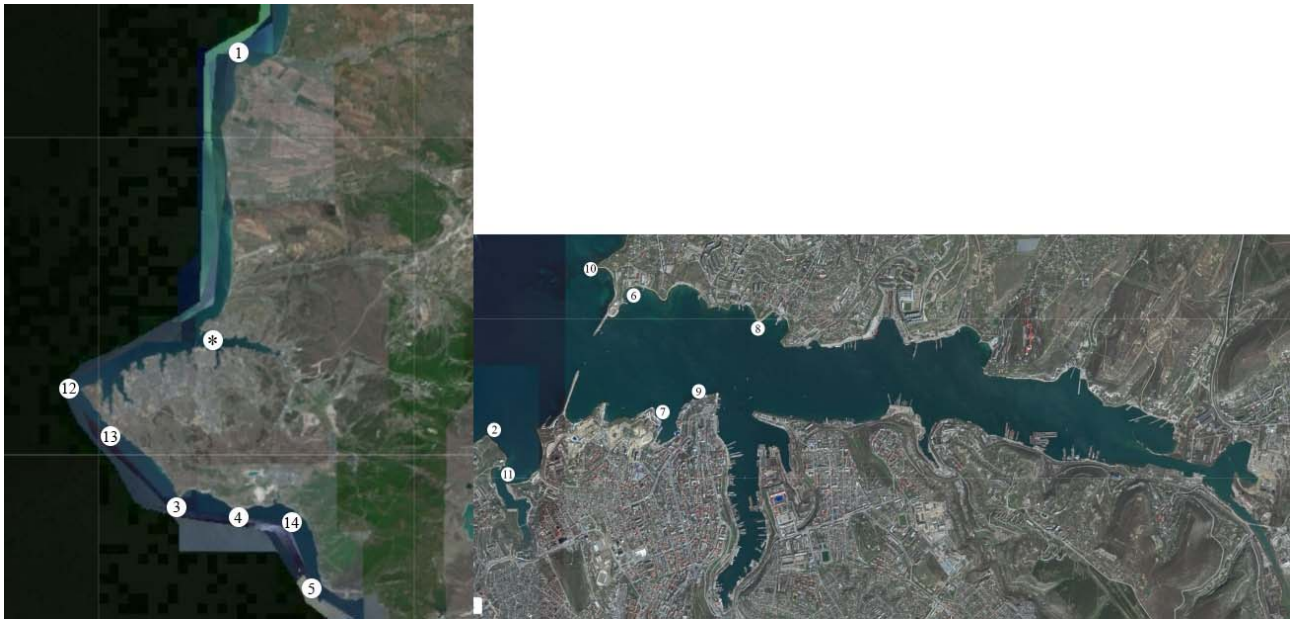

Fig. 1. Map of the location of sampling stations for the study of macrophytobenthos in the coastal zone of the Southwestern Crimea (Sevastopol region) in 2015–2021: 1, natural monument Coastal Aquatic Complex near Cape Lukull; 2, natural monument Coastal Aquatic Complex near the Chersonesus Nature Reserve; 3, natural monument Coastal Aquatic Complex near the Cape Fiolent; 4, state natural landscape reserve Karansky; 5, state natural landscape reserve Cape Aya; 6, the Konstantinovskaya Bay; 7, the Cape Khrustalny; 8, the Cape Kordon; 9, water area near the Monument to the Sunken Ships; 10, the Cape Severnaya Kosa; 11, the Karantinnaya Bay, an entrance Cape Vostochny; 12, the Cape Chersonesus; 13, the Golubaya Bay; 14, water area off the Seraya Rock (near Balaklava); 15, the Streletskaya Bay; *, stations within the Sevastopol Bay

Brown algae were sampled at depths of 1.0–1.5 m, with water temperature measured at 0.3 m using a Lowrance Hook-5 fishfinder equipped with a GPS navigator. Tidal and seiche variations in bay waters were recorded (those did not exceed 0.2–0.4 m), along with meteorological conditions. When the wind speeds exceeded 8 $m \cdot s^{-1}$ or there was precipitation, sampling was not carried out. As known [AlgaeBase, 2024], brown algae *Cystoseira crinita* and *Cystoseira barbata* have been reclassified: now, these ones are *Ericaria* sp. *crinita* and *Gongolaria* sp. *barbata*, respectively. No genus-specific differences in phosphorus metabolism were recorded for these algae. In tables with processed data and figures with mineral phosphorus concentrations, algae were reported exclusively as *Ericaria crinita*. It was assumed that variability from unaccounted hydrodynamic, meteorological, hydrochemical, and biological factors fell within the confidence intervals of parameter distributions; those were determined at a significance level of $\alpha = 0.05$.

To analyze the composition and structure of the macrophytobenthos and the *Ericaria*-dominated phytocenosis, *Ericaria crinita* + *Gongolaria barbata* – *Cladostephus spongiosus* – *Ellisolandia elongata*, and to investigate the biomass distribution of dominant and associated species, we used hydrobotanical survey data (Fig. 1) obtained during summer in the coastal zone (Fig. 2) of the Southwestern Crimea (Sevastopol region). Survey transects were laid in sites with differing land-use types: in waters within SPNAs of Sevastopol and in spots adjacent to shipping lanes and recreational areas.

Fig. 2. Biotope of *Ericaria crinita* and *Gongolaria barbata* in the coastal zone of the Southwestern Crimea (the Cape Fiolent, depth of 1 m, photo by S. Raksha)

Quantitively, macrophytobenthos was sampled along 12 hydrobotanical transects following a standardized hydrobotanical method [Kalugina-Gutnik, 1975]. At each depth (0.5, 1, 3, 5, and 10 m), a 25 × 25 cm recording frame was laid in four replicates deployed by scuba divers from the small

research vessel "Viktoriya" (IBSS). For each station, the following parameters were recorded: total projective cover (%), type of bottom sediments, and condition of benthic phytocenoses and key species populations. A total of 268 quantitative macrophytobenthic samples were processed.

Methods of macrophytobenthic sample processing. Macrophytes were rinsed with flowing seawater to remove impurities: benthic sediments and epiphytic organisms. For each sample, we established wet weight (> 0.1 g) of lithophytic species and their epiphytic synusiae, total phytomass of macrophytes (g), and number of dominant species (ind.). For each depth stratum, species-specific biomass ($g \cdot m^{-2}$) and abundance ($ind. \cdot m^{-2}$) were calculated to characterize macrophytobenthic community development and the specificity of its spatial distribution.

Macroalgae were identified in accordance with monographic references [Vinogradova, 1974; Zinova, 1967] considering updates: taxonomic revisions and nomenclatural changes [AlgaeBase, 2024]. When describing the macrophytobenthos structure, we used the classification of the Black Sea benthic vegetation established by A. Kalugina-Gutnik [1975].

Methods for hydrochemical water analysis and macroalgal chemical composition determination. For chemical analysis, we selected apical thallus branches of algae [Kompleksnaya adaptatsiya, 1985] which showed the highest physiological activity based on results of algological assessments and ^{32}P experiments [Popovichev, Egorov, 2009]. Sample preparation followed standard methods [GOST 26263-84, 1985], while mineral phosphorus content was determined according to [Metody, 1988]. Mineral phosphorus concentrations in both water and algal samples were measured in triplicate. Analyzed algal fragments consisted of the 3rd to 4th order branches. For phosphorus quantification, a 0.1 g of aliquot (prewashed, dried, and ground) was ashed in a muffle furnace at +750 °C until converted to light grey powder. An ashed sample was dissolved in 1 mL of concentrated hydrochloric acid and diluted to 100 mL with distilled water. Subsequent analysis involved the phosphomolybdenum complex and its further restoration to an intensely blue compound with maximum wave absorbance at 885 nm (Murphy–Riley method). The wet-to-dry biomass conversion factor, k, was 4.11.

Computational and statistical data processing methods. Obtained results were analyzed using ratios derived from the theory of radioisotope and chemical homeostasis of marine ecosystems [Egorov, 2021; Polikarpov, 1964]. The phosphorus accumulation factor (K_n) in *E. crinita* thalli was calculated by the following formula accounting for parameter dimensionality:

$$K_n = 1,000 \times C_{erc}/C_w\,, \tag{1}$$

where C_{erc} and C_w are concentrations of mineral phosphorus in algae ($mg \cdot kg^{-1}$ wet weight) and in water ($\mu g \cdot L^{-1}$), respectively.

Based on observational data, the relationships between parameters of the power function (C_{erc} and K_n) and the independent variable (C_w) were determined by equations:

$$C_{erc} = C_w^{\,b}$$

or

$$K_n = C_w^{\,b1}\,, \tag{2}$$

where b and b1 are indicators of degree representing process rates.

The mineral phosphorus pool (in %) in benthic phytocenoses (P_{alg}) relative to its content in aquatic environment (P_w) was estimated as follows:

$$P_{alg}(\%) = 100 \times (1 + 1/(m_{sp}1,000(C_{alg}/C_w))) \quad (3)$$

and

$$P_{alg}(\%) = 100 \times (1 + 1/(m_{sp}K_n/10^6 h)) , \quad (4)$$

where m_{sp} is *E. crinita* biomass ($g \cdot m^{-2}$ wet weight);

h is algal growth depth (m).

Data were statistically processed in Statistica 12; the standard deviation (σ) and the coefficient of determination (R^2) were calculated for hydrochemical and phytocenotic parameters. The statistical significance of regression coefficients and the linearity of dependencies were assessed using Student's *t*-test [Parchevskaya, 1969].

RESULTS AND DISCUSSION

Monitoring data on the mineral phosphorus content in surface waters and in *E. crinita* obtained from the estuarine zone of the Streletskaya Bay are detailed in Table 1.

Table 1. Results of determination of nutrient concentration in water and a brown alga *Ericaria crinita* in the Streletskaya Bay

Date	Day number of the year	Water temperature (°C)	H_2PO_4 concentration in water ± σ (μg $P \cdot L^{-1}$)	Phosphorus concentration in *E. crinita* ± σ (mg·kg^{-1} wet weight)	Phosphorus accumulation factor (K_n) in *E. crinita* (*per* wet weight)
09.04.2023	99	+13.2	3.8 ± 0.10	377.1 ± 45	99,244
28.05.2023	149	+16.0	9.0 ± 0.14	194.6 ± 23	21,627
24.06.2023	174	+20.0	7.0 ± 0.11	184.9 ± 22	26,416
24.07.2023	206	+25.3	10.5 ± 0.16	187.3 ± 22	17,872
23.08.2023	236	+25.6	6.0 ± 0.09	197.0 ± 24	32,846
14.09.2023	258	+25.3	7.0 ± 0.11	192.2 ± 23	27,459
20.10.2023	294	+23.4	6.4 ± 0.11	219.0 ± 26	34,215
22.11.2023	316	+14.1	7.0 ± 0.11	238.4 ± 29	34,063
25.12.2023	360	+11.3	7.0 ± 0.11	235.0 ± 28	35,576
18.01.2024	18	+8.8	4.0 ± 0.06	253.0 ± 30	63,260
28.02.2024	57	+9.6	14.0 ± 0.21	248.0 ± 30	17,714
31.03.2024	91	+12.5	11.0 ± 0.17	170.0 ± 20	15,454
Mean			7.7 ± 2.90	224.7 ± 27	35,300 ± 27,800

Note: σ, standard deviation.

The results of monitoring (Table 1) revealed weakly pronounced decreasing tendencies in mineral phosphorus concentrations within a year both in surface waters and in *E. crinita* from the Streletskaya Bay (see Fig. 3B, C). H_2PO_4 content in water ranged 3.8 to 14.0 μg·L^{-1}; mean values of C_w

were of (7.7 ± 2.9) μg·L^{-1}. In *E. crinita*, concentrations varied within 170.0–377.1 mg·kg^{-1} wet weight, and C_{erc} averaged (224.7 ± 55.3) mg·kg^{-1}. The phosphorus accumulation factor for this alga ranged 15,454 to 99,244; mean K_n values were of (35,300 ± 27,800).

Comparative analysis of development of macrophytobenthos and accompanying species showed as follows: regardless of location, the *Ericaria*-dominated phytocenosis reached maximum biomass values at depths of 0.5–1 m, particularly in open coastal waters (Tables 2, 3). *E. crinita* and *G. barbata* contribution to total phytocenosis biomass consistently decreased with depth, namely 1.5-fold in zones of SPNAs and coastal waters and 4.3-fold in the Sevastopol Bay (Table 3). Importantly, with a drop in *E. crinita* and *G. barbata* contribution to the total phytocenosis biomass, the role of accompanying species increased, including epiphytic synusiae. This indicated a shift in growing conditions, irradiance, water transparency, and the composition of bottom sediments. Furthermore, the combined effect of these factors largely determined the structural features and development of the macrophytobenthos in the studied areas. The greatest increase in the contribution of accompanying species with depth was recorded within a range of 5 to 10 m, especially in the areas of the Sevastopol Bay and its inner part (Table 3), where this indicator reached 61.2–95.2%.

Table 2. Changes in biomass (g·m^{-2}) of the *Ericaria*-dominated phytocenosis by depth in various areas of the coastal zone of Sevastopol (the Southwestern Crimea, 2015–2021)

Polygon	Biomass at different depths				
	0.5 m	1 m	3 m	5 m	10 m
Coastal zones of SPNAs (polygon 1)					
Natural monument Coastal Aquatic Complex near Cape Lukull	754	4,751	3,635	3,556	3,134
Natural monument Coastal Aquatic Complex near the Chersonesus Nature Reserve	1,780	2,627	3,904	2,310	751
Natural monument Coastal Aquatic Complex near the Cape Fiolent	4,445	3,480	1,892	4,461	1,995
State natural landscape reserve Karansky	6,471	8,475	4,382	3,739	1,307
State natural landscape reserve Cape Aya	5,819	3,352	1,953	4,716	3,432
The Sevastopol Bay (polygon 2)					
The Konstantinovskaya Bay, entrance cape	992	423	424	35	–
The Cape Khrustalny	745	1,224	1,310	306	13
The Cape Kordon	4,700	5,064	2,323	1.2	–
Water area near the Monument to the Sunken Ships	5,483	3,416	1,864	655	–
Open coastal waters (polygon 3)					
The Cape Severnaya Kosa	11,458	12,889	5,572	3,157	131
The Karantinnaya Bay, an entrance Cape Vostochny	7,035	5,286	4,450	1,621	702
The Cape Chersonesus	7,727	11,755	14,068	9,045	2,391
The Golubaya Bay	5,224	3,817	3,039	5,741	4,906
Water area off the Seraya Rock	8,000	5,465	8,376	3,839	3,945

Table 3. Change in biomass ($g \cdot m^{-2}$) of *Ericaria crinita*, *Gongolaria barbata*, and associated species, as well as change in their contribution (%) to biomass of the *Ericaria*-dominated phytocenosis, by depth in the coastal zone of Sevastopol (2015–2021)

Polygon	Biomass and contribution at different depths				
	0.5 m	1 m	3 m	5 m	10 m
Coastal zones of SPNAs (polygon 1)					
Natural monument Coastal Aquatic Complex near Cape Lukull	653 (86.6) / 101 (13.4)	4,588 (96.6) / 163 (3.4)	2,751 (75.7) / 884 (24.3)	2,544 (71.5) / 1,012 (28.5)	2,600 (83) / 534 (17)
Natural monument Coastal Aquatic Complex near the Chersonesus Nature Reserve	1,629 (91.5) / 151 (8.5)	2,369 (90.2) / 260 (9.8)	2,813 (72.1) / 1,091 (27.9)	1,335 (57.8) / 975 (42.2)	292 (38.9) / 459 (61.1)
Natural monument Coastal Aquatic Complex near the Cape Fiolent	4,324 (97.3) / 121 (2.7)	3,220 (92.5) / 260 (7.5)	1,266 (66.9) / 626 (33.1)	2,909 (65.2) / 1,552 (34.8)	1,376 (69) / 619 (31)
State natural landscape reserve Karansky	5,621 (86.9) / 850 (13.1)	7,603 (89.7) / 872 (10.3)	3,440 (78.6) / 942 (21.4)	2,603 (66.6) / 1,136 (33.4)	716 (54.8) / 591 (45.2)
State natural landscape reserve Cape Aya	5,016 (86.2) / 803 (13.8)	3,025 (90.2) / 327 (9.8)	1,666 (85.3) / 287 (14.7)	3,912 (83) / 804 (17)	1,537 (44.8) / 1,895 (55.2)
The Sevastopol Bay (polygon 2)					
The Konstantinovskaya Bay, entrance cape	623 (62.8) / 369 (37,2)	310 (73.4) / 113 (26.6)	185 (43.6) / 239 (56.4)	3 (9.3) / 32 (90.7)	–
The Cape Khrustalny	522 (70.1) / 223 (29.9)	980 (80.1) / 244 (19.9)	588 (44.9) / 722 (55.1)	168 (54.7) / 138 (45.3)	9 (71.7) / 4 (28.3)
The Cape Kordon	4,060 (86.4) / 640 (13.6)	4,415 (87.2) / 649 (12.8)	1,823 (78.5) / 500 (21.5)	no *Cystoseira*	–
Water area near the Monument to the Sunken Ships	4,766 (86.9) / 717 (13.1)	2,894 (84.7) / 522 (15.3)	727 (39.0) / 1,137 (61.0)	212 (32.4) / 453 (67.6)	–
Open coastal waters off Sevastopol (polygon 3)					
The Cape Severnaya Kosa	10,765 (94.0) / 693 (6.0)	12,314 (95.5) / 575 (4.5)	4,333 (77.8) / 1,239 (22.2)	2,042 (64.7) / 1,115 (35.3)	7 (5.3) / 124 (94.7)
The Karantinnaya Bay, an entrance Cape Vostochny	6,166 (87.7) / 869 (12.3)	4,883 (92.4) / 403 (7.6)	2,878 (64.7) / 1,572 (35.3)	1,035 (63.8) / 586 (36.2)	456 (65.1) / 246 (34.9)
The Cape Chersonesus	6,713 (86.9) / 1,014 (13.1)	10,658 (90.7) / 1,097 (9.3)	11,197 (79.6) / 2,871 (20.4)	6,157 (68.1) / 2,888 (31.9)	1,789 (74.8) / 602 (25.2)
The Golubaya Bay	4,384 (83.9) / 840 (16.1)	2,798 (73.3) / 1,019 (26.7)	2,301 (75.7) / 738 (24.3)	3,496 (60.9) / 2,245 (39.1)	4,243 (86.5) / 663 (13.5)
Water area off the Seraya Rock	6,943 (86.8) / 1,057 (13.2)	4,441 (81.3) / 1,024 (18.7)	5,586 (66.7) / 2,790 (33.3)	2,253 (58.7) / 1,586 (41.3)	2,203 (55.8) / 1,742 (44.2)

Note: in the numerator, the total biomass of *E. crinita* and *G. barbata* is provided, and in brackets, the proportion of these species (%) in the phytocenosis biomass is given. In the denominator, the biomass of associated species is provided, and in brackets, their contribution (%) to the phytocenosis biomass is given.

Based on mean values of the specific biomass of the phytocenosis (m_{sp}) across areas and depths, *E. crinita* and *G. barbata* contribution to it was assessed (Tables 2, 3). For these species, the mean m_{sp} values (converted to wet weight) at depths of 0.5, 1, 3, 5, and 10 m were as follows:

- in area 1, (3,853 ± 2,980), (4,537 ± 2,930), (3,153 ± 1,155), (3,756 ± 3,153), and (2,132 ± 1,151) $g \cdot m^{-2}$, respectively;
- in area 2, (2,980 ± 2,461), (2,636 ± 2,280), (1,864 ± 816), (181 ± 316), and (6 ± 3) $g \cdot m^{-2}$;

- in area 3, (7,906 ± 2,305), (7,842 ± 4,158), (7,101 ± 4,359), (4,680 ± 2,353), and (2,445 ± 2,323) $g \cdot m^{-2}$.

Contribution of *E. crinita* and *G. barbata* biomass to the specific biomass of the phytocenosis at depths of 0.5, 1, 3, 5, and 10 m was estimated as follows:

- in area 1, (89.7 ± 4.8), (81.8 ± 2.9), (75.7 ± 6.9), (68.8 ± 9.3), and (58.1 ± 18.0) %, respectively;
- in area 2, (76.5 ± 12.0), (81.3 ± 6.1), (51.5 ± 18.2), (25.0 ± 24.5), and (17.9 ± 35.8) %;
- in area 3, (87.9 ± 3.7), (86.6 ± 9.1), (72.9 ± 6.7), (63.2 ± 3.6), and (57.4 ± 31.5) %.

Involving the obtained data and applying equations (3) and (4), we established the contribution of the *Ericaria*-dominated phytocenosis to water de-eutrophication and the capacity of *E. crinita* and *G. barbata* to concentrate mineral phosphorus. The results of monthly measurements of the annual water temperature cycle and changes in the phosphorus concentration characteristics in water and in the brown algae from the inner part of the Streletskaya Bay are presented in Fig. 3.

The analysis of features of mineral phosphorus concentration in the brown algae (Fig. 3) revealed patterns related to its content in the aquatic environment. When examining the C_w and C_{alg} relationship in linear coordinates, the accumulation capacity of the brown algae was found to decrease with $R^2 = 0.193$. Student's *t*-test for the linear regression coefficient significance showed its calculated value, $t_{obs} = 1.54$, to be below the critical one, $t_{cr} = 2.228$, at the significance level of $\alpha = 0.05$ (with $n - 2 = 10$ degrees of freedom). Consequently, the observed decreasing tendency in algal mineral phosphorus concentration with rising aquatic content was statistically insignificant.

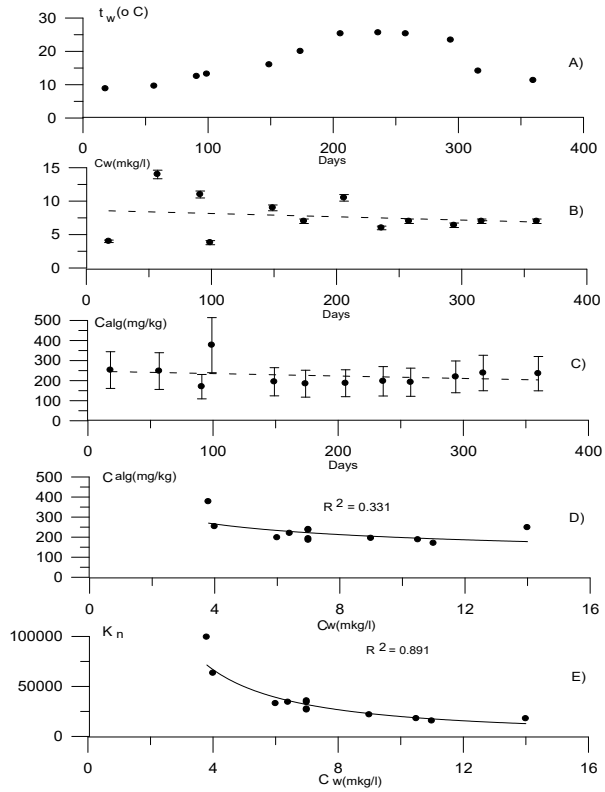

Fig. 3. Changes in temperature (A), concentration of mineral phosphorus in the surface layer of water (B) and in brown algae (C), and dependence of concentration (D) and accumulation coefficients (E) of mineral phosphorus by algae in the Streletskaya Bay (2023–2024)

The data plotted on double logarithmic axes, corresponding to a power-law dependence between C_w and C_{alg}, are presented in Fig. 3D. In this case, the correlation between mineral phosphorus concentrations in water and in *E. crinita* was characterized by a coefficient of determination $R^2 = 0.331$. For this function, the parameters of Student's *t*-test were as follows: the calculated value, t_{obs}, was 2.224, and its critical value, t_{cr}, was 1.812 (at $\alpha = 0.100$). These results were interpreted from the perspective of a type II error [Nalimov, 1971], *i. e.*, the probability of rejecting the hypothesis that a power function reliably describes the experimental observations. The analysis indicated as follows: in 90% of cases, the sample parameters of the power-law dependence between C_w and C_{alg} shown in Fig. 3D fell within the range of parameter scatter for the general population.

Data analysis on the change in the algae concentrating function, expressed *via* accumulation factors (K_n), showed that the relationship between C_w and K_n was described by a linear regression equation

with $R^2 = 0.562$. This relationship corresponds to $t_{obs} = 3.567$ (higher than $t_{cr} = 2.228$). Accordingly, it can be considered significant at $\alpha = 0.05$. A comparison of the linearity index ($\xi = 0.439$) of this function with its error estimate ($O_\xi = 0.209$) demonstrated that the relationship between C_w and K_n is non-linear. However, it (see Fig. 3E) can be approximated by a power function with high statistical significance ($R^2 = 0.891$):

$$K_n = 417,000 C_w^{-1.321}. \quad (5)$$

This function was further applied to determine the mineral phosphorus pool in the algae.

Based on calculations by formula (4), the mineral phosphorus pools in the *Ericaria*-dominated phytocenosis and in *E. crinita* specifically were determined (Table 4). These values are presented relative to the total phosphorus content under 1 m^2 of the water column, incorporating the scatter of the accumulation factor values (Table 1).

Table 4. Changes in the mean proportion of mineral phosphorus pool (%) (the numerator) and its range (the denominator) in the biomass of the *Ericaria*-dominated phytocenosis by depth in the coastal zone of Sevastopol (2015–2021)

Polygon	Depth, m				
	0.5	1	3	5	10
1, coastal zones of SPNAs	99.5 / 99.2–99.9	99.9 / 99.6–99.8	96.1 / 94.2–99.1	95.6 / 92.1–98.7	86.1 / 76.7–95.5
2, the Sevastopol Bay	99.3 / 98.7–99.8	98.5 / 97.8–99.7	91.5 / 85.6–97.5	84.7 / 74.4–94.9	78.0 / 64.0–92.0
3, open coastal waters	99.8 / 99.5–99.9	99.5 / 99.2–99.9	98.5 / 97.4–99.6	96.7 / 93.6–99.9	77.1 / 78.9–96.0

Note: numbers and names of polygons correspond to those in Tables 2, 3.

The data presented in Table 4 evidence for the fact that the highest phosphorus pool values and its most pronounced decrease were observed in open coastal waters: 99.5% at a depth of 0.5 m and 77.1% at 10 m. The pool dropped in water areas from the upper to middle sublittoral zone (from 0.5 to 10 m). The data in Table 4 indicate as follows: in a depth range down to 10 m, the *Ericaria*-dominated phytocenosis can almost completely extract mineral phosphorus from the aquatic environment, thereby limiting its availability for other primary producers.

Nearly all macrophytic communities in the Crimea have coastal and dynamic boundaries. The content of biogenic elements in these areas is governed by both biogeochemical factors and external effects. *Via* biogeochemical processes, biogenic elements are extracted from dissolved state and concentrated in living and abiotic components of ecosystems thus acquiring densities differing from seawater's specific density and becoming incorporated into biogeochemical cycles which involve their turnover, coastal deposition, and elimination into aquatic and geological reservoirs. Experimental studies using radioactive ^{32}P labeling have shown that phosphorus exchange kinetics in *E. crinita* follows a compartmental model, according to which algal uptake of mineral phosphorus from water environment follows Michaelis–Menten equation [Patton, 1968], and its lifetime excretion is described by first-order metabolic reactions [Popovichev, Egorov, 2009]. *E. crinita* maintains phosphorus pools, dynamics of which depends on the volume–mass ratios of branches of different orders and which exchange at varying rates. Thus, the mean phosphorus exchange rate in this species was 0.16 day^{-1}, and the phosphorus turnover period was approximately 6 days.

The influx of biogenic elements *via* precipitation, slope runoff, and river discharge can alter chemical limitation characteristics in primary production processes [Egorov et al., 2023]. Advective processes and the Rim Current with velocity up to 1 $m \cdot s^{-1}$ facilitate biogenic element exchange with adjacent areas and open waters [Egorov et al., 2018]. Macrobiocenoses function as open systems, where steady-state concentrations of dissolved biogenic elements are determined by the balance between input and elimination fluxes. This equilibrium results from the combined effect of all the accounted and unaccounted factors. In this context, effective application of biogeochemical criteria requires either assessment of dissolved nutrient thresholds leading to water hypereutrophication or development of regulatory standards for maximum permissible input fluxes, particularly in areas with high recreational or touristic value. It is known that power functions of the type (2) are widely used to describe biogeochemical interactions between biotic and abiotic components with radioactive and chemical substances of marine environment. When parameters b and b1 are positive, the power function corresponds to the Freundlich equation characterizing sorption saturation in solids. With negative values of b and b1, the equation (2) reflects concurrent sorption and metabolic processes. Asymptotic estimates of K_n and C_{alg} values calculated *via* equation (2) as functions of C_w enable prediction of water self-purification capacity limits [Egorov, 2021]. Therefore, the data presented in this study constitute a phase of research aimed at investigating the sequestration of mineral phosphorus by macrophytocenoses as a factor determining their role as a barrier to water de-eutrophication, and also a parametric database for utilizing biogeochemical criteria to regulate the maximum permissible flows of anthropogenic effect.

Conclusions:

1. At mineral phosphorus concentrations in water of 3.8–10.5 $\mu g \cdot L^{-1}$, a brown alga *Ericaria crinita* accumulates it within a range of 170.0–377.1 $mg \cdot kg^{-1}$ wet weight, with a mean value of (224.7 ± 55.7) $mg \cdot kg^{-1}$; accumulation factor values range 15,454 to 92,244 units, with a mean of (35,300 ± 27,800). The concentrating capacity of perennial brown algae, expressed as K_n, decreases with rising mineral phosphorus content in the aquatic environment. This relationship follows a power function with a negative exponent indicating the rate of decrease. The strength of the dependence between the mineral phosphorus concentration in water C_w and the accumulation factor K_n is characterized by a high coefficient of determination: $R^2 = 0.891$. The probability of rejecting the hypothesis of a power-law relationship between the mineral phosphorus concentration in water and in algae is 90%.
2. The mineral phosphorus pool within the *Ericaria*-dominated phytocenosis dropped with depths 0.5 to 10.0 m in all investigated areas: in zones of specially protected natural areas, from 99.5 to 86.1%; in the Sevastopol Bay, from 99.3 to 78.0%; and in open coastal waters, from 96.8 to 77.1%. In general, this phytocenosis absorbs and retains over 80% of the mineral phosphorus occurring in the water column, while releasing back only up to 16% of maximum absorbed flux daily.
3. The perennial *Ericaria*-dominated phytocenosis that prevails off the Southwestern Crimea can extract mineral phosphorus almost completely from the aquatic environment, thereby limiting its availability for other producers. This study is the first to reveal its significant role in sequestering mineral phosphorus in the Black Sea waters off the coast of the Southwestern Crimea.
4. These results can be used to develop measures for improving coastal water quality in the context of intensifying natural resource use. Moreover, they can help in forecasting probable changes in coastal ecosystems under increasing anthropogenic load and other adverse factors, particularly those arising from the development of industrial, transport, recreational, and other zones along the Russian coast of the Black Sea.

This work was carried out within the framework of IBSS state research assignment "Study of biogeochemical patterns of radioecological and chemoecological processes in the ecosystems of water bodies of the Sea of Azov–Black Sea Basin in comparison with other areas of the World Ocean and individual aquatic ecosystems of their drainage basins to ensure sustainable development in the southern seas of Russia" (No. 124030100127-7) and "Biodiversity as the basis for the sustainable functioning of marine ecosystems, criteria and scientific principles for its conservation" (No. 124022400148-4).

REFERENCES

1. Aleksandrov B. G. *Gidrobiologicheskie osnovy upravleniya sostoyaniem pribrezhnykh ekosistem Chernogo morya.* Kyiv : Naukova dumka, 2008, 343 p. (in Russ.)
2. Vernadsky V. I. *Khimicheskoe stroenie biosfery Zemli i ee okruzheniya.* Moscow : Nauka, 1965, 374 p. (in Russ.)
3. Vinogradova K. L. *Ul'vovye vodorosli (Chlorophyta) morei SSSR.* Leningrad : Nauka, Leningr. otd-nie, 1974, 166 p. (in Russ.)
4. GOST 26263-84. *Pochvy. Metody opredeleniya valovogo fosfora i valovogo kaliya* : gosudarstvennyi standart Soyuza SSR : utverzhden i vveden v deistvie Postanovleniem Gosudarstvennogo komiteta SSSR po standartam ot 21.08.1984 No. 2939 : vveden vpervye : data vvedeniya 1985-07-01 / podgotovlen Ministerstvom sel'skogo khozyaistva SSSR. Moscow : Izdatel'stvo standartov, 1985, 11 p. (in Russ.)
5. Gubanov V. I., Mal'chenko Yu. A., Kuftarkova E. A., Kovrigina N. P. Diagnosis of modern state of coastal water near Sevastopol (the Black Sea) according to monitoring of chemical parameters. *Ekologicheskaya bezopasnost' pribrezhnoi i shel'fovoi zon i kompleksnoe ispol'zovanie resursov shel'fa*, 2004, iss. 10, pp. 141–148. (in Russ.). https://elibrary.ru/ymtpgd
6. Egorov V. N. *Theory of Radioisotope and Chemical Homeostasis of Marine Ecosystems.* Sevastopol : IBSS, 2019, 356 p. (in Russ.). https://doi.org/10.21072/978-5-6042938-5-0
7. Egorov V. N., Plugatar Yu. V., Malakhova L. V., Mirzoeva N. Yu., Gulin S. B., Popovichev V. N., Sadogurskii S. E., Malakhova T. V., Shchurov S. V., Proskurnin V. Yu., Bobko N. I., Marchenko Yu. G., Stetsyuk A. P. Ekologicheskoe sostoyanie akvatorii osobo okhranyaemoi prirodnoi territorii "Mys Mart'yan" i problema realizatsii ee ustoichivogo razvitiya po faktoram evtrofikatsii, radioaktivnogo i khimicheskogo zagryazneniya vod. In: *Sokhranenie biologicheskogo raznoobraziya i zapovednoe delo v Krymu* : materialy nauchno-prakticheskoi konferentsii s mezhdunarodnym uchastiem, Yalta, 23–26 oktyabrya 2018 g. Yalta, 2018, pp. 36–40. (Nauchnye zapiski prirodnogo zapovednika "Mys Mart'yan" ; iss. 9). (in Russ.). https://doi.org/10.25684/NBG.scnote.009.2018.04
8. Egorov V. N., Mirzoyeva N. Yu., Artemov Yu. G., Proskurnin V. Yu., Stetsiuk A. P., Marchenko Yu. G., Evtushenko D. B., Moseichenko I. N., Chuzhikova-Proskurnina O. D. The possibility of implementation of the sustainable development concept for the recreational coastline of Yalta city regarding biogenic elements, radionuclides, heavy metals, and organochlorine compounds (Crimea, Black Sea). *Marine Biological Journal*, 2023, vol. 8, no. 3, pp. 12–32. https://elibrary.ru/yhovfn
9. Zaitsev Yu. P., Garkavaya G. P., Nesterova D. A., Polishchuk L. N. The Danube as a basic source of the Black Sea

eutrophication. *Gidrobiologicheskii zhurnal*, 1989, vol. 25, no. 4, pp. 21–23. (in Russ.)
10. Zilov E. A. *Gidrobiologiya i vodnaya ekologiya (organizatsiya, funktsionirovanie i zagryaznenie vodnykh ekosistem).* Irkutsk : Izd-vo Irkutskogo gos. un-ta, 2009, 147 p. (in Russ.). https://elibrary.ru/qkspbj
11. Zinova A. D. *Opredelitel' zelenykh, burykh i krasnykh vodoroslei yuzhnykh morei SSSR.* Moscow ; Leningrad : Nauka, 1967, 400 p. (in Russ.)
12. Ivanov V. A., Ovsyany E. I., Repetin L. N., Romanov A. S., Ignatyeva O. G. *Hydrological and Hydrochemical Regime of the Sebastopol Bay and Its Changing Under Influence of Climatic and Anthropogenic Factors* / NAS of Ukraine, Marine Hydrophysical Institute. Sevastopol, 2006, 90 p. (in Russ.). https://elibrary.ru/yriouu
13. Izrael Iu. A., Tsyban A. V. On the assimilation capacity of the World Ocean. *Doklady Akademii nauk SSSR*, 1983, vol. 272, no. 3, pp. 702–704. (in Russ.)
14. Kalugina-Gutnik A. A. *Fitobentos Chernogo morya.* Kyiv : Naukova dumka, 1975, 248 p. (in Russ.). https://repository.marine-research.ru/handle/299011/5645
15. *Kompleksnaya adaptatsiya tsistoziry k gradientnym usloviyam: nauchnye i prikladnye problemy* / S. A. Kovardakov, A. V. Prazukin, Yu. K. Firsov, A. E. Popov. Kyiv : Naukova dumka, 1985, 216 p. (in Russ.). https://repository.marine-research.ru/handle/299011/8319
16. *Red Book of the Republic of Crimea. Plants, Algae, and Fungi* / A. V. Yena, A. V. Fateryga (Eds). Simferopol : ARIAL, 2015, 480 p. (in Russ.). https://elibrary.ru/wxeqef
17. Kuftarkova E. A., Gubanov V. I., Kovrigina N. P., Eremin I. Yu., Senicheva M. I. Ecological assessment of modern state of waters in the region of interaction of the Sevastopol Bay and part of the sea contiguous to it. *Morskoj ekologicheskij zhurnal*, 2006, vol. 5, no. 1, pp. 72–91. (in Russ.). https://repository.marine-research.ru/handle/299011/851
18. *Metody gidrokhimicheskikh issledovanii osnovnykh biogennykh elementov.* Moscow : VNIRO, 1988, 119 p. (in Russ.)
19. *Marine Protected Areas of the Crimea. Scientific Handbook* / N. A. Milchakova, V. V. Aleksandrov, L. V. Bondareva, T. V. Pankeeva, E. B. Chernysheva / N. A. Milchakova (Ed.). Simferopol : N.Orianda, 2015, 312 p. (in Russ.). https://repository.marine-research.ru/handle/299011/1399
20. Nalimov V. V. *Teoriya eksperimenta.* Moscow : Nauka, 1971, 207 p. (in Russ.). https://elibrary.ru/rxymdy
21. Patton A. R. *Biochemical Energetics and Kinetics* : transl. from Engl. by Z. F. Bogautdinov. Moscow : Mir, 1968, 159 p. (in Russ.)
22. Parchevskaya D. S. *Statistika dlya radioekologov (prakticheskoe rukovodstvo po statistike i planirovaniyu eksperimentov v radioekologii).* Kyiv : Naukova dumka, 1969, 114 p. (in Russ.). https://repository.marine-research.ru/handle/299011/1109
23. Polikarpov G. G. *Radioekologiya morskikh organizmov.* Moscow : Atomizdat, 1964, 295 p. (in Russ.). https://repository.marine-research.ru/handle/299011/12748
24. Polikarpov G. G., Egorov V. M. Zdatnist' mors'kykh ekosystem do vydalennya radioaktyvnykh i khimichnykh zabrudnen' z fotychnogo sharu. *Visnyk AN URSR*, 1981, no. 2, pp. 73–81. (in Ukr.). https://repository.marine-research.ru/handle/299011/11224
25. Polikarpov G. G., Egorov V. N. *Morskaya dinamicheskaya radiokhemoekologiya.* Moscow : Energoatomizdat, 1986, 176 p. (in Russ.). https://repository.marine-research.ru/handle/299011/7683

26. Popovichev V. N., Egorov V. N. Kinetic regularities of exchange of phosphorus by the Black Sea brown seaweed *Cystoseira barbata*. *Morskoj ekologicheskij zhurnal*, 2009, vol. 8, no. 1, pp. 55–66. (in Russ.). https://repository.marine-research.ru/handle/299011/1000
27. Yunev O. A., Konovalov S. K., Velikova V. *Anthropogenic Eutrophication in the Black Sea Pelagic Zone: Long-term Trends, Mechanisms, Consequences* / A. O. Kovalevsky Institute of Biology of the Southern Seas of RAS ; Marine Hydrophysical Institute of RAS. Moscow : GEOS, 2019, 164 p. (in Russ.). https://repository.marine-research.ru/handle/299011/7989
28. Egorov V. N. *Theory of Radioisotopic and Chemical Homeostasis of Marine Ecosystems.* Cham, Switzerland : Springer, 2021, 320 p. https://doi.org/10.1007/978-3-030-80579-1
29. Fiori E., Zavatarelli M., Pinardi N., Mazziotti C., Ferrari C. R. Observed and simulated trophic index (TRIX) values for the Adriatic Sea basin. *Natural Hazards and Earth System Sciences*, 2016, vol. 16, iss. 9, pp. 2043–2054. https://doi.org/10.5194/nhess-16-2043-2016
30. *AlgaeBase.* World-wide electronic publication, National University of Ireland, Galway / M. D. Guiry, G. M. Guiry (Eds) : [site], 2024. URL: http://www.algaebase.org [accessed: 09.10.2024].
31. Mee L. D. The Black Sea in crisis: A need for concerted international action. *Ambio*, 1992, vol. 21, pp. 278–286.
32. Oguz T., Gilbert D. Abrupt transitions of the top-down controlled Black Sea pelagic ecosystem during 1960–2000: Evidence for regime-shifts under strong fishery exploitation and nutrient enrichment modulated by climate-induced variations. *Deep Sea Research Part I: Oceanographic Research Papers*, 2007, vol. 54, iss. 2, pp. 220–242. https://doi.org/10.1016/j.dsr.2006.09.010
33. Redfield A. C. The biological control of chemical factors in the environment. *American Scientist*, 1958, vol. 46, no. 3, pp. 205–221.
34. Slepchuk K. A., Khmara T. V., Man'kovskaya E. V. Comparative assessment of the trophic level of the Sevastopol and Yuzhnaya bays using E-TRIX index. *Physical Oceanography*, 2017, no. 5, pp. 60–70. http://doi.org/10.22449/1573-160X-2017-5-60-70

МАКРОФИТОЦЕНОЗЫ КАК БИОГЕОХИМИЧЕСКИЕ БАРЬЕРЫ ГИПЕРЭВТРОФИКАЦИИ ВОД МИНЕРАЛЬНЫМ ФОСФОРОМ В АКВАТОРИЯХ ЮГО-ЗАПАДНОГО КРЫМА

В. Н. Егоров, Н. А. Мильчакова, Н. И. Бобко, Ю. Г. Марченко

ФГБУН ФИЦ «Институт биологии южных морей имени А. О. Ковалевского РАН»,
Севастополь, Российская Федерация
E-mail: *egorov@ibss-ras.ru*

Цель работы заключалась в изучении особенностей концентрирования минерального фосфора занесёнными в Красную книгу Республики Крым бурыми водорослями *Cystoseira crinita* и *Cystoseira barbata* и в оценке роли макрофитобентоса прибрежной экосистемы Юго-Западного Крыма в создании биогеохимических барьеров, регулирующих конкурентные отношения продуцентов за биогенные элементы. Определено, что *Cystoseira crinita* и *Cystoseira barbata* концентрируют минеральный фосфор до уровней 170,0–377,1 мг·кг$^{-1}$, в среднем (224,7 ± 55,7) мг·кг$^{-1}$ сырой массы, с коэффициентами накопления 15 454–92 244 единицы, в среднем (35 300 ± 27 800).

По новой номенклатуре семейства Sargassaceae Kützing, эти виды водорослей входят в состав эрикариевого фитоценоза *Ericaria crinita* + *Gongolaria barbata* – *Cladostephus spongiosus* – *Ellisolandia elongata* (*Ericaria* sp.). В целом бурые водоросли прибрежных биотопов поглощают и задерживают свыше 80 % объёма минеральных форм фосфора, содержащихся в водной среде, и ежедневно возвращают в неё лишь до 16 % его максимально поглощаемого потока, что является значимым фактором кондиционирования биогенного состава вод.

Ключевые слова: биогенные элементы, макрофитобентос, пул минерального фосфора в воде и водорослях, Юго-Западный Крым, Чёрное море

1871
ИнБЮМ – IBSS

Морской биологический журнал
Marine Biological Journal
2025, vol. 10, no. 2, pp. 18–33
https://marine-biology.ru

UDC 574.587(265.54.04)

INTERANNUAL CHANGES IN THE STRUCTURE OF MEIOBENTHOS IN SANDY SHALLOWS OF THE TRIOZERYE BAY (SEA OF JAPAN)

© 2025 **A. Karpova[1,2] and N. Fadeeva[1]**

[1]Far Eastern Federal University, Vladivostok, Russian Federation
[2]A. V. Zhirmunsky National Scientific Center of Marine Biology, FEB RAS, Vladivostok, Russian Federation
E-mail: *lyuney@gmail.com*

Received by the Editor 31.05.2024; after reviewing 07.07.2024;
accepted for publication 20.03.2025.

This paper is the first one to provide results of the study on the dynamics of biological parameters of the meiobenthos within the coastal strip of sandy sediments in the Triozerye Bay (Sea of Japan) in July–August 2021–2023. During the investigation, 20 taxa of the meiofauna were registered, with the basis formed by representatives of Harpacticoida, Nematoda, Copepoda, Turbellaria, Gastrotricha, Annelida, Halacaridae, and Ostracoda. The nematofauna mostly covered free-living nematodes *Daptonema normandicum*, *Enoplolaimus pectinatus*, *Metadesmolaimus innii*, and *Parascolaimus proprius*. In general, the structure of qualitative and quantitative indicators of meiobenthos and nematofauna changed annually due to fluctuations in the grain size distribution of bottom sediments.

Keywords: Sea of Japan, interannual changes, grain size distribution, organic matter, meiobenthos, nematofauna

Information on coastal ecosystems of the Sea of Japan shoreline is still scarce. While the taxonomic composition and distribution of meiobenthos in relation to environmental factors have been studied in several areas of Peter the Great Bay [Pavlyuk, 2004; Smirnova, Fadeeva, 2012; Trebukhova, Pavlyuk, 2006; *etc.*], the structural organization and spatial and temporal variability of interstitial communities in low-tidal beaches dominated by wave action have been poorly investigated [Fadeeva, 1991; Smirnova, Fadeeva, 2012].

In the upper subtidal zone, in open bays, bottom sediments are formed under active hydrodynamics (both wave action and current-related) and are characterized by intensive water exchange with the open sea. On sandy shores, an environment of high physical stress for marine fauna is formed; consequently, relatively few species inhabit this unique transitional ecosystem laying between terrestrial and marine habitats. At first sight, sandy beaches appear lifeless, resembling 'biological deserts'; however, rich meiobenthic communities are formed in interstitial areas.

The Triozerye Bay, an open and sandy one, is known for its three freshwater lakes bordering saline waters. It is a popular beach destination in summer. It is located in the southeastern Primorye, in the Partizansky District, along the western coast of the Sea of Japan (see Fig. 1). Several marine biological studies carried out in the Triozerye Bay were focused only on some macrobenthic species and abundant macrophytes [Kulepanov et al., 2023].

The aim of this work is to examine interannual variations in the density of meiobenthic and nematode communities in the upper subtidal zone (at depths down to 1 m) of open shallows in the Triozerye Bay in 2021–2023 in relation to environmental conditions.

MATERIAL AND METHODS

The study area was the Triozerye Bay: a shallow sandy open site in the western Sea of Japan. Its central part is dominated by the dome-shaped landscapes extending from the northeast. Those are bordered by extensive arenoid fields. To the northwest, those are bordered by the littoral zone; to the north, by concizium; and to the southwest, by landscapes adjacent to a group of rocks [Arzamastsev, Preobrazhensky, 1990; Preobrazhensky et al., 2000]. A sandy beach stretches for over 1.5 km. Three lakes near the bay are located 200 m from the shoreline; those do not affect directly water conditions. The mean salinity ranges 30 to 33‰.

The morphometric index determining the degree of a bay openness was established as the ratio of depth of the bay's incision into the land to the distance between the entrance capes [Manuilov, 1990]. This index was calculated using the 'ruler and planimeter' tool in a mapping service Yandex.Maps (https://yandex.ru/maps). A schematic map was built using Ocean Data View software package and Yandex.Maps.

The investigation was carried out in July–August 2021–2023 (at temperature of +18.5…+24 °C) in the Triozerye Bay (the Sea of Japan) (Fig. 1), within a depth range of 0.5–1.0 m.

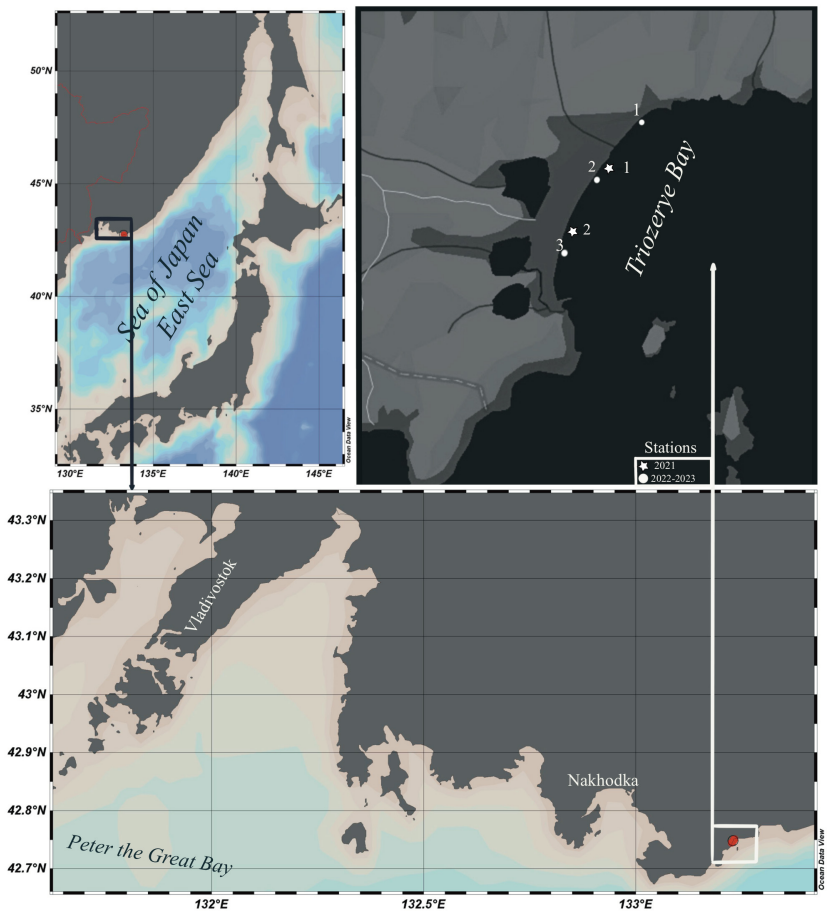

Fig. 1. Scheme map of the Triozerye Bay study area. White dots mark stations 1, 2, and 3 of 2022–2023 (st1_22, st2_22, and st3_22 in 2022; st1_23, st2_23, and st3_23 in 2023). White stars mark stations 1 and 2 of 2021 (st1_21 and st2_21). Sources: Ocean Data View and Yandex.Maps

Over the study period, 24 samples were collected in the Triozerye Bay: on 19 August, 2021, 6 samples at two stations; on 19 July, 2022, and 10 August, 2023, 9 samples at three equally spaced stations. Weather data for the sampling periods were obtained from an open-source archive [Arkhivy pogody, 2024]. Alongside the quantitative sampling, we sampled material to analyze organic matter content and grain size distribution of sediments.

Bottom sediments were sampled with a tubular corer with an inner diameter of 2.2 cm and a sediment column height of 5 cm. The core cross-sectional area was 3.8 cm^2. Grain size was analyzed by the standard sieve method [Petelin, 1967], and the obtained data were classified according to the dominant grain fraction [GOST 12536-2014, 2015]. Organic matter content was determined following the State Standard 26213-91: carbon content was assessed by wet combustion by the Tyurin method [GOST 26213-91, 1992]. Meiobenthic organisms were extracted from sediments by a standard method using sieves with mesh sizes of 32–40 μm and fixed in filtered seawater with buffered 4% formaldehyde.

All meiobenthos was counted and taxonomically classified. Species identification of nematodes and measurements of key morphological parameters (body length and maximum diameter) were carried out under a stereo microscope Axio Imager applying AxioVision software v4.8.

To characterize the taxocene structure of meiobenthos and nematodes, we calculated the Shannon index (H), the Margalef index (D_{Mg}), the Pielou index (E), and the Simpson index ($1 - D$). Estimations and similarity analysis between the sampling stations were carried out applying the Bray–Curtis dissimilarity (PRIMER v6), while correlation analysis involved Pearson coefficient (PAST 4.04). The trophic structure of the Nematoda community was preliminarily evaluated based on W. Wieser's classification [1953] categorizing nematodes according to their buccal cavity morphology.

Index of Trophic Diversity, *ITD*, was calculated by the formula:

$$ITD = g_1^2 + g_2^2 + ... + g_n^2 ,$$

where g is the relative contribution of each trophic group to the total number of individuals;

n is the number of trophic groups [Heip et al., 1985].

In literature, the more common form is $1 - ITD$, where the value ranges 0 to 0.75.

The biomass (M) of nematodes was determined by the formula:

$$M = V \times p \times N ,$$

where V is volume of organisms;

p is specific density (1.13 $mg \cdot m^{-3}$ for Nematoda);

N is the number of organisms *per* 1 m^2.

The volume (V) of organisms was calculated in accordance with the formula:

$$V = k \times L \times w ,$$

where k is the conversion factor (530 for Nematoda);

w is the maximum body width;

L is the body length [Chislenko, 1968].

Qualitatively, the community was assessed applying the ABC method (Abundance–Biomass Comparison) based on plotting two cumulative curves – the abundance and biomass ones:

$$ABC_{index} = \sum_{i=1}^{N}(B_i - A_i)\ ,$$

where B_i and A_i are cumulative values of relative biomass and abundance of the *i*-th species, %;

N is the number of species.

If the index value is positive, communities are considered undisturbed; if it is negative, those are under stressful conditions; and if value is close to zero, those experience minor or negligible effects. To have more data and to compare ABC curves, we calculated Clarke's *W* statistics [Clarke, 1990]. It assesses the area between two cumulative curves – the biomass and abundance ones:

$$W = \frac{\sum(B_i - A_i)}{[50(S-1)]}\ ,$$

where B_i are accumulated biomass values for the *i*-th ranked species;

A_i are accumulated abundance values for the *i*-th ranked species;

S is the number of species.

W statistics defines the ABC effect and ranges −1 to +1. Its value approaches −1 in highly disturbed communities and +1 in undisturbed ones (PRIMER v6).

To fully characterize the grain size distribution of sediments, the percentage content of grain fractions of certain size was calculated. Then, the median (mean grain size, Md), sorting coefficient (S_0), and asymmetry coefficient (S_k) were established. These coefficients were determined by constructing cumulative curves from which quartile values were derived. The degree of sediment sorting S_0 was evaluated according to P. D. Trask [1932]: well sorted sediments (S_0 = 1.0…1.58), moderately sorted (S_0 = 1.58…2.12), and poorly sorted (S_0 > 2.12).

For multivariate assessment of communities, cluster analysis and non-metric multidimensional scaling were applied. Station clustering was performed using the Bray–Curtis dissimilarity (PRIMER v6). Univariate parametric correlation coefficients were calculated between numerical environmental parameters, meiofaunal density, biomass of nematodes, and various diversity indices. The relationship between the environmental variables and the structure of meiofaunal and Nematoda community was examined using the BEST procedure with Spearman's rank correlation coefficient (PRIMER v6).

Statistical analysis was carried out using MS Office Excel, PRIMER v6, and PAST 4.04 software packages.

RESULTS

The Triozerye Bay features active hydrodynamic regime and absence of silts, with a morphometric index of 0.2; this allows for classifying it as an open-type bay. According to [Arkhivy pogody, 2024] data for Nakhodka city district, during sampling in August 2021 and July 2022, weather conditions were similarly moderate. In both periods, the sea was calm; there was no precipitation; and air temperature ranged +25…+32 °C. During the first decade of August 2023, strong wind gusts, up to 13 $m \cdot s^{-1}$, occurred intermittently. From the beginning of the month until the sampling day, cloud cover prevailed,

10/10, with air temperature not exceeding +23 °C; precipitation was recorded daily. On 10 August, 2023, rainfall reached 27 mm *per* day (a heavy rain occurred). In August 2023 (during sampling), the water temperature in the Triozerye Bay was lower than +18 °C.

Over the three years, the composition of bottom sediments changed. Specifically, the proportion of coarse particles increased. The predominant fractions shifted from fine sand in 2021 to medium and coarse sand in 2022 and to medium gravel at st1_23 in 2023. Cumulative curves (Fig. 2) clearly illustrate the differences in composition in 2021 and 2023.

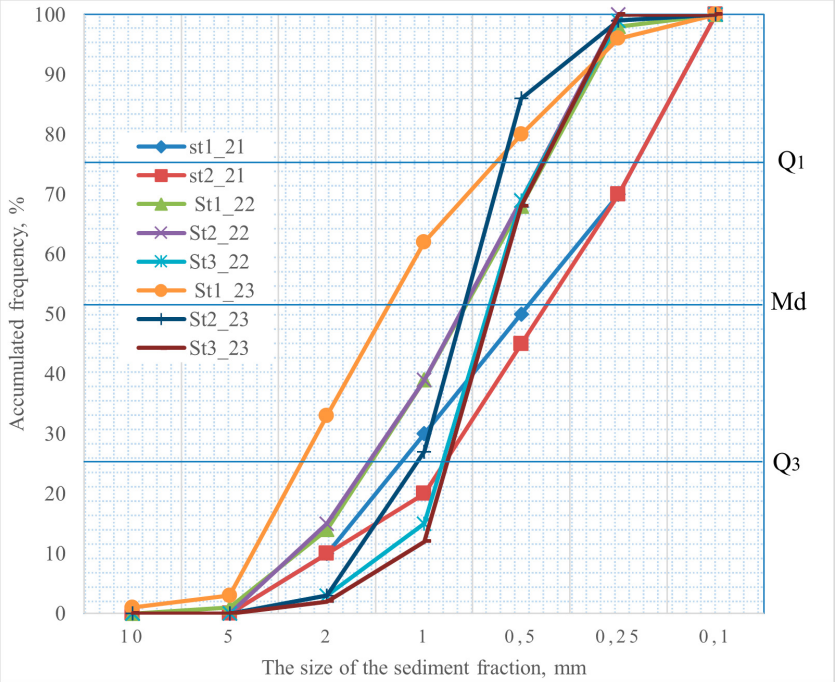

Fig. 2. Cumulative curves of the grain size distribution of bottom sediments in the Triozerye Bay in 2021–2023

Despite low organic matter content recorded in bottom sediments at all the stations in 2021–2023, there was a gain in its concentration from 0.03 to 0.08% within this period (Table 1).

Table 1. Characteristics of the stations: parameters of the grain size distribution of bottom sediments (S_0, sorting coefficient; S_k, asymmetry coefficient; Md, mean grain size of sediments) and organic matter content (C_{org}, %)

Station	S_0	S_k	Md	Sorting characteristics [Trask, 1932]	Predominant fraction, mm [Bezrukov, Licitzin, 1960]		C_{org}, %
st1_21	2.54	0.45	0.75	poorly sorted	0.25–0.01	fine sand	0.03
st2_21	2.12	0.9	0.45	moderately sorted	0.25–0.01	fine sand	0.03
st1_22	2.06	1.06	0.8	moderately sorted	0.5–0.25	medium sand	0.05
st2_22	2.06	1	0.8	moderately sorted	0.5–0.25	medium sand	0.05
st3_22	1.4	0.88	0.6	well sorted	1–0.5	coarse sand	0.05
st1_23	1.96	0.84	1.5	moderately sorted	5–2	medium gravel	0.05
st2_23	1.3	0.9	0.8	well sorted	1–0.5	coarse sand	0.08
st3_23	1.4	0.9	0.6	well sorted	1–0.5	coarse sand	0.05

During investigations in the Triozerye Bay in 2021–2023, a total of 20 meiofaunal taxa were identified. The interstitial community was primarily formed by Harpacticoida, Nematoda, Copepoda, Turbellaria, Gastrotricha, Annelida, Halacaridae, and Ostracoda (Fig. 3). The number of taxa *per* station ranged 9 to 12. In 2022 and 2023, 13 taxa were recorded in the bay, and in 2021, 14 taxa were noted.

The dominant taxa varied throughout the study period (Fig. 3). In 2021, the proportion of Nematoda was the largest in the meiobenthos, 71%. In 2022, it dropped to less than 5%, while crustaceans (Harpacticoida and Copepoda) became predominant accounting for more than 80%. In 2022, the mean meiofaunal density across three stations reached (2,196.8 ± 1,407) ind. *per* 10 cm^2 being the highest during the research. In 2023, taxa distribution was more uniform, with no clearly prevailing groups. Turbellaria, Annelida, and Harpacticoida occurred in almost equal proportions (see Fig. 3); Ostracoda accounted for 16%. This year also showed the lowest nematode abundance: 6% of total meiofauna in the bay. Moreover, in 2023, at all the three stations, the lowest meiofaunal density was revealed: (288.3 ± 212) ind. *per* 10 cm^2.

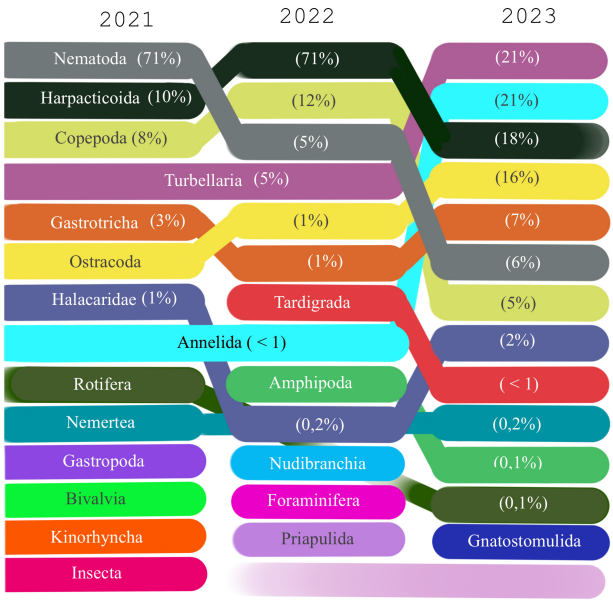

Fig. 3. Dynamics of changes in the share of main taxa in meiobenthos in the Triozerye Bay in 2021–2023

A total of 33 Nematoda species from 29 genera and 15 families were identified in the Triozerye Bay. The highest species diversity was recorded for Xyalidae (6 species), Axonolaimidae, and Chromadoridae (4 species each). All the registered species are listed in Table 2. The number of species varied 1 to 21 *per* station peaking at st2_21 in 2021 and reaching minimum at st3_23 in 2023. Notably, euryhaline free-living nematodes were observed in the bay: Linhomoeidae gen. sp. and *Leptolaimoides propinquus* at st3_23 in 2023 and *Anoplostoma cuticularia* at st1_21 in 2021.

Table 2. List of nematode species found in the Triozerye Bay in 2021–2023, their frequency of occurrence, and trophic affiliation

No.	Species	Family	Trophic index according to [Wieser, 1953]*	Frequency of occurrence, %	Ind. *per* 10 cm^2		
					2021	2022	2023
1	*Daptonema normandicum* (de Man, 1890) Lorenzen, 1977	Xyalidae	1B	71	34.2	57.5	2.2
2	*Parascolaimus proprius* Belogurov & Kartavseva, 1975	Axonolaimidae	1B	50	9	22.8	2.7
3	*Metadesmolaimus innii* Fadeeva & Karpova, 2024	Xyalidae	1B	42	35.6	0.9	4
4	*Enoplolaimus pectinatus* Fadeeva & Zograf, 2010	Thoracostomopsidae	2B	42	31.6	4.7	1.3

Continued on the next page…

No.	Species	Family	Trophic index according to [Wieser, 1953]*	Frequency of occurrence, %	Ind. *per* 10 cm^2		
					2021	2022	2023
5	*Ascolaimus elongatus* (Bütschli, 1874) Shuurmans Stekhoven & de Coninck, 1932	Axonolaimidae	1B	38	1.8	2.9	0
6	*Neochromadora poecilosoma* (de Man, 1893) Micoletzky, 1924	Chromadoridae	2A	21	60.5	0	0
7	*Theristus macroflevensis* Gerlach, 1954	Xyalidae	1B	21	13.2	0	1.3
8	*Oncholaimus domesticus* (Chitwood & Chitwood, 1938) Rachor, 1969	Oncholaimidae	2B	21	11.1	0.9	2.2
9	*Oncholaimus* sp. Dujardin, 1845	Oncholaimidae	2B	21	3	8,1	0
10	*Parachromadorita* sp. nov. Blome, 1974	Chromadoridae	2A	21	10.4	0	0.7
11	*Bolbolaimus* sp. 1 Cobb, 1920	Microlaimidae	2A	21	8,4	0	0
12	*Bathylaimus anatolii* Smirnova & Fadeeva, 2011	Tripyloididae	1B	21	3.2	1.6	0
13	*Desmodora* sp. de Man, 1889	Desmodoridae	2A	17	8.2	0	0
14	*Trileptium* sp. Cobb, 1933	Thoracostomopsidae	2B	17	1.6	4.3	0.7
15	*Microlaimus* sp. de Man, 1880	Microlaimidae	2A	17	0.6	0	1.6
16	*Axonolaimus seticaudatus* Platonova, 1971	Axonolaimidae	1B	13	0.4	6.3	0
17	*Theristus* sp. Bastian, 1865	Xyalidae	1B	13	4	1.7	0
18	*Tripyloides* sp. de Man, 1886	Tripyloididae	1B	13	4.1	0	0
19	*Chromaspirina* sp. Filipjev, 1918	Desmodoridae	2A	13	0	2.5	0.9
20	*Chromadora heterostomata* Kito, 1978	Chromadoridae	1A	13	0	0	3
21	*Enoplus* sp. Dujardin, 1845	Enoplidae	1B	13	0	1.1	0
22	*Daptonema* sp. nov. Cobb, 1920	Xyalidae	1B	8	3	0	0
23	*Lauratonema juncta* Fadeeva, 1989	Lauratonematidae	1A	8	0	0.9	0.9
24	*Metachromadora itoi* Kito, 1978	Desmodoridae	2A	8	1	0	0.5
25	*Leptolaimoides propinquus* Fadeeva & Morduchovic, 2007	Leptolaimidae	1A	8	0	0	1.4
26	Linhomoeidae gen. sp. Filipjev, 1922	Linhomoeidae	1B	8	0	0	1.3
27	*Desmoscolex* sp. Claparède, 1863	Desmoscolecidae	2A	8	0.6	0	0
28	*Dichromadora* sp. Kreis, 1929	Chromadoridae	2A	4	4	0	0
29	*Viscosia epapillosa* Platonova, 1971	Oncholaimidae	2B	4	0	0	1
30	*Metadesmolaimus canicula* (Wieser & Hopper, 1967) Gerlach & Riemann, 1973	Xyalidae	1B	4	1	0	0
31	*Nudora* sp. nov. Cobb, 1920	Monoposthiidae	1A	4	1	0	0
32	*Parodontophora* sp. Timm, 1963	Axonolaimidae	2B	4	0.3	0	0.5
33	*Anoplostoma cuticularia* Belogurov & Alekseev, 1977	Anoplostomatidae	1B	4	0	0	0.5

Note: *, see Fig. 6 caption for explanation.

Over the three years, the Nematoda community showed shifts with changes in dominants. Five species forming the basis demonstrated both highest frequency of occurrence and density: *Daptonema normandicum*, *Parascolaimus proprius*, *Metadesmolaimus innii*, *Ascolaimus elongatus*, and *Enoplolaimus pectinatus*. *Oncholaimus domesticus* also had high frequency of occurrence in the bay, but lower values of density.

Certain interannual fluctuations in Nematoda density were observed in the Triozerye Bay. Specifically, within 2021–2023, total meiofaunal abundance has undergone some changes. The highest mean nematode density was recorded in 2021 at st2_21: (370 ± 296) ind. *per* 10 cm^2. The lowest value was noted in 2023 at st3_23: (5 ± 1.8) ind. *per* 10 cm^2 (Table 2). Within 2021–2022, the mean density across stations decreased by 2.2 times. In 2021–2023, it declined 10-fold evidencing for substantial interannual variability.

In 2021, the short-lived phytophagous species *Neochromadora poecilosoma* dominated: its proportion was 24% (Fig. 4). Interestingly, it was absent in subsequent years in the Triozerye Bay suggesting that its abundance is tightly associated with its feeding strategy depending on microphytobenthos dynamics. At the stations of 2021, half of the Nematoda community was formed by juveniles, and males accounted for only 12%. A shift in dominant species occurred in 2022, and *D. normandicum* proportion was 51%. This was reflected in the values of the Simpson index (1 – *D*) (Table 3): those were < 0.7 at st3_22. In 2023, the prevailing forms have changed, and there were no dominants among 18 Nematoda species recorded. The proportions were as follows (Fig. 4): *M. innii*, 14%; *Chromadora heterostomata*, 12%; and *A. elongatus*, *O. domesticus*, and *D. normandicum*, 9–10% each. Age and gender structures were similar in the samples of 2022–2023: females dominated at a level of 50%, and proportions of juveniles and males accounted for 30 and 20%, respectively.

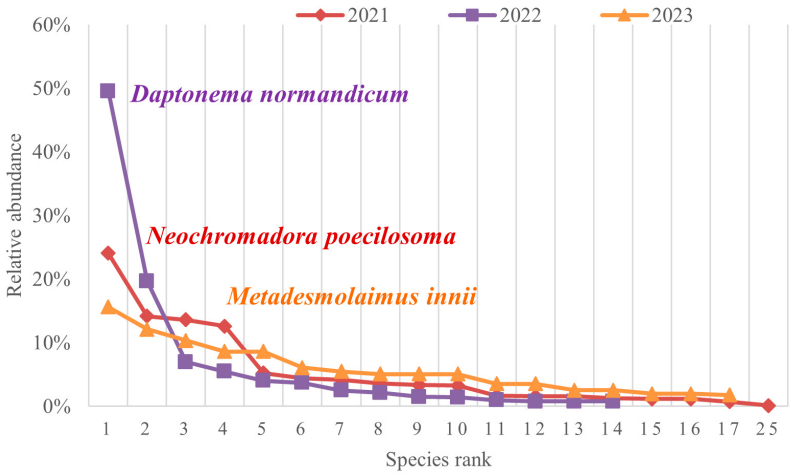

Fig. 4. Curves of the rank distribution of nematode relative abundance in 2021–2023 and dominant nematode species (the signature color corresponds to the dominance curve color)

Applying the ABC method, we revealed that in 2021–2023, the biomass curve was typically located above the abundance curve (Fig. 5) evidencing for the lack of physical stress.

In 2021 and 2022, the biomass of Nematoda remained relatively at the same level: 1,090 and 960 μg·m^{-2}. In 2023, the value dropped 10-fold, to 90 μg·m^{-2}. In 2021, 6 out of 25 registered species accounted for 80% of the total biomass, while in 2022, only 3 out of 14. The mean length of the found nematodes ranged 498 to 5,241 μm.

Table 3. Indices of biological diversity for the stations studied in 2021–2023

Index	2021		2022			2023		
	st1_21	st2_21	st1_22	st2_22	st3_22	st1_23	st2_23	st3_23
Shannon (H)	2.3	2.4	1.4	1.9	1.2	2.0		
Simpson ($1 - D$)	0.9		0.7	0.8	0.6	0.9		
Margalef (D_{Mg})	3.7	3.4	1.1	2.2	1.4	2.5		
Pielou (E)	0.8		0.8	0.8	0.6	0.9	0.9	1.0
$1 - ITD$	0.66		0.55			0.74		
ABC_{index}	1.6		0.97			3.6		

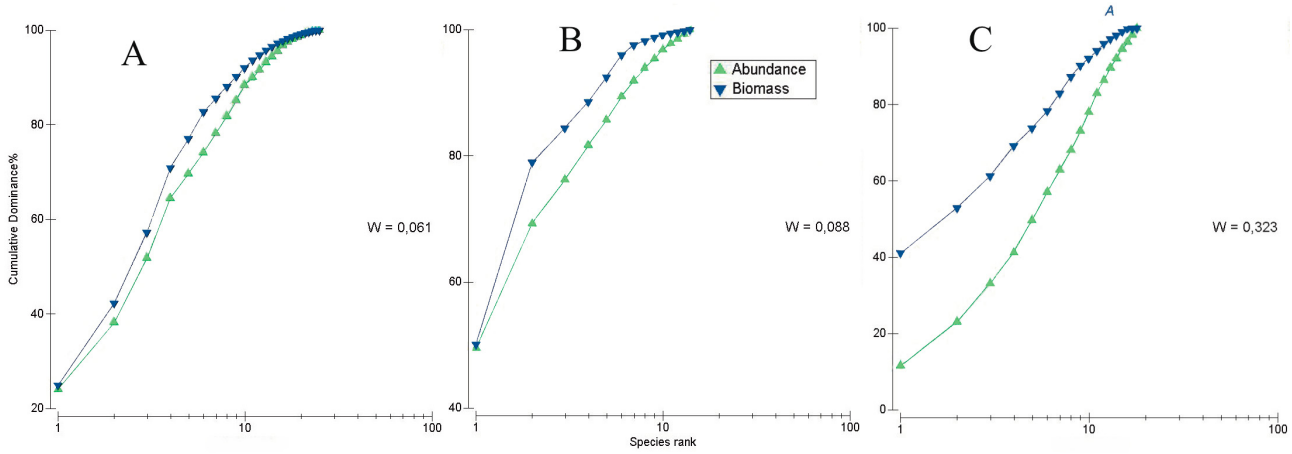

Fig. 5. Cumulative curves of abundance and biomass according to the data of 2021 (A), 2022 (B), and 2023 (C)

A large nematode *P. proprius* was the primary contributor to the nematocene biomass in the bay's community annually (Table 2). Some specimens reached a length of 6,500 μm. In 2021, the proportion of *P. proprius* in the total biomass was 17%, and in 2022, it increased to 50%. In 2023, the main contribution to the biomass was made by 7 out of 18 species of free-living nematodes, including *P. proprius* (up to 40%).

The maximum ABC_{index} values, at the level of 3.6, were recorded in 2023; those were 2.25-fold higher than in 2022 (Table 3). The values of three indices, ABC_{index}, $1 - ITD$, and Pielou index (E), rose within 2021–2023 (see Table 3), and the values of the Pearson correlation coefficient between them were not lower than 0.8. However, at the stations of 2023, relatively high values of biological diversity indices were noted. Also, there were no dominant taxa in both meiobenthic and Nematoda communities. The maximums of the Shannon index (H) and Margalef index (D_{Mg}) were characteristic of the stations of 2021. Thus, st1_21 featured a high value of D_{Mg}, about 3.7, indicating significant species diversity in the Triozerye Bay in 2021 (Table 3).

The trophic structure of Nematoda communities is illustrated in the diagram (Fig. 6). Despite a sharp rise in the proportion of non-selective deposit feeders (1B) in 2022, omnivores/predators (2B) maintained a proportion of 20% of the total nematofauna in the trophic structure within 2021–2023 and were represented by 6 species (see Table 2). Three omnivores, *E. pectinatus*, *O. domesticus*, and *Trileptium* sp., were found in the bay every year.

In 2021, the prevailing trophic groups were non-selective deposit feeders (1B) and epistratum feeders (2A), with proportions of 44 and 36%, respectively (Fig. 6). Importantly, there were no selective deposit feeders (1A) in several samples of 2021 and 2022; this fact manifested itself in the index 1 – *ITD* (Table 3). Its minimum occurred at the stations of 2022, where non-selective deposit feeders (1B) dominated, 81% (Fig. 6). Out of the stations surveyed, st2_23 exhibited the highest trophic diversity (all four feeding types were equally represented) (Fig. 6, Table 3) and had the index value of 0.74. The year of 2023 was marked by a notable rise in the proportion of selective deposit feeders (1A). Those accounted for 22% (Fig. 6, Table 2), and this value was an order of magnitude higher than in previous years.

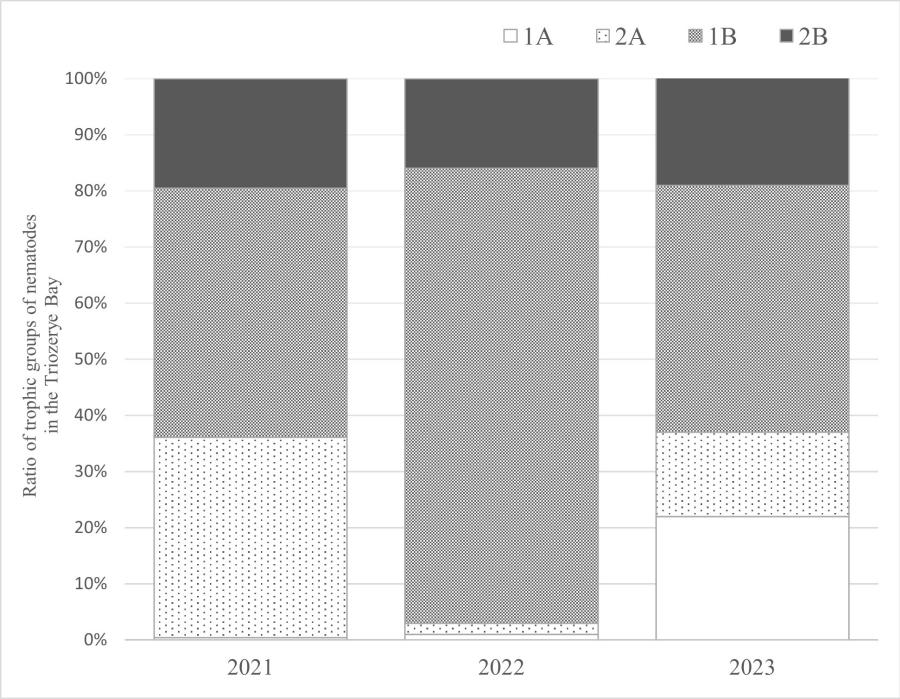

Fig. 6. Trophic structure of the nematofauna compiled according to W. Wieser classification based on the structure of the oral cavity of nematodes [1953]: 1A, deposit feeders, with no buccal armature; 1B, non-selective deposit feeders, oral cavity without weapons; 2A, epistratum feeders with a developed oral cavity surrounded by sclerotized teeth or plates; 2B, omnivores/predators with a large oral cavity armed with powerful teeth, jaws, and onchas

According to the results of the cluster analysis, nematocenes feature low levels of both interspecies and interstation similarity. The highest similarity (up to 60%) was found between two stations of 2022, st1_22 and st2_22, and between all the stations of 2021. Classification and ordination performed using non-metric multidimensional scaling (Fig. 7) revealed clear grouping of the stations by the sampling year (with a stress value of 0.02). These data combined with the values of diversity indices evidence for interannual variability in environmental conditions (Table 3).

The BIOENV procedure allowed for evaluating multiple combinations of abiotic variables to identify an optimal one explaining structural patterns of the Nematoda community [Clarke, Gorley, 2006].

Grain size distribution was the primary factor affecting the community structure. We revealed a weak positive effect (Spearman's rank correlation coefficient was about 0.31) (Table 4) between nematode distribution depending on predominant grain fraction that varied interannually from fine sand to medium gravel (see Table 1).

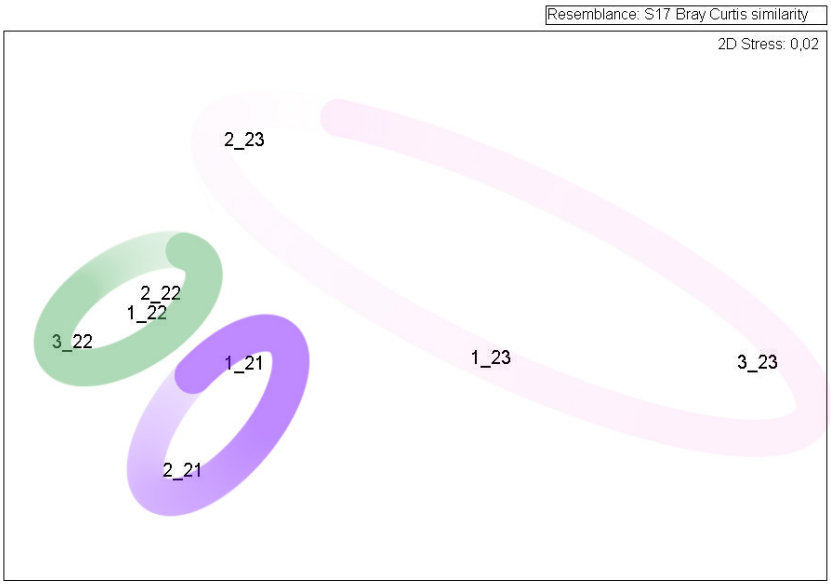

Fig. 7. Scheme of multidimensional scaling (MDS) by species composition of nematodes

Table 4. The best combination of abiotic variables according to results of the BEST analysis, with variables divided by station (year) using the LINKTREE procedure

Period	Spearman's rank correlation coefficient	Combination of variables
July 2021	0.31	fraction < 0.5 mm
August 2022	0.31	fraction ≥ 0.5 mm, C_{org} = 0.05%
August 2023	0.3	fraction ≥ 1 mm, C_{org} = 0.05%, S_0 < 2

Note: fraction, predominant fraction of bottom sediment (see Table 1); C_{org}, organic matter content; S_0, sorting coefficient.

DISCUSSION

In the Triozerye Bay, the species richness in the sandy zone of the upper sublittoral horizon was formed by 33 species. This bay featured active hydrodynamics. Its surface layer of bottom sediments experienced the strongest wave action at depths down to 1 m. Accordingly, the distribution of sediments was uneven.

Constant mixing of bottom sediments mediates a decrease in food availability and provides unfavorable conditions for meiofaunal organisms, as small ones struggle to stay attached to such a surface [Galtsova, 1991]. The taxonomic composition of meiobenthos and the species composition of nematodes are often poorer in shallow areas than in deeper ones [Pavlyuk et al., 2012].

Interannual changes in the meiobenthic community covered fluctuations in biomass and a rise in evenness of the species structure. Within 2021–2023, there were shifts in benthic biocenotic complexes governed by coarsening of sand particles and changes in dominant forms of meiobenthos and nematofauna. Cumulative curves of the grain size distribution (see Fig. 2) reflect significant differences between bottom sediment composition. The BIOENV procedure showed a direct effect of sediment indicators on Nematoda communities in the bay.

Meiobenthos is known to be unevenly distributed even in seemingly homogeneous bottom sediments, as small-scale changes in physical conditions occur in visually uniform sediments [Chesunov, 2006; Galtsova, 1991]. Environmental heterogeneity is primarily mediated by microtopography of the seabed and the type of food distribution [Galtsova, 1991]. Within the study period, Nematoda communities differed in terms of dynamics, and changes in sediment types govern a shift in dominant species.

Sampling in the Triozerye Bay in 2023 was carried out during prolonged rainfall and strong wave action that affected meiofaunal composition. Moreover, heavy rainfall in tidal shallows caused abrupt salinity changes triggering migration into deeper sediment layers and an increase in euryhaline nematode abundance. This is consistent with literature data [Steyaert et al., 2001].

The prevalence of Turbellaria at st1_23 and Annelida at st2_23 (see Fig. 3) was associated with bottom sediments dominated by grain fractions of 0.5–5 mm (coarse sand to medium gravel) in 2023 (see Table 1). According to regional studies, other groups become the key ones in meiofauna: oligochaetes, turbellarians, polychaetes, and nemerteans; the significance of macrobenthic larvae may rise as well [Giere, 2009; Gowing, Hulings, 1976; McLachlan, 1985; Mokievsky, 2009; Udalov, Burkovskii, 2002; Udalov et al., 2005]. In the Triozerye Bay, *D. normandicum* were consistently abundant across all the stations. *Ascolaimus*, *Axonolaimus*, and *Enoplolaimus* nematodes were significant in fine sands. On sandy beaches, Xyalidae often occur among the most common taxa. This family is typically represented by several genera (the most characteristic are *Daptonema*, *Theristus*, and *Metadesmolaimus*), and some genera are represented by several species [Fadeeva, Karpova, 2024; Gheskiere et al., 2005; Heip et al., 1985; Lee, Riveros, 2012; Nicholas, Hodda, 1999]. In literature, their prevalence is associated with high organic matter content, 0.5–2% [Gheskiere et al., 2005; Maria et al., 2012]. However, species we recorded inhabit the Triozerye Bay against the backdrop of much lower organic matter content, 0.03–0.05%.

Nematode density and biomass decreased 10-fold within 2021–2023. The ABC method showed as follows: in the Triozerye Bay, the biomass curves were located above the abundance ones, and *W* statistics rose 5-fold since 2021. A community is considered undisturbed when the biomass curve lies entirely above the abundance one (the ABC method). Under enhancing environmental stress, biomass and abundance curves converge and may cross. Sometimes, the abundance curve may surpass entirely the biomass one, and *W* statistics reaches its minimum [Shitikov, Golovatyuk, 2013; Warwick, Clarke, 1994]. As known, physically stressed communities are typically dominated by small and abundant organisms with high reproductive rates and short lifespan (r-strategists), while stable communities are inhabited by larger and less abundant ones with lower fecundity and longer lifespan (K-strategists) [Warwick, Clarke, 1994].

In the Triozerye Bay, the ABC method revealed prevalence of large species by biomass and small ones by abundance. The role of a nematode *P. proprius* is especially important: it is 4-fold larger in size than the most abundant species in the bay, *D. normandicum*. These data align with low values of diversity indices, including *ITD* (see Table 3), and the registration of pronounced dominants in the Nematoda community in 2022. The key reasons for restructuring of the community during the study period could be shifts in population density of some prevailing species and changes in their spatial distribution, as well as alterations in regional climatic and hydrological factors.

Conclusion. During short-term observations in the Triozerye Bay, we analyzed sandy shallow-water biotopes and registered a typical psammophilic fauna showing genus-level similarity with that in other areas. Within 2021–2023, structural shifts occurred in the meiobenthos: in composition

and ratio of high-rank taxa and mass species affected by hydrodynamics and salinity. The Nematoda community exhibited both qualitative and quantitative changes, with notable alterations in dominant forms. Currently observed variability in meiobenthic community structure was also governed by life cycles of organisms and their migrations into deeper and more stable layers of bottom sediments.

REFERENCES

1. Arzamastsev I. S., Preobrazhensky B. V. *Atlas of Underwater Landscapes of Sea of Japan.* Moscow : Nauka Publishers, 1990, 224 p. (in Russ.). https://elibrary.ru/toigon
2. Arkhivy pogody. In: *Pogoda i klimat* : [site], 2024. (in Russ.). URL: http://www.pogodaiklimat.ru/archive.php [accessed: 29.03.2024].
3. Bezrukov P. L., Licitzin A. P. Classification of bottom sediments in recent marine basins. *Trudy Instituta okeanologii*, 1960, vol. 32, pp. 3–14. (in Russ.)
4. Galtsova V. V. Meiobenthos in marine ecosystems (with special reference to freeliving nematodes). *Trudy Zoologicheskogo instituta AN SSSR*, 1991, vol. 224, 240 p. (in Russ.)
5. GOST 12536-2014. *Soils. Methods of Laboratory Granulometric (Grain-size) and Microaggregate Distribution* : natsional'nyi standart Rossiiskoi Federatsii : izdanie ofitsial'noe : utverzhden i vveden v deistvie Prikazom Federal'nogo agenstva po tekhnicheskomu regulirovaniyu i metrologii ot 12.12.2014 No. 2022-st : vzamen GOST 12536-79 : data vvedeniya 01.07.2015 / razrabotan Otkrytym aktsionernym obshchestvom "Proizvodstennyi i nauchno-issledovatel'skii institut po inzhenernym izyskaniyam v stroitel'stve" (OAO "PNIIIS"). Moscow : Standartinform, 2015, 20 p. (in Russ.)
6. GOST 26213-91. *Pochvy. Metody opredeleniya organicheskogo veshchestva* : vzamen GOST 26213-84; vveden 01.07.1993. Moscow : Izdatel'stvo standartov, 1992, 8 p. (in Russ.)
7. Kulepanov V. N., Sokolenko D. A., Vlasenko R. V. The state of thickets of mass species of macrophytes in the coastal region of Primorye. In: *Ratsional'naya ekspluatatsiya vodnykh biologicheskikh resursov* : materialy mezhdunarodnoi nauchno-tekhnicheskoi konferentsii, Vladivostok, 26–27 oktyabrya 2023 g. Vladivostok : Dal'rybvtuz, 2023, pp. 59–65. (in Russ.). https://elibrary.ru/cfyqah
8. Manuilov V. A. *Podvodnye landshafty zaliva Petra Velikogo.* Vladivostok : Izd-vo Dal'nevostochnogo universiteta, 1990, 168 p. (in Russ.)
9. Mokievsky V. O. *Ekologiya morskogo meiobentosa.* Moscow : KMK Scientific Press, 2009, 286 p. (in Russ.). https://elibrary.ru/qksklt
10. Pavlyuk O. N. Meiobenthos of bays of Furugelm Island and Sivuchya Bight (Peter the Great Bay, Sea of Japan). *Biologiya morya*, 2004, vol. 30, no. 3, pp. 183–190. (in Russ.). https://elibrary.ru/ebrwdf
11. Pavlyuk O. N., Trebukhova Yu. A., Propp L. N. Interannual variations of the meiobenthic community structure in Boisman Bay (Peter the Great Bay, Sea of Japan). *Biologiya morya*, 2012, vol. 38, no. 6, pp. 428–439. (in Russ.). https://elibrary.ru/pjgzbn
12. Petelin V. P. *Granulometricheskii analiz*

morskikh donnykh osadkov. Moscow : Nauka, 1967, 128 p. (in Russ.)

13. Preobrazhensky B. V., Zharikov V. V., Dubeikovsky L. V. *Basics of Underwater Landscape Studies (Management of Marine Ecosystems)*. Vladivostok : Dal'nauka, 2000, 352 p. (in Russ.). https://elibrary.ru/tvbslt
14. Smirnova E. V. *Struktura i dinamika soobshchestv peschanykh gruntov pribrezhnoi melkovodnoi zony severo-zapadnoi chasti Yaponskogo morya.* [dissertation] / Dal'nevostochnyi federal'nyi universitet. Vladivostok, 2012, 128 p. (in Russ.). https://elibrary.ru/qfylqh
15. Smirnova E. V., Fadeeva N. P. Raspredelenie interstitsial'noi fauny v morskikh peskakh melkovodnoi zony otkrytykh bukht zaliva Petra Velikogo, Yaponskoe more. In: *Aktual'nye problemy osvoeniya biologicheskikh resursov Mirovogo okeana* : materialy II Mezhdunarodnoi konferentsii, Vladivostok, 22–24 maya 2012 g. Vladivostok : Dal'rybvtuz, 2012, pp. 436. (in Russ.)
16. Trebukhova Yu. A., Pavlyuk O. N. Species composition and distribution of free-living marine nematodes in Vostok Bay, Sea of Japan. *Biologiya morya*, 2006, vol. 32, no. 1, pp. 8–16. (in Russ.). https://elibrary.ru/hzjjvd
17. Udalov A. A., Burkovskii I. V. The role of the mesobenthos in the size structure of an intertidal ecosystem. *Okeanologiya*, 2002, vol. 42, no. 4, pp. 527–536. (in Russ.)
18. Udalov A. A., Mokievskii V. O., Chertoprud E. S. Influence of the salinity gradient on the distribution of meiobenthos in the Chernaya River estuary (White Sea). *Okeanologiya*, 2005, vol. 45, no. 5, pp. 719–727. (in Russ.). https://elibrary.ru/hrwtep
19. Fadeeva N. P. Raspredelenie svobodnozhivushchikh nematod v raione bukhty Kievki. In: *Biologicheskie issledovaniya bentosa i obrastaniya v Yaponskom more*. Vladivostok : DVO AN SSSR, 1991, pp. 66–84. (in Russ.)
20. Chesunov A. V. *Biologiya morskikh nematod.* Moscow : KMK Scientific Press, 2006, 367 p. (in Russ.). https://elibrary.ru/otyhal
21. Chislenko L. L. *Nomogrammy dlya opredeleniya vesa vodnykh organizmov po razmeram i forme tela (morskoi mezobentos i plankton).* Leningrad : Nauka, Leningrad. otd-nie, 1968, 106 p. (in Russ.)
22. Shitikov V. K., Golovatyuk L. V. ABC method and the domination specificity of species in bottom river communities. *Povolzhskii ekologicheskii zhurnal*, 2013, no. 1, pp. 088–097. (in Russ.). https://elibrary.ru/qzbzmp
23. Clarke K. R., Gorley R. N. *PRIMER v6: User Manual. Tutorial.* Plymouth : PRIMER-E, 2006, 190 p.
24. Clarke K. R. Comparisons of dominance curves. *Journal of Experimental Marine Biology and Ecology*, 1990, vol. 138, iss. 1–2, pp. 143–157. https://doi.org/10.1016/0022-0981(90)90181-B
25. Fadeeva N. P., Karpova A. A. New species of *Metadesmolaimus*, *Rhynchonema* and *Gairleanema* (Nematoda) from the sandy beaches of the Sea of Japan. *Zootaxa*, 2024, vol. 5537, no. 1, pp. 115–132. https://doi.org/10.11646/zootaxa.5537.1.6
26. Gheskiere T., Vincx M., Urban-Malinga B., Rossano C., Scapini F., Degraer S. Nematodes from wave-dominated sandy beaches: Diversity, zonation patterns and testing of the isocommunities concept. *Estuarine, Coastal and Shelf Science*, 2005, vol. 62, iss. 1–2, pp. 365–375. https://doi.org/10.1016/j.ecss.2004.09.024
27. Giere O. *Meiobenthology. The Microscopic Motile Fauna of Aquatic Sediments.* 2nd edition.

Berlin ; Heidelberg : Springer-Verlag, 2009, 538 p. https://doi.org/10.1007/978-3-540-68661-3

28. Gowing M. M., Hulings N. C. A spatial study of meiofauna on a sewage-polluted Lebanese sand beach. *Acta Adriatica*, 1976, vol. 18, pp. 341–363.
29. Heip C. H. R., Vincx M., Vranken G. The ecology of marine nematodes. *Oceanography and Marine Biology: An Annual Review*, 1985, vol. 23, pp. 399–489.
30. Lee M. R., Riveros M. Latitudinal trends in the species richness of free-living marine nematode assemblages from exposed sandy beaches along the coast of Chile (18–42 °S). *Marine Ecology*, 2012, vol. 33, iss. 3, pp. 317–325. https://doi.org/10.1111/J.1439-0485.2011.00497.X
31. Maria T. F., Vanaverbeke J., Esteves A. M., De Troch M., Vanreusel A. The importance of biological interactions for the vertical distribution of nematodes in a temperate ultradissipative sandy beach. *Estuarine, Coastal and Shelf Science*, 2012, vol. 97, pp. 114–126. https://doi.org/10.1016/j.ecss.2011.11.030
32. McLachlan A. The ecology of two sandy beaches near Walvis Bay. *Madoqua*, 1985, vol. 14, no. 2, pp. 155–163.
33. Nicholas W. L., Hodda M. Free-living nematodes of a temperate, high-energy sandy beach: Faunal composition and variation over space and time. *Hydrobiologia*, 1999, vol. 394, pp. 113–127. https://doi.org/10.1023/A:1003544115600
34. Steyaert M., Herman P. M. J., Moens T., Widdows J., Vincx M. Tidal migration of nematodes on an estuarine tidal flat (the Molenplaat, Schelde Estuary, SW Netherlands). *Marine Ecology Progress Series*, 2001, no. 224, pp. 299–304. https://doi.org/10.3354/meps224299
35. Trask P. D. *Origin and Environment of Source Sediments in Petroleum*. Houston : Gulf Publishing Company, 1932, 324 p.
36. Warwick R. M., Clarke K. R. Relearning the ABC: Taxonomic changes and abundance/biomass relationships in disturbed benthic communities. *Marine Biology*, 1994, vol. 118, iss. 4, pp. 739–744. https://doi.org/10.1007/BF00347523
37. Wieser W. Die Beziehung zwischen Mundhöhlengestalt, Ernährungsweise und Vorkommen bei freilebenden marinen Nematoden: eine ökologisch-morphologische Studie. *Arkiv för Zoologi*, 1953, vol. 2, pp. 439–484.

МЕЖГОДОВЫЕ ИЗМЕНЕНИЯ СТРУКТУРЫ МЕЙОБЕНТОСА ПЕСЧАНОГО МЕЛКОВОДЬЯ БУХТЫ ТРИОЗЕРЬЕ (ЯПОНСКОЕ МОРЕ)

А. А. Карпова[1,2], Н. П. Фадеева[1]

[1]Дальневосточный федеральный университет, Владивосток, Российская Федерация
[2]Национальный научный центр морской биологии имени А. В. Жирмунского, Владивосток, Российская Федерация
E-mail: *lyuney@gmail.com*

Впервые представлены результаты анализа динамики биологических параметров мейобентоса прибрежной полосы песчаных грунтов в бухте Триозерье (Японское море) в июле — августе 2021–2023 гг. За время исследования зарегистрировано 20 таксонов мейофауны, которую формировали представители Harpacticoida, Nematoda, Copepoda, Turbellaria, Gastrotricha, Annelida,

Halacaridae и Ostracoda. Основой нематоцена являлись свободноживущие нематоды *Daptonema normandicum*, *Enoplolaimus pectinatus*, *Metadesmolaimus innii* и *Parascolaimus proprius*. В целом структура качественных и количественных показателей мейобентоса и нематофауны ежегодно менялась в связи с гранулометрическим составом грунтов.

Ключевые слова: Японское море, межгодовые изменения, гранулометрический состав, органическое вещество, мейобентос, нематофауна

1871
ИнБЮМ – IBSS

Морской биологический журнал
Marine Biological Journal
2025, vol. 10, no. 2, pp. 34–60
https://marine-biology.ru

UDC 594-155.3(262.5)

TAXOCENE OF MOLLUSCS OF COASTAL SOFT SEDIMENTS IN THE NORTHEASTERN SECTOR OF THE BLACK SEA AT THE BEGINNING OF THE XXI CENTURY

© 2025 **G. Kolyuchkina[1], I. Lyubimov[1], and N. Danilova[1,2]**

[1]Shirshov Institute of Oceanology of Russian Academy of Sciences, Moscow, Russian Federation
[2]Russian State Agrarian University – Moscow Timiryazev Agricultural Academy, Moscow, Russian Federation
E-mail: *galka.sio@gmail.com*

Received by the Editor 13.11.2023; after reviewing 19.04.2024;
accepted for publication 20.03.2025.

The key question of modern ecology is to understand the relationship between changes in marine ecosystems and the environment under ongoing climate change and increasing anthropogenic load. However, not all changes occurring in marine shelf ecosystems can be explained by the action of external factors, since the dynamics of ecosystems associated with internal processes, such as natural succession, is poorly understood. Benthic communities play a crucial role in ecosystem functioning by modifying habitats and affecting nutrient cycling and primary productivity. Bottom ecosystems are associated with the potential for carbon immobilization and sequestration the assessment of which remains a fundamental scientific challenge. Coastal communities of the Black Sea are a convenient model for such studies. Carbonate-producing organisms – molluscs – dominate in benthic ecosystems of this basin. The aim of the present work was to investigate the dynamics of abundance and population structure of molluscs in soft sediments of the coastal zone of the Black Sea at the North Caucasus in 2015–2022. Annual sampling was carried out at depths of 10 and 25 m. The structure of the mollusc taxocene and the dynamics of the size structure of populations of its main dominants were analyzed: at 10-m depth, *Chamelea gallina* and *Lucinella divaricata*; at 25-m depth, *Gouldia minima* and *Pitar rudis*. Fluctuations in their abundance reached orders of magnitude. The highest taxocene biomass was recorded in 2020 which coincided with the maximum surface water temperature and salinity (a drought period). Successful annual recruitment and multimodal appearance of size–frequency diagrams of these species were observed, except for *G. minima*, as its juvenile stages were almost absent in the samples. Based on the analysis of size–frequency diagrams, an attempt was made to estimate the mean limiting age of individuals in the population of these species. No linear relationships were revealed between values of abiotic factors and the taxocene structure. Trends of parallel changes in abundance of juveniles in a population and total biomass of each of the studied species were characterized.

Keywords: Black Sea, bivalves, macrozoobenthos, population dynamics

Benthic communities play a key role in functioning of marine ecosystems by modifying habitats and affecting nutrient cycling and primary productivity. Benthic ecosystems are associated with the possibility of carbon immobilization and sequestration, and their assessment remains a fundamental scientific problem [Romankevich, Vetrov, 2001]. In the context of more and more active climate and anthropogenic changes, the main issue of modern ecology is to study the formation of the response of marine ecosystems: structural rearrangements of communities, alterations in trophic interactions, and species

adaptation to fluctuating environmental conditions. Interestingly, not all changes occurring in benthos of the marine shelf can be explained by the effect of external factors alone. The dynamics of ecosystems driven by the effect of internal processes, such as natural successions, has been studied fragmentary [Zhirkov, 2010]. Macrozoobenthic communities of soft bottom sediments of the Black Sea are a convenient model for this kind of research. There are no papers on the dynamics of Black Sea macrozoobenthos analyzing a unified series of long-term data (4–5 years and more). However, the Black Sea benthic ecosystems are known to have undergone dramatic changes in the late XX–early XXI century. The reasons for these transformations are rooted in uncontrolled overfishing, regulation of large watercourses flowing into the Black Sea, anthropogenic hypereutrophication of the basin, and its increased pollution in the early XX century [Bologa et al., 1995]. Invasion of alien species has governed the transformation of communities as well. As a result, in the 1970s, there was a shift in biodiversity indices and macrozoobenthos abundance, with the northwestern Black Sea being most affected [Exotic Species in the Aegean, 2001; Marinov, Stoykov, 1990; Mitilidy, 1990; Revkov, 2003; Tiganus, 1997]. Hypereutrophication resulted in outbreaks in plankton proliferation followed by a gain in organic carbon content in the water column, an increase in sedimentation, and a drop in oxygen concentration in the bottom layer [Bologa et al., 1995]. In the northwestern Black Sea, annual hypoxia areas were formed, suffocation of the benthic community occurred, and the structure of bivalve population changed: juveniles became the predominant class [Bologa et al., 1995]. Subsequently, in the 1980s, there were an almost twofold decrease in the number of macrozoobenthos species, mainly due to crustaceans, a drop in the role of psammophiles, and a rise in pelophiles, *inter alia* far invaders [*Anadara kagoshimensis* (Tokunaga, 1906), Bivalvia] [Alekseev, Sinegub, 1992; Bologa et al., 1995]. Importantly, by the beginning of the XXI century, after disastrous transformations, a trend towards recovery of species diversity and community structure was observed in the northwestern Black Sea [Dumitrache, Abaza, 2004; Revkov et al., 2018].

Conversely, on the northeastern coast of the Black Sea, a decrease in species diversity of macrozoobenthos was recorded in 1999–2005 against the backdrop of significant annual fluctuations in abundance and biomass in *Chamelea gallina* (Linnaeus, 1758) biocenosis [Chikina, Kucheruk, 2005; Kucheruk et al., 2002]. This biocenosis was registered in the early XX century at depths of 10–30 m [Kiseleva, 1981, 1992]. By 1999, due to double pressure by predatory invaders [the warty comb jelly *Mnemiopsis leidyi* A. Agassiz, 1865 affected planktonic larval stages; a gastropod *Rapana venosa* (Valenciennes, 1846) affected adult bottom stages], bivalves were not found at 10–30 m [Kucheruk et al., 2002]. In the autumn of 1999, *Beroe ovata* Bruguière, 1789 – a new invasive obligate ctenophore – became highly abundant. The pressure on larval stages was weakened, and mass settling of bivalves was recorded along the entire coast of the North Caucasus from Gelendzhik to Adler [Chikina, Kucheruk, 2005; Kucheruk et al., 2002]. In 2001, biomass of the main dominants was more than 1 kg·m^{-2}, and abundance was about 2.5 thousand ind.·m^{-2} [Chikina, Kucheruk, 2005]; by 2005, these indicators dropped to almost zero values [Kucheruk et al., 2012]. At a depth of 10–15 m, *Ch. gallina* remained the dominant, the same as in the XX century. However, at 20–30 m, the key species was *A. kagoshimensis*, an invader. By 2005, due to a re-gain in *R. venosa* pressure on bivalves, macrozoobenthos abundance and biomass decreased by an order of magnitude: down to 340–554 ind.·m^{-2} and 12–146 g·m^{-2}, respectively [Chikina, 2009]. In 2005–2007, at depth of 10–15 m, *Ch. gallina* prevailed; at 20–30 m, *Pitar rudis* (Poli, 1795) dominated, the former minor species of its biocenosis [Chikina, 2009; Kucheruk et al., 2012]. The belt community was clearly divided into two zones in the 2010s as well [Kolyuchkina et al., 2020]. At the same time, in 2014–2017, an increasing role of a bivalve *Gouldia minima* (Montagu, 1803) was noted. Not registered in the early 2000s, this mollusc was one of the key

species of *Ch. gallina* community in the XX century [Kiseleva, 1981]. Lately, there have been reports on stabilization of macrozoobenthos abundance and species diversity off the North Caucasus [Frolenko, Zhivoglyadova, 2020; Frolenko et al., 2019; Kolyuchkina et al., 2020; Selifonova, Chasovnikov, 2017], but none of the papers has analyzed long-term series of macrobenthos abundance and populations dynamics of the chief community dominants, bivalves. Researchers of the Shirshov Institute of Oceanology of RAS carried out annual monitoring of macrozoobenthos state in a narrow shelf area (the Inal Bay). The aim of this work was to study the structure and dynamics of Mollusca taxocene, as well as the dynamics of the population structure of dominant bivalves, and to reveal factors causing changes of mollusc taxocene in the Inal Bay at depths of 10 and 25 m in 2015–2022.

MATERIAL AND METHODS

The studies were carried out in 2015–2022 in late June–early July on the narrow shelf of the northeastern Black Sea near the Inal Bay (Tuapsinsky District, Krasnodar Krai, Russian Federation) during annual expeditions of the Shirshov Institute of Oceanology on the small research vessel "Ashamba." Sampling was carried out with an Ocean grab, with a capture area of 0.1 m^2, at depths of 10 m (N44.3276°, E38.6146°) and 25 m (N44.3212°, E38.6024°) in three replicates *per* station, except for samples from a depth of 25 m in 2021–2022 (there were two replicates). In total, 46 samples from 16 stations were analyzed. Upper 5 cm of bottom sediments were sampled from an additional grab with a plastic cylinder to determine the grain size. The mean surface water temperature in February–March at the Tuapse weather station area was derived from the website http://portal.esimo.ru/portal. Water temperature at the survey time was measured by a portable data logger Star-Oddi DST centi-TD (±0.1 °C).

Right after sampling, macrozoobenthic samples were thoroughly washed through a sieve with a mesh diameter of 0.5 mm and then fixed in 4% buffered formalin diluted by seawater. In a laboratory, all molluscs were picked from each sample, transferred to 75% ethanol, and taxonomically identified. Abundance and wet biomass of species in the samples were determined (on scales with a resolution up to 0.001 g), and the mean weight of individuals was established (the quotient of biomass and abundance). For each sample, the obtained data on abundance and biomass were recalculated *per* 1 m^2. Identification keys of the Black Sea fauna guide [1972] and lists of alien species [Shalovenkov, 2020] were used. The validity of species names (as of December 2023) was checked in the WoRMS taxonomic database [2023].

The grain size of sediments was analyzed by the staff of the analytical laboratory at the Shirshov Institute of Oceanology by the water–sieve method. The content of key fractions was determined: from < 0.01 to > 10 mm.

The main statistical data on the taxocene structure were processed in PRIMER v6.1.16 with PERMANOVA+ v1.0.6 add-on. The species diversity was assessed using the cumulative curve of accumulation of species abundance with an increase in the number of samples. The expected total number of species was established with the Chao2 estimator for the occurrence rate of rare species [Chao, 1987]. To identify sample groupings, cluster analysis was carried out. Similarity matrices were calculated using the Bray–Curtis index for log(x + 1)-transformed biomass. *R. venosa*, a migratory predator feeding on other molluscs, was preliminarily excluded from the species list for the analysis of taxocene structure. In the present study, the rapa whelk abundance was considered as a factor. The SIMPROF method was used to determine the significance of differences between clusters (significance level

of 0.01). The significance of differences between data sets was tested by non-parametric Permutational ANOVA (PERMANOVA). To confirm the adequacy of the methods applied (to assess the contribution of spatial and temporal factors to the variability of community structure), an additional two-factor PERMANOVA was performed on data on the log-transformed biomass of species in the samples for depths of 10 and 25 m (factor 1, depth; factor 2 nested in depth, year).

To identify the taxocene dynamics, we averaged similarity matrices of biomass data ('distance among centroids' procedure, PERMANOVA+); the year of the study served as a grouping factor [Anderson, 2001]. To reveal species with the greatest contribution to similarities and differences in clusters, we used the SIMPER procedure for the log(x + 1)-transformed biomass in the samples. Species contributing most to the taxocene biomass were considered dominant ones. Based on data on species occurrence rate in the samples within each cluster (sample grouping), we distinguished [Vorob'ev, 1949]: leading species ('constants'), with the occurrence rate of 50–100%; characteristic ones, 25–50%; and rare ones, less than 25%.

To analyze correlations between the macrozoobenthos structure and environmental factors, we applied the non-parametric regression analysis DistLM [Clarke, Gorley, 2006]; the Bray–Curtis index for log(x + 1)-transformed biomass of species in the samples was used as a measure of similarity. As predictors, we applied year from the beginning of the study, geographic coordinates reflecting spatial location of stations, grain size of sediments (10 fractions), the mean surface water temperature in February–March at the Tuapse weather station area, and abundance of a predatory gastropod *R. venosa*. Before the analysis, predictor data were normalized. The predictors were grouped by type (using 'group variables'); the selection criterion was Adjusted R^2, and the selection procedure was Stepwise. In all cases, $p < 0.001$ was considered a reliable value. For unified data (the number of species *per* station, as well as taxocene abundance and biomass), non-parametric Spearman correlation analysis was performed (the rank correlation coefficient R_{Sp}) with the same predictors; correlation was considered significant at $p < 0.001$. Pairwise differences between independent samples were assessed by the non-parametric Mann–Whitney test; differences were considered significant at $p < 0.001$.

For dominant species, we investigated the dynamics of the size structure of their populations analyzing totally all specimens of each species in two samples *per* station. If the total sample volume was less than 100 ind., material from three samples was united. If the number of individuals *per* sample exceeded 300, material from one sample was used. The number of studied samples could differ from the species number in a sample, since some molluscs were lost during repeated measurements, or their shells were damaged. We did nor re-measure damaged specimens. In total, 89.4–97.9% of individuals in the samples were measured. Shell length was determined for all specimens: totally, molluscs of each species from every investigated sample were separately placed on a flat surface and photographed with a scale ruler (division value of 0.1 mm), with a camera oriented parallel to the surface. The images obtained (300 dpi) were analyzed using ImageJ 1.53a (Wayne Rasband, National Institutes of Health, the USA). The accuracy of the software determination exceeded the division value of the scale ruler; so, values were rounded to 0.1 mm. The deviation of shell lengths obtained using the program and a caliper (division value of 0.02 mm) was 2.4%, or 0.3 mm (threefold measurement of shell lengths in the program; results of measurements with a caliper were taken as 100%). Thus, the accuracy of digital measurements was 0.3 mm. The size–frequency distributions were formed and analyzed in PAST 4.03 ('mixture analysis'). The procedure was based on the EM algorithm [Dempster et al., 1997] allowing to reveal local optima. The procedure automatically runs 20 times, each time with new random

starting positions for a data array. The stability of the solution was checked by re-running the algorithm three times. The optimal solution (number of groupings) was chosen with simultaneous minimum value of the Akaike information criterion [Akaike, 1974] and maximum value of the logarithmic likelihood.

RESULTS

Habitat characteristics. The study area features sandy sediments (at a depth of 10 m) and sandy-gravel ones (at a depth of 25 m). At 10 m, there was practically no gravel fraction in sediments, (0.4 ± 0.8) %, in contrast to a depth of 25 m, where the gravel fraction reached (15.2 ± 8.9) % (Fig. 1). Siltation degree between 10 and 25 m differed insignificantly. In 2015–2022, a weakly noticeable trend of increasing pelite content was observed at a depth of 25 m (R_{Sp} = 0.69; p = 0.06).

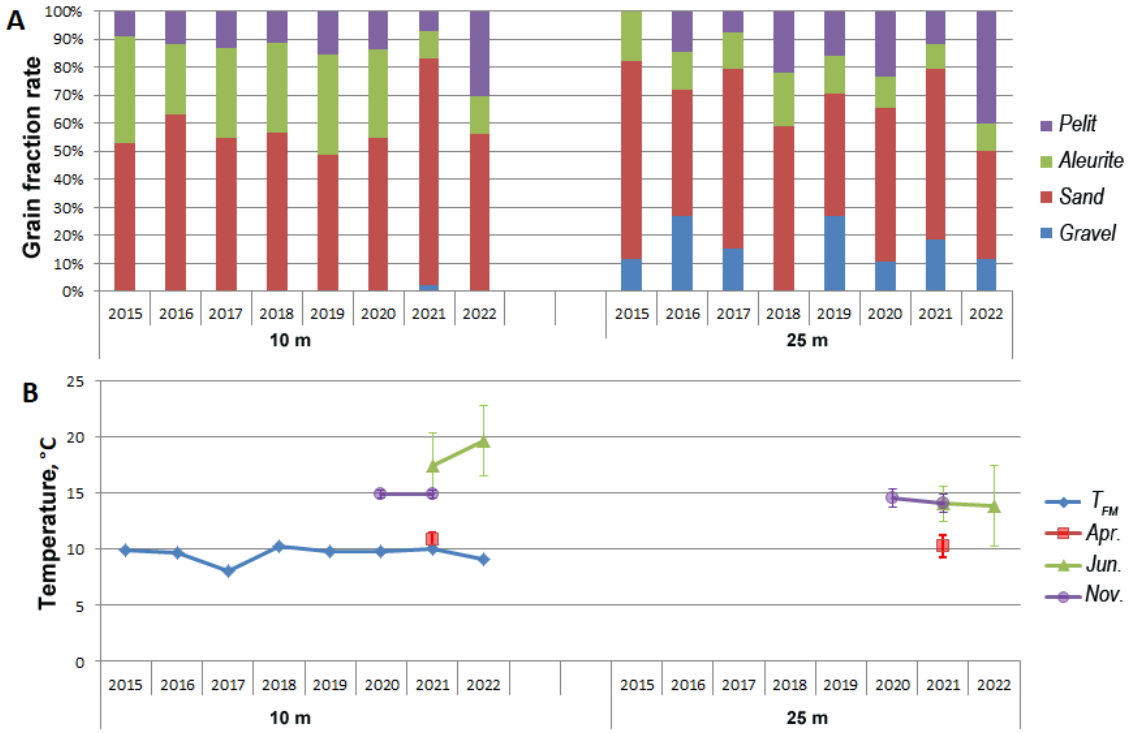

Fig. 1. Grain-size distribution of bottom sediments (A); mean water surface temperatures in February–March (T_{FM}) according to the Tuapse weather station data and water temperatures at observation sites in different seasons (B) at depths of 10 and 25 m in the Inal Bay in 2015–2022

The temperature regime at 10 and 25 m differed only during summer. For both 2021 and 2022, a noticeably higher water temperature was recorded: in 2021, (+17.4 ± 2.9) °C *vs.* (+14.1 ± 2.9) °C; in 2022, (+19.7 ± 3.1) °C *vs.* (+13.9 ± 2.6) °C (Fig. 1B). No significant trends in the mean temperature in February–March were observed during the study. The minimum values were registered in 2017 (+8.1 °C). Also, a lower value, compared to the mean for the period, was recorded in 2022 (+9.1 °C).

Structure and dynamics of Mollusca taxocene. In 2015–2022, 29 mollusc species were found at depths of 10 and 25 m. At 10 m, 20 species were noted in 27 samples, 3–12 *per* sample [(7 ± 2) on average; hereinafter mean ± standard deviation] (Fig. 2A). The expected number of species with the Chao2 correction was (21 ± 1) evidencing for a fairly high representativeness of our sample. No trends in the species number over time were revealed; differences were reliable for 2019 and 2020 only,

when the species number increased almost twofold. At a depth of 25 m, 24 species were recorded in 25 samples [(30 ± 8) with the Chao2 estimator], 3–14 *per* sample [(8 ± 3) on average] (Fig. 2A). The species number fluctuated, with a minimum in 2016–2017 and a maximum in 2020 (differences were significant, $p < 0.05$).

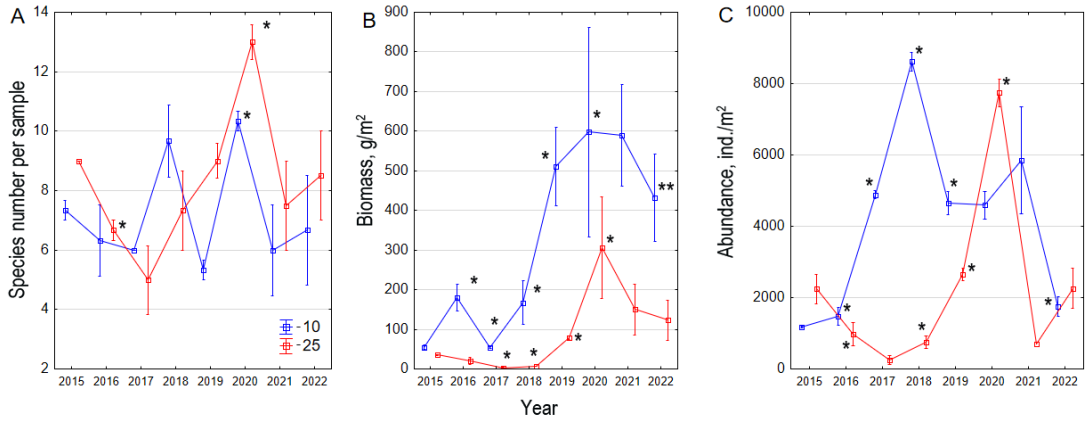

Fig. 2. Dynamics of the species number *per* sample (A), total biomass (B), and abundance (C) of Mollusca taxocene at depths of 10 and 25 m. * marks values of the parameter that significantly differ from those of the previous year; ** mark values that significantly differ from those of 2020. Error bars are standard error of the mean; points are the mean

Within 2015–2022, the total biomass in the Mollusca taxocene varied widely: 45.8–869.1 g·m^{-2} at 10 m and 0.3–513.8 g·m^{-2} at 25 m (Fig. 2B). In 2015–2018, the biomass at a depth of 10 m changed annually (interannual differences were significant, $p < 0.05$) reaching minimum values in 2015 and 2017 and maximum ones in 2016 and 2018. In 2019, the taxocene biomass at this depth rose more than 2 times compared to that of 2018 (Fig. 2B). The biomass growth trend continued in 2020. In 2021–2022, there was a downward trend in biomass, and differences between the values of 2020 and 2022 were significant (Fig. 2B). At 25-m depth, biomass dropped from (35.1 ± 3.5) g·m^{-2} in 2015 to (3.4 ± 2.7) g·m^{-2} in 2017. Within 2018–2020, the taxocene biomass increased (interannual differences were significant, $p < 0.05$) by two orders of magnitude. Already in 2021, the value decreased threefold (differences from 2020 were unreliable due to a small number of samples). In 2022, biomass remained at approximately the same level (differences from 2020 were unreliable). When uniting samples from 2021 and 2022, their differences in biomass from the values of 2020 became significant. Thus, both at 10-m and 25-m depths, a rise in biomass in the Mollusca taxocene was observed in 2018–2020, and a decrease was recorded in 2021 (it was reliably determined in 2022).

The abundance in Mollusca taxocene fluctuated widely during these years: from 60 to 10,050 ind.·m^{-2} (Fig. 2C). At a depth of 10 m, abundance was low in 2015–2016; it reliably increased by 3.3 times in 2017 and almost doubled in 2018. In 2019, a noticeable drop in abundance to the values of 2017 was revealed. In 2020 and 2021, no significant interannual differences were found; in 2022, abundance in the taxocene decreased by half. At a depth of 25 m, within 2015–2017, a decline in abundance by an order of magnitude was registered. In 2018–2020, a rise in abundance by an order of magnitude was noted. In 2021 and 2022, the values were similar and noticeably differed from those of 2020 by 4.5 times.

R. venosa was found only in six samples in 2017, 2018, 2021, and 2022 (Fig. 3). No significant trends in abundance of this predatory gastropod were revealed.

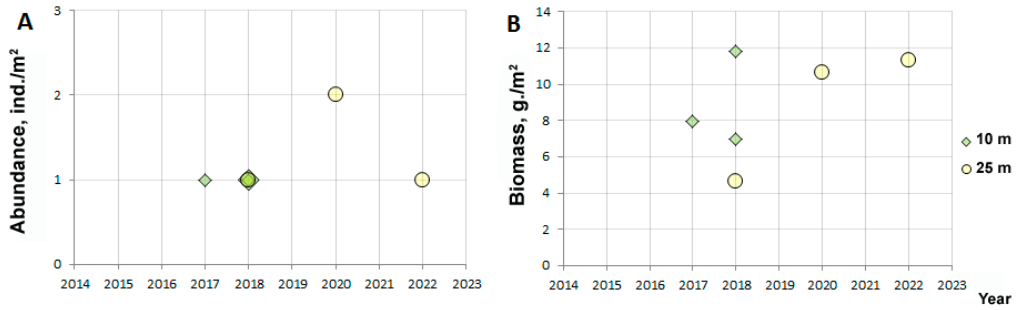

Fig. 3. *Rapana venosa* abundance (A) and biomass (B) in samples of 2015–2022 at depths of 10 and 25 m in the Inal Bay

A two-factor analysis (PERMANOVA) showed as follows: the contribution of depth to the overall biomass data variability was greater than that between years within each depth range (Table 1). Accordingly, we reject the null hypothesis that there are no statistically significant differences between the taxocene structure at 10 and 25 m and that there are no interannual differences.

Table 1. Results of two-way analysis of variance (PERMANOVA) for log(x + 1)-transformed biomass of species of Mollusca taxocene at depths of 10 and 25 m in the Inal Bay in 2015–2022

Factor	Degree of freedom	Sum of squares	Mean sum	Pseudo-*F*	*P* (permutational)	Number of permutations	Proportion of explained variation (SS/SS_{total}), %
Depth, m	1	38,827	38,827	94,303	0.001	999	48
Year (depth, m)	14	28,849	2,060.7	5,005	0.001	999	36
Residual variation	31	12,763	411.7				
Total variation	46	80,636					

Cluster analysis of biomass data allowed us to identify four main groupings of samples (Fig. 4). Species composition and occurrence rates are provided in Table 2.

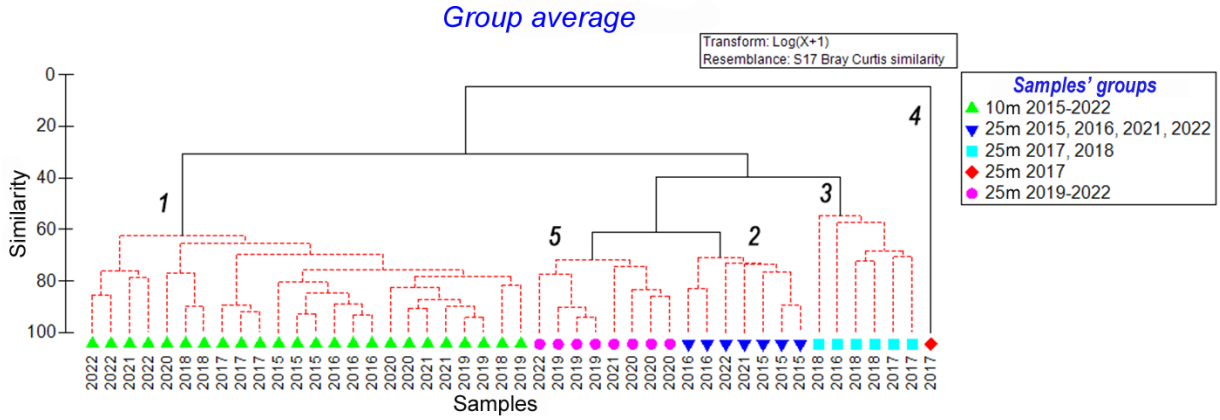

Fig. 4. Results of cluster analysis of Mollusca taxocene structure based on values of the Bray–Curtis similarity index calculated from the log(x + 1)-transformed biomass for samples of 2015–2022 in the Inal Bay. Red dotted lines show the groupings identified by SIMPROF procedure (confidence level of 1%). Digits indicate numbers of the groupings

Table 2. Mollusca occurrence in 2015–2022 in the Inal Bay (%). The groupings: 1, a depth of 10 m, 2015–2022; 2, a depth of 25 m, 2015, 2016, 2021, and 2022; 3, a depth of 25 m, 2016–2018; 4, a depth of 25 m, 2017; 5, a depth of 25 m, 2019–2022

Class	Species	Grouping				
		1	2	3	4	5
Bivalvia	*Abra alba* (W. Wood, 1802)	4	29	17	38	0
	Abra nitida (O. F. Müller, 1776)	0	0	0	13	0
	Acanthocardia paucicostata (G. B. Sowerby II, 1834)	0	0	17	25	0
	Anadara kagoshimensis (Tokunaga, 1906)	50	86	67	100	0
	Parvicardium simile (Milaschewitsch, 1909)	0	14	17	0	0
	Chamelea gallina (Linnaeus, 1758)	100	100	100	100	0
	Donax semistriatus Poli, 1795	88	0	33	63	0
	Gouldia minima (Montagu, 1803)	46	100	100	100	100
	Lentidium mediterraneum (O. G. Costa, 1830)	42	0	0	0	0
	Lucinella divaricata (Linnaeus, 1758)	100	100	100	100	0
	Mytilaster lineatus (Gmelin, 1791)	17	0	33	38	0
	Mytilus galloprovincialis Lamarck, 1819	4	14	17	38	0
	Pitar rudis (Poli, 1795)	25	100	100	100	100
	Spisula subtruncata (da Costa, 1778)	92	100	83	100	100
	Fabulina fabula (Gmelin, 1791)	83	43	0	63	0
	Bela nebula (Montagu, 1803)	4	0	0	0	0
Gastropoda	*Bittium reticulatum* (da Costa, 1778)	4	0	0	0	0
	Brachystomia scalaris (MacGillivray, 1843)	25	0	0	13	0
	Calyptraea chinensis (Linnaeus, 1758)	0	14	0	63	0
	Epitonium clathrus (Linnaeus, 1758)	0	0	0	13	0
	Hydrobia acuta (Draparnaud, 1805)	0	14	0	0	0
	Parthenina interstincta (J. Adams, 1797)	8	0	0	0	0
	Parthenina terebellum (R. A. Philippi, 1844)	0	14	0	0	0
	Retusa truncatula (Bruguière, 1792)	0	14	0	25	0
	Retusa variabilis (Milaschewitsch, 1912)	0	14	0	0	0
	Rissoa splendida Eichwald, 1830	4	14	0	25	0
	Tragula fenestrata (Jeffreys, 1848)	13	29	0	0	0
	Tritia neritea (Linnaeus, 1758)	4	0	0	0	0
	Tritia reticulata (Linnaeus, 1758)	8	0	0	13	0
	Rapana venosa (Valenciennes, 1846)	13	14	17	13	0
Number of samples *per* a grouping		24	7	6	1	8

The grouping 1 included all 24 samples from a depth of 10 m in 2015–2022. The average sample similarity (SIMPER) in this grouping accounted for 71%. The main contributors to the sample similarity (96%) were three species: *Ch. gallina*, *Donax semistriatus* Poli, 1795, and *Lucinella divaricata* (Linnaeus, 1758). Two main dominants of the taxocene had an occurrence rate of 100%: *Ch. gallina* and *L. divaricata* (Table 2). These two species, along with *D. semistriatus* (occurrence rate of 88%) and *A. kagoshimensis* (occurrence rate of 50%), ensured the major contribution to the intra-complex similarity by log-transformed biomass (up to 96–100% in total). In this grouping, the leading species were *Spisula subtruncata* (da Costa, 1778) and *Fabulina fabula* (Gmelin, 1791), but their contribution to the intra-complex similarity in the taxocene biomass did not exceed 3%. Gastropods were characterized by a lower occurrence rate than bivalves (up to 25%) and low biomass. Only 3 ind. of a predatory gastropod *R. venosa* were noted: in 2017 (a weight of a specimen was 7.9 g) and in 2018 (11.7 and 6.9 g).

All the other groupings included samples from 25-m depth. The grouping 2 united 7 samples from 2015, 2016, 2021, and 2022. The species number *per* sample ranged 6–11, (8 ± 2) on average, and biomass was (45.0 ± 24.5) g·m^{-2}. This grouping included samples with low biomass. Abundance varied 700 to 3,040 ind.·m^{-2}. The average sample similarity (SIMPER) accounted for 74%. The chief contributors to the sample similarity (96%) were three species: *G. minima*, *P. rudis*, and *Ch. gallina*. These ones, as well as *S. subtruncata* and *L. divaricata*, had an occurrence rate of 100%. The main contribution to the intra-complex similarity in biomass in this grouping was made by *G. minima* (35–83%) and *P. rudis* (4–49%) providing a total of 56–93% of biomass. *Ch. gallina* contributed 3–17%, *S. subtruncata*, 1–7%, and *L. divaricata*, 2–10%. The characteristic species of the taxocene in this grouping was an invader *A. kagoshimensis* recorded at 86% of the stations. Its contribution to biomass ranged 1–3%; only in one sample, where one large specimen (shell length of 36.2 mm) with a weight of 10.8 g was found, the contribution of this species accounted for 32%. The occurrence rate of Gastropoda representatives did not exceed 29%. The only *R. venosa* individual was registered in 2022 (its weight was 11.3 g).

The grouping 3 included 6 samples of 2016–2018. The average sample similarity (SIMPER) accounted for 54%. The number of species was 5–10, (7 ± 2) *per* sample. The taxocene biomass was (6.2 ± 1.3) g·m^{-2} there, and abundance was (560 ± 293) ind.·m^{-2}. Thus, this grouping united the samples with minimum values of biomass and abundance during the study period. The key contributors to the sample similarity (96%) were four species: *G. minima*, *P. rudis*, *Ch. gallina*, and *L. divaricata*. They were found in all samples of the grouping and provided 63–92% of the taxocene biomass. The characteristic species were also *A. kagoshimensis* (occurrence rate of 67%) and *S. subtruncata* (occurrence rate of 83%); in one sample, their biomass reached 12 and 16%, respectively. Gastropoda were not found there, except for *R. venosa*: 1 ind. was noted in one of the samples in 2017 (its weight was 4.7 g).

One sample – that from a depth of 25 m in 2017 – was not included in any other grouping (marked with number 4). There, only three species were recorded: *S. subtruncata* (79% of biomass), *P. rudis* (18%), and *G. minima* (3%). The total biomass was 0.33 g·m^{-2}. *R. venosa* was not registered.

The grouping 5 united 8 samples of 2019–2022. The average sample similarity (SIMPER) accounted for 49%. The species number *per* sample ranged 7–14, (11 ± 3) on average. Taxocene biomass was (250.5 ± 182.6) g·m^{-2}, and abundance was (4,444 ± 2,799) ind.·m^{-2}. This grouping united the samples with high abundance, biomass, and species diversity. The major contributors to the sample similarity (96%) were four species: *G. minima*, *P. rudis*, *Ch. gallina*, and *A. kagoshimensis*. They accounted for 88–98% of the biomass, with the highest values for *G. minima* (27% on average) and *P. rudis* (33% on average). *Ch. gallina* biomass accounted for a mean of 18% (3–28%), and *A. kagoshimensis* biomass, 15% (3–42%). In each of two samples with a high contribution of *A. kagoshimensis* to biomass, 1 ind. of this species was found: with a shell length of 31.2 mm and a weight of 7.1 g and with a shell length of 19.8 mm and a weight of 2.4 g. Characteristic Bivalvia species were *S. subtruncata* and *L. divaricata* recorded in 100% of the samples (total contribution to biomass was < 5%), as well as *F. fabula* and *D. semistriatus* identified in 63% of the samples (2–9% of biomass in total). The only characteristic Gastropoda species was *Calyptraea chinensis* (Linnaeus, 1758) also registered in 63% of the samples (< 1% of biomass). Two *R. venosa* individuals were noted in one sample in 2020 (a weight of 4.7 and 5.9 g).

So, at a depth of 25 m, a change in the taxocene structure was determined during the study period. The trend is well illustrated by a non-metric multidimensional scaling (MDS) diagram constructed on the matrix of distances between centroids of samples with a grouping factor of year (Fig. 5). Two states

of the system were identified: 1) 2015 and 2019–2022; 2) 2016–2018. Differences between them are significant (PERMANOVA pseudo-F = 9.1; p = 0.02). SIMPER analysis showed that it was mediated by the difference in biomass of three leading species. Their biomass was high in 2015 and 2019–2022 (on average, 126.2 g·m^{-2} for *P. rudis*, 86.6 g·m^{-2} for *G. minima*, and 66.6 g·m^{-2} for *Ch. gallina*) and low in 2016–2018 (on average, 8.1 g·m^{-2} for *P. rudis*, 9.9 g·m^{-2} for *G. minima*, and 4.6 g·m^{-2} for *Ch. gallina*).

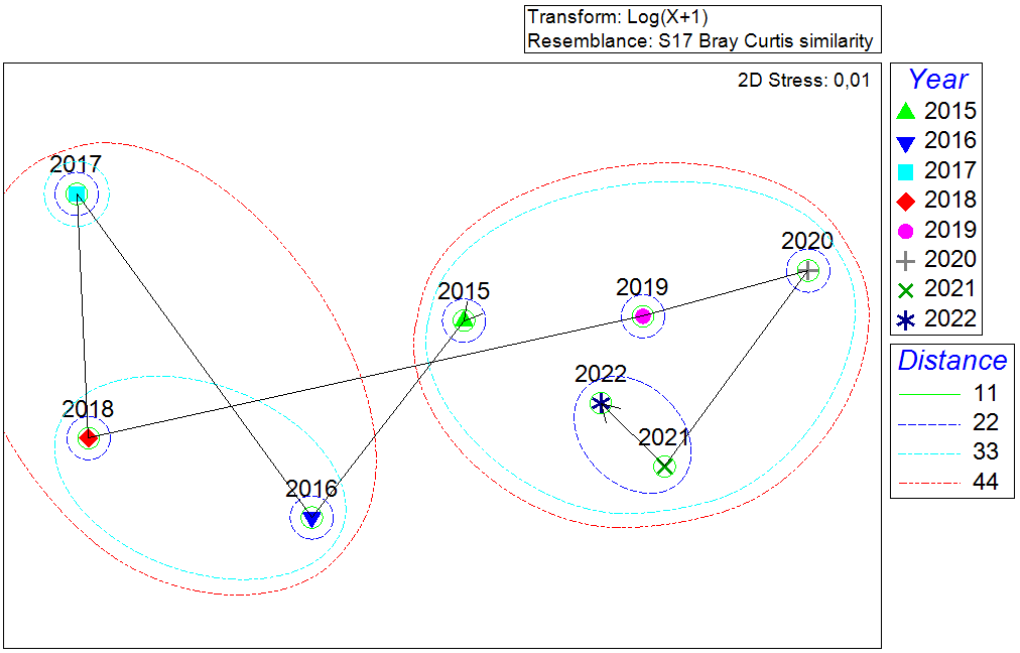

Fig. 5. MDS diagram constructed on the basis of a matrix of distances between centroids of samples from a depth of 25 m with a grouping factor of year

Dynamics of abundance and size structure of dominant species. The major contribution to biomass and its interannual variability was made by dominants of the communities: at 10 m, *Ch. gallina* and *L. divaricata*; at 25 m, *P. rudis* and *G. minima*, and also *Ch. gallina* in 2019–2022 (Fig. 6). Biomass of *Ch. gallina*, *P. rudis*, and *G. minima* underwent the greatest changes during the study period. At a depth of 10 m, the basis of abundance was ensured by *L. divaricata* and *Ch. gallina*; at 25 m, by *G. minima* and *P. rudis*, and also *Ch. gallina* in 2019–2020.

***Chamelea gallina*.** Quantitative characteristics of *Ch. gallina* samples in 2015–2022 are provided in Table 3. Abundance of the key dominant at 10-m depth fluctuated during the study period (Fig. 6A). The highest biomass was recorded in 2020–2021: the species formed 82 to 96% of the total taxocene biomass. The period of the highest abundance (2018) preceded the period of the maximum biomass (Fig. 6C). In 2018, the minimum mean weight of *Ch. gallina* individuals in the samples was registered; also, their low weight was noted in 2017 (Fig. 6E). Analysis of the size–frequency distributions showed as follows: in 2017–2018, the population consisted of 81–95% individuals with a shell length < 3 mm. Within 2017–2019, only two maximums were revealed in histograms (Fig. 7). However, in 2019, molluscs with a shell length < 3 mm (juveniles) accounted for only 20% of the studied ones, while most of them had a shell length of 7–12 mm. A similar distribution pattern was established for 2015 and 2016, but with an intermediate peak of 4–7-mm individuals. In 2020–2021, a gap between the first and second population peaks widened. There were two main population peaks: juveniles and 10–18-mm adults;

between these groups, single individuals of medium sizes were found (4–6 and 7–10 mm). In 2022, the number of population peaks increased. We have identified five maximums, but conditionally, as the sample was insufficient. The first two peaks seem to refer to juveniles, and the last one is an aggregate one, since the sample of 2022 included individuals of the maximum size for this population (in 2015–2022) – 19.7 mm.

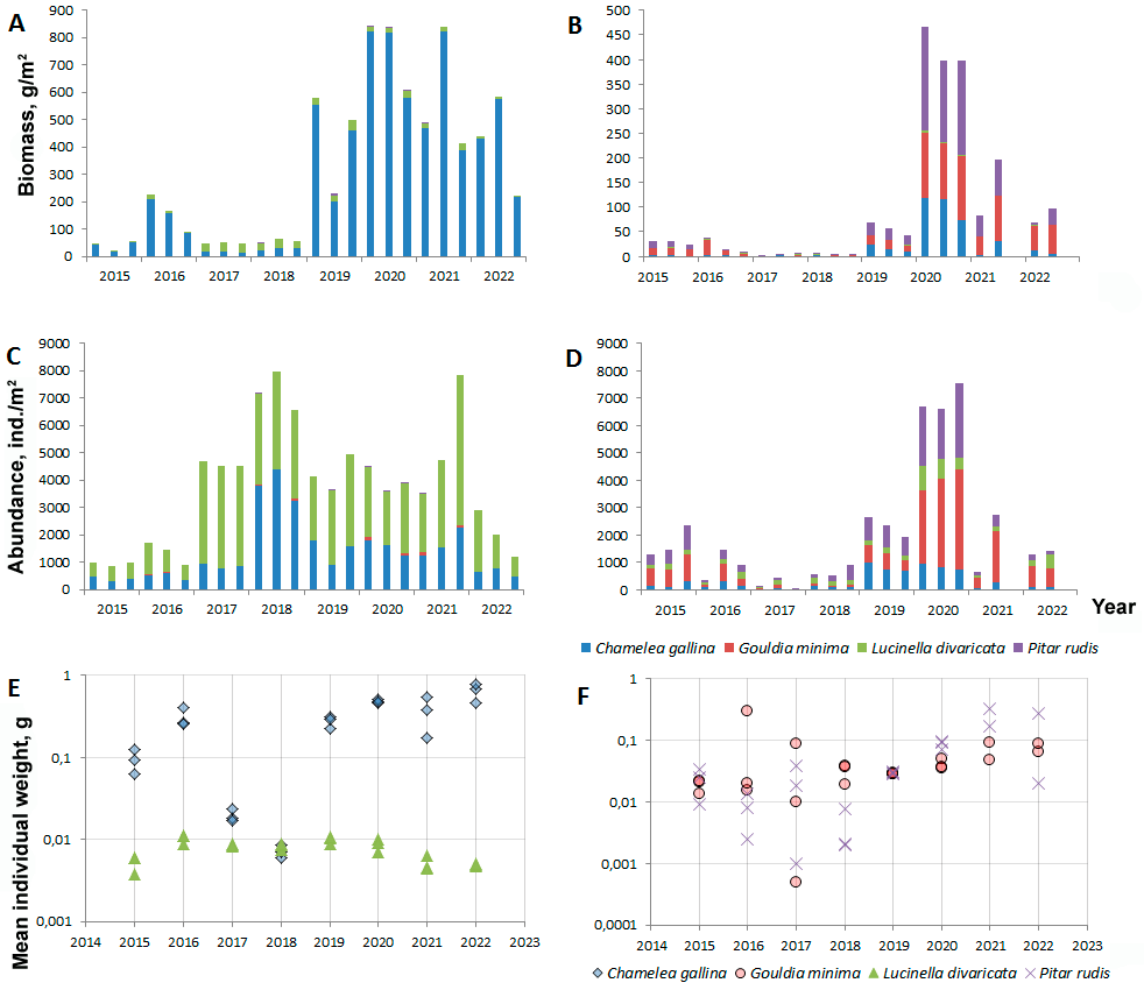

Fig. 6. Dynamics of biomass (A, B), abundance (C, D), and mean weight of individuals (E, F) of the main dominants at depths of 10 m (A, C, E) and 25 m (B, D, F) in the Inal Bay in 2015–2022

Table 3. Quantitative characteristics of *Chamelea gallina* samples in 2015–2022

Characteristics of the samples	Year							
	2015	2016	2017	2018	2019	2020	2021	2022
Total number of samples	2	3	3	1	2	2	2	3
Total number of studied individuals	84	137	228	366	249	327	329	184
Minimum shell length, mm	0.8	0.7	0.5	0.5	0.9	0.6	0.5	1.0
Mean shell length, mm	5.6	8.1	2.3	1.8	7.6	9.7	6.7	10.4
Maximum shell length, mm	12.2	17.1	13.0	8.9	13.8	17.3	19.7	19.0

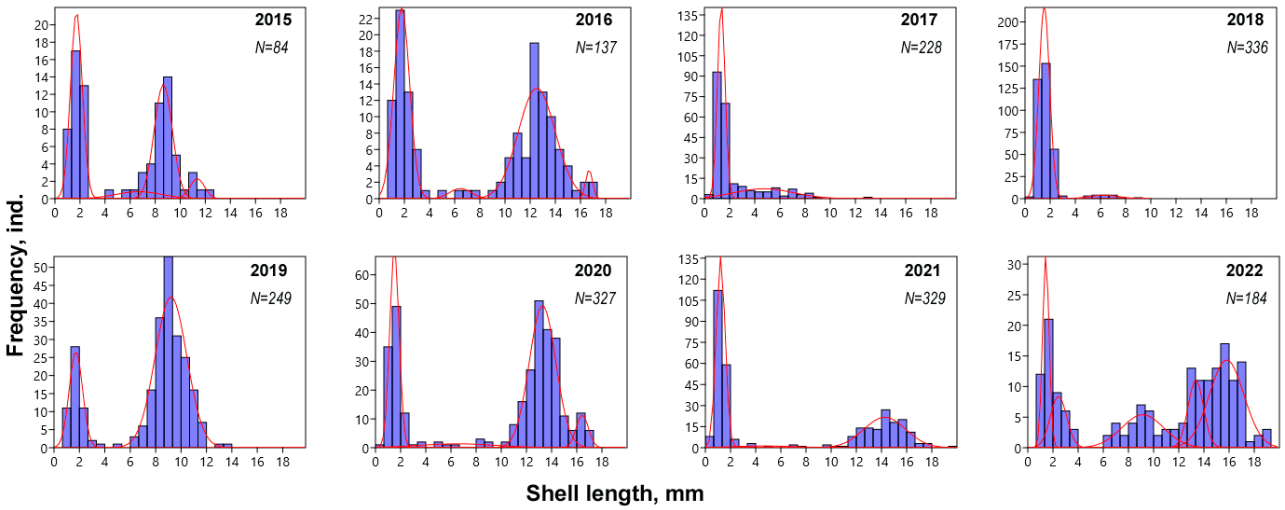

Fig. 7. Size structure of *Chamelea gallina* population in different years in the Inal Bay at a depth of 10 m. Red curves are approximation curves of normal distribution for abundance peaks (hereinafter); *N* is sample size

***Pitar rudis*.** Quantitative characteristics of *P. rudis* samples in 2015–2022 are provided in Table 4. In 2015–2016, its abundance and biomass were similar, and a mean weight of molluscs was 0.02–0.03 g. The population was represented by different-sized individuals of three size groups: 0–4, 4–6, and 6–10 mm (Fig. 8). In 2017–2018, biomass dropped by an order of magnitude, down to 1.6 g·m^{-2}. In 2017, abundance was minimum and valued to 20–60 ind.·m^{-2}. In 2017–2018, the population consisted chiefly of juveniles, and the mean weight of individuals was the lowest for the entire study period. In 2018–2020, a trend of increasing *P. rudis* biomass, abundance, and mean weight was revealed. In 2019, the population included three size groups: juveniles up to 4 mm and adults of 4–8 and 9–10 mm. In 2020, after settling of molluscs of the previous year, the population was replenished, and the proportion of juveniles reached 48%. Groups of adults identified for 2019 were indistinguishable from each other, and the histogram had only two maximums. In 2021, there were a decline in biomass and abundance and a rise in the mean size of individuals. At the same time, the proportion of juveniles accounted for only 27% of the total abundance, and this evidenced for the lack of mass settling in 2020. The view of the histogram for 2022 was similar to that for 2021, but low abundance did not allow us to reveal four peaks. Only two ones were reliably identified: those of juveniles and adults. The largest size of specimens in the samples was 15.6 mm.

Table 4. Quantitative characteristics of *Pitar rudis* samples in 2015–2022

Characteristics of the samples	Year							
	2015	2016	2017	2018	2019	2020	2021	2022
Total number of samples	3	3	3	3	3	2	2	2
Total number of studied individuals	180	64	13	76	221	427	56	37
Minimum shell length, mm	0.7	0.7	1.5	0.9	0.8	0.4	0.7	0.6
Mean shell length, mm	3.1	2.5	2.7	2.2	3.7	4.9	7.5	6.1
Maximum shell length, mm	9.5	6.8	7.8	5.5	10.2	13.2	15.6	12.9

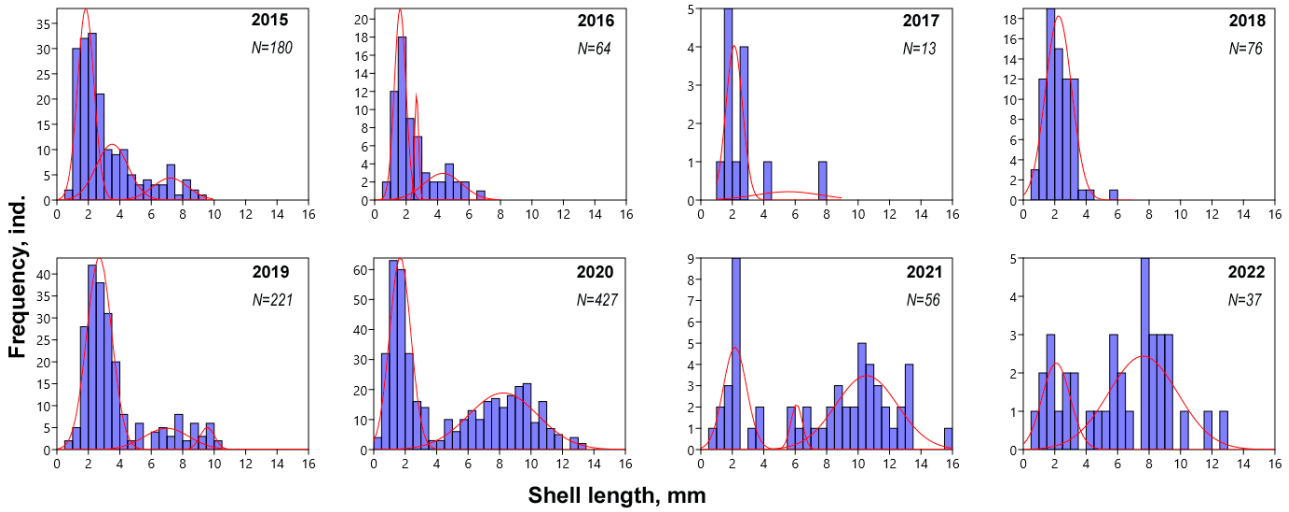

Fig. 8. Size structure of *Pitar rudis* population in different years in the Inal Bay at a depth of 25 m

Gouldia minima. Quantitative characteristics of *G. minima* samples in 2015–2022 are provided in Table 5. The pattern of changes in abundance of its population over time was generally similar to that for *P. rudis* population (these two species co-inhabit one biotope). In most cases, *G. minima* exceeded *P. rudis* in abundance, but had lower biomass. The mean weight of *G. minima* and *P. rudis* was similar. In 2016, the mean weight of *G. minima* was the highest, 0.3 g; in 2017, it had a wide range, 0.001 to 0.04 g. There were no reliable differences in the mean weight of individuals of this species in the population. Within the study period, similar to *P. rudis*, *G. minima* had the lowest biomass in 2017–2018. In 2019, biomass and abundance increased, and in 2020, they reached their maximums. In 2021–2022, a gradual decrease in these parameters was observed, but the only statistically significant difference was that between 2020 and 2022.

Table 5. Quantitative characteristics of *Gouldia minima* samples in 2015–2022

Characteristics of the samples	Year							
	2015	2016	2017	2018	2019	2020	2021	2022
Total number of samples	3	3	3	3	3	2	2	2
Total number of studied individuals	211	102	14	20	156	626	224	140
Minimum shell length, mm	0.9	1.1	2.1	2.2	1.5	0.6	0.6	1.1
Mean shell length, mm	3.9	5.0	3.3	4.2	4.6	4.6	4.7	5.9
Maximum shell length, mm	6.6	8.2	7.0	8.5	8.2	10.1	11.7	9.6

G. minima differs from the two species described above in its smaller size. The maximum shell length recorded in our survey was 11.7 mm (in 2021). Up to three peaks were observed in the histograms (Fig. 9). The first one was formed by individuals with a shell length up to 3 mm; the second, 3–6 mm; and the third, more than 6 mm. The proportion of juveniles did not exceed 29%, and this is in sharp contrast to the pattern recorded for the two previous species. Molluscs of 1.0–2.5 mm were abundant only in the samples of 2015 and 2021. The highest abundance in almost all years was provided by specimens with a shell length of 4–9 mm. There were no shifts in peaks between years. The pattern

for *G. minima* differed from that for the first two species: for this hydrobiont, in most cases, no clear separation of peaks was revealed (with no intermediate-sized individuals). The exceptions were the size histograms of 2015, 2021, and 2022.

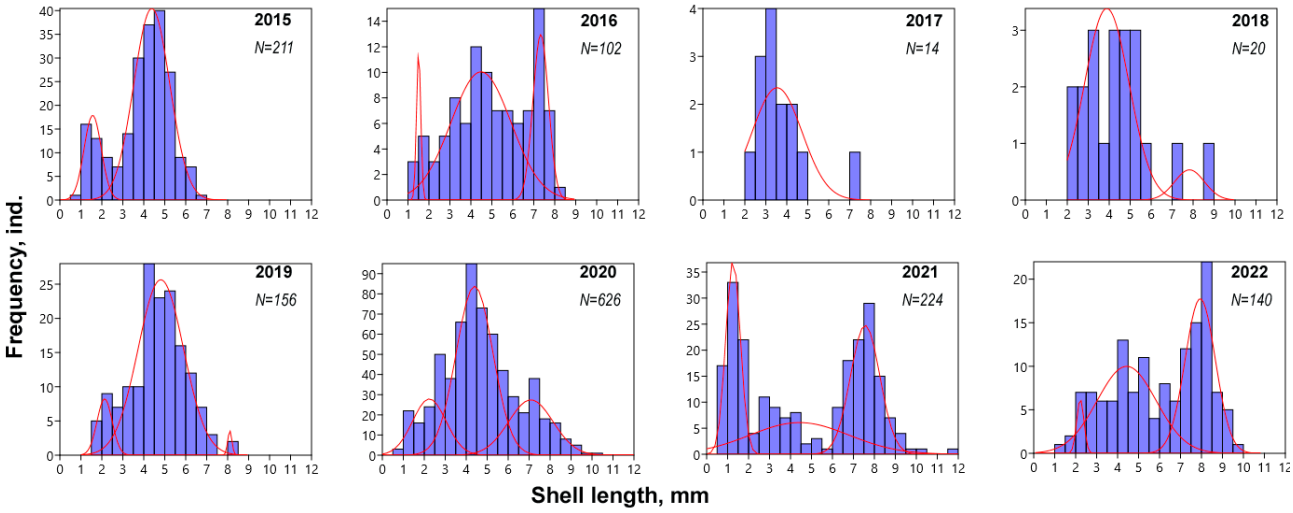

Fig. 9. Size structure of *Gouldia minima* population in different years in the Inal Bay at a depth of 10 m

Lucinella divaricata. Quantitative characteristics of *L. divaricata* samples in 2015–2022 are provided in Table 6. It is the smallest species inhabiting a depth of 10 m. This mollusc was characterized by the lowest amplitude of fluctuations in abundance, biomass, and mean weight of individuals (see Fig. 6). In 2015–2016, its abundance was low and comparable to that of the main dominant, *Ch. gallina*. Already in 2017, *L. divaricata* abundance increased fourfold compared to that for previous years and *Ch. gallina* abundance. Biomass of *L. divaricata* population rose as well. Both parameters remained stable during 2017–2021, and their values decreased slightly in 2022. *L. divaricata* population in the Inal Bay in 2015–2022 was characterized by the presence of two or three peaks in the size–frequency histograms (Fig. 10). The first one – peak of the smallest individuals with a shell length of about 0.5–2 mm (juveniles) – was registered in all years, except for 2019. The second peak, extremely abundant, included *L. divaricata* with a shell length of 2–4 mm and was also recorded in all years of the study. The third peak – that of 4–5.3-mm individuals – was the least abundant and formed by single molluscs. No shifts in peaks were noted between years, and the general view of the histograms was relatively stable.

Table 6. Quantitative characteristics of *Lucinella divaricata* samples in 2015–2022

Characteristics of the samples	Year							
	2015	2016	2017	2018	2019	2020	2021	2022
Total number of samples	3	3	1	3	2	2	2	2
Total number of studied individuals	146	256	370	570	404	373	297	353
Minimum shell length, mm	0.9	0.7	0.9	0.9	0.5	0.7	0.5	0.6
Mean shell length, mm	2.2	2.7	2.2	2.6	2.7	2.5	1.8	1.9
Maximum shell length, mm	4.5	5.1	4.9	5.3	5.3	4.6	4.7	4.9

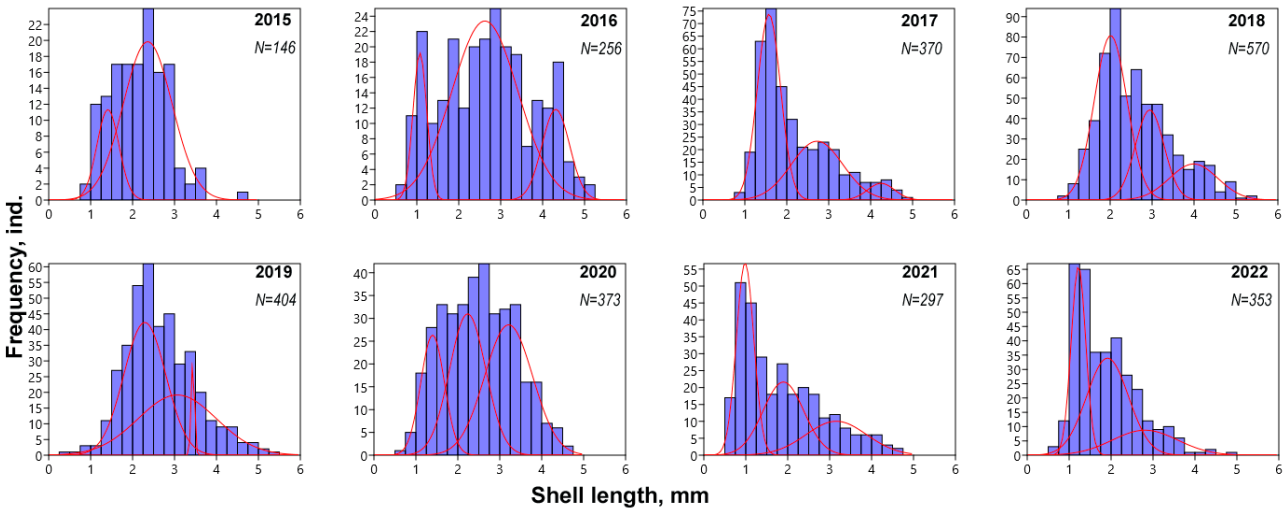

Fig. 10. Size structure of *Lucinella divaricata* population in different years in the Inal Bay at a depth of 10 m

Factors driving the taxocene structure and dynamics. We carried out a non-parametric analysis of correlations between available data on abiotic factors (mean surface water temperature in February–March at the Tuapse weather station area and grain size of sediments), *R. venosa* abundance in the samples, information on complex characteristics (abundance, biomass, and species number in the samples), and the taxocene structure (based on log-transformed biomass of species in the samples). No reliable correlations between complex characteristics and aforementioned factors were established. Habitats at 10-m and 25-m depths differed significantly in the rate of the sediment gravel fraction and summer temperature.

DistLM analysis (sequential tests) showed as follows: for a depth of 10 m, the selected predictors accounted for 45.9% of the variability. The grain size of sediments and the mean surface water temperature in February–March had a reliable linear correlation with the biotic data (Table 7, Fig. 11). The only reliable factor turned out to be the aleurite content (Table 8). It was significantly lower in the samples of the last two years (2021 and 2022). However, contribution of this factor to the explained variation of biotic data was small (21.8% only), since the population structure in 2021–2022 did not differ noticeably from that of previous years (see Fig. 4). For the taxocene at a depth of 25 m, no reliable correlations were revealed with any of the predictors available.

When comparing biomass dynamics of studied species and the proportion of juveniles in their populations, we identified no reliable relationships because of the fact that time series were too short. However, certain trends can be recorded. An outbreak of abundance of *Ch. gallina* juveniles was registered against the backdrop of low population biomass (in 2017–2018), and with a subsequent rise in biomass, there was a parallel drop in abundance of juveniles (in 2019) (Fig. 12A). A similar pattern was revealed for *G. minima* and *P. rudis* (Fig. 12C, D). It was the period of minimum mean temperatures for February–March.

In 2019–2020, there was a parallel increase in biomass and abundance of juveniles for *Ch. gallina* and *G. minima*, and in 2021, a parallel decline in these parameters. For *P. rudis*, the same as for the other two venerids, a peak in biomass was observed in 2020, but it occurred against the backdrop of a steady decrease in abundance of juveniles in the samples since 2017.

Table 7. Results of DistLM analysis of the effect of abiotic factors on Mollusca taxocene structure (optimal combinations obtained in sequential tests)

Predictor	Adjusted determination coefficient	Pseudo-*F*	*P*-value	Proportion of explained total variation
Depth of 10 m				
+Grain size	0.326	3.777	0.001	0.443
+Spatial position	0.449	3.116	0.006	0.149
+Temperature	0.649	10.710	0.001	0.163
Depth of 25 m				
+Spatial position	0.172	3.181	0.009	0.251
+Grain size	0.364	2.438	0.004	0.295
+Year	0.413	2.248	0.059	0.063
+Temperature	0.460	2.210	0.062	0.057

Table 8. Results of DistLM analysis of the effect of abiotic factors on Mollusca taxocene structure (optimal combinations obtained in sequential tests) at a depth of 10 m

Factor	Adjusted determination coefficient	Pseudo-*F*	*P*-value	Proportion of explained total variation
+Aleurite	0.183	6.137	0.001	0.218
+Temperature	0.253	3.066	0.016	0.100
+Pelite	0.329	3.387	0.017	0.099
+Sand	0.346	1.506	0.227	0.043
+Gravel	0.406	2.944	0.034	0.076

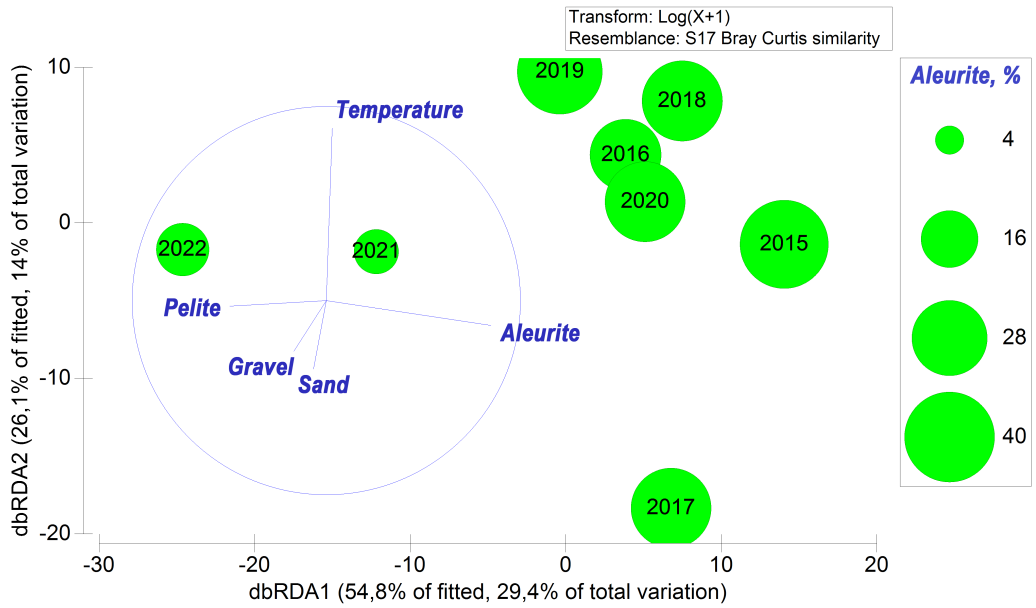

Fig. 11. Analysis of the effect of abiotic factors on Bivalvia taxocene structure by the dbRDA method within 2015–2022; similarity measure is Bray–Curtis index (based on log(x + 1)-transformed biomass); different-sized circles indicate the percentage of aleurite in bottom sediments

The dynamics of *L. divaricata* settlements was different: there were two periods with abundance of juveniles and total biomass changing in antiphase (2015–2017 and 2020–2022) and one period with parallel changes (2017–2019) (Fig. 12B). The period of the highest biomass coincided with that of the lowest temperature, when *Ch. gallina* abundance was minimal. Unlike *Ch. gallina* biomass, *L. divaricata* biomass decreased in 2017–2020.

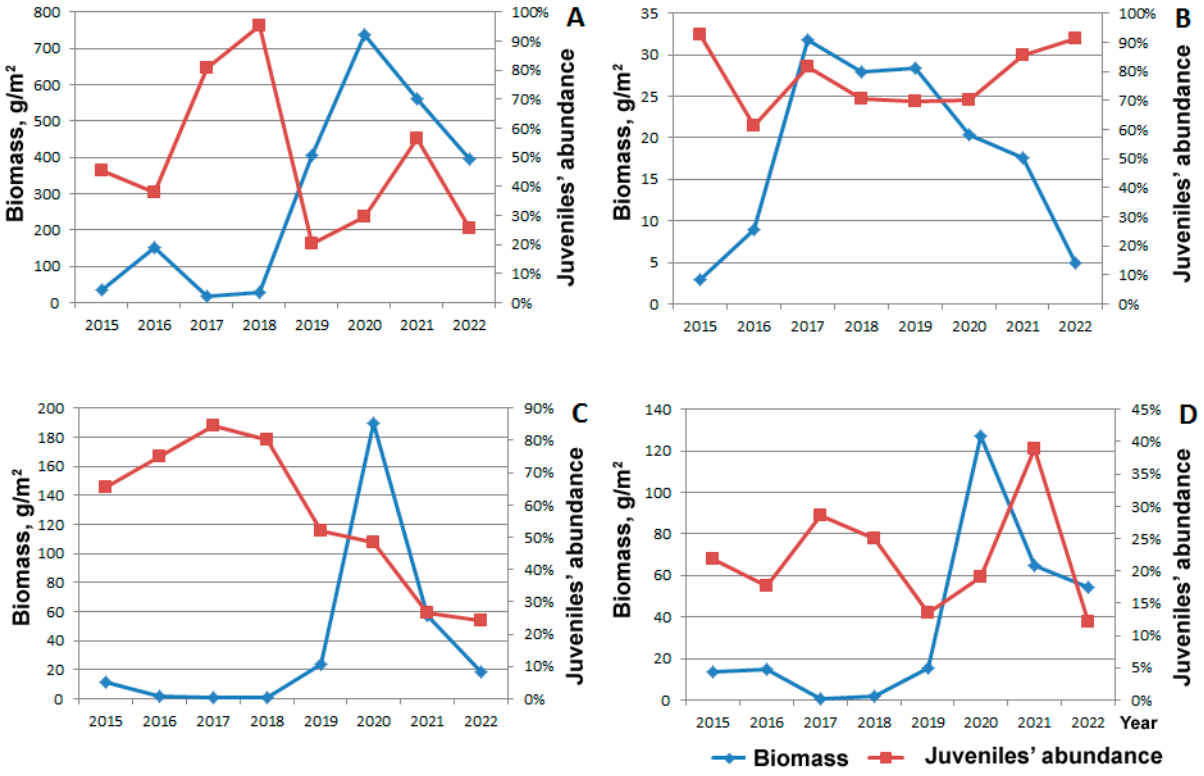

Fig. 12. Parallel changes in total biomass of population and abundance of juveniles of *Chamelea gallina* (A), *Lucinella divaricata* (B), *Pitar rudis* (C), and *Gouldia minima* (D) in the Inal Bay in 2015–2022

DISCUSSION

Dynamics of size structure and age of molluscs. In the Black Sea, all the four mollusc species studied in this work are known to have a single peak of reproduction *per* year, although extended in time [Kiseleva, 1981; Revkov et al., 2014]. *Ch. gallina* reproduces mostly in late summer, and just-settled individuals occur in samples in early autumn [Kiseleva, 1981]. Larvae are found in plankton until February [Vinogradova, 1950]. We carried out sampling in late June–early July, before new individuals of the current year appeared. In addition, the mesh size of the sieve we used (0.5 × 0.5 mm) does not allow taking into account the earliest stages, while settling *Ch. gallina* specimens have a size of 0.2 mm [Kiseleva, 1981; Zakhvatkina, 1959]. Therefore, the first peak of individuals with a shell length up to 3 mm in the size–frequency histograms for this species most likely includes molluscs that settled in autumn–winter of the previous year (a generation 0+). In winter, their growth seems to be extremely slow [Revkov et al., 2014]; according to our data, they grow only to 2.5 mm by July. A cohort 1+ covered specimens of 5–10 mm in different years, and this is consistent with the data of M. Kiseleva [1981] on growth rates of this species in the Black Sea. Adults – representatives of cohorts 1+ and more – mostly formed a continuous smoothed peak in the histograms.

In 2018, high abundance of small-sized *Ch. gallina* (0–3 mm) was recorded in benthic samples from a 10-m depth. This generation (molluscs that settled in the autumn of 2017) was found in the samples of the following year (2019) and boosted biomass in 2019. At the same time, there was no new mass settling in the autumn of 2018, and, accordingly, there was no corresponding high peak of juveniles in 2019. The mean size of individuals in the population and its total biomass increased. As a result, the next year (2020), a gap was formed between generations: either small-sized specimens of a cohort 0+, up to 3 mm, were registered or individuals larger than 10 mm were recorded, while the cohort 1+ was represented by single molluscs. This gap persisted in 2021. It allowed us to fully examine the generation of 2017 (in 2019, these individuals were aged 1+; in 2020, 2+; in 2021, 3+; and in 2022, 4+). Its abundance dropped over time, and by 2020, it became difficult to clearly distinguish it from later generations. In the autumn of 2020, there was a new abundant replenishment of *Ch. gallina* population evidenced by a peak of juveniles in the histograms of 2021. In 2022, after successful settling of molluscs of 2020, individuals of the cohort 1+ appeared again, and specimens that settled in 2017 still occurred forming a cohort 4+. In 2020, molluscs of this generation reached about 13 mm in length (2+), and in 2021, 15 mm (3+). Apparently, in 2022, size of these individuals ranged 17 to 20 mm (4+). Throughout the entire study period, there were no *Ch. gallina* with a shell length more than 20 mm, whereas in the middle of the XX century, the largest recorded size was 27 mm [Kiseleva, 1981]. Thus, according to our data, the maximum age of molluscs was at least 4.5 years. The extended period of the population replenishment during the year governs the fact that the histograms have a narrow peak of juveniles and a flatter total peak of adults which is wide due to the combination of generations with different time of settling [Chukhchin, 1965; Kiseleva, 1981; Revkov et al., 2014]. This is exactly the pattern for most cases in 2015–2022 (with the exception of 2017 and 2018). However, the population structure of this species still experiences annual fluctuations. After it was eliminated by the rapa whelk in 2003–2006, small-sized juveniles alone were noted in samples; gradual recovery began only in 2007, after a decrease in *R. venosa* abundance [Kucheruk et al., 2012]. In the early 2000s, due to massive simultaneous settling of bivalves, all individuals in the population were of similar sizes, but since the mid-2010s, the occurrence of several size groups is registered, with a dominance of juveniles.

For another species, *P. rudis*, inhabiting the Black Sea at a depth of 25 m, no published data on the lifespan were found. Our material may indirectly indicate the highest mean age of this mollusc in the study area. According to available literature information, larvae of this species are recorded in plankton in June–August [Kiseleva, 1978]. The same as *Ch. gallina*, *P. rudis* has one peak of reproduction, distributed over time, and settling occurs in autumn [Kiseleva, 1978]. Thus, the smallest individuals (1–4 mm) were apparently about 8–10 months old (0+). Such specimens formed a peak in all years of observation and, with the exception of 2021–2022, dominated in the population. We identified four size groups which seem to correspond to different mollusc generations: 0+ (up to 4 mm), 1+ (4–8 mm), 2+ (9–13 mm), and 3+ (more than 13 mm, singly registered in 2021). Individuals larger than 16 mm were not included in this sample. Importantly, hydrobionts with a shell length of 19 mm were noted in the Gelendzhik Bay in 2023 (own unpublished data); in the XX century, size of *P. rudis* reached 25 mm in the Black Sea [Kiseleva, 1981]. We found no information on the maximum age of this species in literature; based on the analysis carried out, we assume that it may be at least about 4 years. However, in most cases, we recorded simultaneously two or three size groups in the population evidently belonging to different generations. Thus, the maximum age seemed to be at least 3 years. The occurrence of younger age groups and their predominance evidence for a stable replenishment of the population, but since 2020, the intensity of replenishment declines.

G. minima was a codominant of *P. rudis* at 25 m in 2015–2022. In our samples, these species were comparable in size (up to 12 mm). Its maximum size in the Black Sea is known to be exactly 12 mm [Kiseleva, 1981]; accordingly, it is a smaller-sized species compared to the previous two. There is no material on exact reproduction period of *G. minima*; the only information covers the fact that it is observed in summer [Kiseleva, 1981]. According to our data, in the Inal Bay populations, there were fewer juveniles (up to 3 mm) in summer than medium-sized individuals in almost all years of the study. To clarify this issue, more detailed research on the maturation and spawning periods is required, along with a seasonal analysis of the population dynamics. Apparently, this species settles already in August and manages to grow by the beginning of winter, unlike *P. rudis* and *Ch. gallina*, or, settling at the same time as they do, it has a higher growth rate. Its high growth rate is confirmed by data of M. Kiseleva [1978]: June to November, *Gouldia* representatives grew by 3–4 mm, *i. e.*, in 5 months, 6-mm individuals became 9–10-mm ones. Interestingly, shell length increased from half the maximum size to almost the maximum size for this species in the Black Sea. The growth rate of *P. rudis* in the same biotope was only 2 mm in 5 months [Kiseleva, 1981]. Thus, the growth rate of *G. minima* seems to be higher than that of *P. rudis*. The maximum age of *G. minima* is also unknown [Kiseleva, 1981]. We assume that its age does not exceed three years in the study area. Firstly, we determined no more than three peaks in the histograms clearly separated from each other. Secondly, the view of the histograms was completely different from the standard form of size–frequency distributions of long-lived species [Revkov et al., 2014] characterized by a narrow and high peak of small-sized individuals and an extended and flat peak of older ones. In *G. minima*, there were no narrow and high peak of juveniles and extended peak of adults, and this may indicate a high growth rate of these molluscs because of their short lifespan. Thirdly, no clear correspondence of peaks was registered in different years. For example, in 2016, there was a peak of individuals with a shell length of about 4.5 mm; in 2017, such a peak was not observed, and the maximum was reached in specimens of about 3 mm.

Finally, *L. divaricata*, the smallest species, an inhabitant of a depth of 10 m, was characterized by the presence of two or three peaks in the histograms, the same as *G. minima*. Their intensity was much lower than even in *G. minima*. No clear separation of peaks was observed. *L. divaricata* was even smaller than *G. minima*: up to 5.3 mm. We failed to find data on the Black Sea *L. divaricata* reproduction, growth rate, and age. According to information for the western Mediterranean basin, this species reproduces in spring, and its juveniles settle in early summer [Sardá et al., 1999]. Assuming that the reproduction period is approximately the same, settling in the studied population could have occurred before we carried out the survey (late June–early July). This may explain the presence of a peak of juveniles in the histograms during the study period. The highest number of peaks we revealed is three. Therefore, we can cautiously assume as follows: off the North Caucasus, the maximum age of *L. divaricata* was no more than three years. However, according to N. Revkov *et al.* [2014], off the Crimea, such a pattern of peak distribution in size–frequency histograms of shell lengths for this species persists in other periods of the year. This contradiction necessitates further investigation on seasonal dynamics of *L. divaricata* size structure on the North Caucasus coast.

Patterns of change in the size structure of bivalves in soft sediments of the North Caucasus have been poorly studied. The latest data on the structure of Bivalvia populations were provided by M. Chikina *et al.* [2003], with a focus on an invader *A. kagoshimensis* prevailing at depths of 20–30 m. As shown, in the early 2000s, its population structure was extremely uniform: most molluscs were of similar size which resulted from mass settling in the autumn of 1999. Their growth rate was low

due to high density of populations: in 2001, *A. kagoshimensis* abundance was 2,462 ind.·m^{-2}, and in 2002, 1,420 ind.·m^{-2} [Chikina et al., 2003]. At the age of two years, the mollusc had a mean size of about 15–16 mm [Chikina et al., 2003]. According to data for the Kerch Strait, the annual growth in the first and second years of life was 17 and 12 mm, respectively (unfortunately, the population density was not indicated by the author) [Zhavoronkova et al., 2022]. In the Black Sea off the Crimea, under conditions of cage culture, this species reached a size of (27.0 ± 1.2) mm in two years [Pirkova, 2012]. A similar decrease in growth rates against the backdrop of high abundance was recorded at a depth of 10 m in the early 2000s for *Ch. gallina* [Chikina, 2009; Kucheruk et al., 2002]. As shown, in the Black Sea, its individuals were of 6–10 mm at the age of one year [Kiseleva, 1981] and 17–25 mm at the age of two years [Boltachova, Mazlumyan, 2001]. In the early 2000s, one-year-old *Ch. gallina* had a shell length of about 2–3 mm, and two-year-old ones were no more than 5 mm [Chikina, 2009]. Currently, its growth rates have risen compared to those of the early 2000s. Apparently, one of the reasons is lower abundance in populations in recent years: the total abundance does not exceed 10 thousand ind.·m^{-2} in 2015–2022 *vs.* 36 thousand ind.·m^{-2} in 2001 [Kucheruk et al., 2002]. The maximum age recorded for this long-lived species has increased as well. In the early 2000s, *Ch. gallina* age did not exceed 3 years [Chikina, 2009; Kucheruk et al., 2012]: individuals settled in 1999 were completely eliminated by 2003 by the rapa whelk. Currently, there is another pattern. Thus, many *Ch. gallina* specimens that settled in 2017 were still alive in 2022 (their age was about 4.5 years).

Dynamics of Mollusca taxocene off the North Caucasus. In the 2000s, invaders (*R. venosa* and *A. kagoshimensis*) played an important role in benthic communities of soft sediments off the North Caucasus [Chikina, 2009; Kucheruk et al., 2012]. Already in the 2010s, according to our data, the former autochthonous dominants came to the forefront: *Ch. gallina*, *L. divaricata*, *P. rudis*, and *G. minima*. Besides, in a community of depths of 10–30 m, minor species began to be recorded again: *S. subtruncata* and *D. semistriatus* [Kolyuchkina et al., 2020; this study]; their abundance was extremely low in the early XXI century [Chikina, 2009; Kucheruk et al., 2002]. This evidences for a gradual recovery of the taxocene structure after disastrous transformations of the early XXI century. However, it is unreasonable to claim that the taxocene structure has returned to the pre-crisis state. Abundance and biomass of dominant species, along with the size structure of their populations, still experience annual fluctuations. Shifts in taxocene abundance and size structure of mollusc populations could be governed by both changes in abiotic factors and food abundance or interspecific/intraspecific interactions. No reliable correlations were established between biomass, abundance, and species number in the taxocene, as well as biomass and abundance of analyzed species, available environmental characteristics, and *R. venosa* abundance. However, the analysis of the taxocene structure by biomass showed that the proportion of explained variation in biotic data for a depth of 10 m due to the grain size of sediments was 44.3%. At the same time, the grain size differed for the last two years only. Thus, in 2021, a low content of silt fractions was determined. In 2021, the content of aleurite was still low, but that of pelite rose by 3.5 times compared to 2021 and was 2 times higher than within 2015–2020 (see Fig. 1A). The second factor that significantly contributed to the variation in biotic data was the mean temperature in February–March. Its variability accounted for 16.3% of the variation. Against the backdrop of relatively similar annual values, temperatures in February–March were lower in 2017 and 2022 (see Fig. 1B).

The study period covered years with different temperature conditions. The winter of 2016–2017 was severe [Podymov et al., 2021]. Back then, abundance and biomass of molluscs were relatively low both at 10 and 25 m, and large individuals occurred rarely. Apparently, it was directly and/or indirectly

driven by temperature conditions. A prolonged cold period could have caused death of both adult molluscs and specimens that settled in autumn. Moreover, cold winters tend to mediate later spring bloom of phytoplankton – the main food source for bivalves. With a gain in water temperature and salinity in 2019–2020 [Chasovnikov, Borodulina, 2022; Podymov et al., 2021], there was a trend of restoring the taxocene abundance and biomass. After low abundance registered by 2020, the taxocene, on the contrary, was characterized by extremely high values of abundance and biomass of molluscs. In 2021, after two years of drought, there was an almost twofold rise in precipitation level, and river runoff increased [Korshenko et al., 2022]. This caused an outbreak of diatoms [Chasovnikov, Borodulina, 2022] which are the key food of the studied bivalves [Kiseleva, 1981]. The trend appeared to continue in 2022: that year, against the backdrop of heavy flood, an extreme outbreak of coccolithophore bloom was recorded in spring [Korshenko et al., 2022]. However, there was no further growth in biomass of molluscs. Quite a similar pattern was observed during the crisis in the northwestern Black Sea in the late XX century, when anthropogenic eutrophication governed a cascade of events that led to annual suffocation in the bottom layer [Bologa et al., 1995]. One of phenomena of that period was annual abundant phytoplankton bloom. Interestingly, despite high food availability, there was no increase in abundance, but rather suppression of benthic filter feeders. However, it is hard to assume that stable hypoxia zones, let alone suffocation zones, can be formed on the open shelf in the upper quasi-homogeneous layer, with its significant and constant wave action. Another explanation for a drop in biomass in 2021–2022 may be the pressure by adults on planktonic larvae: a phenomenon reported for coastal ecosystems [André et al., 1993]. According to our data, after the mass settling of *Ch. gallina* in 2017 which resulted in a peak of juveniles in July 2018, high abundance of large molluscs was noted in the next two years (2019 and 2020), and juveniles were approximately 2–3 times less abundant than large individuals (see Fig. 12). A new abundant replenishment occurred only in 2021 – against the backdrop of a decrease in abundance of large specimens parallel with a gain in their mean size.

We cannot rule out the role of interspecific interactions in regulating abundance of the surveyed bivalve populations. Thus, mass settling in 1999 was most likely caused by limitation of the pressure by a planktotrophic species *M. leidyi* on larval stages of bivalves and absence of adults due to predation by the rapa whelk [Kucheruk et al., 2002]. During the study period (2015–2022), cases of mass settling of bivalves were registered as well: in 2017, *Ch. gallina* and *L. divaricata*; in 2020, *P. rudis*; and in 2021, *G. minima*. The same as in 1999, this was preceded by a drop in abundance of adult individuals. However, in 2015–2022, a decline in abundance was not so dramatic: values of macrozoobenthos biomass roughly corresponded to those of the middle of the XX century [Kiseleva, 1981]. In the mid-2010s, no outbreaks of *R. venosa* abundance were recorded; within the study period, single medium-sized rapa whelks were occasionally found in samples. Thus, the pressure by this predator unlikely triggered mass settling. The pressure by jellyfish on planktonic mollusc larvae in the mid-2010s significantly decreased, and the planktonic community reached an equilibrium state by 2014 [Arashkevich et al., 2015]. Apparently, this largely governs the occurrence of annual replenishment by juveniles for all benthic species. During the study period, the species under the most pressure by jellyfish were those whose larvae appeared in plankton during late spring–early summer, *i. e.*, in the season of mass reproduction of *M. leidyi*, their main consumer [Louppova, 2017]. However, due to water warming off the northeastern Black Sea in recent years, *Beroe ovata*, an obligate ctenophore feeding on the warty comb jelly, appears already in June-July, not in August, as in the early 2000s [Martynyuk, 2017]. This reduces the probability of the fact that *M. leidyi* would eat away planktonic larvae of benthic animals

during summer and autumn. *M. leidyi* could affect *L. divaricata* alone if its reproduction occurred in late spring–early summer. However, very high abundance was recorded for this species, and this may indirectly evidence for success of its population in the study area. Abundant settling of *L. divaricata* in 2017 may have resulted from the suppression of *Ch. gallina* populations inhabiting the same biotope during this period.

Conclusions:

1. In 2015–2022, *Chamelea gallina* and *Lucinella divaricata* dominated at a depth of 10 m, and *Pitar rudis* and *Gouldia minima* prevailed at 25 m. No stabilization of abundance of these species was revealed during the study period. In 2020, an outbreak of their biomass was recorded at depths of 10 and 25 m. In 2021–2022, a decline in biomass was observed.
2. The size structure of populations of the surveyed species was unstable in 2015–2021, but small-sized molluscs from the previous-year settling were registered in the populations almost every year. The only exception was *G. minima*: its small-sized individuals were noted in 2015 and 2021 alone. The most successful generation was that of *Ch. gallina* – the generation of 2017.
3. The highest age of molluscs determined by the cohort method in the investigated populations in 2015–2022 was 4.5 years for *Ch. gallina*, 3.5 years for *P. rudis*, and about 3 years for *G. minima*. To confirm an assumption that *L. divaricata* reproduction is confined to the late spring, additional research is required covering seasonal changes in the size structure of populations and the stage of gonad maturation.
4. The key factors driving the population dynamics of the analyzed species in the modern period seem to be abiotic ones (grain size of sediments and temperature). The period of low temperatures coincided with low abundance of the leading species of the taxocene: *Ch. gallina*, *P. rudis*, and *G. minima*. The period of their declining biomass coincided with a decrease in the content of aleurite in bottom sediments.

The work was supported by the Russian Science Foundation grant No. 23-27-00181

Acknowledgments. The authors are extremely grateful to all colleagues who participated in sampling in 2015–2022: U. Simakova, A. Basin, M. Simakov, V. Timofeev, V. Syomin, A. Vedenin, V. Kokarev, and V. Svasyan, as well as the crew of the small research vessel “Ashamba.”

REFERENCES

1. Alekseev R. P., Sinegub I. A. Macrozoobenthos and bottom biocenoses from the Black Sea shelves off the Caucasus, Crimea and Bulgaria. In: *Ecology of the Black Sea Coastal Areas* : collected papers / V. V. Sapozhnikov (Ed.). Moscow : VNIRO, 1992, pp. 218–234. (in Russ.)
2. Arashkevich E. G., Louppova N. E., Nikishina A. B., Pautova L. A., Chasovnikov V. K., Drits A. V., Podymov O. I., Romanova N. D., Stanichnaya R. R., Zatsepin A. G., Kuklev S. B., Flint M. V. Marine environmental monitoring in the shelf zone of the Black Sea: Assessment of the current state of the pelagic ecosystem. *Okeanologiya*, 2015, vol. 55, no. 6, pp. 964–970. (in Russ.). https://doi.org/10.7868/S0030157415060015
3. Boltachova N. A., Mazlumyan S. A. The linear growth and lifetime of *Chamelea gallina* (Bivalvia: Veneridae) in the Black Sea. *Ekologiya morya*, 2001, iss. 55, pp. 50–52. (in Russ.). https://repository.marine-research.ru/handle/299011/4385

4. Vinogradova Z. A. Materialy po biologii mollyuskov Chernogo morya. *Trudy Karadagskoi biologicheskoi stantsii*, 1950, iss. 9, pp. 100–159. (in Russ.). https://repository.marine-research.ru/handle/299011/6718
5. Vorob'ev V. P. *Bentos Azovskogo morya.* Simferopol : Krymizdat, 1949, 193 p. (Trudy AzCherNIRO ; iss. 13). (in Russ.)
6. Golikov A. N., Starobogatod Ya. I. Klass bryukhonogie molluski – Gastropoda. In: *Opredelitel' fauny Chernogo i Azovskogo morei*. Vol. 3 : *Svobodnozhivushchie bespozvonochnye. Chlenistonogie (krome rakoobraznykh), mollyuski, iglokozhie, shchetinkochelyustnye, khordovye* / V. A. Vodyanitsky (Ed.). Kyiv : Naukova dumka, 1972, pp. 65–166. (in Russ.). https://repository.marine-research.ru/handle/299011/6078
7. Zhavoronkova A. M., Sytnik N. A., Zolotnitsky A. P. Age composition and linear growth of the invasive ark clam species (*Anadara kagoshimensis* (Tokunaga, 1906)) in the Kerch Strait. *Vodnye resursy i sreda obitaniya*, 2022, vol. 5, no. 1, pp. 45–55. (in Russ.). https://elibrary.ru/jgjqki
8. Zhirkov I. A. *Zhizn' na dne. Bioekologiya i biogeografiya bentosa.* Moscow : KMK Scientific Press, 2010, 453 p. (in Russ.). https://elibrary.ru/qksrxf
9. Zakhvatkina K. A. Lichinki dvustvorchatykh mollyuskov Sevastopol'skogo raiona. *Trudy Sevastopol'skoi biologicheskoi stantsii*, 1959, vol. 11, pp. 108–152. (in Russ.). https://repository.marine-research.ru/handle/299011/5397
10. Kiseleva M. I. *Bentos rykhlykh gruntov Chernogo morya.* Kyiv : Naukova dumka, 1981, 165 p. (in Russ.). https://repository.marine-research.ru/handle/299011/8133
11. Kiseleva M. I. Peculiarities of size composition of bivalves populations inhabiting different zones of biotope. *Gidrobiologicheskii zhurnal*, 1978, vol. 14, no. 1, pp. 54–58. (in Russ.). https://repository.marine-research.ru/handle/299011/10110
12. Kiseleva M. I. Sravnitel'naya kharakteristika donnykh soobshchestv u poberezh'ya Kavkaza. In: *Mnogoletnie izmeneniya zoobentosa Chernogo morya* / V. E. Zaika (Ed.). Kyiv : Naukova dumka, 1992, pp. 84–99. (in Russ.). https://repository.marine-research.ru/handle/299011/5644
13. Kolyuchkina G. A., Syomin V. L., Grigorenko K. S., Basin A. B., Lyubimov I. V. The role of abiotic factors in the vertical distribution of macrozoobenthos on the northeastern Black Sea coast. *Zoologicheskii zhurnal*, 2020, vol. 99, iss. 7, pp. 784–800. (in Russ.). https://doi.org/10.31857/S0044513420070053
14. Korshenko E. A., Panasenkova I. I., Osadchiev A. A., Belyakova P. A. Synoptic and seasonal variability of small river plumes in the northeastern part of the Black Sea. In: *Marine Research and Education (MARESEDU) – 2022* : proceedings of the XI International conference, Moscow, 24–28 October, 2022. Tver : PoliPRESS, 2022, vol. 2 (4), pp. 236–240. (in Russ.). https://elibrary.ru/ehtque
15. Kucheruk N. V., Basin A. B., Kotov A. V., Chikina M. V. Macrobenthos of crumbly sediments of the Black Sea Caucasian coast: Long-term dynamics of the communities. In: *Multi-Disciplinary Investigations of the North-Eastern Part of the Black Sea* / A. G. Zatsepin, M. V. Flint (Eds). Moscow : Nauka, 2002, pp. 289–297. (in Russ.)

16. Kucheruk N. V., Flint M. V., Maksimova O. V., Chikina M. V., Simakova U. V. Sovremennaya dinamika bentosnykh soobshchestv severo-vostochnogo shel'fa Chernogo morya. In : *The Change of the Natural Environment of Russia in the XX Century* / V. M. Kotlyakov, D. I. Lyuri (Eds). Moscow : Molnet, 2012, pp. 274–287. (in Russ.)
17. Louppova N. E. Coadaptation of Black Sea cross-crops *Beroe ovata* Mayer and *Mnemiopsis leidyi* A. Agassiz. *Mezhdunarodnyi zhurnal gumanitarnykh i estestvennykh nauk*, 2017, no. 9, pp. 12–15. (in Russ.). https://elibrary.ru/zhzkxt
18. Martynyuk M. L. Features of development of invasive Ctenophora *Mnemiopsis leidyi* (A. Agassiz, 1865) and *Beroe ovata* Mayer, 1912 in the north-eastern Black Sea. In: *Proceedings of AzNIIRKh (rezul'taty rybokhozyaistvennykh issledovanii v Azovo-Chernomorskom basseine)* : sbornik nauchnykh trudov po rezul'tatam issledovanii za 2014–2015 gg. / V. N. Belousov (Eds). Rostov-on-Don : AzNIIRKh, 2017, vol. 1, pp. 97–103. (in Russ.). https://elibrary.ru/vlcolz
19. *Mitilidy Chernogo morya* / V. E. Zaika (Ed.) ; AN USSR, Institut biologii yuzhnykh morei imeni A. O. Kovalevskogo. Kyiv : Naukova dumka, 1990, 208 p. (in Russ.). https://repository.marine-research.ru/handle/299011/1459
20. Pirkova A. V. Growth of bivalve mollusk *Anadara inaequivalvis* (Bivalvia) in the Black Sea while growing in cages. In: *Current Fishery and Environmental Problems of the Azov–Black Sea Region* : materials of VII International conference, Kerch, 20–23 June, 2012. Kerch : YugNIRO Publishers, 2012, vol. 2, pp. 73–78. (in Russ.). https://elibrary.ru/yscpwo
21. Revkov N. K., Timofeev V. A., Lisitskaya E. V. Composition and seasonal dynamics of macrozoobenthos in local biotic complex *Chamelea gallina* (Western Crimea, the Black Sea). *Ekosistemy*, 2014, no. 11 (30), pp. 247–259. (in Russ.). https://elibrary.ru/vkczqp
22. Revkov N. K. Fluffy bottom bed zoobenthos longstanding changes in the southwest Crimea region. In: *Modern Condition of Biological Diversity in Near-shore Zone of Crimea (the Black Sea Sector)* / V. N. Eremeev, A. V. Gaevskaya (Eds) ; NAS of Ukraine, Institute of Biology of the Southern Seas. Sevastopol : EKOSI-Gidrofizika, 2003, pp. 222–229. (in Russ.). https://repository.marine-research.ru/handle/299011/1467
23. Romankevich E. A., Vetrov A. A. *Tsikl ugleroda v arkticheskikh moryakh Rossii.* Moscow : Nauka, 2001, 302 p. (in Russ.)
24. Selifonova Zh. P., Chasovnikov V. K. Ecological condition of zoobenthos on the Caucasus coast near Dzhubga – Khosta (the Black Sea). *Sistemy kontrolya okruzhayushchei sredy*, 2017, no. 10 (30), pp. 119–128. (in Russ.). https://elibrary.ru/qjgrpb
25. Frolenko L. N., Zhivoglyadova L. A. Status of the *Chamelea gallina* and *Pitar rudis* communities in the north-eastern Black Sea in the autumn of 2019. *Vodnye resursy i sreda obitaniya*, 2020, vol. 3, no. 3, pp. 45–55. (in Russ.). https://doi.org/10.47921/2619-1024_2020_3_3_45
26. Frolenko L. N., Zhivoglyadova L. A., Kovalev E. A. Results of the zoobenthos studies in the north-eastern Black Sea according to the data obtained in 2016–2017. *Vodnye resursy i sreda obitaniya*, 2019, vol. 2, no. 4, pp. 85–97.

(in Russ.). https://doi.org/10.47921/2619-1024_2019_2_4_85
27. Chasovnikov V. K., Borodulina P. A. Trends in the interannual variability of nutrients in the northeastern part of the Black Sea according to ship observations for 2017–2021. *Ekologiya gidrosfery*, 2022, no. 2 (8), pp. 37–46. (in Russ.). https://doi.org/10.33624/2587-9367-2022-2(8)-37-46
28. Chikina M. V. *Makrozoobentos rykhlykh gruntov severokavkazskogo poberezh'ya Chernogo morya: prostranstvennaya struktura i mnogoletnyaya dinamika.* [dissertation]. Moscow, 2009, 116 p. (in Russ.). https://elibrary.ru/nqjfxd
29. Chikina M. V., Koluchkina G. A., Kucheruck N. V. Some features of reproduction biology of *Scapharca inaequivalvis* (Bruguière) (Bivalvia, Arcidae) in the Black Sea. *Ekologiya morya*, 2003, iss. 64, pp. 72–77. (in Russ.). https://repository.marine-research.ru/handle/299011/4597
30. Chukhchin V. D. Biologiya razmnozheniya *Venus gallina* L. (Lamellibranchiata) v Chernom more. In: *Bentos* : sbornik statei. Kyiv : Naukova dumka, 1965, pp. 15–23. (in Russ.). https://repository.marine-research.ru/handle/299011/97
31. Shalovenkov N. N. Tendencies of invasion of alien zoobenthic species into the Black Sea. *Rossiiskii zhurnal biologicheskikh invazii*, 2020, vol. 13, no. 1, pp. 72–80. (in Russ.). https://elibrary.ru/bpcrvn
32. Akaike H. A new look at the statistical model identification. *IEEE Transactions on Automatic Control*, 1974, vol. 19, no. 6, pp. 716–723. https://doi.org/10.1109/TAC.1974.1100705
33. Anderson M. J. A new method for non-parametric multivariate analysis of variance. *Austral Ecology*, 2001, vol. 26, iss. 1, pp. 32–46. https://doi.org/10.1111/j.1442-9993.2001.01070.pp.x
34. André C., Jonsson P. R., Lindegarth M. Predation on settling bivalve larvae by benthic suspension feeders: The role of hydrodynamics and larval behaviour. *Marine Ecology Progress Series*, 1993, vol. 97, no. 2, pp. 183–192.
35. Bologa A. S., Bodeanu N., Petranu A., Țigănuș V., Zaitsev Yu. P. Major modifications of the Black Sea benthic and planktonic biota in the last three decades. In: *Les mers tributaires de Méditerranée* / F. Briand (Éd.). Monaco : Musée océanographique, 1995, pp. 85–110. (Bulletin de l'Institut oceanographique, Monaco, n° special 15 ; CIESM, Science Series no. 1).
36. Chao A. Estimating the population size for capture-recapture data with unequal catchability. *Biometrics*, 1987, vol. 43, iss. 4, pp. 783–791. https://doi.org/10.2307/2531532
37. Chikina M. V., Kucheruk N. V. Long-term changes in the structure of coastal benthic communities in the northeastern part of the Black Sea: Influence of alien species. *Oceanology*, 2005, vol. 45, suppl. 1, pp. 176–182. https://elibrary.ru/ljkvgr
38. Clarke K. R., Gorley R. N. *PRIMER v6: User Manual. Tutorial.* Plymouth : PRIMER-E, 2006, 190 p.
39. Dempster A. P., Laird N. M., Rubin D. B. Maximum likelihood from incomplete data *via* the EM algorithm. *Journal of the Royal Statistical Society: Series B (Methodological)*, 1977, vol. 39, iss. 1, pp. 1–22. https://doi.org/10.1111/j.2517-6161.1977.tb01600.x
40. Dumitrache C., Abaza V. The present state

of benthic communities in the Romanian coastal waters. *Cercetări Marine – Recherches Marines*, 2004, no. 35, pp. 61–75.

41. *Exotic Species in the Aegean, Marmara, Black, Azov and Caspian Seas* / Yu. P. Zaitsev, B. Öztürk (Eds). Istanbul : Turkish Marine Research Foundation, 2001, 267 p.
42. Marinov T., Stoykov S. Seasonal investigations of macrozoobenthos in the Bulgarian shelf of Black Sea. *Oceanology [Bulgarian Academy of Sciences]*, 1990, vol. 19, pp. 49–62. (in Bulg.)
43. Podymov O. I., Zatsepin A. G., Ocherednik V. V. Increase of temperature and salinity in the active layer of the north-eastern Black Sea from 2010 to 2020. *Physical Oceanography*, 2021, vol. 28, no. 3, pp. 257–265. https://doi.org/10.22449/1573-160X-2021-3-257-265
44. Revkov N. K., Boltacheva N. A., Timofeev V. A., Bondarev I. P., Bondarenko L. V. Macrozoobenthos of the Zernov's *Phyllophora* field, northwestern Black Sea: Species richness, quantitative representation and long-term variations. *Nature Conservation Research. Zapovednaya nauka*, 2018, vol. 3, no. 4, pp. 32–43. https://doi.org/10.24189/ncr.2018.045
45. Sardá R., Pinedo S., Martin D. Seasonal dynamics of macroinfaunal key species inhabiting shallow soft-bottoms in the Bay of Blanes (NW Mediterranean). *Acta Oecologica*, 1999, vol. 20, iss. 4, pp. 315–326. https://doi.org/10.1016/S1146-609X(99)00135-6
46. Tiganus V. Present state of marine biodiversity in the Romanian Black Sea waters. In: *CIESM Workshop on Mediterranean Marine Biodiversity*, Nicosia (Cyprus), 1–3 May, 1997. [Monaco] : [Commission International pour l'Exploration Scientifique de la Mer Méditerranée], 1997, pp. 61–62. (CIESM Workshop Series ; n° 1).
47. *WoRMS. World Register of Marine Species* : [site]. URL: https://www.marinespecies.org/ [accessed: 10.10.2023].

ТАКСОЦЕН МОЛЛЮСКОВ РЫХЛЫХ ГРУНТОВ ПРИБРЕЖНОЙ ЗОНЫ СЕВЕРО-ВОСТОЧНОГО СЕКТОРА ЧЁРНОГО МОРЯ В НАЧАЛЕ XXI ВЕКА

Г. А. Колючкина[1], И. В. Любимов[1], Н. А. Данилова[1,2]

[1]Институт океанологии имени П. П. Ширшова РАН, Москва, Российская Федерация

[2]Российский государственный аграрный университет — МСХА имени К. А. Тимирязева, Москва, Российская Федерация

E-mail: *galka.sio@gmail.com*

В условиях нарастающих климатических и антропогенных изменений одной из наиболее актуальных задач современной экологии является понимание взаимосвязи динамики морских экосистем и окружающей среды. В то же время далеко не все происходящие в морских шельфовых экосистемах изменения можно объяснить влиянием внешних факторов, поскольку динамика экосистем, связанная с действием внутренних процессов, таких как естественные сукцессии, известна фрагментарно. Донные сообщества играют ведущую роль в функционировании экосистем, модифицируя среду обитания, влияя на круговорот питательных веществ и первичную продуктивность. С донными экосистемами связывают возможность иммобилизации и секвестра углерода, оценка которых остаётся фундаментальной научной задачей. Прибрежные сообщества Чёрного моря являются удобной моделью для такого рода исследований. Здесь доминирующие позиции в бентосе занимают карбонатпродуцирующие организмы — моллюски.

Целью настоящей работы было изучение динамики обилия и популяционной структуры моллюсков рыхлых грунтов прибрежной зоны северокавказского побережья Чёрного моря в 2015–2022 гг. Выполнены ежегодные сборы материала на глубинах 10 и 25 м. Проанализированы структура таксоцена моллюсков и динамика размерной структуры поселений его основных доминантов: на 10-м глубине — *Chamelea gallina* и *Lucinella divaricata*, а на 25-м глубине — *Gouldia minima* и *Pitar rudis*. Колебания обилия этих видов достигали порядка величин. Наибольшие биомассы таксоцена отмечены в 2020 г., что совпало с максимальными значениями температуры и солёности поверхностных вод (с засушливым периодом). Выявлено успешное ежегодное пополнение, установлен мультимодальный вид размерно-частотных диаграмм этих моллюсков, за исключением *G. minima*, ювенильные стадии которой в пробах практически не встречались. На основании анализа размерно-частотных диаграмм сделана попытка оценить средний предельный возраст особей в поселениях этих видов. Не выявлено линейных зависимостей между значениями абиотических факторов и структурой таксоцена. Охарактеризованы тенденции параллельного изменения обилия ювенильных особей в поселениях и общей биомассы каждого из исследованных видов.

Ключевые слова: Чёрное море, двустворчатые моллюски, макрозообентос, динамика поселений

1871
ИнБЮМ – IBSS

Морской биологический журнал
Marine Biological Journal
2025, vol. 10, no. 2, pp. 61–66
https://marine-biology.ru

UDC 591.69-731.77-512.2

FIND OF A TREMATODE *HELICOMETRA FASCIATA* (RUD., 1819) SENSU LATO FROM THE BLACK SEA COMMON STINGRAY *DASYATIS PASTINACA* (LINNAEUS, 1758)

© 2025 **Yu. Kornyychuk**

A. O. Kovalevsky Institute of Biology of the Southern Seas of RAS, Sevastopol, Russian Federation
E-mail: *kornyychuk@ibss-ras.ru*

Received by the Editor 10.12.2024; after reviewing 12.02.2025;
accepted for publication 20.03.2025.

A trematode belonging to *Helicometra fasciata* sensu lato (family Opecoelidae) was found for the first time from the Black Sea common stingray, *Dasyatis pastinaca* (Linnaeus, 1758), caught in the Karkinitsky Bay (western coast of the Crimean Peninsula). A drawing and a morphological description of marita are provided. The find of this trematode from the common stingray is consistent with the data on *Helicometra* life cycle in the Black Sea. This is the first record of *Helicometra* spp. from cartilaginous fishes. The common stingray is classified as an accidental definitive host of these trematodes in the Black Sea. Dasyatidae is believed to be an undersampled host group for digenean infection in the Black Sea.

Keywords: Trematoda, Opecoelidae, Chondrichthyes, Batomorphi, Dasyatidae, new definitive host, Black Sea, food webs

Trematodes *Helicometra fasciata* (Rudolphi, 1819) Odhner, 1902 feature extremely broad specificity to final hosts – bony fishes from 51 families [Blend, Dronen, 2015]. For the first time, we have registered these trematodes from a cartilaginous fish – a stingray *Dasyatis pastinaca* (Linnaeus, 1758) caught in the Black Sea.

This article is focused on the morphological description of this extremely interesting find.

MATERIAL AND METHODS

The total balsam slide of a trematode No. 1439.Tr.39 is studied [label: the host, *D. pastinaca*, intestine, 16.05.2015; the Black Sea, the Karkinitsky Bay (Swan Islands); sampler, M. Maslennikova]. It is deposited in a subcollection of parasitic organisms of the IBSS Collection of Hydrobionts of the World Ocean (http://marineparasites.org/). For species identification of a trematode, we used an Olympus CX41 microscope with a CAM SC50 digital camera and CellSens Standard v. 1.18 software. In the text, all measurements are given in micrometers. Shape index is calculated as the ratio of the object length to its width. When describing eggs, their maximum sizes (min–max) and arithmetic means are provided.

RESULTS

On a slide, there is one mature marita of *Helicometra fasciata* (Rudolphi, 1819) sensu lato (Fig. 1).

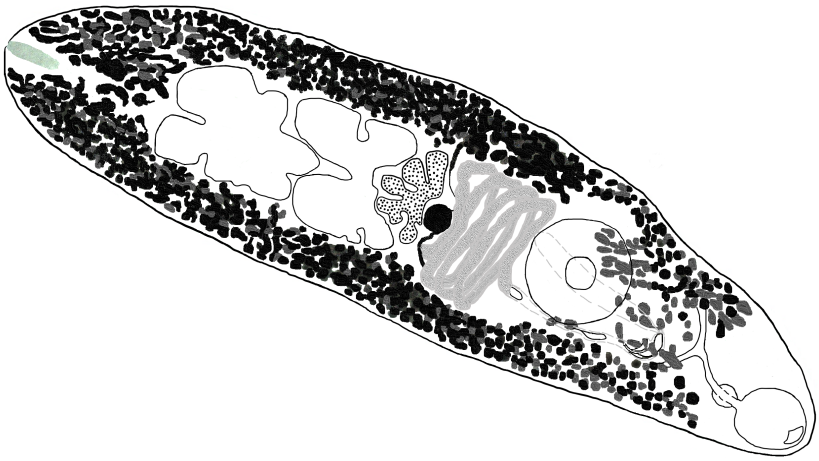

Fig. 1. *Helicometra fasciata* sensu lato marita from the Black Sea common stingray *Dasyatis pastinaca*, ventral view of general morphology

Sizes of the trematode body and organs are provided in Table 1.

Table 1. Measurements of *Helicometra fasciata* sensu lato marita from the Black Sea common stingray *Dasyatis pastinaca* compared to the ones from other Black Sea fish hosts

Parameter		*Helicometra fasciata* maritae from the Black Sea fishes	
		From *D. pastinaca*	From other fish hosts*
Body	length	1,489.81	0.414–3.795
	width	400.54	0.179–1.007
Oral sucker	length	143.80	0.041–0.193
	width	123.45	0.043–0.179
Ventral sucker	length	205.69	0.073–0.290
	width	207.37	0.073–0.331
Pharynx	length	41.64	0.030–0.110
	width	75.65	0.027–0.097
Anterior testis	length	218.58	0.024–0.552
	width	219.87	0.027–0.649
Posterior testis	length	213.92	0.024–0.731
	width	199.47	0.022–0.635
Ovary	length	114.88	0.016–0.276
	width	173.06	0.019–0.483
Bursa cirri	length	265.0	0.041–0.511
	width	71.63	0.011–0.110
Eggs (n = 14)	length	52.6–65.12 (58.19)	0.052–0.073
	width	23.7–25.6 (25.13)	0.023–0.041
Posttesticular space		296.71	–
Forebody		413.6	–

Note: *, according to [Korniychuk, 2009a; Kornyychuk, 2023].

Description of marita.

Body elongated-oval (shape index 3.71).

Tegument unarmed.

Oral sucker subterminal, slightly elongated along the longitudinal axis (shape index 1.16).

Ventral sucker (acetabulum) rounded (shape index 0.99). The length ratio of the oral and ventral suckers is 1 : 1.43; their width ratio is 1 : 1.68.

There are a short prepharynx, pharynx, and esophagus.

Forebody is 28% of the marita body length. Thus, the ventral sucker is located on the border of the first and second thirds of the worm body.

Gonads tandem.

Ovary five-lobed, submedian; its posterior edges at the level of the anterior edge of the anterior testis.

Testes contiguous, tandem, lobed.

Posttesticular space 19.9% of the body length.

Bursa cirri straight, elongated, club-shaped; its posterior end at the level of the posterior edge of the ventral sucker.

Metraterm extends along the left side of the bursa cirri.

Genital pore submedian, between bifurcation of intestine and anterior edge of the ventral sucker.

Vitelline glands follicular, in lateral fields, extend from the level of posterior border of pharynx to posterior end of the body; follicles are dorsally, laterally, and ventrally to intestinal branches. Vitelline follicles form “dorsolateral arch” [Korniychuk, 2009a] on the dorsal side of the worm body in the area from anterior border of ventral sucker to posterior border of pharynx. In the posttesticular space, the left and right vitelline fields are in contact with separate follicles, on the ventral side of the worm body only (Fig. 2).

Vitelline reservoir round, in front of the ovary, median.

Uterus between the ventral sucker and the ovary, helical. Uterus rings are parallel to the transverse axis of the body.

Eggs oval (shape index 2.31), with a long unipolar filament (Fig. 3).

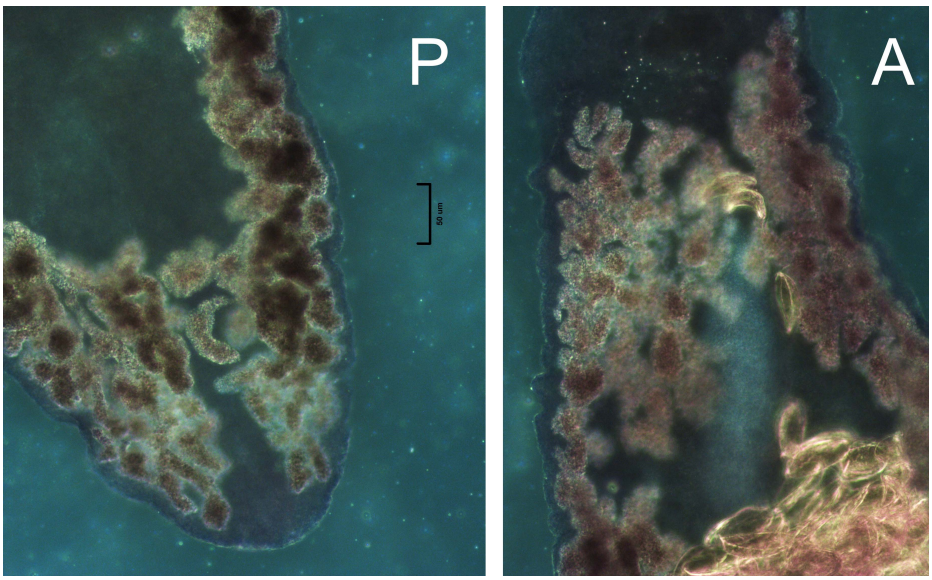

Fig. 2. The location of the vitellaria follicles at the posterior (P) and anterior (A) ends of the marita body of *Helicometra fasciata* sensu lato from the Black Sea common stingray *Dasyatis pastinaca*

Fig. 3. Filamented egg of *Helicometra fasciata* sensu lato from the Black Sea *Dasyatis pastinaca*

DISCUSSION

The studied specimen corresponds in morphology to the diagnosis of *H. fasciata* sensu lato [Blend, Dronen, 2015; Naidenova, Dolgikh, 1969]: oral sucker subterminal, almost rounded; ventral sucker in the anterior part of the marita body; uterus helical; eggs with a long unipolar filament; genital pore median, before the intestinal bifurcation; vitelline glands in lateral fields and enter the anterior part of the body; lobed gonads are tandem.

Sizes of the body and eggs of the marita analyzed, the shape of gonads, and the values of taxonomically significant morphological indices are within the limits previously established for sexually mature representatives of *H. fasciata* sensu lato from the Black Sea fish hosts (see Table 1).

As assumed, at least the Black Sea representatives of *H. fasciata* are a complex of cryptic species [Katokhin, Kornyychuk, 2020; Sokolov et al., 2022]. More precise taxonomic identification of these trematodes from the stingray implies molecular studies which could be carried out only after repeated finds.

D. pastinaca is the 34th known definitive fish host species of *H. fasciata* sensu lato complex in the Black Sea; out of them, 33 are bony fishes. This find is very interesting: trematodes identified as *H. fasciata* have not been known earlier from Dasyatidae family or from cartilaginous fishes in general anywhere in the World Ocean [Blend, Dronen, 2015].

Stingrays are common along all the Black Sea shores, where they inhabit shallows in the summer and move to deeper areas when it gets colder. Stingrays stay near the bottom and feed mainly on bottom and demersal crustaceans and fish [Svetovidov, 1964]. Various shrimps and crabs are common food for the Black Sea stingrays [Saglam et al., 2010; Smirnov, 1959].

Infection of the Black Sea stingrays with *H. fasciata* metacercariae is possible, for example, when feeding on a green crab *Carcinus aestuarii* Nardo, 1847, as well as rockpool and grass shrimps *Palaemon elegans* Rathke, 1836 and *Palaemon adspersus* Rathke, 1836; these species are involved in the life cycle of these trematodes in the Black Sea as the second intermediate hosts [Korniychuk, 2008, 2009b; Kornijchuk, Lozovsky, 2005; Mordvinova, 1980; Tkachuk, Mordvinova, 1999]. As the find of *H. fasciata* is a single one, despite the large number of the Black Sea stingrays studied by parasitologists, and as the trematode found is sexually mature, with a large number of eggs, we classify the stingray as an accidental definitive host of *H. fasciata* in the Black Sea.

Before this find, information on the trematode fauna of the Black Sea stingrays was limited to a single record of parasitism of a marita of *Nagmia yorkei* Nagaty, 1930 [syn. *Petalodistomum yorkei* (Nagaty, 1930)] from a stingray caught off the city of Yevpatoriya [Pogorel'tseva, 1964]. We conclude that Dasyatidae are evidently an undersampled host group for digenean infection in the Black Sea.

This work was carried out within the framework of IBSS state research assignment "Biodiversity as the basis for the sustainable functioning of marine ecosystems, criteria and scientific principles for its conservation" (No. 124022400148-4).

REFERENCES

1. Katokhin A. V., Kornyychuk Yu. M. Genotyping of Black Sea trematodes of the family Opecoelidae by mitochondrial markers. *Marine Biological Journal*, 2020, vol. 5, no. 4, pp. 15–27. (in Russ.). https://doi.org/10.21072/mbj.2020.05.4.02
2. Korniychuk Yu. M. Additional description of hermaphroditic generation of trematodes of Black Sea fishes, *Helicometra fasciata* (Trematoda, Opecoelidae). *Vestnik zoologii*, 2009a, spec. iss. no. 23, pp. 63–68. (in Russ.). https://elibrary.ru/zifvir
3. Korniychuk Yu. M. Seasonal dynamics of abundance and qualitative composition of trematode, *Helicometra fasciata*, metacercaria hemipopulation in coastal biocenosys of Southwestern Crimea. *Ekologiya morya*, 2008, iss. 75, pp. 9–15. (in Russ.). https://repository.marine-research.ru/handle/299011/4793
4. Korniychuk Yu. M. Parasite fauna of shrimps in the Black Sea and the Sea of Azov. *Ekologiya morya*, 2009b, iss. 77, pp. 44–48. (in Russ.). https://repository.marine-research.ru/handle/299011/4836
5. Kornijchuk Ju. M., Lozovsky V. L. Black Sea crab *Carcinus aestuarii* – a new intermediate host for the trematode *Helicometra fasciata*. *Morskoj ekologicheskij zhurnal*, 2005, vol. 4, no. 2, pp. 38. (in Russ.). https://repository.marine-research.ru/handle/299011/803
6. Mordvinova T. N. *Gel'mintofauna vysshikh rakoobraznykh krymskogo poberezh'ya i severo-zapadnoi chasti Chernogo morya (sistematika, faunistika, ekologiya)* : avtoref. dis. … kand. biol. nauk : 03.00.20. Moscow, 1980, 24 p. (in Russ.). https://repository.marine-research.ru/handle/299011/9577
7. Naidenova N. N., Dolgikh A. V. On revision of some species of the genus *Helicometra* Odhner, 1902 (Trematoda, Opecoelidae). *Nauchnye doklady vysshei shkoly. Biologicheskie nauki*, 1969, no. 7 (67), pp. 7–12. (in Russ.). https://repository.marine-research.ru/handle/299011/11182
8. Pogorel'tseva T. P. *Fauna parazitov ryb Chernogo morya (sistematika, ekologiya, zoogeografiya, filogeniya).* [dissertation], 1964, vol. 1, 391 p. (manuscript). (in Russ.)]
9. Svetovidov A. N. *Ryby Chernogo morya.* Moscow ; Leningrad : Nauka, 1964, 551 p. (in Russ.). https://repository.marine-research.ru/handle/299011/8655
10. Smirnov A. N. Materialy po biologii ryb Chernogo morya v raione Karadaga. *Trudy Karadagskoi biologicheskoi stantsii*, 1959, iss. 15, pp. 31–109. (in Russ.). https://repository.marine-research.ru/handle/299011/6943
11. Tkachuk L. P., Mordvinova T. N. On parasite infection of food-fishes from south-western part of the Indian Ocean. *Ekologiya morya*, 1999, iss. 49, pp. 21–23. (in Russ.). https://repository.marine-research.ru/handle/299011/3664
12. Blend C. K., Dronen N. O. A review of the genus *Helicometra* Odhner, 1902 (Digenea: Opecoelidae: Plagioporinae) with a key to species including *Helicometra overstreeti* n. sp. from the cusk-eel *Luciobrotula corethromycter* Cohen, 1964 (Ophidiiformes: Ophidiidae) from the Gulf of Mexico. *Marine Biodiversity*, 2015, vol. 45, iss. 2, pp. 183–270. https://doi.org/10.1007/s12526-014-0250-3
13. Kornyychuk Yu. M. *Helicometra fasciata* (Rudolphi, 1819) complex from new fish host

in the Black Sea, the broadnosed pipefish *Syngnathus typhle* Linnaeus, 1758, with notes on biology of this trematode species. *Parazitologiya*, 2023, vol. 57, no. 6, pp. 498–503. https://doi.org/10.31857/S0031184723060042

14. Saglam H., Ak O., Kutlu S., Aydin I. Diet and feeding strategy of the common stingray *Dasyatis pastinaca* (Linnaeus, 1758) on the Turkish coast of southeastern Black Sea. *Cahiers de Biologie Marine*, 2010, vol. 51, no. 1, pp. 37–44. https://doi.org/10.21411/CBM.A.C51293DF
15. Sokolov S. G., Shchenkov S. V., Khasanov F. K., Kornyychuk Y. M., Gordeev I. I. Redescription and phylogenetic assessment of *Helicometra antarcticae* Holloway & Bier, 1968 (Trematoda, Opecoelidae), with evidence of non-monophyletic status of the genus *Helicometra* Odhner, 1902. *Zoosystema*, 2022, vol. 44, iss. 15, pp. 423–433. https://doi.org/10.5252/zoosystema2022v44a15

О НАХОДКЕ ТРЕМАТОД *HELICOMETRA FASCIATA* (RUD., 1819) SENSU LATO У ЧЕРНОМОРСКОГО МОРСКОГО КОТА *DASYATIS PASTINACA* (LINNAEUS, 1758)

Ю. М. Корнийчук

ФГБУН ФИЦ «Институт биологии южных морей имени А. О. Ковалевского РАН»,
Севастополь, Российская Федерация
E-mail: *kornyychuk@ibss-ras.ru*

У черноморского ската-хвостокола (морского кота) *Dasyatis pastinaca* (Linnaeus, 1758) из Каркинитского залива (западное побережье Крыма) впервые обнаружена трематода *Helicometra fasciata* sensu lato (семейство Opecoelidae). Приведены рисунок и морфологическое описание найденной единственной половозрелой мариты. Обнаружение этой трематоды у морского кота согласуется с данными об особенностях протекания жизненного цикла хеликометр в Чёрном море. Это первая находка представителей рода *Helicometra* у хрящевых рыб; черноморский морской кот отнесён к категории случайных дефинитивных хозяев *H. fasciata* sensu lato. Dasyatidae, в том числе черноморские, — семейство рыб, недостаточно исследованное в отношении их заражённости трематодами.

Ключевые слова: Trematoda, Opecoelidae, Chondrichthyes, Batomorphi, Dasyatidae, новый дефинитивный хозяин, Чёрное море, пищевые сети

1871
ИнБЮМ – IBSS

Морской биологический журнал
Marine Biological Journal
2025, vol. 10, no. 2, pp. 67–86
https://marine-biology.ru

UDC 581.526.323(262.5.04)

COMPOSITION AND STRUCTURE OF MACROPHYTOBENTHOS OFF THE COAST OF THE NATURAL MONUMENT KUCHUK-LAMBAT STONE CHAOS (CRIMEA, BLACK SEA)

© 2025 **S. Sadogurskiy, T. Belich, and S. Sadogurskaya**

Nikitsky Botanical Gardens – National Scientific Center of RAS, Yalta, Russian Federation
E-mail: *ssadogurskij@yandex.ru*

Received by the Editor 29.01.2024; after reviewing 13.03.2024;
accepted for publication 20.03.2025.

The southern coast of the Crimea (SCC) is characterized by a high level of anthropogenic transformation; therefore, the areas preserved in a natural or quasi-natural state are of a certain nature conservation value. Those include the territorial-aquatic complex uniting the geological natural monument Kuchuk-Lambat Stone Chaos and the adjacent coastal waters of the Black Sea. The water area has never been studied from the hydrobotanical point of view and is not included in any list of protected natural sites. Considering this, the research was carried out based on data of 2015 and 2022; it was aimed at characterizing species composition, biomass, and spatial structure of macrophytobenthos to clarify information on distribution and dynamics of the benthic vegetation cover off the SCC and in relation with the prospect for conservation of this area. Macroscopic vegetation was found to develop on hard and soft substrata which determines its general nature. In total, 63 species of macrophytes were recorded: Chlorophyta, 14 (22.2%); Ochrophyta, 9 (14.3%); Rhodophyta, 39 (62.0%); and Tracheophyta, 1 (1.6%). The total number of species (NS) and the ratio of systematic groups by NS in both years are similar. However, the composition of the flora and the biomass (BM) ratio of dominant species and ecological-floristic groups changed significantly at minimum and maximum depths, and this governed the transformation of the vegetation cover. In the shallows, their dynamics has a fluctuating character, and it is driven by local disturbance and subsequent recovery of macrophytobenthos after a mudflow. At depth, the changes are caused by the invasion of the transformer species *Bonnemaisonia hamifera* into natural communities. These changes seem to have a long-term character. To reveal their degree and reversibility, it is necessary to monitor the distribution of the invasive species off the SCC and within the boundaries of the Sea of Azov–Black Sea region in general. Currently, along the surveyed shore, macrophytes form five belt-like communities with BM 0.2–6.0 kg·m^{-2} and NS 14–27. The extreme values of these indicators are registered in the sublittoral zone: maximum ones, on hard substrata in the upper and central spots of a *Cystoseira* belt (*Cystoseira* s. l. species), and minimum ones, on soft substrata in the deepest seagrass community (*Nanozostera noltei*). In general, perennial macrophytes dominate in the BM, and short-vegetating macrophytes prevail in the NS. Phytobenthos has a pronounced oligosaprobic marine warm-water character. The vegetation cover of the water area shows a high degree of preservation; its spatial distribution, composition, and structure (except for changes caused by biological invasion) are typical for the Black Sea hydrobotanical region "SCC." The rare species fraction of the flora covers 12 taxa; biotopes formed by macrophyte communities are listed in Directive 92/43/EEC. It is expedient to form a complex territorial-aquatic nature reservation which will unite the existing natural monument and the adjacent water area.

Keywords: Black Sea, southern coast of the Crimea, Kuchuk-Lambat, macrophytobenthos, species composition, biomass, spatial structure

Due to its unique geographical location and favorable combination of natural and climatic conditions, the Crimean Peninsula is one of European centers of biological diversity; at the same time, it is characterized by a significant level of anthropogenic transformation [Johnson, 1995; Sovremennoe sostoyanie, 2015]. This applies in full to the southern coast of Crimea (hereinafter SCC): a narrow strip stretching between the Main Ridge of the Crimean Mountains and the Black Sea. Recreational development of this area began 1.5 centuries ago and acquired an industrial scale by the second half of the XX century. By now, the shore is much reinforced with concrete hydraulic structures and is occupied by recreational and tourist infrastructure; importantly, its density is continuously increasing. However, some of its spots, usually confined to inconvenient areas, escaped a similar fate and now are of great conservation importance [Sadogurskiy et al., 2017]. Thus, near the settlement of Utes, where a village of Kuchuk-Lambat was located, the marine area and the adjacent section of the shore have been preserved almost in their natural state, unlike the surrounding sites. This is governed by the active dynamics of the gravitational relief of the coastal zone formed by the Kuchuk-Lambat Stone Chaos. It is a picturesque pile of rock debris extending for 1 km along the coast and 1.5 km up the slope to a height of 0–235 m above sea level [Vakhrushev, Amelichev, 2000]. More than 50 years ago, part of this tract with a total area of 5 hectares (protected zone of 7.1 hectares) received the status of a geological natural monument (by decision of the Regional Executive Committee No. 19/8-67, 30.01.1969). Later, it was highlighted that its territory is also of high botanical value, and this made it possible to raise an issue of transferring the object to the category of complex natural monuments [Ryff, 2013; Vakhrushev, Amelichev, 2000]. The water area at the foot of the tract does not have a nature conservation status; it remained unexplored until recently. Previously, we noted as follows: given the inextricable structural and functional relationship between territorial and aquatic components of integral territorial-aquatic ecosystems mediated by material and energy flows, it is advisable to form territorial-aquatic protected objects and elements of econetworks in the marine coastal zone that will be common in terms of area and management [Sadogurskiy et al., 2017; Sadogursky et al., 2009, 2013]. In this regard, a hydrobotanical study of this water area was initiated, and preliminary data were provided on phytobenthos of its supra- and pseudolittoral, where a direct contact between land and sea occurs [Belich et al., 2020].

The aim of this work is to characterize species composition, biomass, and spatial structure of macrophytobenthos of the marine water area at the foot of the natural monument Kuchuk-Lambat Stone Chaos in order to clarify the ideas about the distribution and dynamics of the benthal vegetation cover off the SCC, with the prospect of conservation taken into account.

RESEARCH AREA, OBJECTS, AND METHODS

The surveyed area is a 300-m site of the natural coast of the Black Sea located between two recreational complexes (Fig. 1a). Along the site, there is a boulder-block beach (sometimes boulder one), up to 10–15 m wide (Fig. 1b). Within the boundaries of the natural monument (I), above the beach, there are block heaps of stone chaos composed in the coastal part mainly of Upper Jurassic limestones and cemented breccias of the Massandra suite (see Fig. 1a, b). In the protected zone of the monument (II), steep coastal slopes are composed of terrigenous flysch of the Tauride series consisting of alternating folded layers of argillites, siltstones, and sandstones. Along the boundary between the territory and the protected zone of the monument, there is a small watercourse into the sea. Its surface runoff is extremely variable: in summer, it disappears for 1–2 months; after heavy rains, it can increase and even form mudflows with a velocity of 1–4 $m \cdot s^{-1}$ and a detrital material content of 100–500 $kg \cdot m^{-3}$ [Vakhrushev,

Amelichev, 2000]. The adjacent water area is located within the boundaries of the hydrobotanical region "SCC" [Kalugina-Gutnik, 1975]. The seabed is deep; in pseudolittoral and sublittoral, to a depth of 5–6 m, block and block-boulder heap (hereinafter heap) dominates sometimes alternating with pebble areas. Sands with a slight admixture of shells extend beyond the lower boundary of hard substrata.

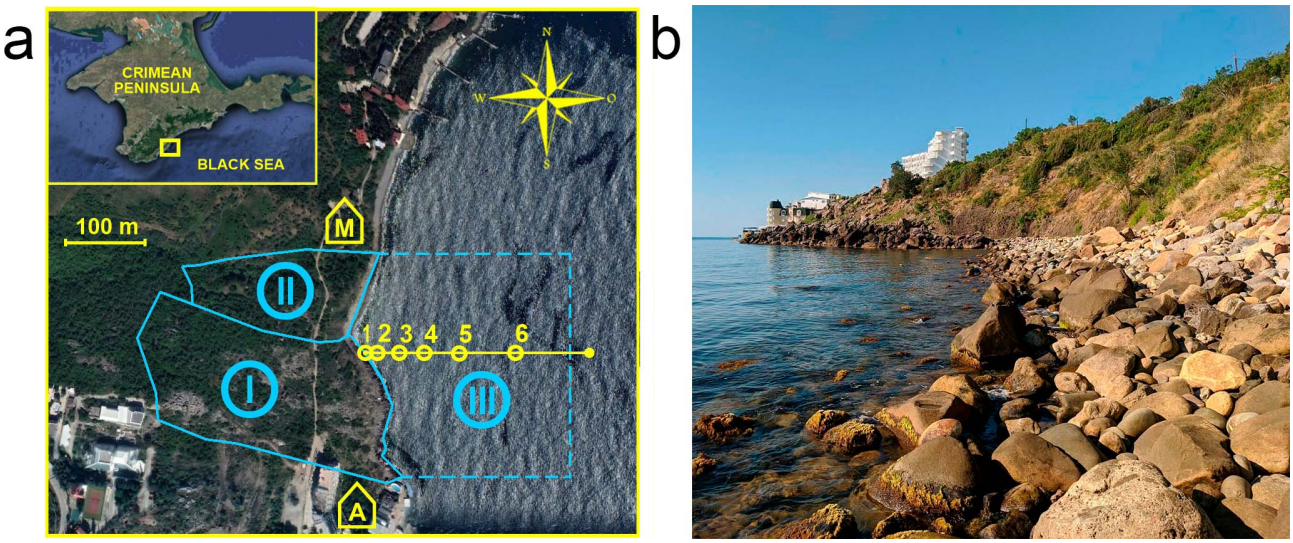

Fig. 1. Research area: a, map of the surveyed area of the coastal zone; 1–6, numbers and location of stations along the hydrobotanical profile (44°36′06.3″N, 34°22′19.9″E at the point of intersection with the water's edge); I, the territory of the geological natural monument Kuchuk-Lambat Stone Chaos; II, the protected zone of the natural monument [Pasport pamyatnika prirody, 2021]; III, the water area recommended to be included in the proposed complex territorial and aquatic reservation; recreational complexes (M, a tourist center Mayak; A, a hotel Arkadia); b, the natural shore of the surveyed area (north to south view), 27.07.2022

Off the SCC, the direction of the coastal current usually coincides with the direction of the Rim Current; the current is directed to the southwest, usually with a speed up to 10 cm·s^{-1}, although with a tailwind, in 5% of cases, a speed exceeds 30 cm·s^{-1} [Belokopytov et al., 2003]. The highest frequency of storm waves is observed from eastern and southeastern directions [Gidrometeorologiya i gidrokhimiya morei SSSR, 1991; Goryachkin, Repetin, 2009]. Off the SCC, fluctuations in sea level of any nature (*inter alia* surges) are insignificant; those are overlapped by surf and wave activity [Gidrometeorologiya i gidrokhimiya morei SSSR, 1991]. The mean temperature of the surface water layer there (according to data for the city of Alushta) varies from +7.4 °C in February–March to +23.3 °C in August. Interestingly, during summer upwellings, the amplitude of temperature fluctuations can exceed 15 °C. The mean annual salinity varies within 17.0–18.2‰, with a minimum in April–May.

The water area was surveyed twice, on 07.08.2015 and 27.07.2022, during independent scuba dives by the generally accepted method [Kalugina, 1969; Kalugina-Gutnik, 1975]. In the central part of the analyzed site of the natural shore, there was a hydrobotanical profile with coordinates 44°36′06.3″N, 34°22′19.9″E at the point of intersection of the water's edge (see Fig. 1a). Sampling was carried out along this profile in a depth interval of 0–8.0 m: at each station, 10 quantitative samples were taken with a frame of 0.01 m^2 in pseudolittoral, and 5 samples were taken with a frame of 0.04 m^2 in sublittoral (the key parameters of stations are provided in Table 1). Visual observations covered all the surveyed water area down to a depth of 10–12 m.

The object of the study is benthic macrophytes. The nomenclature of Chlorophyta, Ochrophyta (class Phaeophyceae), Rhodophyta, and Tracheophyta representatives is given according to AlgaeBase [2024]; surnames of the authors of taxa are provided in the standard abbreviation, as recommended by IPNI [2024]. The identification guide of A. Zinova [1967] is used as a basic one for identifying macroalgae. Ecological-floristic characteristics are given according to A. Kalugina-Gutnik [1975]; saprobiological and halobic ones are based on unpublished data of A. Kalugina-Gutnik and T. Eremenko. The projective cover (hereinafter PC) was determined visually; the mean biomass (hereinafter BM) was established for each species separately: $\bar{x} \pm S_{\bar{x}}$ (wet weight). Layers in communities were identified by aspective species taking into account BM; the vegetation height (hereinafter VH) was given by mean values of the length of thalli (shoots) of dominants in the upper layer. Underwater pictures were taken with an Olympus TG-835 digital camera. Temporary preparations of algae were studied by light microscopy under a Leica DM2500 microscope.

Table 1. Characteristics of sampling stations (No. 1–6) and benthic vegetation cover in the coastal-marine water area off the coast of the Kuchuk-Lambat tract

07.08.2015						
Parameter	PSL*	SBL				
	No. 1	No. 2	No. 3	No. 4	No. 5	No. 6
Depth, m**	±0.25	–0.5	–1.0	–3.0	–5.0	–8.0
Distance from the shore, m	0	3–5	30	60–70	110–120	170–200
Plant community	*Ulva intestinalis* + *Ulva kylinii*	*Ericaria bosphorica* – *Padina pavonica* + *Dictyota fasciola*	*Ericaria bosphorica* + *Gongolaria barbata* + *Vertebrata subulifera* – *Cladostephus hirsutus*			*Nanozostera noltei*
Projective cover, %	85–90	55–60	60–65	95–100	85–90	25–30
Vegetation height, cm	7.41	8.17	17.41	27.02	29.08	22.89
27.07.2022						
Plant community	*Ceramium ciliatum*	*Ericaria bosphorica* + *Gongolaria barbata* – *Padina pavonica* + *Dictyota fasciola*	*Ericaria bosphorica* + *Gongolaria barbata* + *Vertebrata subulifera* – *Cladostephus hirsutus*	*Ericaria bosphorica* + *Gongolaria barbata* + *Vertebrata subulifera* – *Bonnemaisonia hamifera*		*Nanozostera noltei*
Projective cover, %	85–90	70–75	95–100	95–100	85–90	25–30
Vegetation height, cm	6.22	12.32	28.60	34.27	32.33	21.67

Note: hereinafter, PSL, pseudolittoral zone; SBL, sublittoral zone (*). For the pseudolittoral zone, indicator is provided within the vertical range of surge fluctuations in water level (**).

RESULTS AND DISCUSSION

Results of the survey of the coastal water area at the foot of the Kuchuk-Lambat Stone Chaos are as follows (the species list and BM values of macrophytes are provided in Table 2).

Table 2. The species list and biomass value ($g \cdot m^{-2}$) of macrophytes off the coast of the Kuchuk-Lambat tract (stations No. 1–6)

Species	2015						2022					
	PSL	SBL					PSL	SBL				
	No. 1	No. 2	No. 3	No. 4	No. 5	No. 6	No. 1	No. 2	No. 3	No. 4	No. 5	No. 6
CHLOROPHYTA Rchb.												
Chaetomorpha aerea (Dillwyn) Kütz.	0.10	m	m	m	6.67			m	m	m	m	
Chaetomorpha gracilis Kütz.	m						m					
Cladophora albida (Nees) Kütz.	106.00			0.42		m	13.70	m	0.83 ± 0.81			
Cladophora sericea (Huds.) Kütz.			0.83	0.41	m		3.10	m	0.67			
Cladophora vadorum (Aresch.) Kütz. ✱	119.30											
Cladophoropsis membranacea (Bang ex C. Agardh) Børgesen ✱	m		23.00 ± 14.89	35.42	10.42	m						m
Ulothrix flacca (Dillwyn) Thur.						m						
Ulva intestinalis L.	541.80						8.20					
Ulva kylinii (Bliding) H. S. Hayden, Blomster, Maggs, P. C. Silva, Stanhope et Waaland	584.60						47.20					
Ulva rigida C. Agardh					2.08							
Ulvella lens P. Crouan et H. Crouan												m
Ulvella leptochaete (Huber) R. Nielsen, O'Kelly et B. Wysor		m	m	m	m		m	m	m	m	m	m
Ulvella scutata (Reinke) R. Nielsen, O'Kelly et B. Wysor											m	m
Ulvella viridis (Reinke) R. Nielsen, O'Kelly et B. Wysor			m	m					m	m	m	

Continued on the next page…

Species	2015						2022					
	PSL	SBL					PSL	SBL				
	No. 1	No. 2	No. 3	No. 4	No. 5	No. 6	No. 1	No. 2	No. 3	No. 4	No. 5	No. 6
OCHROPHYTA Caval.-Sm.												
Cladostephus hirsutus (L.) Boudour. et M. Perret ex Heesch et al. ✱		4.75	192.58 ± 105.7	895.83 ± 318.06	371.67 ± 137.93	32.50		10.08	832.50 ± 31.45	203.25	29.92 ± 9.07	
Dictyota fasciola (Roth) J. V. Lamour.		118.08 ± 49.16	120.42 ± 20.63				47.30	55.67 ± 31.69	0.83			
Ericaria bosphorica (Sauv.) D. Serio et G. Furnari ★○▲		348.75 ± 109.68	590.83	2,157.92 ± 1,898.27	1,904.17 ± 1,524.67		23.30	467.92	2,572.50 ± 51.98	2,245.00	1,713.58 ± 777.40	
Eudesme virescens (Carmich. ex Berk.) J. Agardh							11.20					
Gongolaria barbata (Stackh.) Kuntze ★○▲			604.17 ± 569.55	1,046.25	832.92			186.42 ± 75.43	629.17	1,924.58	1,554.92 ± 754.90	
Myriactula rivulariae (Suhr ex Aresch.) Feldmann	m							m	m	m		
Padina pavonica (L.) Thivy □		246.83 ± 33.12	29.25 ± 21.46				19.10	308.75 ± 39.03	10.55			
Scytosiphon lomentaria (Lyngb.) Link, nom. cons.	1.70											
Sphacelaria cirrosa (Roth) C. Agardh	m	m	m	m	m	m		m	m	m	m	
RHODOPHYTA Wettst.												
Acrochaetium parvulum (Kylin) Hoyt				m								
Acrochaetium secundatum (Lyngb.) Nägeli	m		m									
Antithamnion cruciatum (C. Agardh) Nägeli									m	m	m	
Apoglossum ruscifolium (Turner) J. Agardh					6.83 ± 6.33					2.08	0.75	
Bonnemaisonia hamifera Har.							m	m	10.00	409.17 ± 110.79	593.00 ± 98.14	0.33 ± 0.14
Carradoriella denudata (Dillwyn) Savoie et G. W. Saunders	1.50			5.00	0.42		49.00	m				
Ceramium ciliatum (J. Ellis) Ducluz.	69.0	1.25		m		m	390.70 ± 357.65					
Ceramium diaphanum (Lightf.) Roth	m	0.75				m						0.25

Continued on the next page…

Species	2015						2022					
	PSL	SBL					PSL	SBL				
	No. 1	No. 2	No. 3	No. 4	No. 5	No. 6	No. 1	No. 2	No. 3	No. 4	No. 5	No. 6
Ceramium siliquosum var. *elegans* (Roth) G. Furnari			m									
Ceramium virgatum Roth	7.20	0.50	1.42	1.67	4.83 ± 4.23	m	27.50	m	1.92 ± 0.63	0.42	0.08	
Chondria capillaris (Huds.) M. J. Wynne		2.50					50.90	0.08	18.92 ± 17.77			1.17
Chondria dasyphylla (Woodw.) C. Agardh			7.92	10.83	2.08	9.17				18.92 ± 10.96		m
Choreonema thuretii (Bornet) F. Schmitz									m	m		
Chroodactylon ornatum (C. Agardh) Basson ✱						m						
Chylocladia verticillata (Lightf.) Bliding				15.0 ± 13.52								
Colaconema daviesii (Dillwyn) Stegenga	m											m
Dasya baillouviana (S. G. Gmel.) Mont.								21.75 ± 16.84				
Gelidium crinale (Hare ex Turner) Gaillon	0.50	18.83	m					m	m	0.58		
Gelidium spinosum (S. G. Gmel.) P. C. Silva			4.33		4.58 ± 4.00	0.83						
Grania efflorescens (J. Agardh) Kylin					m	m						
Jania rubens (L.) J. V. Lamour.			1.01	34.51 ± 20.48	27.13 ± 25.56				69.33 ± 45.79	16.25		
Jania virgata (Zanardini) Mont.	1.5	0.92	2.32 ± 2.15	145.49 ± 43.23	80.95 ± 74.43	1.83 ± 1.61			99.42 ± 83.46	10.92 ± 9.36	2.25	
Laurencia coronopus J. Agardh ✱▲									153.50 ± 134.80	22.58 ± 16.38	1.75	
Laurencia obtusa (Huds.) J. V. Lamour.		1.25			37.50 ± 33.07				13.42	164.17 ± 86.30	26.67 ± 14.34	
Leptosiphonia brodiei (Dillwyn) Savoie et G. W. Saunders					1.67 ± 1.44							
Lithophyllum cystoseirae (Hauck) Heydr.									m	m	m	

Continued on the next page…

Species	2015						2022					
	PSL	SBL					PSL	SBL				
	No. 1	No. 2	No. 3	No. 4	No. 5	No. 6	No. 1	No. 2	No. 3	No. 4	No. 5	No. 6
Lomentaria compressa (Kütz.) Kylin ✚▲			4.33		8.75				m	m	m	
Lophosiphonia obscura (C. Agardh) Falkenb.	3.00						64.20	m			m	
Palisada perforata (Bory) K. W. Nam			13.33				90.60					
Palisada thuyoides (Kütz.) Cassano, Sentíes, Gil-Rodríguez et M. T. Fujii									0.42			
Peyssonnelia rubra (Grev.) J. Agardh						m						
Phyllophora crispa (Huds.) P. S. Dixon ★✚▲											28.25	
Pneophyllum confervicola (Kütz.) Y. M. Chamb.		m	m	m	m	m	m	m	m	m	m	m
Pneophyllum fragile Kütz.						m						m
Polysiphonia opaca (C. Agardh) Moris et De Not.								0.67 ± 0.52				
Pterothamnion plumula (J. Ellis) Nägeli	1.50											
Stylonema alsidii (Zanardini) K. M. Drew ✱		m	m	m		m		m				m
Vertebrata fucoides (Huds.) Kuntze							0.50					
Vertebrata subulifera (C. Agardh) Kuntze		14.25	77.92	213.33	282.08 ± 69.42	22.08 ± 16.65		4.92 ± 3.17	889.17 ± 545.64	827.42 ± 666.64	389.08 ± 99.72	0.67
TRACHEOPHYTA Sinnott ex Caval.-Sm.												
Nanozostera noltei (Hornem.) Toml. et Posl. ★▲❖						203.42 ± 20.45						193.70 ± 8.76

Note: cells are empty if a species is absent from samples. The error of the mean (± $S_{\bar{x}}$) is given for cases where the coefficient of variation $v < 100\%$. Hereinafter, m is minor quantity (less than 0.01 g in a sample). Conservation status of taxa: ○, Convention for the Protection of the Mediterranean Sea Against Pollution (Barcelona Convention, 1976) [2009]; ✱, Red Data Book of Ukraine [2009]; ✚, Red Book of the Russian Federation [2008]; □, Red Data Book of the Republic of Bulgaria [2015a; 2015b]; ★, Black Sea Red Data Book [1999]; ▲, Red Book of the Republic of Crimea [2015]; ❖, Red Data Book of Priazovsky Region [2012].

Results of 2015. In **pseudolittoral** (PSL) on the heap (sta. No. 1), the vegetation cover was a well-separated belt, not divided into subzones and layers, 0.25–0.45 m wide. It was formed by the community *Ulva intestinalis* + *Ulva kylinii* (see Table 1). BM was 1,438 g·m^{-2}; PC, 85–90%; VH, 7.4 cm; and the number of species (hereinafter NS), 20 (Tables 3, 4).

Table 3. The number of species of macrophytes in ecological-floristic groups (GR) off the coast of the Kuchuk-Lambat tract

GR	Number of species / % (stations No. 1–6)													
	2015							2022						
	PSL	SBL					Total	PSL	SBL					Total
	No. 1	No. 2	No. 3	No. 4	No. 5	No. 6		No. 1	No. 2	No. 3	No. 4	No. 5	No. 6	
Ch	7 / 35.00	1 / 6.25	5 / 20.83	6 / 28.57	5 / 22.72	3 / 15.79	12 / 24.00	6 / 31.58	4 / 18.18	5 / 18.52	3 / 13.04	4 / 19.05	4 / 28.57	11 / 22.45
Oh	3 / 15.00	5 / 31.25	6 / 25.00	4 / 19.05	4 / 18.18	2 / 10.53	8 / 16.00	4 / 21.05	7 / 31.82	7 / 25.93	5 / 21.74	4 / 19.05	0 / 0	8 / 16.33
Rh	10 / 50.00	10 / 62.50	13 / 54.17	11 / 52.38	13 / 59.09	13 / 68.42	29 / 58.00	9 / 47.37	11 / 50.00	15 / 55.56	15 / 65.22	13 / 61.90	9 / 64.29	29 / 59.18
Th	0 / 0	0 / 0	0 / 0	0 / 0	0 / 0	1 / 5.26	1 / 2.00	0 / 0	0 / 0	0 / 0	0 / 0	0 / 0	1 / 7.14	1 / 2.04
Os	7 / 35.00	12 / 75.00	18 / 75.00	15 / 71.43	16 / 72.73	9 / 47.37	26 / 52.00	10 / 52.63	13 / 59.09	21 / 77.78	19 / 82.61	16 / 76.19	8 / 57.14	32 / 65.31
Ms	9 / 45.00	2 / 12.50	5 / 20.83	5 / 23.81	5 / 22.73	7 / 36.84	19 / 38.00	6 / 31.58	8 / 36.36	5 / 18.52	3 / 13.04	3 / 14.29	4 / 28.57	12 / 24.49
Ps	3 / 15.00	2 / 12.50	1 / 4.17	1 / 4.76	1 / 45.55	3 / 15.79	4 / 8.00	2 / 10.53	1 / 4.55	1 / 3.70	1 / 4.35	2 / 9.52	2 / 14.29	4 / 8.16
?	1 / 5.00	0 / 0	0 / 0	0 / 0	0 / 0	0 / 0	1 / 2.00	1 / 5.26	0 / 0	0 / 0	0 / 0	0 / 0	0 / 0	1 / 2.04
An	13 / 65.00	6 / 37.50	10 / 41.67	12 / 57.14	11 / 50.00	9 / 47.37	27 / 54.00	13 / 68.42	10 / 45.45	11 / 40.74	9 / 39.13	10 / 47.62	10 / 71.43	24 / 48.98
Ss	3 / 15.00	4 / 25.00	5 / 20.83	3 / 14.29	1 / 4.55	4 / 21.05	8 / 16.00	3 / 15.79	5 / 22.73	3 / 11.11	1 / 4.35	0 / 0	2 / 14.29	7 / 14.29
Sw	1 / 5.00	0 / 0	0 / 0	0 / 0	0 / 0	0 / 0	1 / 2.00	0 / 0	0 / 0	0 / 0	0 / 0	0 / 0	0 / 0	0 / 0
Pr	3 / 15.00	6 / 37.50	9 / 37.90	6 / 29.57	10 / 45.45	6 / 31.58	14 / 28.00	2 / 10.53	6 / 27.27	11 / 40.74	11 / 47.83	10 / 47.62	1 / 7.14	16 / 32.65
?	0 / 0	0 / 0	0 / 0	0 / 0	0 / 0	0 / 0	0 / 0	1 / 5.26	1 / 4.55	2 / 7.41	2 / 8.70	1 / 4.76	1 / 7.14	2 / 4.08
Mr	10 / 50.00	12 / 75.00	18 / 75.00	14 / 66.67	17 / 77.27	14 / 73.68	34 / 68.00	11 / 57.89	14 / 63.64	20 / 74.07	18 / 78.26	16 / 76.19	10 / 71.43	37 / 75.51
Bm	9 / 45.00	4 / 25.00	6 / 25.00	7 / 33.33	5 / 22.72	5 / 26.32	14 / 28.00	7 / 36.84	8 / 36.36	7 / 25.93	5 / 21.74	5 / 23.81	4 / 28.57	11 / 22.45
Bw	1 / 5.00	0 / 0	0 / 0	0 / 0	0 / 0	1 / 5.26	2 / 4.00	1 / 5.26	0 / 0	0 / 0	0 / 0	0 / 0	0 / 0	1 / 2.04
Ww	9 / 45.00	12 / 75.00	16 / 66.67	12 / 57.14	13 / 59.09	12 / 63.16	29 / 58.00	9 / 47.37	13 / 59.09	15 / 55.56	12 / 52.17	11 / 52.38	10 / 71.43	31 / 63.27
Cw	9 / 45.00	3 / 18.75	6 / 25.00	7 / 33.33	8 / 36.36	6 / 31.58	18 / 36.00	7 / 36.84	7 / 31.82	8 / 29.63	7 / 30.43	6 / 28.57	3 / 21.43	13 / 26.53
Cp	2 / 10.00	1 / 6.25	2 / 8.33	2 / 9.52	1 / 4.55	1 / 5.26	3 / 6.00	3 / 15.79	2 / 9.09	3 / 11.11	3 / 13.04	3 / 14.29	1 / 7.14	4 / 8.16
En	0 / 0	0 / 0	0 / 0	0 / 0	0 / 0	0 / 0	0 / 0	0 / 0	0 / 0	1 / 3.70	1 / 4.35	1 / 4.76	0 / 0	1 / 2.04
Σ	20 / 100	16 / 100	24 / 100	21 / 100	22 / 100	19 / 100	50 / 100	19 / 100	22 / 100	27 / 100	23 / 100	21 / 100	14 / 100	49 / 100

Note. Hereinafter, systematic groups: Ch, Chlorophyta; Oh, Ochrophyta (class Phaeophyceae); Rh, Rhodophyta; Th, Tracheophyta. Saprobiological groups: Os, oligosaprobes; Ms, mesosaprobes; Ps, polysaprobes. By the duration of the vegetation period: An, annuals; Ss, seasonal summer; Sw, seasonal winter; Pr, perennials. In relation to halobility: Mr, marine; Bm, brackish–marine; Bw, brackish. Phytogeographical groups: Ww, warm-water; Cw, cold-water; Cp, cosmopolitan; En, endemic. ?, no data available.

In **sublittoral** (SBL), all hard substrata were occupied by communities of a so-called *Cystoseira* belt (with the dominance of *Cystoseira* s. l. representatives).

In the shallowest spots, the community *Ericaria bosphorica* – *Padina pavonica* + *Dictyota fasciola* developed (see Table 1). At sta. No. 2, BM was 758 g·m^{-2}; PC, 55–60%; VH, 8.2 cm; and NS, 16 (see Tables 3, 4).

Table 4. The biomass of macrophytes in ecological-floristic groups (GR) off the coast of the Kuchuk-Lambat tract

GR	Biomass, g·m^{-2} / % (stations No. 1–6)													
	2015							2022						
	PSL	SBL					Mean	PSL	SBL					Mean
	1	2	3	4	5	6		1	2	3	4	5	6	
Ch	1,351.80 94.02	m 0	23.83 1.42	36.25 0.80	19.17 0.54	0 0	238.51 11.74	72.20 8.53	m 0	1.50 0.02	m 0	m 0	m 0	12.28 0.42
Oh	1.70 0.12	718.41 94.69	1,537.25 91.85	4,100.00 89.87	3,108.76 86.72	32.50 10.95	1,583.11 77.12	100.90 11.92	1,028.84 97.40	4,045.55 76.29	4,372.83 74.81	3,298.42 76.00	m 0	2,141.10 73.04
Rh	84.20 5.86	40.25 5.31	112.58 6.73	425.83 9.33	456.82 12.74	33.91 11.42	192.26 9.47	673.40 79.55	27.42 2.60	1,256.10 23.69	1,472.51 25.19	1,041.83 24.00	2.42 1.23	745.61 25.44
Th	0 0	0 0	0 0	0 0	0 0	203.42 68.53	33.90 1.67	0 0	0 0	0 0	0 0	0 0	193.70 98.77	32.28 1.10
Os	70.60 4.91	738.58 97.35	1,667.08 99.61	4,554.58 99.83	3,572.84 99.67	65.58 24.30	1,778.21 86.84	633.60 74.85	1,055.59 99.94	5,289.73 99.74	5,435.17 92.98	3,747.17 86.34	1.84 0.94	2,693.85 91.90
Ms	233.50 16.24	18.83 2.48	5.16 0.31	5.83 0.13	7.08 0.20	204.25 75.70	79.11 3.86	130.00 15.35	0.67 0.06	11.50 0.22	409.75 7.01	593.00 13.66	194.03 98.93	223.16 7.61
Ps	549.00 38.19	1.25 0.16	1.42 0.08	1.67 0.04	4.83 0.13	m 0	93.03 4.54	35.70 4.22	m 0	1.92 0.04	0.42 0.01	0.08 0.002	0.25 0.13	6.40 0.22
?	584.6 40.66	0 0	0 0	0 0	0 0	0 0	97.43 4.76	47.20 5.58	0 0	0 0	0 0	0 0	0 0	7.86 0.27
An	1,365.00 94.94	18.00 2.37	92.42 5.52	246.66 5.41	306.50 8.55	31.25 11.58	343.31 16.77	275.50 32.55	5.00 0.47	911.51 17.19	827.84 14.16	389.16 8.96	2.09 1.06	401.85 13.71
Ss	69.00 4.80	366.16 48.26	172.67 10.32	35.42 0.78	10.42 0.29	m 0	108.94 5.32	457.10 53.99	386.17 36.56	11.38 0.21	m 0	m 0	m 0	142.44 4.86
Sw	1.70 0.12	0 0	0 0	0 0	0 0	0 0	0.28 0.01	0 0	0 0	0 0	0 0	0 0	0 0	0 0
Pr	2.00 0.14	374.5 49.36	1,408.57 84.16	4,280.00 93.82	3,267.83 91.16	238.58 88.42	1,595.25 77.90	113.90 13.46	665.09 62.97	4,370.26 82.41	4,608.33 78.84	3,358.09 77.37	193.70 98.77	2,218.23 75.67
?	0 0	0 0	0 0	0 0	0 0	0 0	0 0	m 0	m 0	10.00 0.19	409.17 7.00	593.00 13.67	0.33 0.17	168.75 5.76
Mr	658.60 45.81	757.41 99.84	1,671.41 99.87	4,554.58 99.83	3,572.83 99.67	269.83 100.00	1,914.11 93.47	745.00 88.01	1,056.26 100.00	5,289.73 99.75	5,435.75 92.99	3,747.17 86.34	195.54 99.70	2,744.91 93.64
Mb	237.30 16.51	1.25 0.16	2.25 0.13	7.50 0.16	11.92 0.33	m 0	43.37 2.12	93.30 11.02	m 0	13.42 0.25	409.59 7.01	593.08 13.66	0.58 0.30	185.00 6.31
Bw	541.80 37.69	0 0	0 0	0 0	0 0	m 0	90.30 4.41	8.2 0.97	0 0	0 0	0 0	0 0	0 0	1.36 0.05
Ww	75.60 5.26	753.41 99.31	1,478.83 88.36	3,663.75 80.31	3,199.75 89.26	237.33 87.96	1,568.11 76.57	735.10 86.84	1,046.18 99.05	4,303.73 81.15	5,207.84 89.09	3,714.75 85.59	195.79 99.83	2,533.90 86.44
Cw	813.10 56.56	4.75 0.63	193.41 11.55	896.66 19.65	380.17 10.61	32.50 12.04	386.77 18.89	75.70 8.94	10.08 0.95	834.00 15.73	205.33 3.51	30.67 0.71	m 0	192.63 6.57
Cp	549.00 38.19	0.50 0.06	1.42 0.08	1.67 0.04	4.83 0.13	m 0	92.90 4.54	35.70 4.22	m 0	11.92 0.22	409.59 7.01	593.08 13.66	0.33 0.17	175.10 5.98
En	0 0	0 0	0 0	0 0	0 0	0 0	0 0	0 0	0 0	153.50 2.90	22.58 0.39	1.75 0.04	0 0	29.64 1.01
Σ	1,437.70 100	758.66 100	1,673.66 100	4,562.08 100	3,584.75 100	269.83 100	2,047.78 100	846.50 100	1,056.26 100	5,303.15 100	5,845.34 100	4,340.25 100	196.12 100	2,931.27 100

In a depth range of 1–5 m, right up to the boundary with sand, the community *Ericaria bosphorica* + *Gongolaria barbata* + *Vertebrata subulifera* – *Cladostephus hirsutus* was recorded (see Table 1). The vegetation cover was fairly uniform, but the ratio of the key quantitative indicators varied with depth. At sta. No. 3–5, BM was 1,674–4,562 g·m^{-2}; PC, from 60–65 to 95–100%; VH, 17.4–29.1 cm; and NS, 22–24 (see Tables 3, 4).

Soft substrata from the boundary with hard substrata to the isobath of 7–7.5 m were devoid of permanent macroscopic vegetation. However, from this mark and down to 8.5–9 m, those were occupied by the community of *Nanozostera noltei* (see Table 1). At sta. No. 6, BM was 270 g·m^{-2}; PC, 25–30%,

VH, 22.9 cm; and NS, 19 (see Tables 3, 4)[1] . Several *N. noltei* clumps, 1–3 m in diameter and 1–5 m apart (sometimes up to 10 m), were formed by vegetative shoots alone. Deeper than 9 m, no permanent vegetation cover was revealed.

In 2015, 50 macrophyte species were registered in the surveyed area: Chlorophyta, 12 (24.0%), Ochrophyta, 8 (16.0%), Rhodophyta, 29 (58.0%), and Tracheophyta, 1 (2.0%) (see Table 3). The minimum species diversity was noted for a depth of 0.5 m (16 species), and the maximum one, for 1 m (24 species); in other cases, NS distribution along the profile was relatively uniform (19–22 species). With the dominance by NS of short-vegetating (annual, seasonal winter, and seasonal summer) species (86.0%), the flora of the water area in general had an oligosaprobic (52.0%) marine (68.0%) warm-water (58.0%) character. In SBL, with increasing depth, there was no clear trend in the shift in the ratio of ecological-floristic groups. However, macrophytobenthos of PSL had a pronounced specificity in NS distribution by ecological-floristic groups, even more evident when analyzing BM. Thus, its overwhelming majority was formed by short-vegetating (99.7%), mainly annual Chlorophyta (94.0%), while proportions of marine (45.8%) oligosaprobic (4.9%) warm-water (5.3%) species were minimal for the surveyed area (see Table 4). At the same time, in SBL on hard substrata, Ochrophyta dominated (86.7–94.7%), while macroalgae species were chiefly oligosaprobic (97.4–99.8%) marine (99.7–99.9%) perennial (49.3–93.8%) warm-water (88.0–99.3%) ones (importantly, with increasing depth, there were no clear trends in the shift in the ratio of BM of these groups). On soft substrata, BM was formed mostly by mesosaprobic (79.1%) Tracheophyta (68.5%); the values of other indicators were close to those on hard substrata.

Results of 2022. The second survey showed that the vegetation belt of **PSL**, not divided into subzones and 25–45 cm wide, is formed by the community of *Ceramium ciliatum* (see Table 1). At sta. No. 1, BM was 847 g·m^{-2}; PC, 85–90%; VH, 6.2 cm; and NS, 19 (see Tables 3, 4).

Soft substrata of **SBL** are occupied by communities of the *Cystoseira* belt.

In the shallowest areas, the community *Ericaria bosphorica* + *Gongolaria barbata* – *Padina pavonica* + *Dictyota fasciola* develops. At sta. No. 2, BM was 1,056 g·m^{-2}; PC, 70–75%; VH, 12.3 cm; and NS, 22 (see Tables 1–4).

A depth of 1 m is still occupied by the community *Ericaria bosphorica* + *Gongolaria barbata* + *Vertebrata subulifera* – *Cladostephus hirsutus* (see Table 1). At sta. No. 3, BM was 5,303 g·m^{-2}; PC, 95–100%; VH, 28.6 cm; and NS, 27 (see Tables 3, 4). In a depth range of 3–5 m, *Bonnemaisonia hamifera* became one of the dominants of the second layer; as a result, the community *Ericaria bosphorica* + *Gongolaria barbata* + *Vertebrata subulifera* – *Bonnemaisonia hamifera* was formed (see Table 1). At sta. No. 4–5, BM was 4,340–5,845 g·m^{-2}; PC, from 85–90 to 95–100%; VH, 32.3–34.3 cm; and NS, 21–23 (see Tables 1–4).

The general character and vegetation distribution on soft substrata did not change. In a depth range from 7–7.5 to 8.5–9 m, the community of *Nanozostera noltei* was recorded (see Table 1). At sta. No. 6, BM was 196 g·m^{-2}; PC, 25–30%; VH, 21.7 cm; and NS, 14 (see Tables 3, 4). However, among vegetative shoots determining VH, a few generative ones were registered; those had a mean length of 13.6 cm and constituted less than 3% of the aboveground BM of *N. noltei*.

[1]For *Nanozostera noltei*, only the biomass (BM) of the aboveground part is given. BM of the underground part (rhizomes and roots) was not taken into account when calculating the total BM of the community and individual ecological-floristic groups.

In 2022, 49 macrophyte species were recorded in the surveyed area: Chlorophyta, 11 (22.5%), Ochrophyta, 8 (16.3%), Rhodophyta, 29 (59.2%), and Tracheophyta, 1 (2.0%) (see Table 3). The minimum species diversity was noted for soft substrata at a depth of 8 m (14 species), and the maximum one, at a depth of 1 m (27 species); in other cases, NS distribution along the profile remained quite stable (19–23 species). By NS, short-vegetating species predominate (63.3%); in general, the flora of the water area has an oligosaprobic (65.3%), marine (75.5%) warm-water (63.3) character. The same as earlier, macrophytobenthos of PSL differs from SBL one by these indicators; the analysis of the ratio of BM of ecological-floristic groups evidences for it even more clearly. However, in 2022, BM in PSL was chiefly formed by Rhodophyta (79.6%) represented mainly by short-vegetating (86.5%) seasonal summer and annual species (see Table 4). At the same time, proportions of most ecological-floristic groups in the total BM were slightly different from values recorded for hard substrata in SBL. It was dominated by Ochrophyta (76.0–97.4%), with high prevalence of oligosaprobic (86.3–99.9%) marine (86.3–100%) perennial (63.0–82.4%) warm-water (81.2–99.1%) species (there are no trends in the shift in the ratio of BM of the listed groups with a change in depth). On soft substrata, BM is chiefly formed by mesosaprobic (98.9%) Tracheophyta (98.8%); the values of other indicators are close to those observed for hard substrata.

As evidenced by generalization of the results obtained in 2015 and 2022, in the surveyed area, macrophytobenthos develops on different natural substrata which determines the nature of the vegetation cover on hard substrata (*Thalassophycion sclerochthonophytia*) and soft ones (*Thalassopoion malacochthonophytia*) [Kalugina-Gutnik, 1975]. In total, 63 macrophyte species were recorded at the analyzed site (see Table 2): Chlorophyta, 14 (22.2%), Ochrophyta, 9 (14.3%), Rhodophyta, 39 (62.0%), and Tracheophyta, 1 (1.6%). The comparison showed: the total NS of macrophytobenthos and the ratio of systematic groups by NS were quite close in two years. But at certain depths, the flora composition and the ratio of species (including dominant ones) and ecological-floristic groups had changed by 2022, and this determined the corresponding transformations in the vegetation cover. To date, along the surveyed shore, macrophytes form five belt-located plant communities (see Table 1). Their total BM has increased significantly on average, and the flora (NS) has acquired a more oligosaprobic marine warm-water character (see Tables 3, 4). The main qualitative and quantitative changes were recorded in the shallowest and deepest areas. Apparently, they occurred mainly for two different reasons.

In 2015, there were obvious signs of a recent mudflow both on the coast and on the seabed. Specifically, we noted fairly fresh gullies in the ravine and beach pebble deposits (sometimes mixed with unrounded rubble and clay) in a shallow area. Approximately 1–1.5 months before our survey, there were heavy rains in this area followed by significant (but not disastrous) floods into the sea. Macrophytobenthos near the water's edge was the first to be subjected to the destructive effect of the flow loaded with solid particles. The vegetation of PSL seems to have quickly recovered: due to the mass development of *Ulva* L. representatives, a community was formed there which is usually more typical of spring period (sometimes autumn) and/or eutrophic waters [Sadogurskiy et al., 2023b]. While the mechanical damage to the seabed vegetation at the ravine mouth was local and rapid, the eutrophication of waters was more large-scale and relatively long-term (due to a summer decrease in storm activity). As *Ulva intestinalis* is one of the fastest growing annual macroscopic polysaprobic species under favorable light and temperature conditions and an increased nutrient concentration [Kim et al., 2021; Parchevsky, Rabinovich, 1991], the 'off-season' transformation of the vegetation cover in the damaged area occurred. Visual observation of the adjacent areas of PSL revealed the widespread dominance of the seasonal

summer oligosaprobic species *Ceramium ciliatum* during this period. And in 2022, when the above- and underwater parts of the coastal zone had no signs of recent mudflow activity, this species continued to form the basis of the vegetation cover of SBL in the entire area, including the spot at the ravine mouth. At the same time, lower values of VH and total BM (see Tables 1, 4) are mostly mediated by morphological differences between *C. ciliatum* and a larger-sized species *U. intestinalis*.

For perennial communities of the shallow part of SBL, the mudflow in 2015 had more long-term consequences. In addition to the fact that the rate of recovery of perennial macroalgae was lower, the situation was worsened by partial burial of the bottom heap by terrigenous sediments. During the initial survey, at a depth of 0.5–1 m, *Cystoseira* s. l. thalli were significantly damaged: there were broken branches, and sometimes, bases of their trunks were covered with pebble and rubble (Fig. 2a). Visual observation showed as follows: the nature of the seabed vegetation at the ravine mouth did not change compared to that of the periphery of the surveyed area and the adjacent waters, but its quantitative indicators obviously dropped. This is sure to have affected the species composition, as other algae species inhabit either *Cystoseira* epilithon or its epiphyton. Although additional sampling along the periphery of the area was not carried out that year, the second survey was planned in a year – to identify the dynamics of macrophytobenthos; however, 7 years had passed before it was carried out. So, we did not establish how long it takes for macrophytobenthos to recover, and we do not have reliable information about whether similar damage occurred during that period (probably, yes), but we know how it ends. More precisely, we can characterize the vegetation cover of this area not subjected to the recent destructive effect of the mudflow that could occur again. Thus, at a depth of 0.5 m (sta. No. 2), where in 2015 the minimum NS and total BM for hard substrata were recorded, the values of 2022 increased by 27–28% (see Tables 3, 4). At 1 m (sta. No. 3), with a three-fold rise in the total BM, the indicators reached maximum or close-to-maximum values. They became comparable with those at greater depths which did not experience such a strong effect of the mudflow in 2015.

The difference between PC and VH values established in different years within the boundaries of the *Cystoseira* belt is quite obvious (see Table 1). Thus, in 2022, compared to 2015, VH increased by depths as follows: at 0.5 m, by 33.7%; at 1 m, by 39.1%; at 3 m, by 21.2%; and at 5 m, by 10.1%. Accordingly, the further from the shore, the less pronounced these changes; this corresponds to the weakening of the mudflow intensity. Therefore, it is quite natural that the total BM of *Cystoseira* s. l. representatives forming the basis of the vegetation cover in a depth range of 3–5 m, least affected by the mudflow (sta. No. 4 and 5), has close values in two analyzed years (see Table 2). An increase in the total BM of macrophytobenthos in this depth range in 2022 was governed by the abundant growth of epiphytes, mainly *Vertebrata subulifera* and *Bonnemaisonia hamifera*.

While the first one is a typical representative of the native flora, the second is a new invasive species for the region [Sadogurskiy et al., 2023a, b]. Developing almost in epiphyton alone, thalli of *B. hamifera* sporophytes occur now in absolutely all samples taken off the SCC. The only difference is that numerous filaments are common in shallow waters, while separate spherical thalli (Ø of 2–3 cm) appear deeper; from a depth of 2.5–3 m, those merge into growths sometimes reaching an area of 1–3 m^2. As a result, to date, the invader has become one of the dominants of the deepest plant communities and even caused their local degradation; it made it possible to classify the species as a transformer one [Sadogurskiy et al., 2023a, b]. In the surveyed area, at depths of 3–5 m, *B. hamifera* forms 6.0–13.7% of the total BM of the community, as well as most of BM and an aspect of the lower layer (previously almost exclusively *Cladostephus* one) (Fig. 2b). Under a dense epiphytic cover, *Cladostephus hirsutus* thalli appear

extremely depressed having lost almost all of their characteristic short branches. This is the key difference from the pattern recorded earlier in other areas off the SCC, where *B. hamifera* developed mostly on *Cystoseira* thalli [Sadogurskiy et al., 2023a, b].

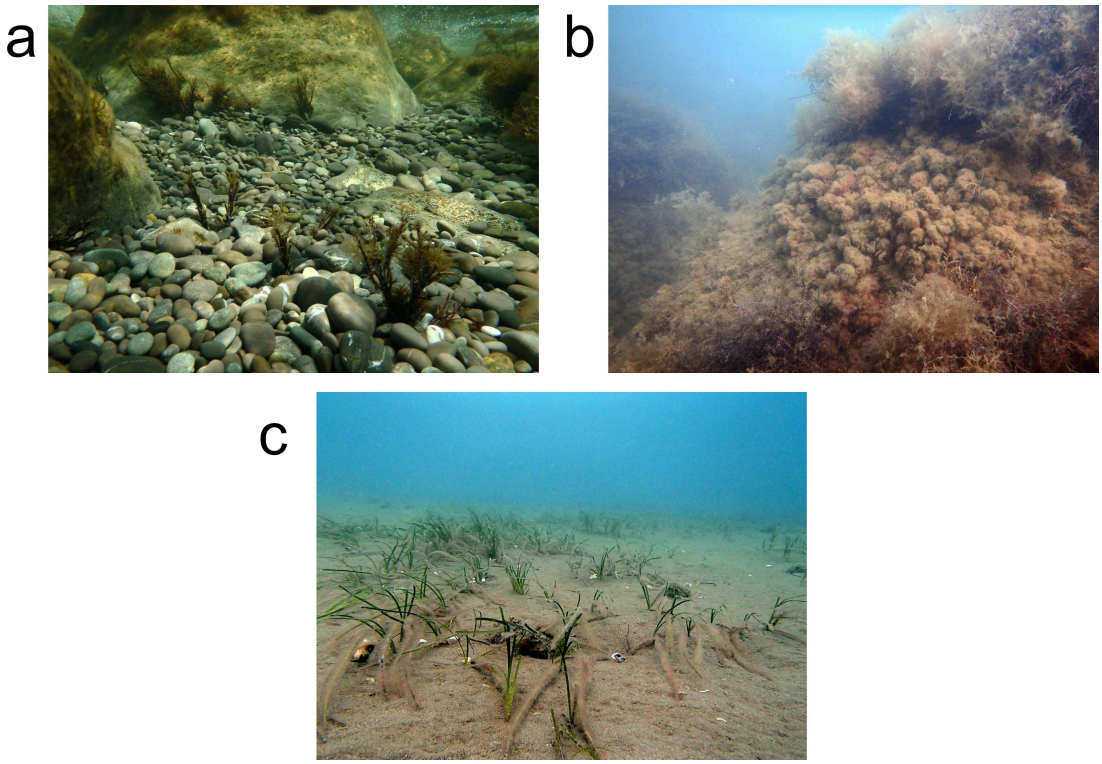

Fig. 2. Some features of macrophytobenthos off the coast of the Kuchuk-Lambat tract: a, community of the *Cystoseira* belt (*Cystoseira* s. l.) damaged by a mudflow, a depth of 0.5 m (07.08.2015); b, *Bonnemaisonia hamifera* growth in the community of the *Cystoseira* belt, a depth of 5 m (27.07.2022); c, laying of *Nanozostera noltei* leaves overgrown by *Bonnemaisonia hamifera*, a depth of 8 m (27.07.2022)

Importantly, *Ericaria bosphorica* and *Gongolaria barbata*, both *Cystoseira* s. l. representatives, used to be quite widespread off the SCC [Maslov, 2004; Maslov, Kuropatov, 1987; Pogrebnyak, Maslov, 1976]. Since about the mid-1990s, abundance and occurrence of the second species have dropped; as a result, its role in the formation of thickets has decreased for more than two decades. At some sites, the species was not registered in samples at all [Sadogursky, 2009, 2014]. Interestingly, within the last 3–5 years, a sudden recovery in quantitative indicators of *G. barbata* was observed, and it has almost returned to its dominant position, along with *E. bosphorica*. Thus, in the surveyed area, *G. barbata* was noted at 0.5 m in 2022 (it was absent there in 2015); in a depth range of 3–5 m, its BM almost doubled (see Tables 2, 4). It is hard to establish the cause for such dynamics, but we have to highlight the fact as follows. Along southern shores of the Sea of Azov, the pattern has been different all these years: most thickets were formed by *G. barbata*, while *E. bosphorica* was rare and non-abundant [Sadogurskiy et al., 2020].

Off the SCC, in the area of capes, mobile soft substrata are usually devoid of permanent macroscopic vegetation. Seagrass communities (with the dominance of *Zostera* L. and *Nanozostera* Toml. et Posl. representatives) develop fragmentarily at significant depths at sites with a concave coastline [Sadogurskiy et al., 2022]. The surveyed area is one of such sites. Seagrasses, unlike *Cystoseira*, belong to a different saprobiological group. Moreover, their thickets have a poorly represented dense substrata suitable

for the attachment of large-thallus species; that is why epiphytic macroalgae settle mostly on leaves. Only some of them develop on a few mollusc shells (scattered over the substrata surface) and less often on rhizomes of seagrasses (if those are exposed from the substrata). Therefore, in seagrass thickets off the SCC, NS and total BM are lower (the second one, by an order of magnitude) than in the *Cystoseira* belt; ecological-floristic indicators also differ much. The mudflow of 2015 did not affect the deep-water community of *N. noltei*; consequently, in both years, BM of the dominant and VH were almost the same (see Tables 1, 4). However, in 2022, NS and BM of epiphytic macroalgae decreased by 26.3–27.3%. The reason was that epiphytic filaments of *B. hamifera* densely covered *N. noltei* shoots; moreover, the oldest leaves were wrapped in continuous fleecy covers and, accordingly, were lying on the seabed (Fig. 2c). This directly reduces the area of substrata available to other epiphytes. In addition, their colonization is hindered by secondary metabolites of *B. hamifera*: according to several studies, they not only have a strong inhibitory allelopathic effect on the native phytobiota, but also definitely repel phytophages [Enge et al., 2012; Svensson et al., 2013]. As a result, due to its morphological plasticity, high stenobiontism, and the formation of a specific phytogenic field, *B. hamifera* successfully competes with native macrophytes. Its rapid distribution along the SCC, a part of the global expansion, poses a serious threat to natural communities and biotopes of the Sea of Azov–Black Sea region [Sadogurskiy et al., 2023a, b].

Thus, the periodic effect of the mudflow on macrophytobenthos of the surveyed area is short-term and reversible, and it weakens with increasing depth. At the same time, transformations caused by *B. hamifera* invasion become more intense with depth and are probably long-term; to date, their reversibility raises reasonable doubts. But in general, despite the close and long-term proximity to urbanized, recreational, and agricultural areas, the benthic vegetation cover shows a high degree of preservation. Its general character, as well as the flora composition and the ratio of the key ecological-floristic indicators (except for transformations mediated by the new biological invasion) are typical for the Black Sea hydrobotanical region "SCC." The rare species fraction of the flora covers 12 taxa listed in environmental documents of various ranks. Biotopes, with the basis formed by macrophyte communities, are listed in the Habitats Directive (Directive 92/43/EEC; codes 1160 and 1170) [Interpretation Manual of European Union Habitats, 2013]. Thus, both the water area and the coast certainly have obvious sozological value. Taking into account the approach proposed earlier [Sadogurskiy et al., 2017; Sadogursky et al., 2009, 2013], we consider it appropriate to establish on their basis a single territorial-aquatic nature reservation. It should unite the existing geological natural monument Kuchuk-Lambat Stone Chaos and its adjacent coastal and marine area of the Black Sea with a length of 300–350 m along the shore to a depth of at least 10 m, at a distance of at least 250–300 m from the water's edge (see Fig. 1a). To a certain extent, the official nature reserve status will protect this territorial-aquatic complex from direct anthropogenic transformation due to gradual absorption by adjacent recreational complexes. Such a nature reserve will not interfere with their functioning; on the contrary, it will increase their tourist attractiveness. Off the SCC, natural and slightly transformed areas have still been preserved, most often confined to hard-to-reach rocky capes and other inconvenient areas (as in the case analyzed). Establishing of small but relatively numerous territorial-aquatic protected areas (cores) on their basis, united into the structure of the ecological network by territorial-aquatic connecting elements (ecocorridors), will allow for the formation of a certain environmental protection framework off the SCC. At the same time, further study of *B. hamifera* invasion is required: this will reveal its dynamics and help in assessing environmental and possible social and economic consequences for the region.

Conclusion. Based on results of the hydrobotanical study carried out in 2015 and 2022, it was established as follows: in the coastal-marine water area adjacent to the geological natural monument Kuchuk-Lambat Stone Chaos, macrophytobenthos develops on natural hard and soft substrata which determines its general character. In total, 63 macrophyte species were recorded: Chlorophyta, 14 (22.2%); Ochrophyta, 9 (14.3%); Rhodophyta, 39 (62.0%); and Tracheophyta, 1 (1.6%). The total number of species and the ratio of systematic groups by the number of species are close for two years. However, the flora composition and the ratio of dominant species and ecological-floristic groups by biomass changed significantly at minimum and maximum depths. This caused a transformation of the vegetation cover. In shallow areas, its dynamics is mediated by local disturbance and subsequent recovery of macrophytobenthos after a mudflow and has a fluctuating character. At depth, the shifts are governed by the invasion of the transformer species *Bonnemaisonia hamifera* into natural communities. These shifts are likely to be of a long-term nature; to uncover their degree and reversibility, it is necessary to monitor the distribution of the invader off the southern coast of Crimea and within the boundaries of the Sea of Azov–Black Sea region in general. At present, along the surveyed coast, macrophytes form five belt-located plant communities. Macrophytobenthos demonstrates a high degree of preservation. Its spatial distribution, composition, and structure (except for changes caused by biological invasion) are typical for the Black Sea hydrobotanical region "Southern Coast of Crimea." Taxa and biotopes subjected to special protection within the framework of regional and international legislation are recorded. To prevent anthropogenic transformation, it is reasonable to form a comprehensive territorial-aquatic nature reserve that will unite the existing geological natural monument and adjacent coastal waters of the Black Sea.

The work was carried out within the framework of NBG–NSC state research assignment No. 122041900097-3.

REFERENCES

1. Belich T. V., Sadogurskaya S. A., Sadogurskiy S. Ye. To the question of species diversity of coastal-marine areas of the south coast of Crimea. *Trudy Karadagskoi nauchnoi stantsii im. T. I. Vyazemskogo – prirodnogo zapovednika RAN*, 2020, no. 4 (16), pp. 3–12. (in Russ.). https://doi.org/10.21072/eco.2021.16.01
2. Belokopytov V. N., Sarkisov A. A., Shchurov S. V. Currents near the part of the Crimean coast from the Sarych Cape to Katsiveli. *Ekologicheskaya bezopasnost' pribrezhnoi i shel'fovoi zon i kompleksnoe ispol'zovanie resursov shel'fa*, 2003, iss. 8, pp. 64–68. (in Russ.). https://elibrary.ru/zaqmqx
3. Vakhrushev B. A., Amelichev G. N. Geologicheskii pamyatnik prirody – Kuchuk-Lambatskii kamennyi khaos – kak element opolznevoi, seismogravitatsionnoi i karstovoi morfoskul'ptury rel'efa Yuzhnogo berega Kryma. *Kul'tura narodov Prichernomor'ya*, 2000, no. 15, pp. 12–17. (in Russ.). https://elibrary.ru/hurprb
4. Goryachkin Yu. N., Repetin L. N. Storm wind and wave regime near the Black Sea coast of Crimea. *Ekologicheskaya bezopasnost' pribrezhnoi i shel'fovoi zon i kompleksnoe ispol'zovanie resursov shel'fa*, 2009, iss. 19, pp. 56–69. (in Russ.). https://elibrary.ru/yktsvr
5. *Gidrometeorologiya i gidrokhimiya morei SSSR.* Vol. 4. *Chernoe more.* Iss. 1. *Gidrometeorologicheskie usloviya* / A. I. Simonov,

E. N. Altman (Eds). Saint Petersburg : Gidrometeoizdat, 1991, 426 p. (in Russ.)
6. Zinova A. D. *Opredelitel' zelenykh, burykh i krasnykh vodoroslei yuzhnykh morei SSSR*. Moscow ; Leningrad : Nauka, 1967, 400 p. (in Russ.)
7. Kalugina A. A. Issledovanie donnoi rastitel'nosti Chernogo morya s primeneniem legkovodolaznoi tekhniki. In: *Morskie podvodnye issledovaniya*. Moscow : Nauka, 1969, pp. 105–113. (in Russ.)
8. Kalugina-Gutnik A. A. *Fitobentos Chernogo morya*. Kyiv : Naukova dumka, 1975, 248 p. (in Russ.). https://repository.marine-research.ru/handle/299011/5645
9. *Red Data Book of Priazovsky Region. Vascular Plants* / V. M. Ostapko, V. P. Kolomiychuk (Eds). Kyiv : Alterpres, 2012, 280 p. (in Russ.). https://elibrary.ru/yhslft
10. *Red Book of the Republic of Crimea. Plants, Algae, and Fungi* / A. V. Yena, A. V. Fateryga (Eds). Simferopol : ARIAL, 2015, 480 p. (in Russ.). https://elibrary.ru/wxeqef
11. *Krasnaya kniga Rossiiskoi Federatsii* (rasteniya i griby). Moscow : Tov-vo nauch. izd. KMK, 2008, 885 p. (in Russ.). https://elibrary.ru/tcnfxr
12. Maslov I. I. *Morskoi fitobentos krymskogo poberezh'ya*. [dissertation]. Yalta, 2004, 358 p. (in Russ.)
13. Maslov I. I., Kuropatov L. A. K detal'nomu opisaniyu biotsenoza tsistoziry zapovednika "Mys Mart'yan". *Byulleten' Gosudarstvennogo Nikitskogo botanicheskogo sada*, 1987, iss. 63, pp. 13–17. (in Russ.). https://elibrary.ru/zwxmst
14. Parchevsky V. P., Rabinovich M. A. Growth rate and harvest of the green alga *Enteromorpha intestinalis* on artificial substrates in a wastewater outfall area. *Biologiya morya*, 1991, no. 2, pp. 30–36. (in Russ.). https://repository.marine-research.ru/handle/299011/10759
15. *Pasport pamyatnika prirody regional'nogo znacheniya "Kuchuk-Lambatskii kamennyi khaos"* : utverzhden prikazom Ministerstva ekologii i prirodnykh resursov Respubliki Krym ot 29.04.2021 no. 523. Simferopol : [s. n.], 2021, 13 p. (in Russ.)
16. Pogrebnyak I. I., Maslov I. I. K izucheniyu donnoi rastitel'nosti raiona mysa Mart'yan. *Byulleten' Gosudarstvennogo Nikitskogo botanicheskogo sada*, 1976, vol. 70, pp. 105–113. (in Russ.). https://elibrary.ru/yoflcx
17. Ryff L. E. Flora of the nature monument "Kuchuk-Lambat stone chaos" (south coast of the Crimea). *Geopolitika i ekogeodinamika regionov*, 2013, vol. 9, no. 2-2, pp. 65–72. (in Russ.). https://elibrary.ru/vmbfup
18. Sadogursky S. Ye. Macrophytobenthos near the coast of the botanical reserve "Kanaka": Its modern state and the ways of preservation (Black Sea). *Zapovidna sprava v Ukraini*, 2009, vol. 15, iss. 1, pp. 31–39. (in Russ.). https://elibrary.ru/ynkixl
19. Sadogursky S. Ye. Composition and distribution of macrophytobenthos near the cape of Svyatoy Troitsy (Black Sea, Crimea, Ukraine). *Morskoj ekologicheskij zhurnal*, 2014, vol. 13, no. 1, pp. 53–62. (in Russ.). https://repository.marine-research.ru/handle/299011/1325
20. Sadogursky S. E., Belich T. V., Sadogurskaya S. A. To problem of separation of territory-aquatic elements of regional econet in Crimea. In: *The Nature Reserves of Crimea. Theory, Practice and Perspectives of Conservation Business in Black Sea Region* : materials of the 5th International scientific-practical conference (Simferopol, 22–23 October, 2009). Simferopol : [s. n.], 2009, pp. 134–139. (in Russ.). https://elibrary.ru/ynijcn
21. Sadogursky S. E., Belich T. V., Sadogurskaya S. A. Some aspects of formation

of territorial aquatic components of the regional and local ecological networks in the Crimea. In: *Priroda Vostochnogo Kryma. Otsenka bioraznoobraziya i razrabotka proekta lokal'noi ekologicheskoi seti* / S. P. Ivanov (Ed.). Kyiv : TOV "DIA", 2013, pp. 79–85. (in Russ.). https://elibrary.ru/zawrhd

22. Sadogurskiy S. Yu., Ryff L. E., Sadogurs'ka S. O., Belich T. V. To the strategy of preserving the natural phytodiversity of the coastal zone of the sea. In: *Proceedings of the 14th Congress of the Ukrainian Botanical Society*, Kyiv, 25–26 April, 2017. Kyiv, 2017, pp. 134. (in Ukr.)
23. *Sovremennoe sostoyanie beregovoi zony Kryma* / Yu. N. Goryachkin (Ed.). Sevastopol : EKOSI-Gidrofizika, 2015, 252 p. (in Russ.). https://elibrary.ru/urttzy
24. *Red Data Book of Ukraine. Flora* / Ya. P. Didukh (Ed.). Kyiv : Globalkonsalting, 2009, 912 p. (in Ukr.)
25. *AlgaeBase.* World-wide electronic publication, National University of Ireland, Galway / M. D. Guiry, G. M. Guiry (Eds) : [site], 2024. URL: http://www.algaebase.org [accessed: 17.01.2024].
26. *Black Sea Red Data Book* / H. J. Dumont (Ed.). New York : United Nations Office for Project Services, 1999, 413 p.
27. Enge S., Nylund G. M., Harder T., Pavia H. An exotic chemical weapon explains low herbivore damage in an invasive alga. *Ecology*, 2012, vol. 93, iss. 12, pp. 2736–2745. https://doi.org/10.1890/12-0143.1
28. *Interpretation Manual of European Union Habitats. EUR 28.* Brussels : European Commission, DG Environment, 2013, 144 p.
29. *International Plant Names Index (IPNI)* : [site], 2024. URL: https://www.ipni.org/ [accessed: 17.01.2024].
30. Johnson N. C. *Biodiversity in the Balance: Approaches to Setting Geographic Conservation Priorities.* Washington, DC : Biodiversity Support Program, 1995, 116 p.
31. Kim J.-H., Zhao Z. X., Kim Y. S. Variation in germling growth in the green tide-forming alga *Ulva intestinalis* (Chlorophyta) in response to gradients in salinity, temperature, light, and nutrients. *Journal of Applied Phycology*, 2021, vol. 33, iss. 6, pp. 3951–3962. https://doi.org/10.1007/s10811-021-02563-4
32. *Proposal for a Council Decision Establishing the Position to be Adopted on Behalf of the European Community with Regard to Proposals for Amending Annexes II and III to the Protocol Concerning Specially Protected Areas and Biological Diversity in the Mediterranean (SPA/BD Protocol) of the Convention for the Protection of the Marine Environment and the Coastal Region of the Mediterranean (Barcelona Convention) at the Sixteenth Meeting of the Contracting Parties.* COM (2009) 585 final. Brussels : Commission on the European Communities, 2009, 13 p. URL: http://eur-lex.europa.eu/legal-content/EN/TXT/PDF/?uri=CELEX:52009PC0585&from=EN [accessed: 17.01.2024].
33. *Red Data Book of the Republic of Bulgaria.* Vol. 1. *Plants and Fungi* / D. Peev, V. Vladimirov (Eds). Sofia : BAS & MoEW, 2015a, 881 p.
34. *Red Data Book of the Republic of Bulgaria.* Vol. 3. *Natural Habitats* / V. Biserkov et al. (Eds). Sofia : BAS & MoEW, 2015b, 422 p.
35. Sadogurskiy S. Ye., Belich T. V., Sadogurskaya S. A. Invasion of the alien species *Bonnemaisonia hamifera* Hariot in coastal phytocenoses near the southern coast of Crimea (the Black Sea). *Inland Water Biology*, 2023a, vol. 16, iss. 1, pp. 65–71. https://doi.org/10.1134/S1995082923010145
36. Sadogurskiy S. Ye., Belich T. V., Sadogurskaya S. A. Macrophytobenthos of the reserved and transformed coastal

marine areas at the south coast of Crimea in conditions of the new biological invasion (the Black Sea). *International Journal on Algae*, 2023b, vol. 25, iss. 4, pp. 365–382. https://doi.org/10.1615/InterJAlgae.v25.i4.50

37. Sadogurskiy S. Ye., Sadogurska S. S., Belich T. V., Sadogurska S. A. Distribution of *Cystoseira* s. l. species in the Sea of Azov. *International Journal on Algae*, 2020, vol. 22, iss. 4, pp. 327–346. https://doi.org/10.1615/InterJAlgae.v22.i4.30
38. Sadogurskiy S. Ye., Sadogurskaya S. A., Belich T. V. Eelgrass beds (gen. *Zostera* Linnaeus, 1753) and the related specific form of the bottom microrelief at the southern coast of Crimea (in the Black Sea). *Russian Journal of Marine Biology*, 2022, vol. 48, iss. 4, pp. 297–301. https://doi.org/10.1134/S1063074022040101
39. Svensson J. R., Nylund G. M., Cervin G., Toth G. B., Pavia H. Novel chemical weapon of an exotic macroalga inhibits recruitment of native competitors in the invaded range. *Journal of Ecology*, 2013, vol. 101, iss. 1, pp. 140–148. https://doi.org/10.1111/1365-2745.12028

СОСТАВ И СТРУКТУРА МАКРОФИТОБЕНТОСА У ПОБЕРЕЖЬЯ ПАМЯТНИКА ПРИРОДЫ «КУЧУК-ЛАМБАТСКИЙ КАМЕННЫЙ ХАОС» (КРЫМ, ЧЁРНОЕ МОРЕ)

С. Е. Садогурский, Т. В. Белич, С. А. Садогурская

ФГБУН «Никитский ботанический сад — Национальный научный центр РАН»,
Ялта, Российская Федерация
E-mail: *ssadogurskij@yandex.ru*

Южный берег Крыма (ЮБК) характеризуется высоким уровнем антропогенной трансформации, поэтому участки, сохранившиеся в природном или квазиприродном состоянии, имеют особую природоохранную ценность. К ним относится территориально-аквальный комплекс, объединяющий геологический памятник природы «Кучук-Ламбатский каменный хаос» и примыкающую прибрежную акваторию Чёрного моря. Акватория в гидроботаническом аспекте не изучена и в состав особо охраняемых природных объектов не включена. В связи с этим выполнено исследование, цель которого — по данным 2015 и 2022 гг. охарактеризовать видовой состав, биомассу и пространственную структуру макрофитобентоса для уточнения представлений о распределении и динамике растительного покрова бентали у ЮБК и в связи с перспективой заповедания указанной акватории. Установлено, что макроскопическая растительность развивается на твёрдых и мягких грунтах, что определяет её общий характер. Всего зарегистрировано 63 вида макрофитов: Chlorophyta — 14 (22,2 %), Ochrophyta — 9 (14,3 %), Rhodophyta — 39 (62,0 %), Tracheophyta — 1 (1,6 %). Общее количество видов (КВ) и соотношение систематических группировок по КВ в оба года близки. Однако состав флоры, а также соотношение по биомассе (БМ) доминирующих видов и эколого-флористических группировок существенно изменились на минимальных и на максимальных глубинах, что определило трансформации растительного покрова. На мелководье их динамика, обусловленная локальным нарушением и последующим восстановлением макрофитобентоса после схода селевого потока, имеет флуктуационный характер. На глубине изменения вызваны инвазией в природные сообщества вида-трансформера *Bonnemaisonia hamifera* и, вероятно, имеют долговременный характер; для выявления их степени и обратимости необходим мониторинг распространения вселенца у ЮБК и в границах Азово-Черноморского региона в целом. В настоящее время вдоль обследованного берега макрофиты формируют пять поясно расположенных растительных сообществ с БМ 0,2–6,0 кг·м$^{-2}$ и КВ 14–27. Крайние значения этих показателей зарегистрированы в сублиторали: максимальные — на твёрдых грунтах в верхней и центральной частях пояса цистозиры (виды *Cystoseira* s. l.), минимальные — на мягких грунтах

в наиболее глубоководном сообществе морских трав (*Nanozostera noltei*). В целом по БМ доминируют многолетние, а по КВ — коротковегетирующие макрофиты; фитобентос имеет выраженный олигосапробный морской тепловодный характер. Растительный покров акватории демонстрирует высокую степень сохранности, его пространственное распределение, состав и структура (за исключением изменений, вызванных биологической инвазией) типичны для гидроботанического района Чёрного моря «ЮБК». Раритетная фракция флоры насчитывает 12 таксонов; биотопы, основу которых формируют сообщества макрофитов, попадают под действие документа Directive 92/43/EEC. Целесообразно создание комплексного территориально-аквального природного заказника, который объединит существующий памятник природы и прилегающую к нему акваторию.

Ключевые слова: Чёрное море, Южный берег Крыма, Кучук-Ламбат, макрофитобентос, видовой состав, биомасса, пространственная структура

1871
ИнБЮМ – IBSS

Морской биологический журнал
Marine Biological Journal
2025, том 10, № 2, с. 87–94
https://marine-biology.ru

UDC 593.12(265.54)

CEPHALOGULLMIA CAUDATA GEN. NOV., SP. NOV. (RHIZARIA, FORAMINIFERA), A MONOTHALAMOUS FORAMINIFERA FROM THE SEA OF JAPAN

© 2025 **N. Sergeeva and O. Anikeeva**

A. O. Kovalevsky Institute of Biology of the Southern Seas of RAS, Sevastopol, Russian Federation
E-mail: *alegria@ibss-ras.ru*

Received by the Editor 02.07.2024; after reviewing 18.10.2024;
accepted for publication 20.03.2025.

We describe a new species and genus of soft-walled monothalamous foraminifera from the Sea of Japan. The material was sampled off the Primorsky shelf during the 64th cruise of the RV "Akademik Oparin" (17 June to 08 July, 2021). Bottom sediments were sampled at 17 stations in a depth range of 0.3–86 m. The species described here was found at depths of 13 and 86 m. An elongated organic-walled test of *Cephalogullmia caudata* sp. nov. has an inflated anterior (apertural) part which gradually narrows towards the adapertural end. The length varies 600 to 1,180 μm; the width at the widest part (the 'head') is 50 to 135 μm, and at the narrowest part, it is 10 to 20 μm. A single apertural structure (10–28 μm in diameter) is located at the widest end of the test. The apertural structure is slightly elevated; in some specimens, it resembles a nipple. The nucleus is visible only in some specimens; its size is from 16 × 12 μm to 30 × 15 μm. The comparative analysis shows that the new genus *Cephalogullmia* differs from *Micrometula* Nyholm, 1952 in the shape of the test: it has more rounded and inflated apertural end, compared to that of the slender conical test of *Micrometula*. The new genus differs from *Cylindrogullmia* Nyholm, 1974 in the shape of the test as well: in the latter one, it is cylindrical. It also differs from another organic-walled monothalamid with the elongated test, *Bowseria* Sinniger et al., 2008, in having a darker protoplasm and a narrowed (tail-shaped) adapertural end.

Keywords: soft-walled foraminifera, Sea of Japan, *Cephalogullmia caudata* gen. nov., sp. nov., monothalamids

Soft-walled monothalamous foraminifera are an important component of meiofauna in many coastal and deepwater habitats [Gooday, 2002; Majewski et al., 2007; Sergeeva, Anikeeva, 2018, 2023], as well as in freshwater ones [Holzmann et al., 2021]. In recent years, scientific interest in this group has increased significantly [Anikeeva et al., 2013; Sergeeva et al., 2010]. Although molecular analysis is now available for many monothalamous foraminifera [Gooday et al., 2011, 2022; Lejzerowicz et al., 2015; Siemensma et al., 2021; Voltski, Pawłowski, 2015], some recent taxonomic descriptions still rely on morphological characteristics alone [Anikeeva et al., 2013; Golemansky, 1999; Gooday et al., 2006; Henderson, 2023; Ohkawara et al., 2009; Sergeeva, Anikeeva, 2008, 2020, 2021]. Here, we describe a new monothalamous taxon, an organic-walled 'allogromiid,' based on its morphological features.

Studies of meiobenthos in the Sea of Japan have been mainly focused on multicellular eukaryotes, especially the dominant group, free-living nematodes. Out of unicellular eukaryotes, only hard-shelled foraminifera have been considered as a component of meiobenthic communities [Preobrazhenskaya, Tarasova, 1990]. The results of detailed studies of the species diversity of hard-shelled foraminifera in the Sea of Japan are provided by T. Lukina and T. Tarasova [2013] in their check-list of free-living

invertebrates in Far Eastern seas of Russia – a publication covering 217 foraminifera species. A representative of a genus of soft-walled foraminifera, *Allogromia* sp. (the family Allogromiidae), is reported to be found in the Bering Sea and off the South Kuril Islands and northeastern Sakhalin Peninsula. This appears to be the only record of soft-walled foraminifera in the Northwestern Pacific reflecting the lack of information on these protists, their specific morphological characteristics, and the need to apply special methods to study them.

For the first time, soft-walled foraminifera were investigated in Far Eastern waters of Russia (the Sea of Japan) in summer 2021, during the research cruise of the RV "Akademik Oparin." In total, 49 species and morphotypes of monothalamids representing the families Allogromiidae and Saccamminidae were recorded in this area [Sergeeva, Anikeeva, 2023]. The fauna of monothalamids in the Sea of Japan included the one that we describe here as the type species of a new genus.

The aim of this paper is to provide a description of *Cephalogullmia caudata* gen. nov., sp. nov., an inhabitant of the Sea of Japan (the Northwestern Pacific).

MATERIAL AND METHODS

Material was sampled off the Primorsky shelf, the Sea of Japan, during the 64th cruise of the RV "Akademik Oparin" (17 June to 08 July, 2021). Bottom sediments were sampled at 17 stations in a depth range of 0.3 to 86 m. The species described was found at sta. 1 and 40 (depths of 13 and 86 m). At shallower stations, divers sampled sediment cores (two replicates), 5 cm long, with a cross-sectional area of 10 cm^2. At greater depths, similar cores were taken from sediment obtained with a Van Veen grab sampler. Samples of bottom sediments were fixed onboard the RV with 75% ethanol and later processed and analyzed in IBSS laboratory (Sevastopol, Russian Federation). Samples were washed through two sieves: an upper one with a mesh size of 1 mm and a lower one with a mesh size of 63 μm. For the second series of samples, we used a lower sieve with a mesh size of 32 μm.

Detailed microscopic analysis of soft-walled foraminifera was performed under MSP-2, Olympus CX41, Nikon, and Mikmed-6 microscopes equipped with photo cameras.

RESULTS

Taxonomy. According to traditional morphology-based classification systems [Kaminski, 2004; Loeblich, Tappan, 1988], the new single-chambered (monothalamous) taxa described here belong to the suborder Allogromiina (organic-walled). However, recent molecular phylogenetic studies, which revealed a series of monophyletic clades that cut across morphology-based taxa, have undermined the traditional higher-level classification of monothalamous organic-walled and agglutinated foraminifera [Habura et al., 2008; Pawlowski et al., 2003, 2013]. Therefore, we avoid formal higher taxa and place the new genera in the informal group of 'monothalamids' [Pawlowski et al., 2013].

Rhizaria Cavalier-Smith, 2002

Foraminifera d'Orbigny, 1826

'Monothalamids' Pawlowski et al., 2013

Genus *Cephalogullmia* Sergeeva et Anikeeva, gen. nov.

Type species *Cephalogullmia caudata* Sergeeva et Anikeeva, sp. nov.

Diagnosis of the genus. A monothalamous foraminifera having an elongated organic-walled test with an inflated anterior (apertural) part that gradually narrows towards the adapertural end (Fig. 1). The width at the inflated front part (the 'head') exceeds the width of the body by 5–6 times at the narrowest

part. A single slightly elevated apertural structure is located at the widest end of the test. In some specimens, it resembles a nipple. The oval nucleus is localized in the widened part of the body before its tapering and is visible only in some specimens.

Derivation of the genus name. The name of the genus indicates its similarity to the genus *Nemogullmia* in terms of test length and the rounded apertural end resembling a head (in Latin, 'cephalo').

Remarks. Comparative analysis showed that the investigated specimens cannot be related to any of the known foraminifera genera. We made a comparative diagnosis of the new genus with three morphologically most similar genera of soft-walled foraminifera. The key difference between the new genus *Cephalogullmia* and *Micrometula* Nyholm, 1952 is in the shape of the test: there is the test with a more rounded and inflated apertural end than the slender conical test of *Micrometula*. The new genus differs from *Cylindrogullmia* Nyholm, 1974 by the presence of a sharply tapering 'tail' part, while the test of *Cylindrogullmia* specimens has approximately the same diameter throughout the body length. It also differs from another elongated organic-walled monothalamid, *Bowseria* Sinniger et al., 2008, in having a darker protoplasm and a narrowed (tail-shaped) adapertural end.

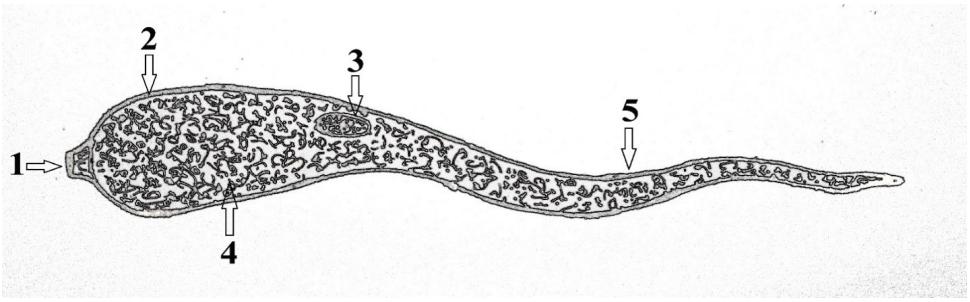

Fig. 1. Schematic image of *Cephalogullmia caudata*: 1, aperture; 2, organic test wall; 3, nucleus; 4, cytoplasm; 5, 'tail' part

Cephalogullmia caudata Sergeeva et Anikeeva, sp. nov. (Fig. 2).

Syn. Allogromiid sp. 9J [Sergeeva, Anikeeva, 2023, pp. 446–447, Fig. 9e, f].

Diagnosis of species. The elongated organic-walled test has an inflated anterior (apertural) part which gradually narrows towards the adapertural end. The body length varies from 600 to 1,180 μm; the width at the widest part (the 'head') is 50 to 135 μm, and at the narrowest part, it is 10 to 20 μm. A single apertural structure (10–28 μm in diameter) is located at the widest end of the test. The apertural structure is slightly elevated; in some specimens, it resembles a nipple. The nucleus is visible only in some specimens, and its size is from 16 × 12 μm to 30 × 15 μm. Coefficient C (length-to-width ratio) ranges 8.7 to 16.5 (based on the maximum width of the body).

Derivation of specific name. Latin 'caudata' = 'tail' refers to the shape of the main part of the body.

Type material. The type specimen (registration number Meib.93.Al.t) and two paratype specimens (registration numbers Meib.94.Al.p.1 and Meib.95.Al.p.2) are mounted in water–glycerol preparations and stored at IBSS. Previous experience has shown that similar organic-walled specimens are too delicate to be mounted in either Canada balsam or a gelatin–glycerol mixture.

Type locality. The type specimen and the paratype specimens (Figs 2–4) are from the Sea of Japan (43°42.7′N, 135°25.6′E; depth of 86 m). They were picked from samples taken during the research cruise of the RV "Akademik Oparin," 17 June to 08 July, 2021.

Other material. Three more specimens from the type locality (Fig. 5) were examined.

Description. The type specimen has an elongated shape (Fig. 2A). The test is organic, thin, and transparent. It gradually narrows from the apertural end to the adapertural one. The cytoplasm is homogeneous and fine-grained. The single aperture is located at the widest end of the test and is 16 μm in diameter (Fig. 2B). The test length is 1,070 μm, and the maximum width is 90 μm. The nucleus is ellipsoidal, oblong (Fig. 2C); it is located in the middle part of the cell, and it is 30 × 15 μm. Coefficient C is about 11.8 (based on the maximum width of the body).

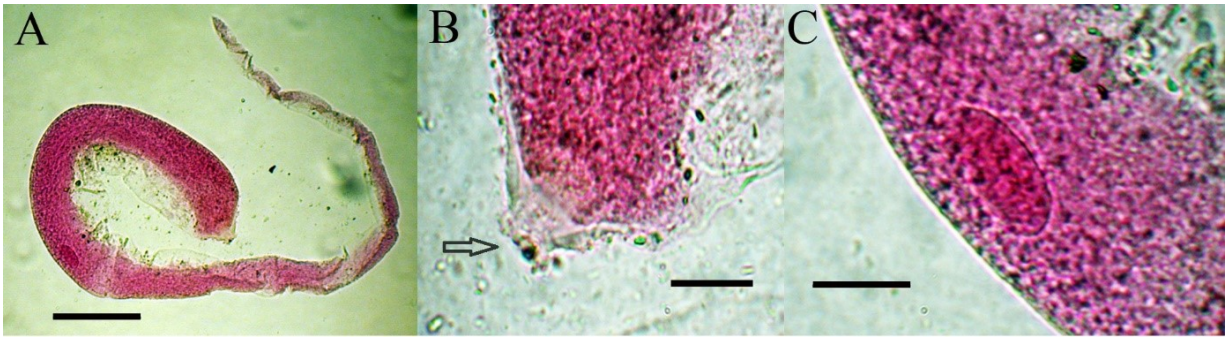

Fig. 2. The type specimen: A, general view; B, aperture; C, nucleus. Scale bars are 100 μm (A) and 20 μm (B, C)

The paratype specimen 1 (Fig. 3A) is 1,150 μm in length and tapers from 110 μm in width at the widest point to 20 μm at the narrow adapertural end (Fig. 3B). The aperture has a diameter of 28 μm. Coefficient C is 10.4.

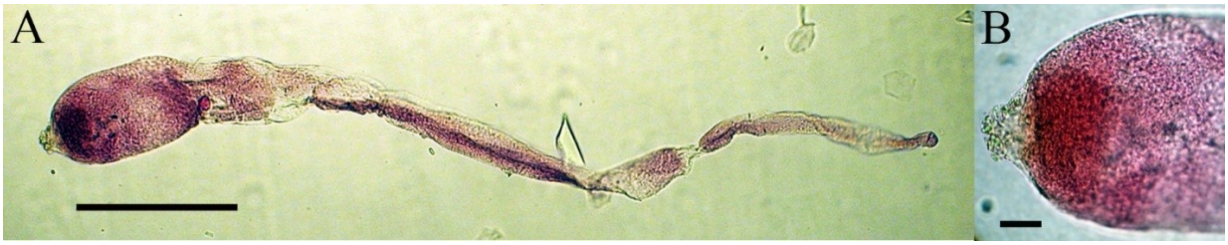

Fig. 3. The paratype specimen 1: A, general view; B, aperture. Scale bars are 200 μm (A) and 20 μm (B)

The paratype specimen 2 (Fig. 4A) is 1,180 μm in length and tapers from 135 μm in width at the widest point to 25 μm at the narrow adapertural end. The aperture (Fig. 4B) is located at the wider end of the body; however, its size cannot be measured, as it is not clearly visible. Coefficient C is 8.7. The nucleus is not clearly visible in either of the paratypes.

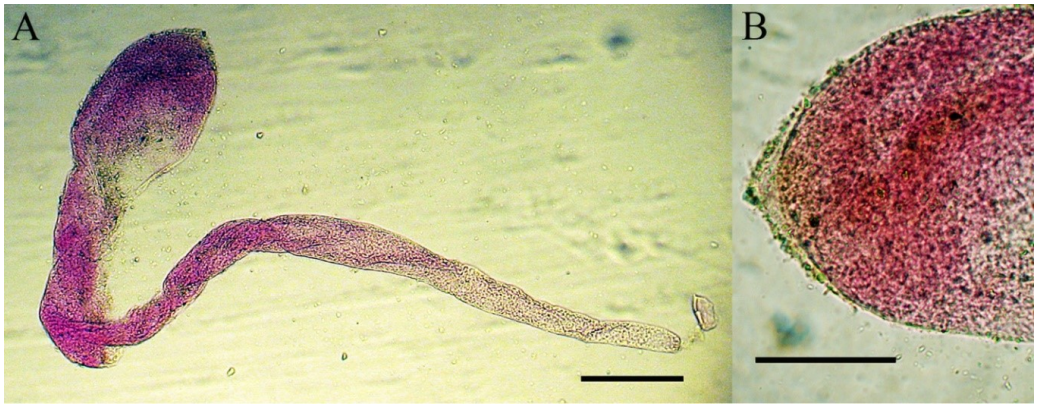

Fig. 4. The paratype specimen 2: A, general view; B, aperture. Scale bars are 100 μm (A) and 50 μm (B)

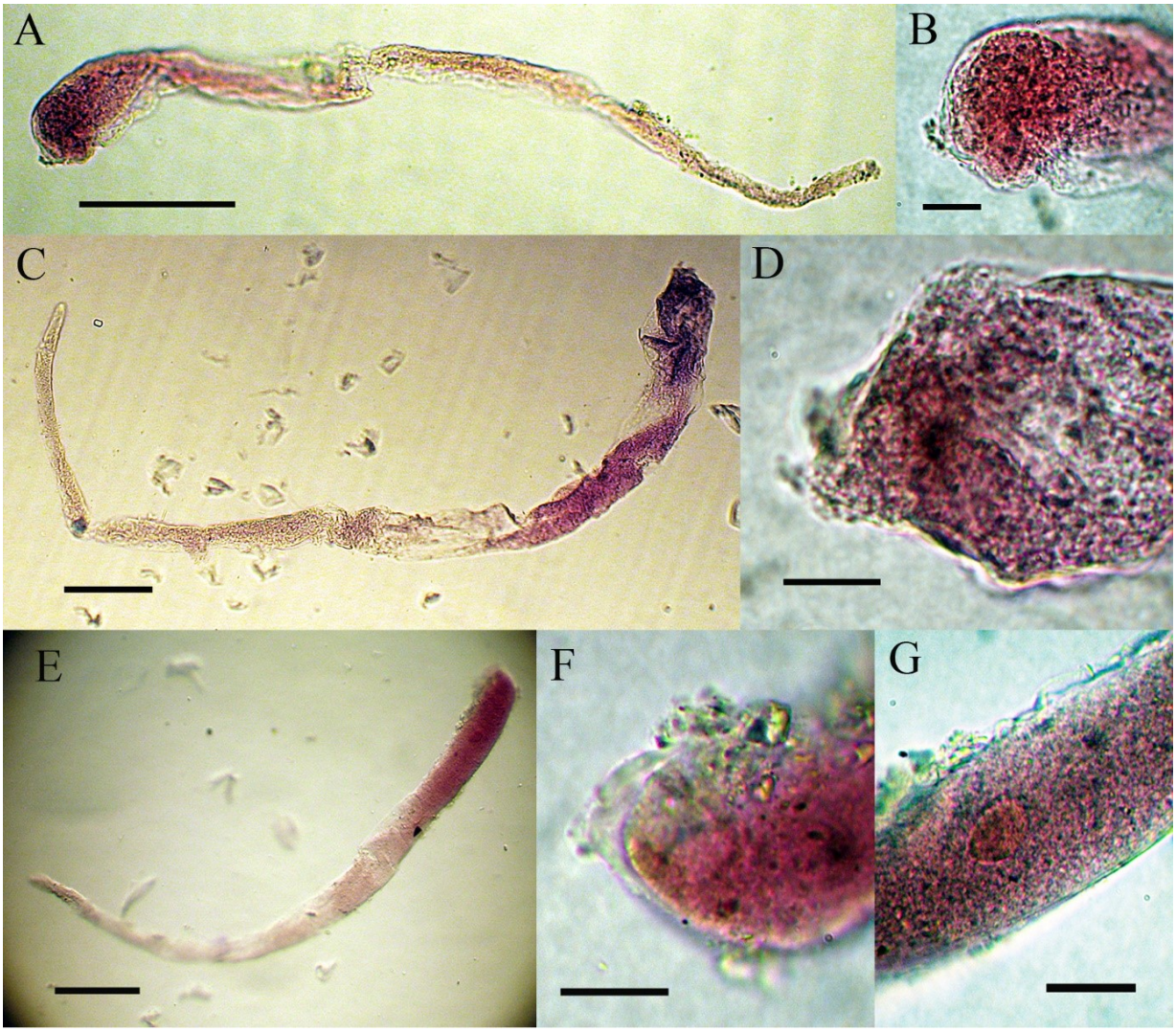

Fig. 5. Specimen 1J ('J' indicates the initial letter in the name of the Sea of Japan): A, general view; B, aperture. Specimen 2J: C, general view; D, aperture. Specimen 3J: E, general view; F, aperture; G, nucleus. Scale bars are 100 μm (A, C, E) and 20 μm (B, D, F, G). Specimens 1J and 2J are partially deformed

We examined in detail only 6 individuals (Table 1), because very delicate and fragile tests of other specimens were significantly deformed or damaged during the samples washing.

Table 1. Morphological parameters (in μm) of the type specimen, the two paratype specimens, and other examined specimens of *Cephalogullmia caudata* (–, not visible)

Specimen	Test length	Test width (maximum)	Diameter of aperture	Nucleus	Coefficient C
Type specimen	1,070	90	16	30 × 15	11.8
Paratype specimen 1	1,150	110	28	–	10.4
Paratype specimen 2	1,180	135	–	–	8.7
Specimen 1J	600	50	13	–	12
Specimen 2J	1,160	70	26	–	16.5
Specimen 3J	640	50	10	16 × 12	12.8

This work was carried out within the framework of IBSS state research assignment "Biodiversity as the basis for the sustainable functioning of marine ecosystems, criteria and scientific principles for its conservation" (No. 124022400148-4).

Acknowledgement. We express our deep gratitude to the administration of the Pacific Institute of Bioorganic Chemistry, Far Eastern Branch of the Russian Academy of Sciences, for the opportunity to sample bottom sediments in the Sea of Japan, as well as to the captain of the RV "Akademik Oparin" and our colleagues S. Trofimov and Yu. Litvin (department of benthic ecology, IBSS) who provided invaluable assistance in obtaining scientific material. We are very grateful to Prof. A. Gooday for his helpful consultations and revision of the English text of the paper. We thank the anonymous reviewers who provided a number of useful tips and recommendations for improving our manuscript.

REFERENCES

1. Anikeeva O. V., Sergeeva N. G., Gooday A. J. Two new genera and species of the monothalamous foraminifera from coastal waters of the Black Sea. *Marine Biodiversity*, 2013, vol. 43, iss. 4, pp. 473–479. https://doi.org/10.1007/s12526-013-0177-0
2. Golemansky V. G. *Lagynis pontica* n. sp., a new monothalamous rhizopod (Granuloreticulosea: Lagynidae) from the Black Sea littoral. *Acta Zoologica Bulgarica*, 1999, vol. 51, pp. 3–13.
3. Gooday A. J. Organic-walled allogromiids: Aspects of their occurrence, diversity and ecology in marine habitats. *Journal of Foraminiferal Research*, 2002, vol. 32, no. 4, pp. 384–399. https://doi.org/10.2113/0320384
4. Gooday A. J., Anikeeva O. V., Sergeeva N. G. *Tinogullmia lukyanovae* sp. nov. – a monothalamous, organic-walled foraminiferan from the coastal Black Sea. *Journal of the Marine Biological Association of the United Kingdom*, 2006, vol. 86, iss. 1, pp. 43–49. https://doi.org/10.1017/S0025315406012847
5. Gooday A. J., Anikeeva O. V., Pawłowski J. New genera and species of monothalamous foraminifera from Balaclava and Kazach'ya Bays (Crimean Peninsula, Black Sea). *Marine Biodiversity*, 2011, vol. 41, iss. 4, pp. 481–494. https://doi.org/10.1007/s12526-010-0075-7
6. Gooday A. J., Holzmann M., Schwarzgruber E., Cedhagen T., Pawłowski J. Morphological and molecular diversity of monothalamids (Rhizaria, Foraminifera), including two new species and a new genus, from SW Greenland. *European Journal of Protistology*, 2022, vol. 86, art. no. 125932 (25 p.). https://doi.org/10.1016/j.ejop.2022.125932
7. Habura A., Goldstein S. T., Broderick S., Bowser S. S. A bush, not a tree: The extraordinary diversity of cold-water basal foraminiferans extends to warm-water environments. *Limnology and Oceanography*, 2008, vol. 53, iss. 4, pp. 1339–1351. https://doi.org/10.4319/lo.2008.53.4.1339
8. Henderson Z. Soft-walled monothalamid foraminifera from the intertidal zones of the Lorn area, north-west Scotland. *Journal of the Marine Biological Association of the United Kingdom*, 2023, vol. 103, art. no. e18 (21 p.). https://doi.org/10.1017/S0025315423000061
9. Holzmann M., Gooday A. J., Siemensma F., Pawłowski J. Review: Freshwater and soil foraminifera – a story of long-forgotten relatives. *Journal of Foraminiferal Research*, 2021, vol. 51, no. 4, pp. 318–331. https://doi.org/10.2113/gsjfr.51.4.318
10. Kaminski M. A. The year 2000 classification of the agglutinated foraminifera. In: *Proceedings of the Sixth International Workshop on Agglutinated Foraminifera, Prague, Czech Republic, 1–7 September, 2001* / M. Bubik, M. A. Kaminski (Eds). Kraków, Poland : Grzybowski Foundation, 2004, pp. 237–255. (Grzybowski Foundation, Special Publication ; no. 8).
11. Lejzerowicz F., Voltski I., Pawłowski J.

Foraminifera of the Kuril–Kamchatka Trench area: The prospects of molecular study. *Deep Sea Research Part II: Topical Studies in Oceanography*, 2015, vol. 111, pp. 19–25. https://doi.org/10.1016/j.dsr2.2014.10.003

12. Loeblich A. R., Tappan J. H. *Foraminiferal Genera and Their Classification.* New York : Van Nostrand Reinhold Company, 1988, 970 p. https://doi.org/10.1007/978-1-4899-5760-3
13. Lukina T. G., Tarasova T. S. Phylum Sarcomastigophora, class Granuloreticulosa. In: *Check-List of Species of Free-Living Invertebrates of the Russian Far Eastern Seas* / B. I. Sirenko (Ed.). Saint Petersburg : [ZIN RAS], 2013, pp. 16–24. (Explorations of the Fauna of the Seas ; 75 (83)). (in Russ.)
14. Majewski W., Lecroq B., Sinniger F., Pawłowski J. Monothalamous foraminifera from Admiralty Bay, King George Island, West Antarctica. *Polish Polar Research*, 2007, vol. 28, no. 3, pp. 187–210.
15. Ohkawara N., Kitazato H., Uematsu K., Gooday A. J. A minute new species of *Saccammina* (monothalamous foraminifera; Protista) from the abyssal Pacific. *Journal of Micropalaeontology*, 2009, vol. 28, iss. 2, pp. 143–151. https://doi.org/10.1144/jm.28.2.143
16. Pawlowski J., Holzmann M., Berney F. C., Gooday A. J., Cedhagen T., Habura A., Bowser S. S. The evolution of early Foraminifera. *Proceedings of the National Academy of Sciences*, 2003, vol. 100, iss. 20, pp. 11494–11498. https://doi.org/10.1073/pnas.2035132100
17. Pawlowski J., Holzmann M., Tyszka J. New supraordinal classification of Foraminifera: Molecules meet morphology. *Marine Micropaleontology*, 2013, vol. 100, pp. 1–10. https://doi.org/10.1016/j.marmicro.2013.04.002
18. Preobrazhenskaya T. V., Tarasova T. S. Donnye foraminifery nekotorykh raionov zaliva Petra Velikogo. In: *Rasprostranenie i ekologiya sovremennykh i iskopaemykh morskikh organizmov*. Vladivostok : Dal'nevostochnoe otdelenie Akademii nauk SSSR, 1990, pp. 11–18. (in Russ.)
19. Sergeeva N. G., Anikeeva O. V. *Goodayia rostellatum* gen. n., sp. n. (Protozoa) – a monothalamous foraminifera from the Black Sea. *Vestnik zoologii*, 2008, vol. 42, no. 5, pp. 467–471. https://elibrary.ru/jxfqsd
20. Sergeeva N. G., Anikeeva O. V. *Soft-shelled Foraminifera of the Black Sea and the Sea of Azov*. Simferopol : ARIAL, 2018, 156 p. (in Russ.). https://doi.org/10.21072/978-5-907118-84-3
21. Sergeeva N. G., Anikeeva O. V. New Black Sea monothalamous Foraminifera from the genus *Nemogullmia* Nyholm, 1953 (Allogromiida: Shepheardellinae). *Invertebrate Zoology*, 2020, vol. 17, no. 2, pp. 176–188. https://doi.org/10.15298/invertzool.17.2.07
22. Sergeeva N. G., Anikeeva O. V. *Vellaria solenta* (Monothalamea: Allogromiidae) – new species of soft-walled foraminifera from Sivash Bay (the Sea of Azov). *Invertebrate Zoology*, 2021, vol. 18, no. 2, pp. 152–158. https://doi.org/10.15298/invertzool.18.2.06
23. Sergeeva N. G., Anikeeva O. V. First investigations of benthic soft-walled foraminifera and gromiids (Protozoa) in the northwestern Sea of Japan. *Russian Journal of Marine Biology*, 2023, vol. 49, no. 6, pp. 435–452. https://doi.org/10.1134/S106307402306007X
24. Sergeeva N. G., Anikeeva O. V., Gooday A. J. Soft-shelled, monothalamous foraminifera from the oxic/anoxic interface (NW Black Sea). *Journal of Micropalaeontology*, 2010, vol. 56, no. 3–4, pp. 393–407. https://elibrary.ru/xmdoph
25. Siemensma F., Holzmann M., Apothéloz-Perret-Gentil L., Clauß S., Voelcker E., Bettighofer W., Khanipour Roshan S., Walden S., Dumack K., Pawlowski J. Broad sampling of monothalamids (Rhizaria, Foraminifera) gives further insight into diversity of non-marine foraminifera. *European Journal of Protistology*, 2021, vol. 77, art. no. 125744 (21 p.). https://doi.org/10.1016/j.ejop.2020.125744
26. Voltski I., Pawłowski J. *Flexammina islandica* gen. nov., sp. nov. and some new phylotypes of monothalamous foraminifera from the coast of Iceland. *Zootaxa*, 2015, vol. 3964, no. 2, pp. 245–259. https://doi.org/10.11646/zootaxa.3964.2.5

CEPHALOGULLMIA CAUDATA GEN. NOV., SP. NOV. (RHIZARIA, FORAMINIFERA) — МОНОТАЛАМУСНАЯ ФОРАМИНИФЕРА ИЗ ЯПОНСКОГО МОРЯ

Н. Г. Сергеева, О. В. Аникеева

ФГБУН ФИЦ «Институт биологии южных морей имени А. О. Ковалевского РАН»,
Севастополь, Российская Федерация
E-mail: *alegria@ibss-ras.ru*

Мы приводим описание нового вида и рода мягкораковинных моноталамусных фораминифер из Японского моря. Материал собран в районе приморского шельфа во время 64-го рейса НИС «Академик Опарин» (17 июня — 08 июля 2021 г.). Пробы донных осадков отобраны на 17 станциях в диапазоне глубин от 0,3 до 86 м. Описываемый здесь вид был найден на глубинах 13 и 86 м. Удлинённая органическая стенка раковины *Cephalogullmia caudata* sp. nov. имеет раздутую переднюю (апертурную) часть, которая постепенно сужается к дистальному концу. Длина тела варьирует от 600 до 1180 мкм; ширина в самой широкой части («голове») — от 50 до 135 мкм, в самой узкой части — от 10 до 20 мкм. Единственная апертурная структура (диаметр 10–28 мкм) расположена на самом широком конце раковины. Апертура слегка приподнята, у некоторых экземпляров напоминает сосок. Ядро видно только у некоторых экземпляров; его размеры составляют от 16 × 12 мкм до 30 × 15 мкм. Сравнительный анализ показал, что новый род *Cephalogullmia* отличается от *Micrometula* Nyholm, 1952 по форме раковины: она более округлая и раздутая в апертурной части, чем узкая раковина конической формы у *Micrometula*. От *Cylindrogullmia* Nyholm, 1974 новый род также отличается по форме раковины: у *Cylindrogullmia* она больше напоминает цилиндр. Описываемый нами род отличается и от другой моноталамиды с удлинённой раковиной и органическими стенками — *Bowseria* Sinniger et al., 2008 — более тёмной протоплазмой и суженным (хвостообразным) дистальным концом.

Ключевые слова: мягкораковинные фораминиферы, Японское море, *Cephalogullmia caudata* gen. nov., sp. nov., моноталамиды

1871
ИнБЮМ – IBSS

Морской биологический журнал
Marine Biological Journal
2025, vol. 10, no. 2, pp. 95–110
https://marine-biology.ru

UDC [502.175:[582.26/.27:574.21]](265.54.04)

ASSESSMENT OF HEAVY METAL POLLUTION OF COASTAL WATERS OFF THE MURAVYOV-AMURSKY PENINSULA USING ALGAE AS BIOINDICATORS

© 2025 **E. Chernova[1,2] and S. Kozhenkova[1]**

[1]Pacific Geographical Institute FEB RAS, Vladivostok, Russian Federation
[2]Far Eastern Federal University, Vladivostok, Russian Federation
E-mail: *elena@tigdvo.ru*

Received by the Editor 18.04.2023; after reviewing 31.10.2023;
accepted for publication 20.03.2025.

Fe, Mn, Cu, Zn, Pb, Cd, and Ni concentrations were measured in brown algae [*Sargassum miyabei* Yendo and *S. pallidum* (Turner) C. Agardh] and green algae [*Blidingia minima* (Nägeli ex Kützing) Kylin, *Ulva lactuca* Linnaeus, and *U. linza* Linnaeus] sampled in July 2017 in coastal waters off the city of Vladivostok, Muravyov-Amursky Peninsula, Sea of Japan. Heavy metal concentrations in algae were determined by atomic absorption spectroscopy after thalli mineralization with nitric acid. Dissolved trace elements in seawater were measured by ultrafiltration of water samples and $CHCl_3$–DDTK-Na method. The degree of pollution in various areas of the coastal zone was assessed applying the hazard coefficient for algae (K_H). It was calculated as the ratio of metal concentration in an alga to the upper threshold level of background concentrations of the element. Also, integral Trace Element Pollution Index (TEPI-threshold) was applied using $K_H \geq 1$. Coastal waters off Vladivostok were slightly polluted by heavy metals. At stations located north and south from a solid waste landfill, TEPI-threshold was 2.4–2.8 due to pollution by Pb and Cu (2.7–12 $C_{threshold}$), as well as Zn, Fe, Mn, and Ni. Algae from upper areas of the Amur and Ussuri bays were Fe- and Mn-enriched because of river discharge; TEPI-threshold was 1.7–3.0. Macrophytes of the Eastern Bosphorus Strait were polluted by Fe (3–10 $C_{threshold}$), as well as Mn, Cu, Zn, and Ni (1–1.5 $C_{threshold}$), which results from port activities, shipping, and construction of bridges; TEPI-threshold was 1.0–2.1. Off the eastern coast of the Muravyov-Amursky Peninsula, there was a local zone of high-degree pollution formed due to rainwater drainage from the reclaimed solid waste landfill in Vladivostok; TEPI-threshold was 16. Out of heavy metals studied, Fe and Cu were main pollutants at this station ($K_H > 80$ in algae), while Pb, Mn, Zn, and Ni were co-pollutants. In seawater at this station, concentrations of dissolved elements exceeded the background levels, and pollution by Cu was equal to 3 MPC for fishery reservoirs.

Keywords: heavy metals, brown algae, green algae, Amur Bay, Ussuri Bay, Peter the Great Bay, Muravyov-Amursky Peninsula, Sea of Japan

Common species of marine algae have long been successfully used as bioindicators of metal and non-metal pollution in the marine environment [Aboal et al., 2023; Bryan, Hummerstone, 1973; Malea, Kevrekidis, 2014; Obluchinskaya et al., 2013; Pan et al., 2018; *etc.*]. Their application is based on the relationship between metal content in the environment and organisms [Rainbow, 2020; Rainbow, Phillips, 1993; *etc.*].

Periodic monitoring of heavy metal concentrations in brown algae from the northwestern Sea of Japan has been carried out since 1976 [Khristoforova, 1989]. Spatial and interannual assessments of metal pollution in coastal waters based on algal data have been obtained for the open sea coast [Shul'kin et al., 2015], Peter the Great Bay, its pristine spots, and areas under significant anthropogenic load [Chernova, Kozhenkova, 2016; Kozhenkova et al., 2006, 2021].

Several localized pollution sites exist in coastal waters of the Russian part of the Sea of Japan [Kozhenkova et al., 2021; Shulkin, 2004]. One of them covers the northwestern Peter the Great Bay off the Muravyov-Amursky Peninsula which is home to the Vladivostok agglomeration.

The aim of this study was to assess heavy metal pollution in coastal waters off the Muravyov-Amursky Peninsula by analyzing content of trace elements in brown algae [*Sargassum miyabei* Yendo, 1907 and *S. pallidum* (Turner) C. Agardh, 1820] and green algae [*Blidingia minima* (Nägeli ex Kützing) Kylin, 1947, *Ulva lactuca* Linnaeus, 1753 (= *U. fenestrata* Postels et Ruprecht), and *U. linza* Linnaeus, 1753].

MATERIAL AND METHODS

Brown algae *S. miyabei* and *S. pallidum* and green algae *U. lactuca*, *U. linza*, and *B. minima* were sampled from coastal waters off the Muravyov-Amursky Peninsula: in the western Amur Bay, the eastern Ussuri Bay, and the Eastern Bosphorus Strait. A total of 27 stations were surveyed (Fig. 1). *S. miyabei* was sampled at 16 stations; *S. pallidum*, at 16 stations; *U. linza*, at 8 stations; *U. lactuca*, at 3 stations; and *B. minima*, at 3 stations.

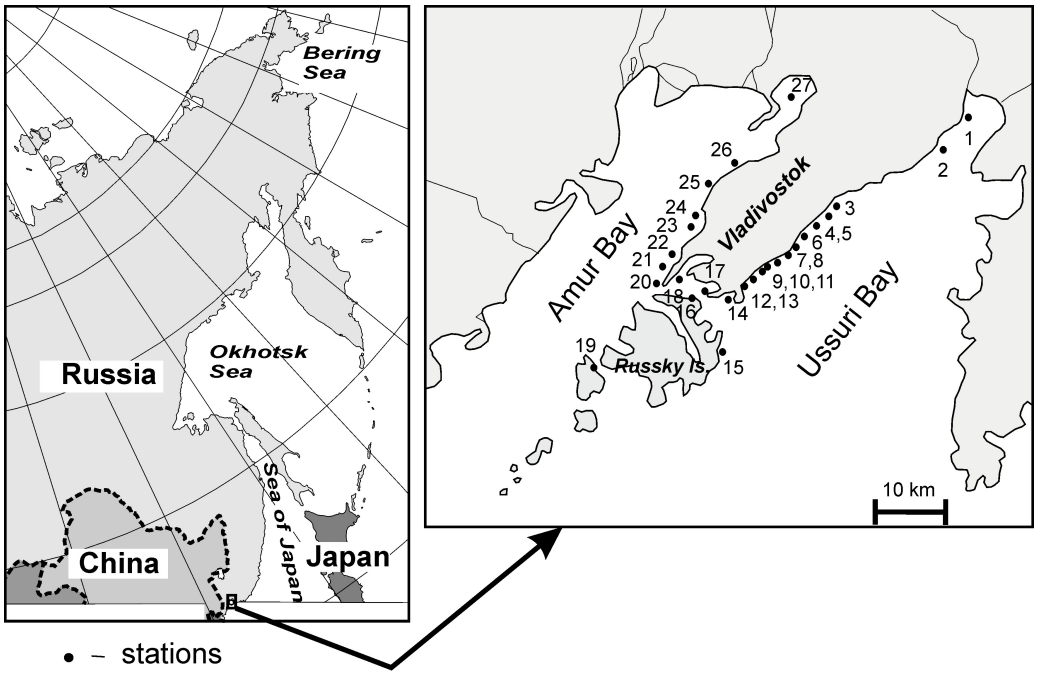

Fig. 1. Sampling stations off the Muravyov-Amursky Peninsula. The Ussuri Bay: 1, Cherepakha Cape; 2, Muravyiny Cape; 3, Lazurnaya Cove, Zeleny Cape; 4, "Politekhnik" recreational base; 5, "Zhemchuzhina" recreational base; 6, Desantnaya Cove; 7, "Gornostay" solid waste landfill; 8, Rybachy village; 9, Gornostay Cove; 10, Promezhutochnaya Cove, north; 11, Promezhutochnaya Cove, south; 12, Sukhoputnaya Cove; 13, Sobol Cove; 14, Patrokl Cove. The Russky Island: 15, Akhlestyshev Cape; 16, Pospelov Cape. The Eastern Bosphorus Strait: 17, Nazimov Cape; 18, Tokarevskaya Koshka Cove. The Popov Island: 19, Stark Strait. The Amur Bay: 20, Tokarevsky Cape; 21, Primorskaya Railway harbor; 22, Bezymyannaya Cove; 23, Kirpichny Zavod Cove; 24, a site between Firsov Cape and Grozny Cape; 25, Krasny Cape; 26, Sanatornaya railway station; 27, Uglovoy Cove

Algae were sampled on 10–17 and 25–27 July, 2017, at depths of 0.5–1.5 m. Depending on size, 5–15 specimens of each species were sampled, washed with seawater, and packed in polyethylene bags. In a laboratory, we cleaned algae of epiphytes and invertebrates, formed 5 samples, and dried them at +85 °C. Dried samples were ground, and 0.5-g subsamples were mineralized in a microwave system with 6 mL of high-purity nitric acid. Concentrations of Fe, Mn, Cu, Zn, Pb, Cd, and Ni were determined by flame and flameless (Pb) atomic absorption spectrometry on a Shimadzu AA-6800 spectrometer at the core facility "Center for Landscape Ecodiagnostics and GIS Technologies" (Pacific Geographical Institute FEB RAS). Quality control for sample preparation and trace element determination was performed using blank samples and international certified reference material (Table 1). Concentrations are presented in $\mu g \cdot g^{-1}$ dry weight.

Table 1. Analysis of standard reference material "Leaf of Birch" (LB-1, GSO 8923-2007, Irkutsk) and "Oyster" (NBS Oyster 1566a)

Parameter	Metal content, $\mu g \cdot g^{-1}$						
	Cu	Mn	Fe	Zn	Cd	Pb	Ni
"Leaf of Birch"							
Certified reference sample	7.3 ± 0.6	930 ± 70	730 ± 70	94 ± 6	0.16 ± 0.03	3.7 ± 0.6	5.8 ± 0.8
Result of control determination	7.4	835	765	95.2	0.13	3.15	6.3
"Oyster"							
Certified reference sample	66.3 ± 4.3	12.3 ± 1.5	539 ± 15	830 ± 57	4.15 ± 0.38	0.37 ± 0.014	2.25 ± 0.44
Result of control determination	64	11.4	517	903	4.65	0.34	2.09

Seawater was sampled in plastic canisters from the undersurface layer at 13 stations. On the same day, 1 L of each sample was filtered through a 0.45-μm membrane filter in the laboratory. Metal complexes were concentrated from 1 L of filtrate using a chloroform–DDTK-Na system. Suspended matter was determined by weighing filters before filtration and after it. Concentrations of dissolved metals were established by atomic absorption spectrometry on a Shimadzu AA-6800 spectrophotometer. Quality of determining Pb and Cd content in water and Pb in algae was additionally controlled using standard additions, with recoveries ranging 80–85%. Salinity was measured conductometrically.

For each station, arithmetic mean and standard deviation of concentrations of trace elements were calculated for algal samples consisting of 5 specimens.

Heavy metal contamination in the Amur and Ussuri bays was assessed by comparing measured concentrations in algae from this study with published upper threshold values of background ranges for corresponding species: $C_{threshold}$ (Table 2). These threshold values were derived as the median plus double median absolute deviation from the sample median (median + 2 MAD) [Chernova, 2012; Chernova, Kozhenkova, 2016] and subsequently validated [Chernova, Shulkin, 2019].

For *U. linza* and *B. minima*, threshold values for metals were adopted from those for *U. lactuca* [Kozhenkova, Chernova, 2017]. The hazard coefficient (K_H) for pollution of an area by an element, defined as the ratio of the *i*-th metal concentration in an alga (C_i) to $C_{threshold}$, was calculated: $K_H = C_i / C_{threshold}$. Stations with $K_H > 1$ were considered polluted.

Table 2. Median and threshold metal concentrations ($C_{threshold}$) in brown algae (*Sargassum miyabei* and *Sargassum pallidum*) and green alga (*Ulva lactuca*) of coastal waters of the Sea of Japan (μg·g^{-1} of dry mass)

Parameter	Taxon	Cu	Mn	Fe	Zn	Pb	Cd	Ni
Median* / $C_{threshold}$	*S. miyabei*	2.9 / 4.7	266 / 714	353 / 746	17.0 / 23.9	0.8 / 1.8	1.6 / 2.9	2.3 / 3.6
	S. pallidum	2.3 / 3.9	168 / 455	317 / 672	15.0 / 23.8	0.6 / 1.5	1.1 / 1.7	2.0 / 3.8
	U. lactuca	4.1 / 7.3	17.2 / 34.6	317 / 672	7.6 / 13.9	1.3 / 3.0	0.07 / 0.15	1.6 / 3.5
World median** / Q3	brown algae	5.7 / 13.0	67 / 135	301 / 848	49 / 120	5.5 / 11.0	1.0 / 2.15	6.0 / 11.4
	green algae	7.1 / 12.6	81 / 182	492 / 1,270	36 / 60.6	5.2 / 11.6	0.42 / 0.90	3.9 / 7.1

Note: *, [Chernova, Kozhenkova, 2016; Kozhenkova, Chernova, 2017]; **, [Sánchez-Quiles et al., 2017]. Q3 is the element concentration corresponding to the value of the third quartile of the sample.

A comprehensive assessment was conducted using the Trace Elements Pollution Index, TEPI [Richir, Gobert, 2014] modified as follows:

$$\text{TEPI-threshold} = (Cf_1 \times Cf_2 \times \ldots \times Cf_n)^{1/n},$$

where Cf_1, Cf_2… Cf_n are normalized concentrations relative to $C_{threshold}$ (Cf_n / $C_{threshold}$);

n is the number of trace elements with $C_i \geq C_{threshold}$.

Stations with TEPI-threshold > 1 were considered polluted.

RESULTS

The hazard coefficients (K_H) for metal pollution in algae from waters off Vladivostok are presented in Figs 2 and 3.

Stations with metal concentrations in *Sargassum* spp. exceeding threshold levels were located in the upper part of the Amur Bay [sta. 26 and 27 (Mn, Fe, and Ni)], in coastal waters off the city [sta. 22 and 23 (Zn and Ni)], in the contact zone between the Amur and Zolotoy Rog bays [sta. 20 (Fe, Mn, and Zn)], and in the Eastern Bosphorus Strait [sta. 19 (Mn, Fe, and Pb)] (Fig. 2). In the Ussuri Bay, metal pollution was noted in algae growing near the "Gornostay" solid waste landfill reclaimed in 2011 [sta. 6–8 (Cu, Mn, Fe, Zn, Pb, Ni, and Cd), sta. 9 (Cu, Zn, Pb, and Ni), and sta. 10 (Ni)], as well as in the upper part of the bay [sta. 1 and 2 (Fe, Mn, and Ni)] (Fig. 3).

The highest K_H values for Fe and Cu were observed in a green alga *B. minima* at sta. 7: values exceeded $C_{threshold}$ by factors of 276 and 82, respectively (Figs 2, 3). Concentrations of Zn, Ni, Pb, Cd, and Mn corresponded to 29, 26, 13, 3, and 3 K_H. Ni content exceeded $C_{threshold}$ in algae at 50% of the stations.

Concentrations of dissolved metals in water from sampling sites were elevated relative to background levels for Peter the Great Bay only at sta. 7 (Mn, Cu, Zn, Cd, Pb, and Ni) and sta. 6 (Zn and Pb). Cu content in water at sta. 7 exceeded $MPC_{fishery}$ (maximum permissible concentration for fishery reservoirs) by a factor of 3 (Table 3). The amount of suspended matter was the highest at sta. 1, near the mouth of the Artemovka River.

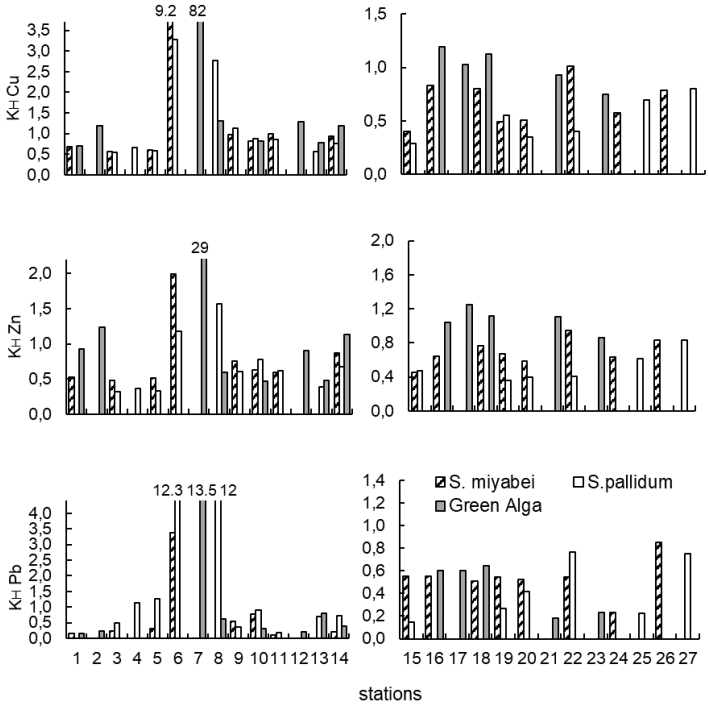

Fig. 2. Hazard coefficient of algae pollution by Cu, Zn, and Pb ($K_H = C_i / C_{threshold}$) (station numbers are as in Fig. 1)

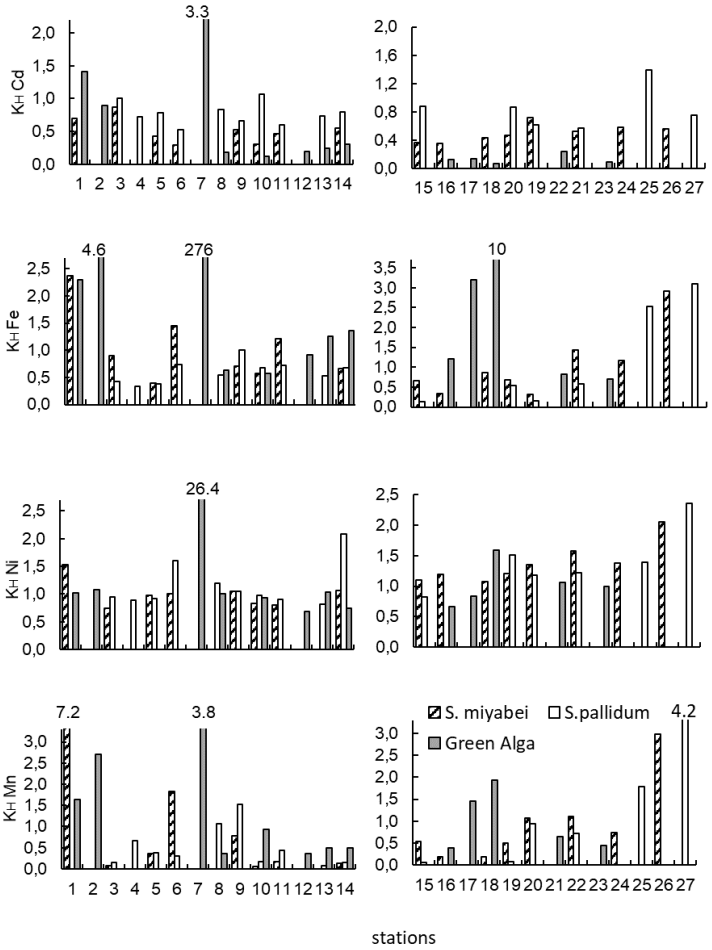

Fig. 3. Hazard coefficient of algae pollution by Cd, Fe, Ni, and Mn ($K_H = C_i / C_{threshold}$) (station numbers are as in Fig. 1)

Table 3. Concentrations of dissolved forms of metals (μg·L^{-1}), salinity (S, ‰), and turbidity (D, mg·L^{-1}) in the water environment of the Ussuri and Amur bays

Station	No.	Date	S	Fe	Mn	Cu	Zn	Cd	Ni	Pb	D
Cherepakha Cape	1	12.07.2017	16.59	1.44	2.12	0.51	1.46	0.009	0.62	0.025	8.68
Muravyiny Cape	2	12.07.2017	24.93	0.59	5.48	0.55	0.86	0.015	0.64	0.029	4.59
Desantnaya Cove, south	6	13.07.2017	32.09	2.08	3.81	0.47	2.73	0.041	0.91	0.238	2.95
Solid waste landfill	7	13.07.2017	31.49	1.24	44.62	16.92	8.62	0.123	1.42	0.159	3.36
Rybachy village	8	12.07.2017	32.32	0.77	1.01	1.36	1.50	0.022	0.64	0.031	3.00
Gornostay Cove	9	13.07.2017	30.62	0.38	3.96	0.66	0.95	0.019	0.57	0.015	4.45
Sukhoputnaya Cove	12	12.07.2017	32.15	0.95	0.89	0.91	0.89	0.020	0.56	0.020	3.14
Patrokl Cove	14	12.07.2017	32.47	1.53	0.64	0.59	2.27	0.021	0.47	0.008	3.04
Stark Strait	19	30.07.2017	28.46	2.92	0.84	1.03	0.49	0.009	0.80	0.019	2.06
Pospelov Cape	16	10.07.2017	30.68	1.52	1.95	0.75	1.04	0.017	0.60	0.017	0.95
Tokarevsky Cape	20	13.07.2017	31.10	1.34	0.77	0.42	0.63	0.012	0.64	0.021	1.09
Primorskaya Railway harbor	21	13.07.2017	30.26	0.89	2.23	0.48	0.90	0.014	0.68	0.022	0.82
A site between Firsov Cape and Grozny Cape	24	10.07.2017	29.07	1.81	6.45	0.41	1.05	0.015	0.63	0.021	1.73
$MPC_{fishery}$			–	100	50	5	50	1	10	6	–
Background for open/sheltered areas of Peter the Great Bay*			–	–	10	0.3 / 1.2	0.5 / 0.8	0.05 / 0.04	0.2 / 1.1	0.05 / 0.06	–

Note: *, [Shulkin, 2004; Shulkin et al., 2013]. A dash denotes no data.

TEPI-threshold values calculated considering only elements with concentrations equal to $C_{threshold}$ or exceeding it are presented in Fig. 4. TEPI-threshold values determined considering all seven studied elements are given in parentheses below.

The highest level of pollution in algae by seven metals, TEPI-threshold = 16, was recorded at sta. 7 (at the solid waste landfill) (Fig. 4). TEPI-threshold at sta. 6 and 8 (in the landfill vicinity) was reduced to 2.4–2.8 (1.6–1.7 when accounting for seven metals). In upper areas of the Ussuri and Amur bays, the index was 1.7–3.0 (1.0–1.2) and 2.6–3.0 (1.2–1.4), respectively. At all other stations off the Muravyov-Amursky Peninsula, TEPI-threshold remained within 1 (< 1 when considering concentrations of seven metals).

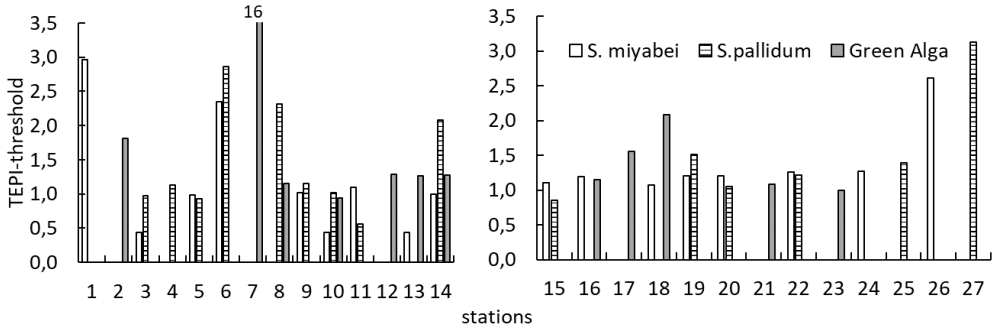

Fig. 4. Trace Element Pollution Index (TEPI-threshold) values for algae off the Muravyov-Amursky Peninsula (station numbers are as in Fig. 1)

DISCUSSION

Sources of metal input into the marine environment off Vladivostok include riverine discharge, atmospheric deposition, municipal and industrial wastewater, surface runoff from urbanized areas, leachate from solid waste landfills, ash ponds, and tailings storage facilities. Also, trace elements can enter the marine environment because of corrosion of port infrastructure facilities and ship hulls, sunken vessels, dredging operations, and sea dumping of dredged material [Kozhenkova et al., 2021; Shul'kin et al., 2017].

Previous studies of coastal waters off Vladivostok revealed that seawater is contaminated with petroleum hydrocarbons, phenols, and organic matter from domestic sewage. Oil pollution in open areas of the Amur and Ussuri bays occurs due to the discharge of ballast and bilge waters from vessels stemming from the absence or insufficient capacity of onshore oil treatment facilities [Marine Water Pollution, 2018]. Bottom sediments off the city are contaminated with petroleum hydrocarbons, phenols, pesticides, cadmium, and mercury [Moshchenko et al., 2019].

Based on metal and petroleum hydrocarbon contamination levels, bottom sediments of the Amur and Ussuri bays are classified as 'moderately polluted' or 'polluted' [Moshchenko et al., 2019]. The high spatial heterogeneity in pollutant distribution within bottom sediments of these bays, along with diverse grain size, results from the hydrodynamics in the region. The most contaminated areas are Zolotoy Rog Bay and Eastern Bosphorus Strait: there, concentrations of metals and hydrocarbons exceed by several times background values and ERL level (effects range-low, *i. e.*, the concentration level at which biological effects are unlikely [Long et al., 1995, cited after: Shulkin, 2004]). The Amur Bay exhibits moderate pollution level. The Ussuri Bay is the cleanest out of the studied areas. Researchers suggest that chemical pollution and eutrophication are currently key factors determining the ecological state of benthos off Vladivostok, and severe pollution of bottom sediments remains localized [Moshchenko et al., 2019].

Algae serve as integrative indicators of heavy metal pollution levels in coastal marine waters [Aboal et al., 2023; Khristoforova, 1989; Pan et al., 2018; Rainbow, Phillips, 1993; *etc.*]. Off Vladivostok, algae grow on rocky substrates in tidal and subtidal zones, primarily accumulating biologically available and highly mobile dissolved metals.

To identify the scale of environmental disturbance and level of metal pollution, researchers compare metal concentrations in macrophytes from studied areas with those from uncontaminated (background) sites [Obluchinskaya et al., 2013; Scanes, Roach, 1999]. However, selecting such background sites can be subjective. Alternatives include using background concentrations calculated as arithmetic or geometric means [Savenko, 2006], truncated means [Sánchez-Quiles et al., 2017], median values [Lukashev, 2007; Reimann et al., 2005; Sánchez-Quiles et al., 2017], or the 85th percentile [Cantillo, 1998]. Sanitary and hygienic MPC values for heavy metals (Hg, Pb, and Cd) and arsenic, used in Russia and abroad, are unsuitable for ecological assessments of natural systems. These standards were developed to determine the safety of food products and raw materials and not to reveal the well-being of hydrobionts themselves.

As already mentioned, to assess the ecological state of the marine environment at different stations off the Amur and Ussuri bays, we used threshold values of background metal concentrations ($C_{threshold}$ = median + 2 MAD) [Chernova, 2012; Chernova, Kozhenkova, 2016; Reimann et al., 2005] and hazard coefficients (K_H) calculated based on them (Figs 2, 3).

Iron and manganese compounds are of low toxicity to hydrobionts, as evidenced by high $MPC_{fishery}$ values for seawater (Table 3). Surface runoff is the primary source of dissolved Fe and Mn entering coastal waters of the bays from the Muravyov-Amursky Peninsula [Shul'kin, 2012]. In areas with high suspended matter content in seawater, metals accumulate in algae not only from the dissolved phase, but also from settling particulate matter [Burdin, Zolotukhina, 1998; Malinovskaya, Khristoforova, 1997]. The contribution of riverine input is maximum in the upper parts of the Amur and Ussuri bays adjacent to the western and eastern Muravyov-Amursky Peninsula, respectively (Fig. 1). There, elevated concentrations of these elements were noted in dissolved form (Table 3), in suspended form [Shulkin, 2004], and in algae (sta. 1, 2, and 27; see Figs 2, 3).

Bottom sediments are an even more indirect source of metals for macrophytes growing on hard substrates than suspended matter. In the Eastern Bosphorus Strait, where bottom sediments exhibit high levels of metal pollution [Moshchenko et al., 2019], elevated content of Fe, Mn, and Zn was also observed in algae (sta. 17 and 18). This is likely associated with the input of insufficiently treated wastewater from Vladivostok (domestic sewage and water from port infrastructure facilities), with shipping, and with large-scale sediment displacement during construction on the coast.

The Amur Bay experiences higher anthropogenic disturbances than the Ussuri Bay but lower ones than the Eastern Bosphorus Strait [Moshchenko et al., 2019; Vashchenko et al., 2010]. Typically, dissolved metal concentrations in seawater of these areas did not exceed $MPC_{fishery}$ [Marine Water Pollution, 2018], while heavy metal content in bottom sediments was elevated compared to permissible concentrations at which biological effects are unlikely [Losev, 2020; Marine Water Pollution, 2018; Petukhov et al., 2018; Vashchenko et al., 2010]. In total, metal concentrations in algae along the western Muravyov-Amursky Peninsula did not exceed thresholds. Fe, Mn, and Ni content was elevated in macrophytes from the shallow Uglovoy Cove (sta. 26 and 27) due to the inflow of several watercourses. Studies of metal and petroleum hydrocarbon pollution in bottom sediments of the Uglovoy Cove across different

seasons indicate the bay's capacity for self-purification facilitated by catastrophic events like typhoons [Losev, 2020]. This contributes to the fact that metals do not accumulate in hydrobionts of the Amur Bay coastal waters at concentrations exceeding $C_{threshold}$.

Leachate both from the former Vladivostok landfill adjacent to the coastline and reclaimed in 2011 (sta. 6–9) and from ash ponds of the thermal power station No. 2 reclaimed before 2018 (sta. 10–12) is a significant anthropogenic source of contamination for coastal waters of the peninsula's eastern coast in the Ussuri Bay. High levels of metal pollution in marine ecosystem components in the landfill vicinity were noted both before its reclamation [Shulkin, 2004; Simokon, 2009] and after it. Importantly, after reclamation, the degree of marine environment pollution decreased [Belcheva et al., 2015; Kozhenkova et al., 2021]. Our results showed as follows: in summer 2017, Fe and Cu compounds were the key pollutants for algae from these stations, while Pb, Mn, Zn, Ni, and Cd were the secondary ones (co-pollutants) (Figs 2, 3). Comparison of dissolved metal concentrations in water (Table 3) with background levels [Shulkin et al., 2013] also revealed high levels of Cu (sta. 7), Zn, Cd, Ni, and Pb (sta. 6 and 7). In summer, leachate from the landfill spread predominantly northward due to prevailing southerly winds. Consequently, maximum metal concentrations in algae and water were observed not only at sta. 7, but also 2 km north, at sta. 6. However, under northerly and westerly winds, pollutants can be transported south and east thus increasing content of trace elements in water and algae at southern stations (sta. 8) (Fig. 2, Table 3). Metal concentrations in algae dropped sharply at the northern cape of the Desantnaya Cove (sta. 7) located 700 m from the southern one [Kozhenkova et al., 2021]. This fact aligns with data from [Chalkley et al., 2019] evidencing for the localized effect of pollution sources in water and a rapid decrease in metal concentrations in macrophytes to near-background levels within 100 m from a source.

Leachate from ash ponds of the thermal power station No. 2, entering Promezhutochnaya and Gornostay coves for many years, was another source of pollution for coastal waters of the western Ussuri Bay [Kozhenkova et al., 2021; Shulkin, 2004; Simokon, 2009]. However, in 2017, metal concentrations in algae at sta. 9–11 were comparable to those at sta. 12–16 within Vladivostok and generally did not exceed $C_{threshold}$ (Figs 2, 3). The levels of dissolved metals in water in this area (sta. 10) corresponded to background values, except for Zn (Table 3). The reclamation of ash ponds seems to be one of the reasons for the reduced input of polluted waters into the marine environment and decreased metal accumulation in water plants.

In the recreational zone of the Ussuri Bay (sta. 3–5), heavy metal concentrations in algae did not exceed $C_{threshold}$. Dissolved metal levels in water at the time of sampling also corresponded to background values for Peter the Great Bay (the Sea of Japan) (Table 3). Importantly, off the Russky and Popov islands (sta. 15, 16, and 20), Ni concentrations were elevated. This is likely associated with the heavy shipping traffic in the Eastern Bosphorus Strait and off Vladivostok in general. Shipping contributes to pollution of Peter the Great Bay waters with both petroleum hydrocarbons [Marine Water Pollution, 2018; Moshchenko et al., 2019] and nickel – a trace impurity in petroleum products [Yakubov et al., 2017].

High concentrations of dissolved metals in seawater in the landfill vicinity (sta. 7) are consistent with elevated content of trace elements in algae (Table 3, Figs 2, 3). However, according the Primorsky Territorial Office on Hydrometeorology and Environmental Monitoring, dissolved metal concentrations exceeding $MPC_{fishery}$ were not recorded in the Ussuri Bay in 2017, although the values registered were slightly higher than background ones [Marine Water Pollution, 2018]. Apparently, the discrepancy

between our data and those of the Primorsky Territorial Office on Hydrometeorology and Environmental Monitoring is due to temporal differences and location of its sampling stations at deeper spots where mixing of leachate and seawater had already occurred. V. Shulkin [2004] also found dissolved metal concentrations in the landfill vicinity in 2001 that were elevated relative to background but did not exceed MPC. The elevated concentration of dissolved copper we detected in the landfill vicinity in 2017 (exceeding $MPC_{fishery}$) was likely related to the location of a sampling site (coastal zone, a depth of 1 m) and period of the study: before sampling, after a relatively dry June, there were more than 40 mm of precipitation in the first decade of July. Heavy precipitation leached mobile chemical elements from the 'body' of the landfill. Contaminated leachate was transported predominantly northward by a current and affected the chemical composition of bioindicators. As experimentally established, accumulation of metals by living algae from contaminated environments by 2 orders of magnitude occurs within 1.5–5 days [Suresh Kumar et al., 2007], while metal elimination occurs significantly slower and at a lower rate [Wang, Dei, 1999].

Metal concentrations in *Sargassum* spp. off the Muravyov-Amursky Peninsula were compared with generalized global indicators: the median and the third quartile (Q3) of element content in brown algae [Sánchez-Quiles et al., 2017]. Minimum Fe concentrations in *Sargassum* spp. from the Ussuri and Amur bays were found to practically correspond to the global median, while maximum ones exceeded Q3. Among Mn content values in *Sargassum* spp. from the study area, some were below the global median, but most concentrations exceeded Q3 (Table 2). The maximum Mn content in algae from the upper part of the Ussuri Bay, (5,063 ± 450) $\mu g \cdot g^{-1}$, was 4 times higher than the known Mn concentration in brown algae according to the compilation by Sánchez-Quiles *et al.* [2017]. We found the highest Mn content in *S. miyabei*, 5,863 $\mu g \cdot g^{-1}$, in the Abrek Cove, Strelok Bay, Sea of Japan [Kozhenkova et al., 2021]. In 2017, stations with Mn concentrations in *Sargassum* spp. exceeding Q3 were located in the upper part of the Ussuri Bay (sta. 1 and 2), where four small rivers inflow, and along the western coast of the bay (sta. 6 and 7). In other bays along the Russian coast of the Sea of Japan, Mn content exceeding Q3 in *Sargassum* spp. were characteristic of estuaries, ports, and spots used to dump dredged material from port operations [Chernova, Kozhenkova, 2016]. Concentrations of Cu, Zn, Pb, Cd, and Ni in *Sargassum* spp. from the study area did not exceed Q3 and were often below the median (Table 2).

Extremely high metal concentrations compared to global data were observed in a green alga *B. minima* at sta. 7, near the reclaimed solid waste landfill, off the western coast of the Ussuri Bay. Iron concentration in *Blidingia*, 38,813 $\mu g \cdot g^{-1}$, significantly exceeded the known maximum Fe value in *Enteromorpha compressa* from the Chilean coast, 23,000 $\mu g \cdot g^{-1}$ [Ratkevicius et al., 2003, cited after: Sánchez-Quiles et al., 2017]. Cu concentration, (601 ± 145) $\mu g \cdot g^{-1}$, was comparable to the known maximum, 750 $\mu g \cdot g^{-1}$ in *E. compressa* from the Chilean coast. Ni value in this alga, (48.6 ± 27.8) $\mu g \cdot g^{-1}$, was also close to the reported maximum, 83.4 $\mu g \cdot g^{-1}$ in *Halimeda tuna* from the Lebanese Mediterranean coast, Beirut [Shiber, Shatila, 1979, cited after: Sánchez-Quiles et al., 2017]. Concentrations of Zn and Pb in *B. minima* from sta. 7 were substantially higher than Q3 as well. Mn value did not exceed Q3. Cd concentration corresponded to the global median for green algae (Table 2).

Thus, manganese concentrations in brown algae off the Muravyov-Amursky Peninsula exhibited extremely high values compared to global literature data, while maximum concentrations of Cu, Zn, Pb, Cd, and Ni did not exceed the global Q3. Mn concentrations higher than Q3 in *Sargassum* spp. were characteristic of estuaries, ports, and spots used to dump dredged material. Maximum Fe and Cu values

in green algae from the most polluted station (in the landfill vicinity) exceeded known literature values; Zn and Pb concentrations were higher than Q3; and Cd value corresponded to the global median for green algae.

There are several systems for the integrated assessment of chemical pollution using biological indicators [Richir, Gobert, 2014; Usero et al., 1996]. One of official systems (Andalusia, Spain) is the Metal Pollution Index, MPI [AMA, 1992, cited after: Usero et al., 1996]:

$$\text{MPI} = (C_{f1} \times C_{f2} \times C_{f3} \times ... \times C_{fn})^{1/n} ,$$

where C_{f1}, C_{f2}… C_{fn} are concentrations of the 1st, 2nd… *n*-th element;

n is the number of elements analyzed in a sample.

J. Richir and S. Gobert [2014] used MPI [Usero et al., 1996] when assessing pollution by both metals and non-metals and named it TEPI. The authors emphasized the need for normalizing concentration of each element by its mean value in a dataset:

$$\text{TEPI} = (Cf_1 \times Cf_2 \times ... \times Cf_n)^{1/n} ,$$

where Cf_1, Cf_2… Cf_n are concentrations normalized by their means (the ratio of a certain metal's concentration in the organism at a certain station to its mean value in the dataset);

n is the number of elements analyzed in a sample.

Normalization is useful when dealing with metals having concentrations that differ by orders of magnitude [Moreda-Piñeiro et al., 2001]. If metal concentration in macrophytes does not exceed the mean value, TEPI is ≤ 1. The higher TEPI, the higher the level of water pollution at the station. The authors [Richir, Gobert, 2014] assume that using this index allows for reliable comparison of global pollution levels across different monitoring periods, even if lists of analyzed elements and/or bioindicator species differ.

Notably, any integrated index averages the overall pollution level: an excess of one chemical element can be compensated by several others with concentration not exceeding threshold values. Specifically, the more metals with concentrations below mean values included in TEPI calculation, the lower (and closer to 1) the resulting calculated pollution level. The occurrence of a single substance with concentration significantly exceeding the regulatory standard can lead to a community distress [Risnik et al., 2012] and its restructuring.

When calculating TEPI for waters off the Muravyov-Amursky Peninsula, we used thresholds of background metal concentrations ($C_{threshold}$ = median + 2 MAD) for normalization instead of their mean values in the dataset (Fig. 4).

To avoid compensating for the excess of some elements (their values being higher than $C_{threshold}$) with others not exceeding thresholds, and to obtain a realistic indicator of metal pollution in macrophytes, TEPI-threshold was calculated only considering elements exceeding $C_{threshold}$ (Fig. 4). If none of the metals exceeded thresholds, one element with a concentration closest to the threshold was selected for TEPI determination.

Overall, the assessment of pollution levels in coastal areas off the Muravyov-Amursky Peninsula using integrated TEPI-threshold confirmed low pollution with heavy metals (Fig. 4). At half of the stations surveyed, TEPI-threshold was less than 1 or equal to it. At other sites, index values ranged 1.1–3.2; this was primarily due to metal input into the coastal environment *via* riverine discharge into the upper

part of the Amur and Ussuri bays. The maximum metal pollution off the peninsula was localized near the reclaimed solid waste landfill (TEPI-threshold = 16).

Conclusions. In July 2017, according to hazard coefficients (K_H) for individual elements and the integrated Trace Element Pollution Index (TEPI-threshold) for algae, coastal waters off Vladivostok exhibited low pollution with trace elements. A localized zone of high contamination formed by surface runoff of pollutants from the territory of the solid waste landfill in Vladivostok (TEPI-threshold = 16) was situated off the eastern coast of the Muravyov-Amursky Peninsula. Out of the elements studied, Fe and Cu were the primary pollutants for macrophytes here ($K_H > 80$), while Pb, Mn, Zn, and Ni were co-pollutants. Values of dissolved metals in seawater at this station exceeded background levels, with copper concentration reaching 3 MPC for fishery reservoirs. Concentrations of dissolved metals in seawater at other stations at the time of sampling generally corresponded to background values for Peter the Great Bay, Sea of Japan, except for Zn.

TEPI-threshold at stations bordering the solid waste landfill to the north and south ranged 2.4–2.8 mostly due to Pb and Cu pollution (2.7–12 K_H), but also due to Zn, Fe, Mn, and Ni contamination. Algae from the upper parts of the Ussuri and Amur bays were Fe- and Mn-enriched because of riverine metal input; TEPI-threshold was 1.7–3.0. In the Eastern Bosphorus Strait, elevated levels of Fe (3–10 K_H), as well as Mn, Cu, Zn, and Ni (1–1.5 K_H), were noted in macrophytes. This was associated with port activities, shipping, and construction; TEPI-threshold was 1.0–2.1.

When calculating TEPI-threshold, normalizing by $C_{threshold}$ and including only elements with content equal to threshold values of background concentrations or exceeding it allow for the most objective assessment of the pollution level of the water area and prevent compensation for the excess of some elements by others not exceeding background levels.

In brown algae (*Sargassum* spp.) off the Muravyov-Amursky Peninsula, extremely high Mn concentrations compared to global data were found. In green algae, Fe and Cu values exceeded natural levels known in literature.

The work was carried out within the framework of the state research assignment of the Ministry of Science and Higher Education of the Russian Federation (No. AAAA-A16-116111610032-5).

Acknowledgments. The authors express their sincere gratitude to A. Plotnikova, G. Vlasova, and N. Bogdanova (Pacific Geographical Institute FEB RAS) for their assistance in sample preparation and analytical procedures.

REFERENCES

1. Burdin K. S., Zolotukhina E. Yu. *Tyazhelye metally v vodnykh rasteniyakh (akkumulyatsiya i toksichnost')*. Moscow : Dialog MGU, 1998, 202 p. (in Russ.)
2. *Marine Water Pollution. Annual Report 2017* / A. Korshenko (Ed.). Moscow : Nauka, 2018, 220 p. (in Russ.)
3. Kozhenkova S. I., Chernova E. N. Background concentrations of metals in green alga *Ulva lactuca* of the north-western Sea of Japan. In: *Geosistemy v Severo-Vostochnoi Azii: territorial'naya organizatsiya i dinamika* : materialy vserossiiskoi nauchno-prakticheskoi konferentsii, Vladivostok, 20–21 aprelya 2017 g. Vladivostok : TIG DVO RAN, 2017, pp. 522–526. (in Russ.). https://elibrary.ru/zmrltf
4. Losev O. V. Heavy metals and petroleum hydrocarbons contents in bottom sediments of Uglovoy Bay (Peter the Great Bay, Sea of Japan). *Vestnik Dal'nevostochnogo otdeleniya Rossiiskoi akademii nauk*, 2020, no. 5 (213), pp. 104–115. (in Russ.). https://elibrary.ru/umooak

5. Lukashev D. V. The method of calculation of background concentrations of trace metals in freshwater mussel tissue for assessment of pollution in River Dnieper. *Biologiya vnutrennikh vod*, 2007, no. 4, pp. 97–106. (in Russ.). https://elibrary.ru/ibkepb
6. Moshchenko A. V., Belan T. A., Borisov B. M., Lishavskaya T. S., Sevastianov A. V. Modern contamination of bottom sediments and ecological state of macrozoobenthos in the coastal zone at Vladivostok (Peter the Great Bay, Japan Sea). *Izvestiya TINRO*, 2019, vol. 196, pp. 155–181. (in Russ.). https://doi.org/10.26428/1606-9919-2019-196-155-181
7. Petukhov V. I., Petrova E. A., Losev O. V. Heavy metals and petroleum hydrocarbons in the waters of the Uglovoy Bay (the Amur Bay, the Sea of Japan) in the warm and cold seasons. *Vestnik Dal'nevostochnogo otdeleniya Rossiiskoi akademii nauk*, 2018, no. 1, pp. 85–93. (in Russ.). https://elibrary.ru/yotixj
8. Risnik D. V., Belyaev S. D., Bulgakov N. G., Levich A. P., Maksimov V. N., Mamikhin S. V., Milko E. S., Fursova P. V., Rostovtseva E. L. Approaches to standardization of environment quality. Legislative and scientific foundations of current ecological normalization systems. *Uspekhi sovremennoi biologii*, 2012, vol. 132, no. 6, pp. 531–550. (in Russ.). https://elibrary.ru/phgcmh
9. Savenko V. S. *Chemical Composition of World River's Suspended Matter*. Moscow : GEOS, 2006, 174 p. (in Russ.). https://elibrary.ru/qkgfwz
10. Simokon M. V. Zagryaznenie donnykh otlozhenii Ussuriiskogo zaliva metallami i metalloidami. In: *Ussuri Bay and Adjacent Water Areas Current Ecology, Resources and Prospects of Nature Management* : materialy mezhdunarodnoi nauchno-prakticheskoi konferentsii, Vladivostok, 29 noyabrya 2008 g. Vladivostok : Izd-vo Dal'nevostochnogo gosudarstvennogo universiteta, 2009, pp. 35–38. (in Russ.)
11. Khristoforova N. K. *Bioindikatsiya i monitoring zagryazneniya morskikh vod tyazhelymi metallami*. Leningrad : Nauka, 1989, 192 p. (in Russ.). https://elibrary.ru/zsyzlv
12. Shulkin V. M. *Metally v ekosistemakh morskikh melkovodii*. Vladivostok : Dal'nauka, 2004, 279 p. (in Russ.). https://elibrary.ru/qkmzkl
13. Shul'kin V. M. Comparative assessment of the aerial and fluvial inputs of matter into marine ecosystems. *Geografiya i prirodnye resursy*, 2012, no. 2, pp. 135–140. (in Russ.). https://elibrary.ru/ozpnyx
14. Aboal J. R., Pacín C., García-Seoane R., Varela Z., González A. G., Fernández J. A. Global decrease in heavy metal concentrations in brown algae in the last 90 years. *Journal of Hazardous Materials*, 2023, vol. 445, art. no. 130511 (14 p.). https://doi.org/10.1016/j.jhazmat.2022.130511
15. Belcheva N., Istomina A., Dovzhenko N., Lishavskaya T., Chelomin V. Using heavy metal content and lipid peroxidation indicators in the tissues of the mussel *Crenomytilus grayanus* for pollution assessment after marine environmental remediation. *Bulletin of Environmental Contamination and Toxicology*, 2015, vol. 95, iss. 4, pp. 481–487. https://doi.org/10.1007/s00128-015-1624-3
16. Bryan G. W., Hummerstone L. G. Brown seaweed as an indicator of heavy metals in estuaries in south-west England. *Journal of the Marine Biological Association of the United Kingdom*, 1973, vol. 53, iss. 3, pp. 705–720. https://doi.org/10.1017/S0025315400058902
17. Cantillo A. Y. Comparison of results of Mussel Watch programs of the United States and France with worldwide Mussel Watch studies. *Marine Pollution Bulletin*, 1998, vol. 36, iss. 9, pp. 712–717. https://doi.org/10.1016/S0025-326X(98)00049-6
18. Chalkley R., Child F., Al-Thaqafi K., Dean A. P., White K. N., Pittman J. K. Macroalgae as spatial and temporal bioindicators of coastal metal pollution following remediation and diversion of acid mine drainage. *Ecotoxicology and Environmental Safety*, 2019, vol. 182, art. no. 109458 (10 p.). https://doi.org/10.1016/j.ecoenv.2019.109458
19. Chernova E. N. Determination of the background ranges of trace metals in the brown alga *Sargassum pallidum* from the Northwestern Sea of Japan. *Russian Journal of Marine Biology*, 2012, vol. 40, iss. 3, pp. 267–274. https://doi.org/10.1134/S1063074012030030

20. Chernova E. N., Kozhenkova S. I. Determination of threshold concentrations of metals in indicator algae of coastal waters in the northwest Sea of Japan. *Oceanology*, 2016, vol. 56, iss. 3, pp. 363–371. https://doi.org/10.1134/S0001437016030024
21. Chernova E. N., Shulkin V. M. Concentrations of metals in the environment and in algae: The bioaccumulation factor. *Russian Journal of Marine Biology*, 2019, vol. 45, iss. 3, pp. 191–201. https://doi.org/10.1134/S1063074019030027
22. Kozhenkova S. I., Chernova E. N., Shulkin V. M. Microelement composition of the green alga *Ulva fenestrata* from Peter the Great Bay, Sea of Japan. *Russian Journal of Marine Biology*, 2006, vol. 32, iss. 5, pp. 289–296. https://doi.org/10.1134/S106307400605004X
23. Kozhenkova S. I., Khristoforova N. K., Chernova E. N., Kobzar A. D. Long-term biomonitoring of heavy metal pollution of Ussuri Bay, Sea of Japan. *Russian Journal of Marine Biology*, 2021, vol. 47, iss. 4, pp. 256–264. https://doi.org/10.1134/S106307402104009X
24. Malea P., Kevrekidis T. Trace element patterns in marine macroalgae. *Science of the Total Environment*, 2014, vol. 494–495, pp. 144–157. https://doi.org/10.1016/j.scitotenv.2014.06.134
25. Malinovskaya T. M., Khristoforova N. K. Characterization of coastal waters of the South Kuril Islands by the trace element content of indicatory organisms. *Russian Journal of Marine Biology*, 1997, vol. 23, iss. 4, pp. 212–218. https://elibrary.ru/ldzuqj
26. Moreda-Piñeiro A., Marcos A., Fisher A., Hill S. J. Evaluation of the effect of data pre-treatment procedures on classical pattern recognition and principal components analysis: A case study for the geographical classification of tea. *Journal of Environmental Monitoring*, 2001, vol. 3, iss. 4, pp. 352–360. https://doi.org/10.1039/b103658k
27. Obluchinskaya E. D., Aleshina E. G., Matishov D. G. Comparative assessment of the metal load in the bays and inlets of Murmansk coast by the Metal Pollution Index. *Doklady Earth Sciences*, 2013, vol. 448, iss. 2, pp. 236–239. https://doi.org/10.1134/S1028334X13020153
28. Pan Y., Wernberg T., de Bettignies T., Holmer M., Li K., Wu J., Lin F., Yu Y., Xu J., Zhou C., Huang Z., Xiao X. Screening of seaweeds in the East China Sea as potential bio-monitors of heavy metals. *Environmental Science and Pollution Research*, 2018, vol. 25, iss. 17, pp. 16640–16651. https://doi.org/10.1007/s11356-018-1612-3
29. Rainbow P. S. Mining-contaminated estuaries of Cornwall – field research laboratories for trace metal ecotoxicology. *Journal of the Marine Biological Association of the United Kingdom*, 2020, vol. 100, iss. 2, pp. 195–210. https://doi.org/10.1017/S002531541900122X
30. Rainbow P. S., Phillips D. J. H. Cosmopolitan biomonitors of trace metals. *Marine Pollution Bulletin*, 1993, vol. 26, iss. 11, pp. 593–601. https://doi.org/10.1016/0025-326X(93)90497-8
31. Reimann C., Filzmoser P., Garrett R. G. Background and threshold: Critical comparison of methods of determination. *Science of the Total Environment*, 2005, vol. 346, iss. 1–3, pp. 1–16. https://doi.org/10.1016/j.scitotenv.2004.11.023
32. Richir J., Gobert S. A reassessment of the use of *Posidonia oceanica* and *Mytilus galloprovincialis* to biomonitor the coastal pollution of trace elements: New tools and tips. *Marine Pollution Bulletin*, 2014, vol. 89, iss. 1–2, pp. 390–406. https://doi.org/10.1016/j.marpolbul.2014.08.030
33. Sánchez-Quiles D., Marbà N., Tovar-Sánchez A. Trace metal accumulation in marine macrophytes: Hotspots of coastal contamination worldwide. *Science of the Total Environment*, 2017, vol. 576, pp. 520–527. https://doi.org/10.1016/j.scitotenv.2016.10.144
34. Scanes P. R., Roach A. C. Determining natural 'background' concentrations of trace metals in oysters from New South Wales, Australia. *Environmental Pollution*, 1999, vol. 105, iss. 3, pp. 437–446. https://doi.org/10.1016/S0269-7491(99)00030-5
35. Shul'kin V. M., Chernova E. N., Khristoforova N. K., Kozhenkova S. I. Effect of mining activities on the chemistry

of aquatic ecosystem components. *Water Resources*, 2015, vol. 42, iss. 7, pp. 843–853. https://doi.org/10.1134/S009780781507012X

36. Shul'kin V. M., Kachur A. N., Kozhenkova S. I. Environmental objectives and indicators of the state of marine and coastal zones in the Northwest Pacific region. *Geography and Natural Resources*, 2017, vol. 38, iss. 1, pp. 52–59. https://doi.org/10.1134/S1875372817010073
37. Shulkin V. M., Orlova T. Yu., Shevchenko O. G., Stonik I. V. The effect of river runoff and phytoplankton production on the seasonal variation of the chemical composition of coastal waters of the Amursky Bay, Sea of Japan. *Russian Journal of Marine Biology*, 2013, vol. 39, iss. 3, pp. 197–207. https://doi.org/10.1134/S1063074013030115
38. Suresh Kumar K., Ganesan K., Subba Rao P. V. Phycoremediation of heavy metals by the three-color forms of *Kappaphycus alvarezii*. *Journal of Hazardous Materials*, 2007, vol. 143, iss. 1–2, pp. 590–592. https://doi.org/10.1016/j.jhazmat.2006.09.061
39. Usero J., González-Regalado E., Gracia I. Trace metals in the bivalve mollusc *Chamelea gallina* from the Atlantic coast of southern Spain. *Marine Pollution Bulletin*, 1996, vol. 32, iss. 3, pp. 305–310. https://doi.org/10.1016/0025-326X(95)00209-6
40. Vashchenko M. A., Zhadan P. M., Almyashova T. N., Kovalyova A. L., Slinko E. N. Assessment of the contamination level of bottom sediments of Amursky Bay (Sea of Japan) and their potential toxicity. *Russian Journal of Marine Biology*, 2010, vol. 36, iss. 5, pp. 359–366. https://doi.org/10.1134/S1063074010050056
41. Wang W.-X., Dei R. C. H. Kinetic measurements of metal accumulation in two marine macroalgae. *Marine Biology*, 1999, vol. 135, iss. 1, pp. 11–23. https://doi.org/10.1007/s002270050596
42. Yakubov M. R., Sinyashin K. O., Abilova G. R., Tazeeva E. G., Milordov D. V., Yakubova S. G., Borisov D. N., Gryaznov P. I., Mironov N. A., Borisova Yu. Yu. Differentiation of heavy oils according to the vanadium and nickel content in asphaltenes and resins. *Petroleum Chemistry*, 2017, vol. 57, iss. 10, pp. 849–854. https://doi.org/10.1134/S096554411710019X

ОЦЕНКА ЗАГРЯЗНЕНИЯ ТЯЖЁЛЫМИ МЕТАЛЛАМИ ПРИБРЕЖНЫХ ВОД ПОЛУОСТРОВА МУРАВЬЁВА-АМУРСКОГО С ИСПОЛЬЗОВАНИЕМ ВОДОРОСЛЕЙ-БИОИНДИКАТОРОВ

Е. Н. Чернова[1,2], С. И. Коженкова[1]

[1]Тихоокеанский институт географии ДВО РАН, Владивосток, Российская Федерация

[2]Дальневосточный федеральный университет, Владивосток, Российская Федерация

E-mail: *elena@tigdvo.ru*

Изучено содержание Fe, Mn, Cu, Zn, Pb, Cd и Ni в бурых водорослях [*Sargassum miyabei* Yendo и *S. pallidum* (Turner) C. Agardh] и зелёных водорослях [*Blidingia minima* (Nägeli ex Kützing) Kylin, *Ulva lactuca* Linnaeus и *U. linza* Linnaeus] из прибрежных вод полуострова Муравьёва-Амурского Японского моря, в окрестностях города Владивостока, собранных в июле 2017 г. Концентрации тяжёлых металлов в водорослях устанавливали методом атомно-абсорбционной спектрофотометрии после минерализации талломов с помощью азотной кислоты. Содержание растворённых элементов в морской воде определяли атомно-абсорбционным методом после ультрафильтрации проб воды и концентрирования металлов с помощью системы хлороформ — ДДТК-Na. На основе коэффициента опасности загрязнения водорослей металлами (K_O), представляющего собой отношение концентрации металла в водоросли к верхнему пороговому уровню фоновых концентраций элемента, а также на основе интегрального коэффициента TEPI-порог, рассчитанного с использованием $K_O \geq 1$, провели оценку степени загрязнения различных участков

прибрежной зоны моря. Прибрежные воды вокруг Владивостока были слабо загрязнены тяжёлыми металлами. Индекс TEPI-порог на станциях к северу и югу от полигона твёрдых бытовых отходов (ТБО) составил 2,4–2,8 в связи с загрязнением Pb и Cu (2,7–12 $C_{порог}$), а также Zn, Fe, Mn и Ni. Водоросли из вершин Уссурийского и Амурского заливов обогащены Fe и Mn из-за выноса металлов водами рек; TEPI-порог — 1,7–3,0. В проливе Босфор Восточный загрязнение макрофитов Fe (3–10 $C_{порог}$), а также Mn, Cu, Zn и Ni (1–1,5 $C_{порог}$) связано с портовой деятельностью, судоходством и строительством мостов; значение TEPI-порог составило 1,0–2,1. Локальная зона высокой степени загрязнения, сформированная за счёт дренирования дождевыми водами рекультивированного полигона ТБО города Владивостока, с TEPI-порог = 16, находится у восточного побережья полуострова Муравьёва-Амурского. Из числа исследованных элементов Fe и Cu были основными загрязнителями макрофитов этой станции ($K_O > 80$ в водорослях), а Pb, Mn, Zn и Ni — сопутствующими. В морской воде с этой станции концентрации растворённых металлов превышали фоновые уровни, содержание растворённой меди составляло 3 ПДК для рыбохозяйственных водоёмов.

Ключевые слова: загрязнение, тяжёлые металлы, бурые водоросли, зелёные водоросли, Амурский залив, Уссурийский залив, залив Петра Великого, полуостров Муравьёва-Амурского, Японское море

1871
ИнБЮМ – IBSS

Морской биологический журнал
Marine Biological Journal
2025, vol. 10, no. 2, pp. 111–113
https://marine-biology.ru

CHRONICLE AND INFORMATION

ON THE 85th ANNIVERSARY OF VICTOR EGOROV, ACADEMICIAN OF RAS

On 21 May, 2025, the outstanding scientist Victor Egorov turns 85: Academician of the Russian Academy of Sciences, D. Sc., Professor, chief researcher of department of radiation and chemical biology, and IBSS supervisor.

Career. V. Egorov was born in 1940 in Sevastopol. He is a fourth-generation Sevastopol resident. He is a graduate of the Sevastopol Shipbuilding College (1955–1959), the Sevastopol Instrument Engineering Institute (1962–1967) as an electrical engineer (mathematical computing devices and units, diploma with honors), and Sevastopol Higher Naval Engineering School (1967–1968) as a senior engineer of the laboratory of electrical training equipment.

Since 1968, Victor Egorov works at IBSS. In 1968–1970, he was senior engineer of the radiobiology department; in 1970–1980, junior researcher; in 1980–1983, senior researcher; in 1983–1990, head of the laboratory; in 1989–1994, deputy director for scientific affairs; and in 1991–2010, head of the department of radiation and chemical biology. Since 2010, V. Egorov works as chief researcher, and since 2018, he is IBSS supervisor.

Scientific career and awards:

- 1975, PhD in marine physics;
- 1984, Veteran of Labor medal;
- 1988, D. Sc. in radiobiology;
- 1995, Corresponding Member of the Crimean Academy of Sciences;
- 2000, senior researcher in hydrobiology;
- 2005, Professor in hydrobiology;
- 2006, a badge of the National Academy of Sciences of Ukraine “For the Training of Qualified Personnel”;
- 2006, Corresponding Member of the NAS of Ukraine in marine biophysics;
- 2007, the State Prize of Ukraine in Science and Technology;
- 2008, an honorary title “Honored Science and Technology Figure of the Autonomous Republic of Crimea”;
- 2010, a badge of the NAS of Ukraine “For Professional Achievements”;
- 2011, Order of Ukraine “For Merit” of the III class;

- 2012–2022, Academician of the NAS of Ukraine in ecosystemology (in June 2022, he was expelled from the membership of the NAS of Ukraine at his own request);
- 2016, Academician of the Department of Agricultural Sciences of the RAS;
- 2022, honored figure of new technologies of the Russian Federation;
- 2023, the Medal of the Order "For Merit to the Fatherland" of the II class;
- 2023, member of the bureau of the Coordinating Council of the Southern Association of Scientific Organizations under the scientific and methodological guidance of the RAS;
- 2024, a jubilee medal "300 Years of the Russian Academy of Sciences."

Marine practice. Victor Egorov is yacht helmsman, motorman, radio operator of the 1st class, and skipper of small vessels. Participated in a round-the-world cruise and researches in 27 seas of the Atlantic, Indian, and Pacific oceans. Worked in more than 45 cruises on research vessels. Headed more than 20 cruises. Out of them, 15 were international ones, with scientists from 16 countries (Belgium, Bulgaria, France, Georgia, Germany, Greece, Holland, Italy, Portugal, Romania, Russia, Spain, Sweden, Turkey, UK, and USA).

Major scientific achievements. V. Egorov is a specialist in studying the interaction between living and inert matter with marine environment's radioactive and chemical components. A semi-empirical theory has been substantiated of mineral and radioisotope exchange of marine organisms and inert matter in the marine environment on the time scale of metabolic and sorption processes and trophic interactions. By parameters, this model is compatible with modern methods of describing the balance of matter and energy in marine ecosystems. The radioecological response of the Black Sea to the Chernobyl Nuclear Power Plant disaster of 1986 has been studied. As established, the radioecological signal from the Chernobyl disaster can be traced in the Black Sea on a half-century time scale. Radiotracer methods have been developed for using post-Chernobyl radionuclides to assess the intensity of biogeochemical processes. A geographical discovery has been made. A previously unknown biogeochemical factor has been registered: methane seeps from the bottom in a depth range of 10–2,100 m. Its environment-forming, resource, and ecological roles have been investigated. Coral-like carbonate bacterial structures with linear dimensions up to 4 m have been discovered in the hydrogen sulfide layer of the Black Sea; those evidence for the existence of the phenomenon of life under anaerobic conditions. As established, the age of bacterial structures at different depths corresponds to trends of hydrogen sulfide contamination of waters during its late geological evolution. A theory of radioisotopic and chemical homeostasis of marine ecosystems has been developed. The term 'ecological capacity' has been proposed to assess the ability of the marine environment to self-purify. The concept of Academician V. Vernadsky on the unity of processes of reproduction of living matter and conditions of its habitat has been quantitatively implemented. Biogeochemical criteria have been substantiated for standardizing maximum permissible flows of marine pollution. Methods for implementing the concept of sustainable development of marine critical and recreational zones have been developed. These methods take into account the ecocentric approach to protecting the biosphere and the balance of anthropogenic consumption and natural reproduction of water quality resources.

Scientific and organizational activities. While participating in numerous research cruises and business trips, Victor Egorov has visited 53 countries in Asia, Africa, Europe, and North and South America, as well as Australia and Oceania. He supervised IBSS research within the framework of international projects as follows: IAEA (1992–1994 and 1997–2002); Volkswagen (Germany, 1993–1995); EROS 2000 and EROS 21 (European Union, 1994–1998); BIG-BLACK (EU, 1998–2000); INCO-COPERNICUS (EU, 2001–2002); The Black Sea Gas Hydrates (EU, 2001–2002); Localization of Methane Seeps in the Black Sea (NATO, 2001–2003); METROL (EU, 2002–2004); CRIMEA (EU, 2003–2005); Mussel Watch (EU, 2004–2007). Moreover, he co-headed the projects Vanco Prikerchenskaya (USA, 2007–2008) and SESAME (EU, 2007–2009).

Scientific and educational work. V. Egorov supervised eight PhDs and one D. Sc. He presented reports at scientific forums in 13 countries (Austria, Belgium, Bulgaria, Czech Republic, France, Germany, Greece, Hungary, Italy, Luxembourg, Monaco, Turkey, and USA). He is the Editor-in-Chief of Marine Biological Journal. He serves on editorial boards of five scientific journals: Biodiversity and Sustainable Development (IBSS, Sevastopol); Civil Security Technologies (All-Russian Research Institute for Civil Defense of the EMERCOM of Russia, Moscow); Ecological Safety of Coastal and Shelf Zones of Sea (Marine Hydrophysical Institute of the RAS, Sevastopol); Ecosystems (V. I. Vernadsky Crimean Federal University, Simferopol); and Monitoring Systems of Environment (Institute of Natural and Technical Systems, Sevastopol). He is the member of the International Union of Radioecology. Member of qualification councils for awarding academic degrees in hydrobiology (biological sciences) and oceanology (geographical sciences). Author of more than 400 scientific papers (with more than 100 published abroad). His works include 15 monographs, with 1 of them published by Wiley and 1 by Springer.

In connection with the glorious anniversary of Academician Victor Egorov, we sincerely wish him consistently good health and further scientific and organizational achievements! We know that with his active work, Victor Egorov will contribute to new accomplishments for the benefit of economic and cultural development of Sevastopol, the Crimea, and Russia. He worthily continues the family tradition to leave a noticeable mark in the history of Sevastopol and the Fatherland glorifying it with discoveries important for science and people.

With deep respect,
staff of IBSS department of radiation and chemical biology

АКАДЕМИКУ РАН ВИКТОРУ НИКОЛАЕВИЧУ ЕГОРОВУ 85 ЛЕТ

21 мая 2025 г. исполняется 85 лет профессору Виктору Николаевичу Егорову — выдающемуся учёному, специалисту в области изучения взаимодействия живого и косного вещества с радиоактивными и химическими компонентами морской среды, главному редактору «Морского биологического журнала». В. Н. Егоров опубликовал 400 работ, принял участие в более чем 40 научных рейсах на океанографических судах, подготовил восемь кандидатов и одного доктора наук.

1871
ИнБЮМ – IBSS

Морской биологический журнал
Marine Biological Journal
2025, vol. 10, no. 2, pp. 114–115
https://marine-biology.ru

IN MEMORIAM: NELLI SERGEEVA (20.11.1940 – 02.02.2025)

On 2 February, 2025, our colleague Nelli Sergeeva passed away – D. Sc., chief researcher at IBSS, and a specialist on Black Sea meiobenthos.

N. Sergeeva was born in the city of Ashgabat (Turkmen SSR). She graduated from school in the city of Alma-Ata (Kazakh SSR) and studied at the faculty of biology and soil science of the Kazakh State University named after S. M. Kirov (now Al-Farabi Kazakh National University). During her final years at the university, she completed coursework and pre-graduation internships in the benthos department at the Institute of Biology of the Southern Seas of Academy of Sciences of the Soviet Union under the supervision of M. Kiseleva and I. Greze. After receiving a diploma in biology, with specialization in hydrobiology and ichthyology, she was assigned to work at the Kazakh Research Institute of Fisheries (the city of Balkhash).

In 1968–1972, Nelli Sergeeva studied in the PhD graduate school in hydrobiology at IBSS under the supervision of V. Vodyanitsky, director of the Institute and corresponding member of the Academy of Sciences of the Soviet Union. Upon successful completion of her studies, she joined the benthos department at IBSS. In 1974, she defended her PhD thesis “Fauna and Some Ecological Aspects of Free-living Nematodes of the Black Sea.” Her subsequent research in biodiversity and life processes in the Black Sea yielded a vast array of new data. In 2000, with advisory support from V. Zaika, the corresponding member of the National Academy of Sciences of Ukraine, she defended her D. Sc. dissertation “Zonal Distribution of Meiobenthos and Its Key Component, Free-living Nematodes in the Black Sea.” Summarizing all the information on nematodes, she described 29 species and 4 genera new for science documenting 30 species and 30 genera previously unrecorded in the Black Sea.

Infinitely in love with science, N. Sergeeva continually expanded the scope of her interests. She studied the taxonomy and ecology of various groups of marine meiofauna, their significance for bioindication, the structure of meiobenthos, and its role in benthic ecosystems. She made a comprehensive inventory of the Black Sea meiobenthos (more than 500 species). Moreover, she conducted a detailed research of specific Black Sea benthic communities formed under extreme conditions: under hypoxia, anoxia, hydrogen sulfide contamination, and anthropogenic pollution, as well as in methane seepage habitats.

Meticulous and observant, Nelli Sergeeva made groundbreaking discoveries in the Black Sea oxygen-depleted depths previously considered lifeless (except for bacterial flora) due to hydrogen sulfide contamination. She recorded previously unknown unicellular organisms (ciliates, soft-shelled foraminifera,

and gromiids), multicellular organisms (rotifers, nematodes, oligochaetes, polychaetes, and tardigrades), and Gastrotricha genus and species that had not been registered in the Black Sea earlier. With this, she actually created a new scientific direction – the study of the Black Sea benthos within the deep-sea periazoic level.

She pioneered large-scale research on soft-shelled foraminifera in the Black Sea and Sea of Azov. She was the first to document the remarkable diversity (extensive spatial and bathymetric distribution) of foraminifera and a closely related group Gromiida. Also, she evaluated their role in benthic communities.

N. Sergeeva participated in 17 research cruises, including international ones. As a hydronaut, she dived aboard a manned submersible "Benthos-300" off the coasts of the Caucasus and Crimea. She coordinated, headed, and implemented several international and national projects and grants of the Russian Foundation for Basic Research. She authored more than 200 scientific papers. In particular, she co-authored two monographs and contributed to chapters of nine collective monographs published both in Russia and abroad. She generously shared her scientific experience with colleagues and students.

She seamlessly balanced her intensive scientific work with organizational leadership. Nelli Sergeeva served as secretary and member of a qualification council for awarding academic degrees. In 2000–2013, she headed the shelf ecosystems department at IBSS. She participated in activities of examination boards and supervised graduate students. In 2017–2018, she served as the advisor for IBSS director. For her lifelong dedication and significant contribution to marine hydrobiology, she was listed on the city Board of Honor (2019) and awarded the Certificate of Honor of the Russian Academy of Sciences (2020).

N. Sergeeva devoted her entire life to science. She enthusiastically dived into every new field of study striving to inspire her colleagues. To her family, she was a loving mother and devoted grandmother.

The bright memory of Nelli Sergeeva, along with endless gratitude and respect for her, will forever remain in our hearts.

Friends and colleagues from IBSS

ПАМЯТИ НЕЛЛИ ГРИГОРЬЕВНЫ СЕРГЕЕВОЙ (20.11.1940 – 02.02.2025)

02 февраля 2025 г. ушла из жизни д. б. н. Нелли Григорьевна Сергеева. Она стала автором более чем 200 научных работ, выполнила инвентаризацию состава мейобентоса Чёрного моря и приняла участие в 17 морских экспедициях, в том числе международных.

1871
ИнБЮМ – IBSS

Морской биологический журнал
Marine Biological Journal
2025, vol. 10, no. 2, pp. 116–118
https://marine-biology.ru

IN MEMORIAM: NIKOLAY BOBKO (19.08.1951 – 11.03.2025)

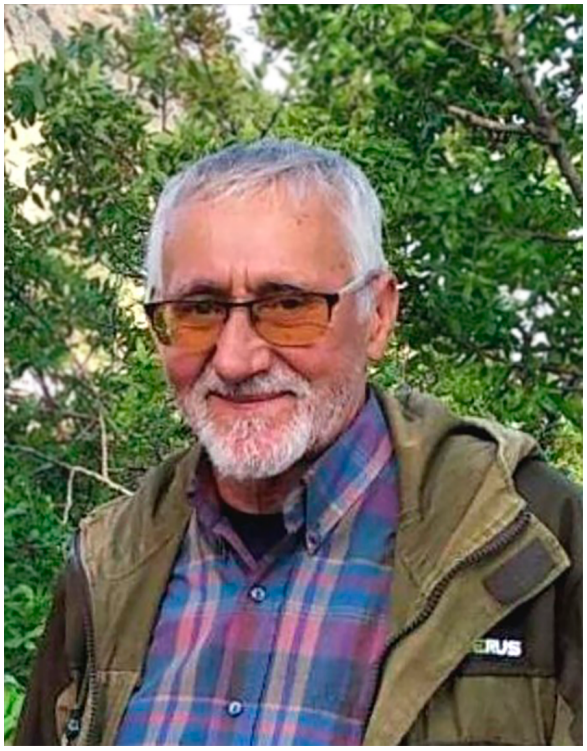

On 11 March, 2025, Nikolay Bobko suddenly passed away – junior researcher at the IBSS department of aquaculture and marine pharmacology, highly qualified hydrochemist and talented mentor.

He was born on 19 August, 1951, in the city of Lutsk, Volyn Oblast, Ukrainian SSR. Like all Soviet children, he went to school, was involved in sports, participated in all school events, and helped his parents about the house. Even then, teachers noticed his sharp mind and thirst for knowledge in physics and chemistry. It was this combination – physics and chemistry – that shaped his future.

In 1968, he entered Taras Shevchenko State University of Kyiv, faculty of chemistry. The competition for admission was very high, and the committee asked questions far beyond the school curriculum. Applicant N. Bobko impressed the committee with the depth of his knowledge of high explosives and received the highest admission score unanimously.

After graduating from the university in 1973, he was assigned to the Sevastopol branch of the N. N. Zubov State Oceanographic Institute. At that time, the USSR increased its activity in exploration of seas and oceans. As the number of research vessels was rising, the country was in dire need of qualified chemists. At this Institute, a young specialist Nikolay Bobko designed various methods of hydrochemical analysis which are still in use.

At the end of 1975, the Special Experimental Design Bureau for Underwater Research was established in Sevastopol (a base “Hydronaut”). As a very passionate person inspired by the sea expeditions of Jacques-Yves Cousteau, N. Bobko decided to try his hand at research at this base. As a result, he was involved in the study of benthos: he dived to a depth of more than 300 m on a famous manned submersible “Benthos-300.”

Since Nikolay Bobko was a highly qualified young specialist, various scientific institutions in Sevastopol were interested in collaborating with him. In 1982, he chose the A. O. Kovalevsky Institute of Biology of the Southern Seas and worked there for 42 years introducing advanced methods of analytical chemistry. He designed modern methods for analyzing almost all elements in hydrobionts. N. Bobko completed scientific internships in Leningrad, Kyiv, and Tartu. He co-authored more than 50 scientific papers,

including 2 monographs and 6 patent. For his inventions, he was awarded a diploma and a gold medal named after Nikola Tesla at the International Fair of Technics and Technical Achievements in Bosnia and Herzegovina in April 2024. Also, he was awarded a gold medal of the XX International Salon of Inventions and New Technologies "New Time."

Nikolay Bobko was one of the best and broad-minded experts in physical and chemical analysis not only in Sevastopol, but also in the entire Southern Federal District. Valuing his skill versatility, various organizations involved in analytical research constantly invited him to work. He managed the flow of tasks in three institutions simultaneously: IBSS, the Sevastopol Regional Center for Standardization, Metrology, and Testing, and "SGS Vostok Limited" providing the analysis of petroleum products. The first two institutions use his technique for sample preparation for elemental analysis.

N. Bobko had extensive experience in marine expeditions. He participated in research cruises to the Pacific, Atlantic, and Indian oceans and to the Black Sea and other seas as a head of the scientific team, deputy head of the expedition, and its head. He studied coral reefs and carried out experiments in hydrochemistry involving deep-sea vehicles. He was always interested in something new and unknown. He could not stand routine; so, he automated all measurements. N. Bobko designed methods using a modern flow analyzer, and this allowed a single researcher to do the work of an entire department of hydrochemists.

He was an unrivaled fisherman: he knew habits of many fish species and always took the first place in fishing tournaments in marine expeditions. In addition to scientific achievements, he demonstrated sport ones winning table tennis matches.

Nikolay Bobko actively participated in the design of new technologies for obtaining bioactive compounds from mariculture objects to create medicines and raw materials for the pharmacological industry. Moreover, he was involved in the development of biotechnology for cultivating microalgae used both as food for molluscs and their larvae and as a source of bioactive compounds.

N. Bobko creatively solved assigned tasks and was a hardworking and proactive researcher. Lately, he was concerned with one of the pressing problems related to the reproduction of marine bioresources and shared his experience gained from long-term studies in the shelf zone of the Black Sea. He investigated hydrochemical factors driving the processes of melioration of the marine environment both in areas of the functioning of farms and in areas chosen for their establishment.

He was an exceptionally conscientious and responsible researcher. He was sociable, responsive, and selfless, maintained good relations with colleagues, and enjoyed well-deserved respect. We are sincerely grateful for everything he taught us.

On 19 August, 2025, Nikolay Bobko would have turned only 74 years old. The memory of a wonderful person, teacher, and friend will forever remain in our hearts.

Students, colleagues, and friends

ПАМЯТИ НИКОЛАЯ ИВАНОВИЧА БОБКО (19.08.1951 – 11.03.2025)

11 марта 2025 г. ушёл из жизни наш коллега — м. н. с. отдела аквакультуры и морской фармакологии ФИЦ ИнБЮМ Николай Иванович Бобко. Он был высококвалифицированным гидрохимиком, наладившим в Институте методы анализа практически всех элементов в гидробионтах. Н. И. Бобко стал соавтором более чем 50 научных работ, среди которых 2 монографии и 6 патентов.

ISSN 2499-9768 25002
9 772499 976005 >

Вниманию читателей!

Зоологический институт РАН,
Институт биологии южных морей
имени А. О. Ковалевского РАН

издают
научный журнал

Морской биологический журнал
Marine Biological Journal

- МБЖ — периодическое издание открытого доступа. Подаваемые материалы проходят независимое двойное слепое рецензирование. Журнал публикует обзорные и оригинальные научные статьи, краткие сообщения и заметки, содержащие новые данные теоретических и экспериментальных исследований в области морской биологии, материалы по разнообразию морских организмов, их популяций и сообществ, закономерностям распределения живых организмов в Мировом океане, результаты комплексного изучения морских и океанических экосистем, антропогенного воздействия на морские организмы и экосистемы.
- Целевая аудитория: биологи, экологи, биофизики, гидро- и радиобиологи, океанологи, географы, учёные других смежных специальностей, аспиранты и студенты соответствующих научных и отраслевых профилей.
- Статьи публикуются на русском и английском языках.
- Периодичность — четыре раза в год.
- Подписной индекс в каталоге «Пресса России» — Е38872. Цена свободная.

Заказать журнал

можно в научно-информационном отделе ИнБЮМ. Адрес: ФГБУН ФИЦ «Институт биологии южных морей имени А. О. Ковалевского РАН», пр-т Нахимова, 2, г. Севастополь, 299011, Российская Федерация.
Тел.: +7 8692 54-06-49.
E-mail: *mbj@imbr-ras.ru*.

Zoological Institute of RAS,
A. O. Kovalevsky Institute of Biology
of the Southern Seas of RAS

publish
scientific journal

Морской биологический журнал
Marine Biological Journal

- MBJ is an open access, peer reviewed (double-blind) journal. The journal publishes original articles as well as reviews and brief reports and notes focused on new data of theoretical and experimental research in the fields of marine biology, diversity of marine organisms and their populations and communities, patterns of distribution of animals and plants in the World Ocean, the results of a comprehensive studies of marine and oceanic ecosystems, anthropogenic impact on marine organisms and on the ecosystems.
- Intended audience: biologists, ecologists, biophysicists, hydrobiologists, radiobiologists, oceanologists, geographers, scientists of other related specialties, graduate students, and students of relevant scientific profiles.
- The articles are published in Russian and English.
- The journal is published four times a year.
- The subscription index in the “Russian Press” catalogue is E38872. The price is free.

You may order the journal

in the scientific information department of IBSS. Address: A. O. Kovalevsky Institute of Biology of the Southern Seas of RAS, 2 Nakhimov avenue, Sevastopol, 299011, Russian Federation.
Tel.: +7 8692 54-06-49.
E-mail: *mbj@imbr-ras.ru*.